Universitetet i Stavanger

FACULTY OF SCIENCE AND TECHNOLOGY

MASTER'S THESIS

Study programme/specialisation: Environmental Engineering/ Offshore Technology	Spring Semester, 2018 Confidential
Author: Elina Alfsvåg	*Elina Alfsvåg* …………………………………………… (signature of author)

Programme coordinator: Supervisor(s):   Malcolm A. Kelland, Rachael Cole, and Tore Nordvik.

Title of master's thesis: New Developments in Demulsifier Chemistry

Credits: 30p

Keywords: Demulsifier, dendrimer, emulsions, dendrimer, crude oil, bottle test, HLB, RSN, ecotoxicity, biodegradation.	Number of pages: ………88………… + Appendix: …61……… Stavanger,……13.07.18.………. date/year

Acknowledgements

Abstract

Sixteen new demulsifier chemicals were prepared based on dendrimer chemistry. They were designed to be amphiphilic with hydrophilic ethoxylated blocks, hydrophobic polyester dendrimer cores and alkyl chains. Three different factors were investigated in the synthesis of Boltorn H311 with the alkyl ether carboxylic acids - the percentage coverage of the dendrimer surface (50 to 100%), the number of the ethylene oxide units (2-10), and the length of the carbon chains (C_{12}/C_{14} and C_{16}/C_{18}). GPC, IR and NMR were successfully used to characterise the reaction products.

The products were systematically investigated as emulsion breakers for resolving water-in-oil (W/O) emulsions by bottle testing on three different crude oils. The best performing products were found to give water separations of >80%. The main trends were improved water separation on increasing coverage of the dendrimer surface, increasing length of EO units and less significantly increasing carbon chain length. Measurements of residual emulsion (BS) were also important in the evaluation of demulsifier performance. The products had a strong affinity for adsorbing at the interface of water droplets in water-in-oil (W/O) emulsions. The demulsifier performance of the best performing products was also correlated to reduction of interfacial tension (IFT) for the 90% coverage range of products.

Biodegradation and ecotoxicity were investigated for the product range (**1-16**). The products had biodegradation measurements between 20-30% on day 28, with the exception of product **5** (15%). EC_{50} was used as the measure of toxicity. For all the products EC_{50} was > 10 mg/L. Fifteen of the products were classified as Y2.

Table of Contents

Table list

Figure list

Nomenclature

Abbreviations

AN	Acid number
ATR	Attenuated total reflection
BDGE	Butyl diglycyl ether
BHT	Butylated hydroxytoluene
BOD	Biochemical oxygen demand
BP	Boiling point
BS&W	Basic sediment and water
CDCl$_3$	Deuterated chloroform
COD	Chemical oxygen demand
DDBSA	Dodecylbenzenesulfonic acid
DETA	Dietylenetriamine
DMI	Dimethyl isosorbide
EB	Emulsion breaker
ECHA	European chemical agency
EDA	Etylenediamine
EGMBE	Ethylene glycol monobutyl ether
EO	Ethylene oxide
EOR	Enhanced oil recovery
Eq.	Equation
EU	European union
FP	Flash point
FT-IR	Fourier transform IR
G	Generation
GPC	Gel permeation chromatography
HLB	Hydrophilic-lipophilic balance
IF	Interface
IFT	Interfacial tension
IR	Infrared
min	Minutes
MP	Melting point
NMR	Nuclear magnetic resonance
O/W	Oil-in-water
OH	Hydroxyl
PAMAM	Polyamidoamine
PD	Polydispersity
PDMS	Poly(dimethylsiloxane)
PEG	Polyethylene glycol
PEO	Poly(ethylene oxide)
PO	Propylene oxide
PPO	Poly(propylene oxide)

PW	Produced water
REACH	Regulation, evaluation, authorization and restriction of chemicals
RPM	Revolutions per minute
RSN	Relative solubility number
RT	Retention time
TEPA	Tetrathylenepentamine
TETA	Triethylenetetramine
ThOD	Theoretical oxygen demand
TMS	Tetramethylsilane
W/O	Water-in-oil

Latin symbols

A	Empirical constant	
B	Empirical constant	
BS	Basic sediment	[mL]
C	Empirical constant	
e	Euler's number	
EC_{50}	Half maximal effective concentration	[mg/L]
LC_{50}	Half lethal concentration	[mg/L]
m	Mass	[g]
M	Molar concentration	[mol/L]
M_W	Molecular weight	[g/mol] [Da]
n	Constant	
$P_{O/W}$	Partition coefficient	
r	Radius	[μm]
T	Temperature	[K]
V	Volume	[cm^3] [mL]
W_B	Weight of bottle and stopper	[g]
W_T	Weight of bottle and stopper with chemicals	[g]
x	Constant	
y	Constant	
z	Constant	

Greek symbols

δ	Chemical shift	[ppm]
η	Viscosity	[cP]
ν	Wavenumber	[cm^{-1}]
ρ	Density	[g/cm^3]
σ	Interfacial tension	[mN/m]
σ_d	Interfacial tension of demulsifier	[mN/m]
σ_{ns}	Interfacial tension of natural surfactant	[mN/m]

1 Introduction

1.1 Background

This master's thesis started with a newly developed demulsifier. Dr. Rachael Cole and Dr. Tore Nordvik from Schlumberger proposed and presented the thesis through Professor Malcolm A. Kelland. The first meeting was arranged between Tore Nordvik and myself on the 22nd of May (2017), where he presented a variety of topics. I accepted the thesis and chose to work on the demulsifier project. The main goals for the thesis is to synthesis the demulsifier and optimize this process, in addition to characterize, test, and analyse the product. The main laboratory work will be performed in Schlumberger's laboratory in the office building located at Forus, Sandnes. Any NMR analyses will be performed at the University of Stavanger. The master's thesis was officially started on the 3rd of January (2018).

1.2 Thesis objective

In this thesis, an array of polymeric syntheses will be performed. The scope of the thesis is to produce a range of new demulsifier products based on dendrimers that differ in structure and properties. Each of the products will be analysed using GPC, IR, and NMR.

The physical properties of the products are important factors in relation to the performance of the demulsifier. Physical properties and parameters such as pH, density, solubility, HLB, and RSN will be investigated and related to demulsifier performance

The most important aspect of this work will be the demulsifier performance testing by bottle test. The bottle testing will be carried out in three different crude oils, where trends between water separation efficiency, chemical structure, and physical properties and water separation will be key. Thieving samples will also be conducted to measure of the amount of residual emulsion and oil dryness. Finally, ecotoxicity and biodegradation will be determined.

2 Theoretical background

2.1 Introduction

In industrial processes, the emulsification of liquid phases can be an undesirable effect, which is especially true for the petroleum industry. An emulsion is defined as a mixture of two liquids that are immiscible in each other [1]. In the mixture, one of the liquids is dispersed (*dispersed phase*) in the other (*continuous phase*) (see Figure 2.1) [1-3]. This is also known as an colloidal dispersion [4]. The dispersion is usually stabilized by the adsorption of a third component, an *emulsifier*, at the liquid-liquid interface [5]. Most emulsions will separate naturally without such an emulsifying agent present. Thus, an emulsion can be described as kinetically stable, but thermodynamically unstable. Emulsions are usually categorized into three types: water-in-oil (W/O), oil-in-water (O/W), and multiple or complex emulsions (see Figure 2.1) [6]. In this thesis, the main focus will be on W/O and O/W emulsions.
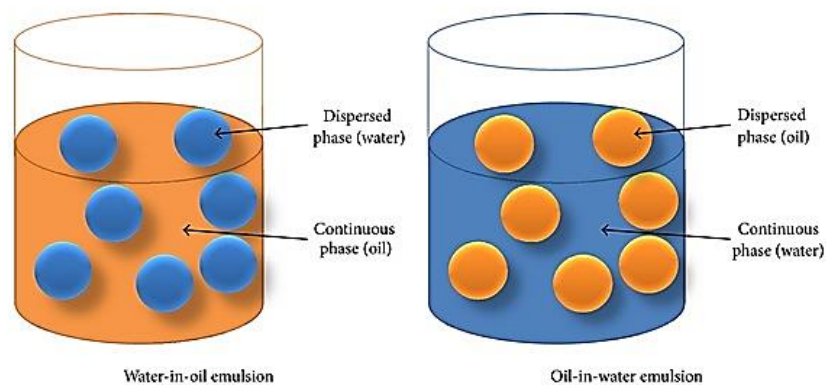
Figure 2. 1 Illustration of W/O (left) and O/W (right) emulsion.

A number of methods have been developed to resolve emulsions, including chemical, mechanical, electrical, acoustic, thermal, and biological treatments [7-11]. Chemical demulsification has been recognized as the most efficient method for resolving petroleum emulsions [12, 13]. Chemical demulsification in the oil industry refers to the process of resolving emulsions to separate water from crude oil, or vice versa, utilizing a class of surface active agents [14]. These chemicals are known as *demulsifiers* or *emulsion breakers*, and will promote coalescence of the dispersed phase and drainage of the interfacial film [15]. Emulsion breaker chemicals are often very efficient at low concentrations, and are generally applied in the concentration range of 1 – 1000 ppm [16].

Undesirable emulsification is particularly a problem in the recovery of petroleum from oil reservoirs. Here, immiscible phases are mixed together with considerable agitation. This phenomenon typically occurs when the oil is in a turbulent environment, such as in in the production tubing, pipeline, and when passing through chokes such as the wellhead [17]. Emulsions can arise in most stages of oil production. Some examples of emulsions in the oil industry are: (1) Emulsion drilling and stimulation fluid, (2) *in situ* reservoir emulsion, (3) process emulsions, (4) transportation emulsions [18, 19].

Water and brine are always factors in crude oil production, and they are both immiscible in the oil. Additionally, the crude oil will also contain natural emulsifying agents, such as asphaltenes, resins, and naphthenic acids [20]. Production chemicals such as corrosion and wax inhibitors are also known to promote emulsification [17]. Finally, solid composites of the oil may accumulate at the interface (IF) and act as stabilizing agents. These include salts, sand, iron, zinc, and crystallized paraffin among others [21]. Such natural and additive emulsifying agents, along with other components of the crude oil, will form a thick, viscous interfacial film surrounding the water droplets dispersed in the oil [3]. The polar group of the emulsifying molecules will orientate toward the water, while the non-polar groups will orientate toward the oil. There are several factors that affect the stability of water-oil (WO) emulsion systems, such as the nature of the emulsifying agent present, oil composition, water cut, oil viscosity, specific gravity of the oil, system agitation, system temperature, and age of emulsion [22].

Moreover, important physical and mechanical properties of the interfacial film are acting as barriers of coalescence. Such properties include [18]:

- Low interfacial tension, thus a large interfacial area can be sustained.
- High surface viscosity (mechanically strong, viscoelastic barrier), which act as a barrier to prevent coalescence and could be enhanced by stabilizing agents.
- Large electric double layer (steric repulsion), which prevent flocculation and coalescence.

Based on the emulsion stability, L.L. Schramm states that it will be easier to form an O/W emulsion than a W/O emulsion. This is due to the electric double layer thickness, which is greater in water than in oil [18].

From an economic perspective, W/O emulsions are troublesome when it comes to maintain a profitable oil production. Crude oil prices are, among other factors, regulated based on °API gravity where high-gravity oils are appraised at a higher price. Too high content of water will drastically lower the crude oil price [22]. Customers usually specify the maximum acceptable contents of water (typically 0.2-0.5% w/w) [17].

In produced water (PW), it is crucial that the concentration of oil is low as possible before discharge to the sea. If the oil content is too high (> 30 mg/L per month, OSPAR 2013), the PW cannot be discharged directly to the sea. Thereby, the oily waste must be further processed or transported to a secondary treatment facility, which is both costly and could occupy valuable transport capacity.

In this chapter, theory will be presented that promotes understanding of how demulsifiers work. Structures and the main components of a demulsifier chemical will be investigated. Additionally, factors affecting the demulsification process will be presented.

2.2   Demulsifiers

2.2.1   Definition and Classification

Chemicals that destabilize emulsions, causing them to separate, are known as demulsifiers[23]. Demulsifiers are surface-active agents that have the chemical function of separating immiscible liquids, in this case WO systems [11]. Thus, emulsion breakers should have a destabilizing effect on such emulsion systems. Additionally, demulsifier should migrate rapidly through the continuous phase and diffuse quickly towards the interface, and lastly promote flocculation and coalescence of the dispersed phase [18].

There are several approaches to classifying demulsifier chemicals. Emulsion breakers can be classified based on their chemical function, structure, and application. With regards to application, the chemical class can be further divided into their water-in-oil and oil-in-water applications [20]. Two major groups exist with respect to the chemical function: (1) non-ionic demulsifiers, and (2) ionic demulsifiers. Moreover, the ionic group may be categorized according to the net charge of the hydrophilic functional group of the molecule; cationic, anionic, or zwitterionic [24]. Based on chemical structure, emulsion breakers are often divided into demulsifier families [25]:

- Ethylene oxide (EO)/Propylene oxide (PO) block copolymers
- Amine derivatives
- Alcohol derivatives
- Aromatic/phenol derivatives
- Silicone derivatives
- Dendritic polymers/Dendrimers

2.2.2   Mechanism

Despite extensive studies of the demulsification process, the mechanism is still elusive. However, overall process of demulsifiers can be broken down into three simplified steps [16, 22, 26, 27]:

1. Strong attraction to the oil-water interface
2. Flocculation or aggregation
3. Coalescence
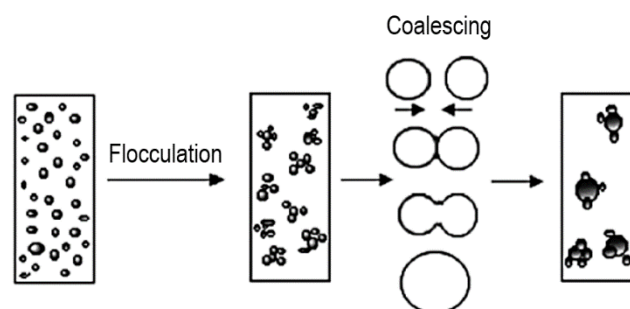
Figure 2. 2 Illustration of the process of flocculation and coalescence.

The otherwise natural process of coalescence in petroleum emulsion systems, is inhibited by natural surfactants of the crude oil such as asphaltenes, resins, naphthenates, and wax particles [28]. By interacting with the WO interface, the emulsifying agents can form a mechanically strong film that often are viscoelastic , retard the film drainage, or form steric hindrance [29]. Nevertheless, the main mechanism of stabilization of emulsion systems encountered in the petroleum industry, are primarily attributed to asphaltenes. This is due to their ability to aggregate and form a gel-like continuum at the oil-water interface [30]. As the demulsifier interacts with the WO interface, it can change the physical properties of the interfacial barrier. Demulsifiers are reported to disrupt the interfacial barrier in three different ways [28]:

1. The demulsifier will overcome the stabilizing agent by having a greater activity, and thus disrupt the stabilizing film.
2. The demulsifier will affect the interfacial barrier by lowering the viscoelasticity of the interface.
3. The demulsifier will disrupt the *interfacial gradient* (Marangoni effect) that is responsible for the stability of the emulsion.

However, it is possible that emulsion breakers may have functions that combine some of these proposed mechanisms, as the complexity of the demulsification mechanism is still not determined.

In W/O emulsions, natural surfactants present at the IF will result in local changes in the surface tension of dispersed water droplet. This is known as the *Marangoni effect* [5]. In this case, the resulting variation in the surface tension is concentration driven and thereby known as *solutecapillary effect* [31]. Consequently, rather strong convective motions may arise which further results in shear stress at the surface [32].

The draining film is located between two dispersed water droplets. At the surface of the draining film, the shear stress (tangential force) resulting from the convective motions can cause some of the natural surfactants to be displaced from the water droplet surface. It follows that the interfacial tension gradient ($\partial\sigma/\partial r$) is negative which reduces the droplets' ability to coalesce (see Figure 2.3) [32].
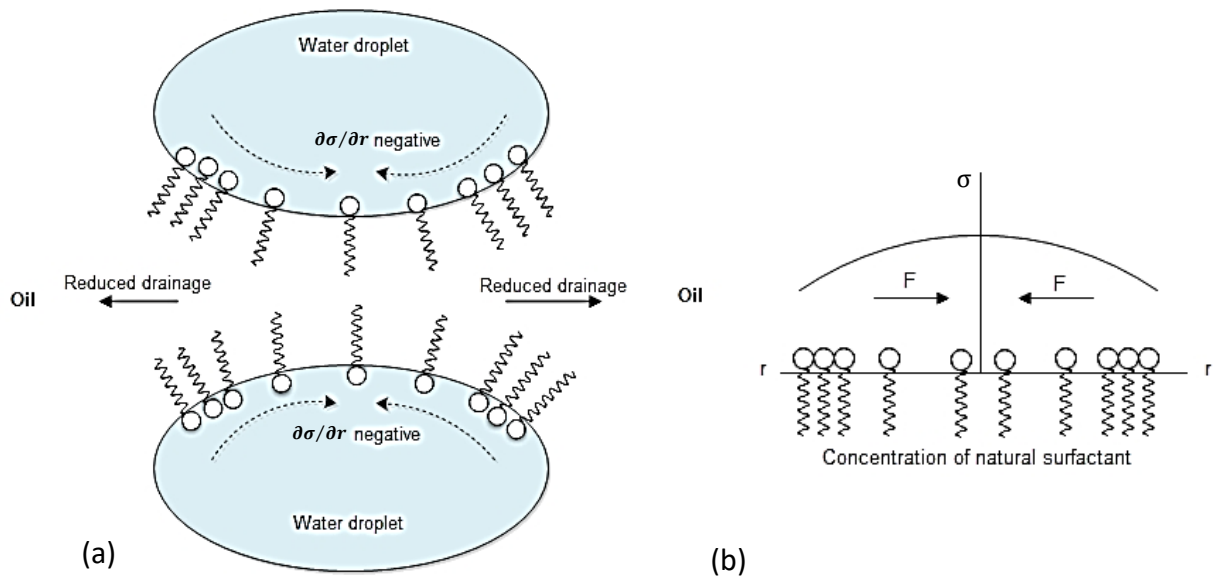
Figure 2. 3 (a) Effect of surface concentration of natural surfactants on film drainage where ∂σ/∂r is negative (where σ is the IFT and r is the radial position in the film). (b) Varying IFT with concentration of natural surfactant concentration within the draining film [32].

When the demulsifier molecules are added to the system, they occupy the vacant surface area of the interfacial film (see Figure 2.4).   As a result, the value of the interfacial tension gradient increases and becomes positive [32]. The tangential force is also reversed. Consequently, the surface mobility increases and the outflow of the interfacial film is enhanced substantially. This phenomenon is also known as *film thinning*, where the film between the water droplets become thinner thus closing the distance between them [11, 33]. The emulsion is thereby destabilized by the demulsifiers' counteraction of the interactions between the water drop and natural emulsifiers [34]. The demulsifiers further displace the native surfactants, advancing the film thinning process, and form a much less rigid and less stable layer at the interface [35, 36]. The interfacial tension (IFT) of the WO system should be reduced considerably below the IFT value of natural surfactants, for a demulsifier to be effective (see Figure 2.5) [11, 32, 37]. As such, dispersed phase is able to flocculate and coalesce.
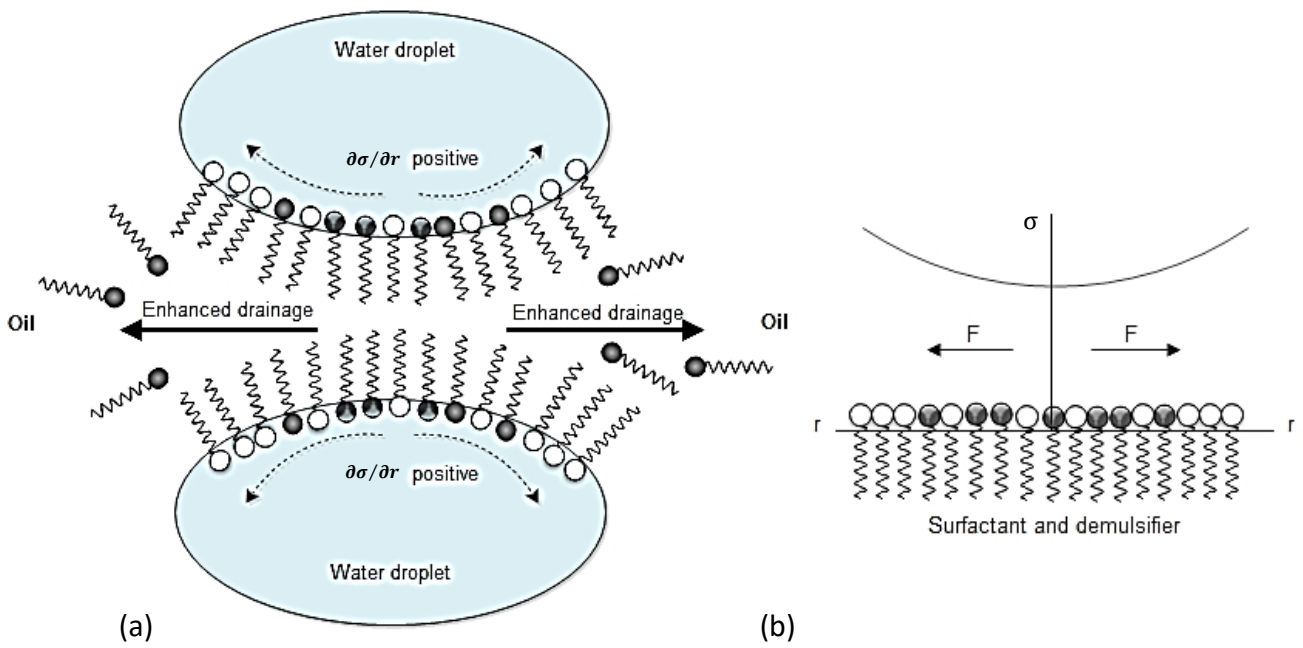
Figure 2. 4 (a) Enhanced film drainage when demulsifier molecules occupy free surface of the interface (giving a positive $\partial\sigma/\partial r$). (b) Effect on IFT by surface concentration of natural surfactants and demulsifiers within the draining film [32].
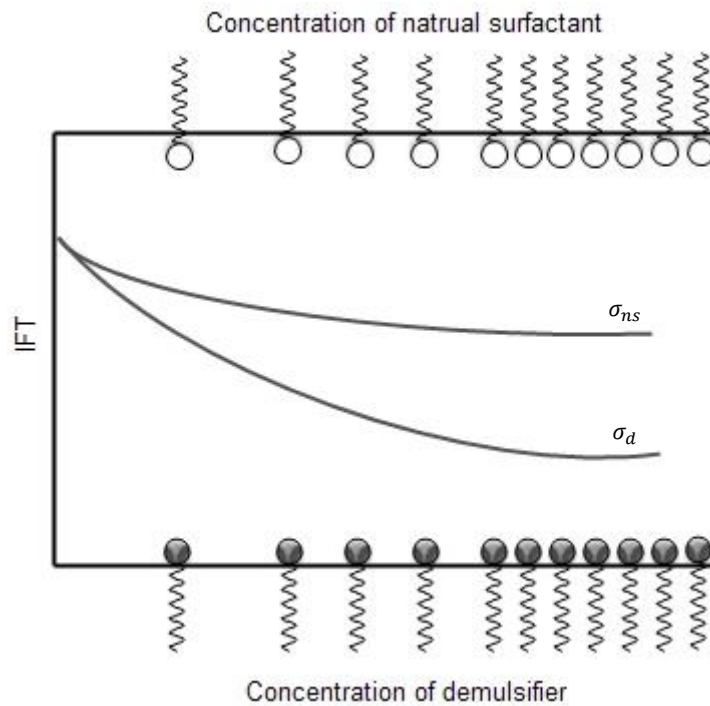
Figure 2. 5 Variation in IFT with surface concentration of natural surfactants (σ_{ns}) and demulsifiers (σ_d) [32].

2.2.3 Chemistry and Structure

The effect of different chemistry and structure on demulsification performance has been investigated extensively. The sections below will further expand on some of the main groups and some of the most common demulsifier components and precursors [38]:

1. Poly(alkylene oxide)s

Poly(alkylene oxide)s are often linearly structured, but also occur in branched structures. Their main polymer chain structure consists of an alkyl with an ether linkage. Poly(alkylene oxide)s are produced in a variety of copolymers, which can be random copolymers or block copolymers. Poly(alkylene oxide) block copolymers have been used for several studies for their surface active properties and have shown good demulsification abilities [39-41].

The process of ethoxylation and propoxylation are widely used in synthesis of emulsion breakers [39, 42-45]. An example of ethoxylation can be seen in Figure 2.6. Compounds that are suitable for such reaction include fatty alcohols, alkyl phenols, fatty amines, fatty acid esters or other chemical compounds containing a nucleophile [38]. Ethoxylation of fatty acids can be traced back to 1935 [22].
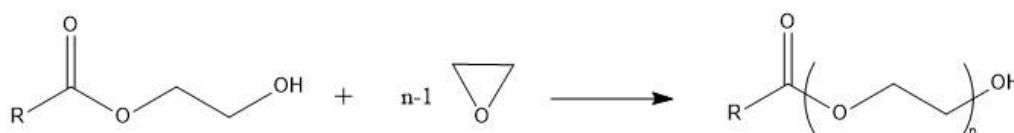
Figure 2. 6 Example of ethoxylation.

Poly(alkylene oxide)s are easily modified, thus the hydrophilic-lipophilic balance (HLB) and molecular weight can easily be varied [17]. The most used components of poly(alkylene oxide)s are ethylene oxide (EO) and propylene oxide (PO), and are generally used for treating W/O emulsions [46]. Vinyl monomers have been used to modify poly(alkylene oxide) block copolymers, in addition to diglycidyl ethers, dicarboxylic acids, di – and trimethylolphenol, poly(amine)s and others [17, 38, 47, 48]. A generic EO/PO block copolymer can be seen in Figure 2.7 [21].
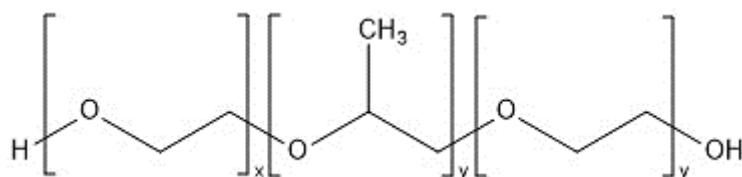
Figure 2. 7 Poly(ethylene glycol)-block-poly(propylene glycol)-block-poly(ethylene glycol) [21].

Al-Sabagh et al. observed the demulsification efficiency in ethoxylated and propoxylated 1,8-diaminooctanes with different degrees of esterification with stearic acid, ranging from monoesterified to tetraesterified [49]. The demulsification efficiency was shown to decrease with increased degree of esterification, where the monoesterified-ethoxylated product had the best performance (100% separation, 400 ppm, 30 min). The propoxylated products performed far below the ethoxylated products. The best propoxylated product, diesterified-propoxylated 1,8-diaminooctane, only reached 100% separation after 4 hours (1000 ppm).

2. Poly(amine)s

Poly(amine)s are usually linear or branched compounds with primary, secondary, or tertiary amino groups in the chain structure [20]. Poly(imine)s are also used without explicit differentiation, and are molecules containing a carbon-nitrogen double bond (=N−) [38]. Many of the smaller poly(amine)s can be alkoxylated, typically with EOs and POs, which achieves a more branched demulsifier molecule [17]. Some examples of polyethyleneamines can be seen in Figure 2.8. Poly(amine)s, like poly(alkylene oxide)s, have been reacted with aliphatic diglycidyl ethers to form polyhydroxyetheramines [50]. Additionally, poly(amine)s have been used particularly for breaking emulsions formed in oil bearing formations as a result of water/surfactant flooding in enhanced oil recovery (EOR) [50, 51].
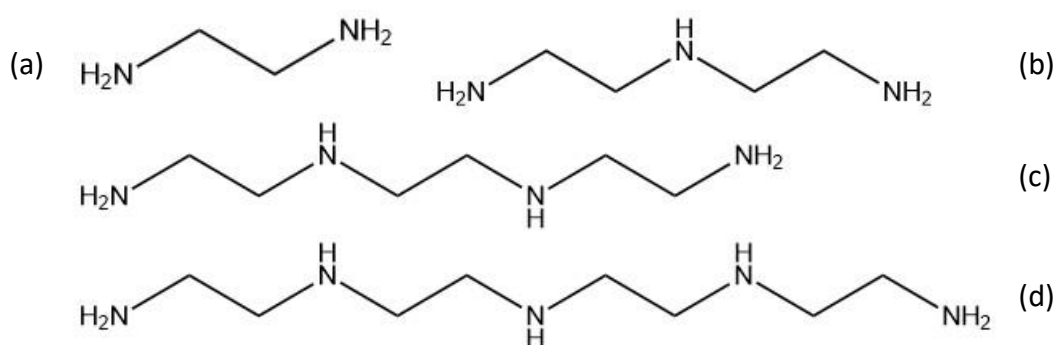
Figure 2. 8 Examples of polyethyleneamines: (a) ethylenediamine (EDA), (b) dietylenetriamine (DETA), (c) triethylenetetramine (TETA), and (d) tetraethylenepentamine (TEPA).

A.A. Abdel-Azim et al. studied various polyoxypropylenated-polyoxyethylenated amines including aliphatic, monocyclic amines with one or two amino groups, and bicyclic aromatic amines [52]. The monocyclic EO/PO amine substituted with two amino groups was found to perform better than the monocyclic EO/PO amine with one amine group. Having the same HLB, the bicyclic EO/PO amine proved to perform better than the monocyclic EO/PO amines. However, the bicyclic EO/PO amine only reached 100% separation efficiency after 24 hours (100 ppm).

3. Polysilicones

Triblock silicon polyethers have been reported to have good demulsification abilities even at low concentrations in crude oils that have different compositions and properties [46, 53]. A study done by D. Daniel-David et al. showed that poly(ethylene oxide)–poly(dimethylsiloxane)–poly(ethylene oxide) block copolymer (PEO-PDMS-PEO) outperformed poly(propylene oxide)–poly(dimethylsiloxane)–poly(propylene oxide) block copolymer (PPO-PDMS-PPO) [54]. See the general structure of PEO-polysiloxane in Figure 2.9.

The same general PEO-polysiloxane structure with four different triblock polymers were investigated as destabilizers of W/O emulsions by Le Follotec et al. [53]. The demulsifier structure can be seen in Figure 2.9, where the PEO units are connected to the central block of polydimethylsiloxane which constituted 13, 24, and 46 monomers. In the study, the longest hydrophobic chain was found to have the least effect (46 monomers), while the shorter hydrophobic chains were observed to be more effective (13 and 24 monomers).
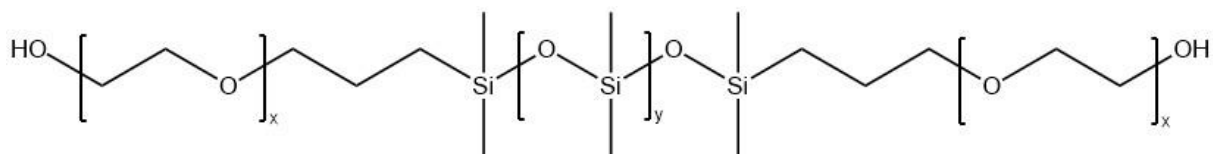
Figure 2. 9 Molecular structure of a siloxane demulsifier. y varied with 13, 24, and 46 monomers [51].

4. Dendrimers

Dendrimers are highly branched structures that often are spherical and symmetrical [55]. These chemicals are easily recognized by their well-defined structures reflecting complete branching and regularity [56]. The branches stretch from a central core and can contain several reactive terminal groups [57]. The terms *dendrimer* and *hyperbranched polymer* are often used interchangeably but should be distinguished. The structure for dendrimer is perfect for each generation, while hyperbranched polymers have imperfections in the branching. The typical structural differences between the two can be seen in Figure 2.10 [58]. The conditions used for preparation of hyperbranched polymers will often result in several related but different structures. Conversely, dendrimers are principally homogeneous products as they are synthesized one step at a time [55].

dendrimer   hyperbranched polymer
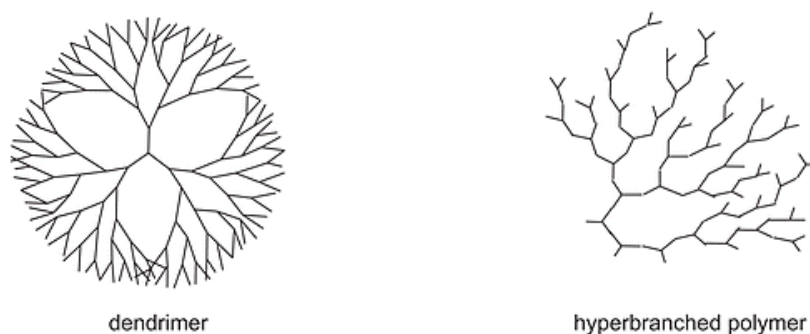
Figure 2. 10 Illustration of the structural differences between dendrimers and hyperbranched polymers [58].

Dendrimers have the advantage of being highly versatile, where the central core and terminal functional groups can be adapted and customized for purpose. The generation (G) of branches can also be controlled; thus, the molecular weight can easily be regulated.

The structural difference between dendrimers and conventional linear polymers is quite clear. However, significant differences are also found between the general properties (see Table 2.1) [59].

Table 2. 1 Different properties between dendrimers and linear polymers [59].

Properties	Dendrimer	Linear Polymer
Structure	Compact and Globular	Not compact
Shape	Spherical	Random coil
Architecture	Regular	Irregular
Synthesis	Stepwise growth	Single step poly condensation
Crystallinity	Non-crystalline and amorphous	Semi-crystalline/crystalline
Aqueous solubility	High	Low
Non-polar solubility	High	Low
Compressibility	Low	High

The effect of additional branches or generations was studied by Zhang et al [60]. The results showed a beneficial effect of additional branches in the demulsification performance in W/O emulsions (see Figure 2.12) [60]. The same principle has been investigated for polyamidoamine (PAMAM) dendrimers. The results showed that higher generation (G) PAMAMs demonstrated enhanced demulsification efficiency [61]. Wang et al. showed that G3 PAMAMs with amine terminal groups were superior to G2 and G1 PAMAMs (see Figure 2.11) [13]. The G3 PAMAM reached a demulsification ratio of 90% in 1 hour (30 ppm, 45°C). Moreover, Bi et al. studied G3 dendrimers with two different cores, namely 1,5-diamino-3-octyl-3-azapentane (octyl-G3) and 1,5-diamino-3-benzyl-3-azapentane (benzyl-G3) [62]. The studies revealed that octyl-G3 was superior to benzyl-G3 at lower concentrations (50 ppm) due to better interaction with the oil phase. Moreover, the two products had high separation efficiency (> 95%, 40 min).
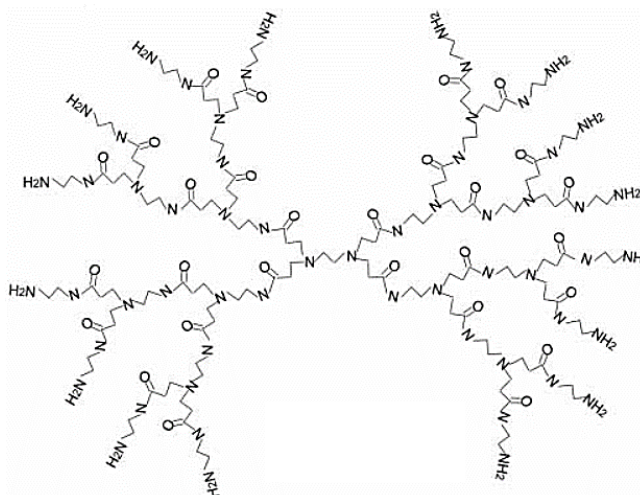
Figure 2. 11 Molecular structure of G3 PAMAM with amine terminal groups [13].

Dendrimers can also assume structurally complex shapes known as *star* structures [55]. Demulsification performance of various star dendrimer block copolymers were investigated by Z. Zhang et al. (see Figure 2.12) [60]. The star dendrimer had a water separation of 80% (60 min) in a heavier asphaltenic crude oil, which was higher than the amount of water separated by linear polymers tested.
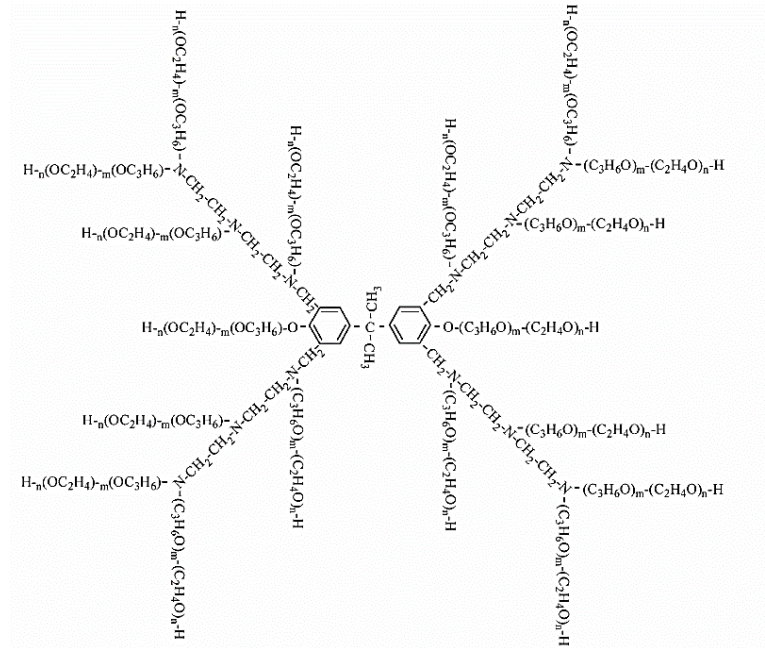
Figure 2. 12 Molecular structure of a star dendrimer (containing EO/PO blocks) [60].

2.3 Influential Demulsification Parameters

2.3.1 Effect of Alkyl Chain Length and Ratio

Abdurahman et al. tested various amines with different structures and length of alkyl chains. The results showed that decylamine performed the best in regard to demulsification efficiency, followed by octylamine, hexylamine, pentylamine, dioctylamine, trioctylamine, and propylamine, respectively [63]. Nevertheless, at a separation time of 85 minutes, the dehydration efficiency of decylamine was only 12%.

Al-Sabagh et al. studied three structures of 1,3,5-triethanolhexahydro-1,3,5-triazine that was ethoxylated with 20 EO units and modified by esterification of different ratios of oleic acid (1:1, 1:2 and 1:3) (see Figure 2.13) [64]. The results showed that the structure containing the highest ratio of oleic acid (1:3) had the best demulsification performance (80-96%, 100-500 ppm, 120 min).
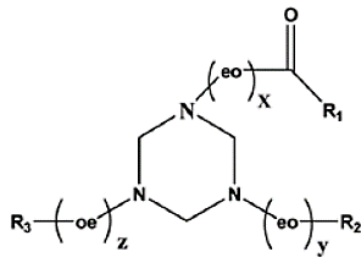
Figure 2. 13 Molecular structure of 1,3,5-triethanolhexahydro-1,3,5-triazine modified with EO units and oleic acid [64].

2.3.2 Effect of HLB and RSN

The hydrophilic-lipophilic balance (HLB) has been used extensively in relation to demulsifier characterization and performance [65-67]. Griffin (1949) described the affinity of a surfactant for water and oil, introducing a dimensionless numerical scale (0-20) [68]. A surfactant with an HLB < 10 is characterised as hydrophobic, while products with HLB > 10 are hydrophilic. Nevertheless, the HLB concept fails to consider variating factors such as temperature, salinity, and the nature of the hydrophilic group. Consequently and practically, the concept applies merely to non-ionic surfactants [69]. Additionally, the experimental method for deciding HLB values is complicated and expensive [11]. Therefore, the relative solubility number (RSN) is often used instead or additionally. The RSN builds on the same theory as the HLB. Higher values of RSN suggest hydrophilicity, while surfactants with lower values are hydrophobic [70]. The numerical scale used for definition of RSN in this thesis can be found in Section 3.2.3.

The HLB values for the products produced in this thesis were calculated by Griffins' equation (see Eq. 2.1) [45].

$$HLB = \frac{\%EO}{5} \qquad (2.1)$$

Zaki et al. studied the correlation between demulsifier performance and found that separation efficiency increases with increasing HLB [65]. Cooper et al. observed that demulsifiers with HLB values between 15-20 had the highest water separation [67]. Wu et al. observed optimum performance for products with RSN between 7.5 and 12.5 [70].

2.3.3 Effect of Dosage Concentration

The general findings of studies relating demulsifier performance to dosage concentration show that performance increases to a certain concentration until the separation rate stagnates [71]. Nevertheless, the effective or optimum dose will vary with the condition and contents of the emulsion. Accordingly, emulsions that are formed during chemical flooding (tertiary enhanced oil recovery, EOR) need substantially higher demulsifier concentration to resolved the emulsion than oil recovered by gas injection or water flooding [11].

2.3.4 Effect of Molecular Weight

There have been different findings and discussions of the effect of molecular weight on demulsification efficiency. Abdel-Azim argued that increasing molecular weight results in expansion of a surfactant's hydrodynamic size [72]. Thus, covering a larger surface area of the interface and displacing or excluding more emulsifier molecules. However, molecules with larger hydrodynamical size may diffuse slower through the interfacial film, which could affect the demulsification efficiency. Berger et al. also found results showing emulsion separation efficiency increasing with increasing molecular weight [73]. A study by Wu et al. revealed optimum demulsification performance for EO/PO block copolymers with molecular weight between 7500 and 15000 Da [70]. However, not enough data points were collected to make conclusions about for demulsifiers with molecular weight over 15000 Da. These results were also correlated to a specific range of RSN (see Section 2.3.2).

2.3.5 Effect of Temperature

With higher temperatures, the amount of Brownian motion will increase, alongside increased mass transfer across the IF [71]. Thus, a higher concentration of demulsifier molecules can be transported toward the IF, enhancing the demulsification performance. The viscosity (η) of the interface decreases with increasing temperature (T), following Vogel's equation (see Eq. 2.2) [74]. This phenomenon should enhance the coalescence of the dispersed phase and the number of droplet collisions will increase [11, 75].

$$\log_e(\eta) = e^{A + \frac{B}{T-C}} \qquad (2.2)$$

Where, A, B, and C are empirical constants.

Nevertheless, when testing a demulsifier product, it is important to consider the environment and temperature range of the oil fields for which the product is targeted for.

2.4 Green Demulsifiers

In the last two decades, the regulation and restriction of chemicals used in the petroleum industry has become progressively rigorous. As such, more and more chemicals are characterized as hazardous to the environment. All chemicals distributed within the EU must comply with ECHA's (European Chemical Agency) regulations within the guidelines of REACH (Regulation, Evaluation, Authorization and restriction of Chemicals) [76]. Thus, there is an increasing drive and need for development of new environmentally friendly oilfield chemicals that match the performance of existing chemicals. This implies that new "green" demulsifiers should have low toxicity and high biodegradability.

For toxicity testing of seawater species, *Skeletoma costatum* (algae, diatom) is one of the most commonly used species. The test duration is 96 hours and the cell count is monitored daily. The endpoint markers can vary with the scope of the test, but are typically changes in biomass, cell number, area underneath growth curve, and chlorophyll content [77]. The results are

often given as LC_{50} (half lethal concentration) or EC_{50} (half maximal effective concentration). Biodegradation is determined by the ratio of biochemical oxygen demand (BOD) to theoretical or chemical oxygen demand (ThOD or COD, respectively). The testing is generally performed according to the OECD 306 standard.

Polymeric alkoxylates are reported to have low toxicity, but EO/PO block copolymers often display low biodegradation due to high molecular weight [78]. However, PPO chains will degrade slower that PEO chains due to the additional methyl side group. Alkylphenol resins have good biodegradation, but may contain traces of toxic monomers or release these as they degrade [17]. Conversely, polyesters are known to have both low toxicity and high biodegradability [78]. Biodegradation is also observed in hyperbranched polymers and dendrimers. Leinweber et al. reported that alkoxylated dendritic polyesters exhibit enhanced biodegradation in respects to other conventional commercial demulsifiers [79]. As the dendrimer base, Leinweber et al. utilized Boltorn® H20 (16 terminal OH groups) and H310. In the same study, the highest value of biodegradation was measured to 45.7% and 62.5% in 14 and 28 days, respectively (in accordance with OCED 306).

Dalmazzone et al. performed a comprehensive study on various demulsifier chemicals in effort to find a chemical family that could be used as "green" or non-toxic emulsion breakers. After screening EO/PO block copolymers, alcohol derivatives, aromatic derivatives, silicone derivatives, and amine derivatives, the results showed that the polysiloxanes had the best separation efficiency (86%, 100ppm at 40°C) [25]. However, no conclusions were given concerning biodegradation. M. Phukan et al. reported a 10% improvement in biodegradation for a silicone polyether-co-caprolactone copolymer (18% biodegradation, day 28) compared to a silicone polyether (8% biodegradation, day 28) [80]. Yet, this may still be considered too low according to today's standards (≥60%) [17].

In demulsifier formulations, solvents are generally used to enhance compatibility and temperature stability. Solvents such as xylene, toluene, methanol, butyl diglycyl ether (BDGE), and ethylene glycol monobutyl ether (EGMBE) are often used [81]. Nevertheless, some of these are not characterized as environmentally friendly.

2.5   References

1. L.L. Schramm, ed. *Emulsions: Fundamentals and Applications in the Petroleum Industry*. 1992, ACS Publications: U.S.A.
2. P.K. Kilpatrick, *Water-in-Crude Oil Emulsion Stabilization: Review and Unanswered Questions.* Energy & Fuels, 2012. **26**(7): p. 4017-4026.
3. M.J. Rosen and J.T. Kunjappu, *Surfactants and Interfacial Phenomena*. 4th ed. 2012, U.S.A, New Jersey: John Wiley & Sons.
4. F. Leal-Calderon, V. Schmitt, and J. Bibette, *Emulsion Science: Basic Principles*. 2007: Springer Science & Business Media.
5. G.T. Barnes and I.R. Gentle, *Interfacial Science: An Introduction*. 2nd ed. 2011, U.S.A, New York: Oxford University Press.
6. S.L. Kokal, *Crude Oil Emulsions: A State-of-the-Art Review.* SPE Production & Facilities, 2005. **20**(1): p. 5-13.
7. A.M. Alsabagh, et al., *Demulsification of W/O emulsion at petroleum field and reservoir conditions using some demulsifiers based on polyethylene and propylene oxides.* Egyptian Journal of Petroleum, 2016. **25**(4): p. 585-595.
8. T. Ichikawa, *Electrical Demulsification of Oil-in-Water Emulsion.* Colloids and Surfaces A: Physicochemical and Engineering Aspects, 2007. **302**(1-3): p. 581-586.
9. G. Ye, et al., *Application of Ultrasound on Crude Oil Pretreatment.* Chemical Engineering and Processing: Process Intensification, 2008. **47**(12): p. 2346-2350.
10. N.H. Abdurahman, et al., *The Potential of Microwave Heating in Separating Water-in-Oil (W/O) Emulsions.* Energy Procedia, 2017. **138**: p. 1023-1028.
11. R. Zolfaghari, et al., *Demulsification Techniques of Water-in-Oil and Oil-in-Water Emulsions in Petroleum Industry.* Separation and Purification Technology, 2016. **170**: p. 377-407.
12. J. Hou, et al., *Understanding Interfacial Behavior of Ethylcellulose at the Water–Diluted Bitumen Interface.* Energy & Fuels, 2012. **26**(3): p. 1740-1745.
13. J. Wang, et al., *Demulsification of Crude Oil Emulsion Using Polyamidoamine Dendrimers.* Separation Science and Technology, 2007. **42**(9): p. 2111-2120.
14. A.M. Al-Sabagh, N.G. Kandile, and M.R. Noor El-Din, *Functions of Demulsifiers in the Petroleum Industry.* Separation Science and Technology, 2011. **46**(7): p. 1144-1163.
15. C.W. Angle, *Chemical Demulsification of Stable Crude Oil and Bitumen Emulsions in Petroleum Recovery — A Review*. 2001, Marcel Dekker: New York, U.S.A. p. 541-594.
16. J. Djuve, et al., *Chemical Destabilization of Crude Oil Based Emulsions and Asphaltene Stabilized Emulsions.* Colloid and Polymer Science, 2001. **279**(3): p. 232-239.
17. M.A. Kelland, *Production Chemicals for The Oil and Gas Industry*. 2nd ed. 2014: CRC Press.
18. L.L. Schramm, *Emulsions, Foams, and Suspensions: Fundamentals and Applications*. 2005, Germany: John Wiley & Sons.
19. L.L. Schramm, ed. *Surfactants: Fundamentals and Applications in the Petroleum Industry*. 2000, Cambridge University Press: Cambridge, UK.
20. J. Fink, *Oil Field Chemicals*. 2003, Burlington, U.S.A: GPP, Elsevier Science.
21. C.M. Ojinnaka, et al., *Formulation of Best-fit Hydrophile/Lipophile Balance - Dielectric Permittivity Demulsifiers for Treatment of Crude Oil Emulsions.* Egyptian Journal of Petroleum, 2016. **25**(4): p. 565-574.
22. P. Jacques, et al., *Alkylphenol Based Demulsifier Resins and Their Continued Use in the Offshore Oil and Gas Industry*, in *Chemistry in the Oil Industry VII: Performance in a Challenging Environment*, T. Balson, et al., Editors. 2002, The Royal Society of Chemistry: Cambridge, UK.
23. R.M. Hill, *Silicone Polymers for Foam Control and Demulsification*. Silicone Surfactants. Vol. 86. 1999, New York, U.S.A: Marcel Dekker.

24.   K. Othmer, *Encyclopedia of Chemical Technology*. 3rd ed. Vol. 8. 1981, New York, U.S.A: Wiley-Interscience Publication.

25.   C. Dalmazzone and C. Noïk, *Development of New "green" Demulsifiers for Oil Production*, in *SPE International Symposium on Oilfield Chemistry*. 2001, Society of Petroleum Engineers: Houston, Texas.

26.   G. Leopold, *Breaking Produced-Fluid and Process-Stream Emulsions*, in *Emulsions: Fundamentals and Applications in the Oil Industry*, L.L. Schramm, Editor. 1992, ACS Publications: DC, U.S.A. p. 341.

27.   H. Celius et. al, *Separation Mechanisms and Fluid Flow in Oil/Water*, in *Oil Field Chemicals, 7th International Symposium*. 1996: Geilo, Norway.

28.   E. Pensini, et al., *Demulsification Mechanism of Asphaltene-Stabilized Water-in-Oil Emulsions by a Polymeric Ethylene Oxide–Propylene Oxide Demulsifier.* Energy & Fuels, 2014. **28**(11): p. 6760-6771.

29.   L.Y. Zhang, Z. Xu, and J.H. Masliyah, *Langmuir and Langmuir– Blodgett Films of Mixed Asphaltene and a Demulsifier.* Langmuir, 2003. **19**(23): p. 9730-9741.

30.   S. Simon, et al., *Relation Between Solution and Interfacial Properties of Asphaltene Aggregates.* Energy & Fuels, 2008. **23**(1): p. 306-313.

31.   Comsol Multiphysics Cyclopedia. *The Marangoni Effect*. 2018 21.02.2017 [cited 2018 10.06]; Available from: https://www.comsol.com/multiphysics/marangoni-effect.

32.   S. Hartland and S.A.K. Jeelani, *Effect of Interfacial Tension Gradients on Emulsion Stability.* Colloids and Surfaces A: Physicochemical and Engineering Aspects, 1994. **88**(2): p. 289-302.

33.   W. Kang, et al., *Influence of Demulsifier on Interfacial Film Between Oil and Water.* Colloids and Surfaces A: Physicochemical and Engineering Aspects, 2006. **272**(1): p. 27-31.

34.   J.B.V. Ramalho, F.C. Lechuga, and E.F. Lucas, *Effect of the Structure of Commercial Poly (Ethylene Oxide-b-Propylene Oxide) Demulsifier Bases on the Demulsification of Water-in-Crude Oil Emulsions: Elucidation of the Demulsification Mechanism.* Quimica Nova, 2010. **33**(8): p. 1664-1670.

35.   S. Kokal, *Crude Oil Emulsions: A State-Of-The-Art Review*, in *SPE Annual Technical Conference and Exhibition*. 2002, Society of Petroleum Engineers: San Antonio, Texas.

36.   K. Salam, et al., *Improving the Demulsification Process of Heavy Crude Oil Emulsion Through Blending with Diluent.* Journal of Petroleum Engineering, 2013. **2013**: p. 1-6.

37.   D. Nguyen, N. Sadeghi, and C. Houston, *Chemical Interactions and Demulsifier Characteristics for Enhanced Oil Recovery Applications.* Energy & Fuels, 2012. **26**(5): p. 2742-2750.

38.   J. Fink, *Petroleum Engineer's Guide to Oil Field Chemicals and Fluids*. 2nd ed. 2015, U.S.A: GPP, Elsevier Science.

39.   P. Alexandridis, *Poly(Ethylene Oxide)/Poly(Propylene Oxide) Block Copolymer Surfactants.* Current Opinion in Colloid & Interface Science, 1997. **2**(5): p. 478-489.

40.   P. Ramírez, et al., *Interfacial Rheology and Conformations of Triblock Copolymers Adsorbed onto the Water–Oil Interface.* Journal of Colloid and Interface Science, 2012. **378**(1): p. 135-143.

41.   G. Cendejas, et al., *Demulsifying Super-heavy Crude Oil with Bifunctionalized Block Copolymers.* Fuel, 2013. **103**: p. 356-363.

42.   A.M. Al-Sabagh, et al., *Investigation of the Demulsification Efficiency of Some Ethoxylated Polyalkylphenol Formaldehydes Based on Locally Obtained Materials to Resolve Water-in-Oil Emulsions.* Journal of Dispersion Science and Technology, 2009. **30**(2): p. 267-276.

43.   A.M. Al-Sabagh, et al., *Demulsification of W/O Emulsion at Petroleum Field and Reservoir Conditions Using Some Demulsifiers Based on Polyethylene and Propylene Oxides.* Egyptian Journal of Petroleum, 2016. **25**(4): p. 585-595.

44.   J. Wu, et al., *Effect of EO and PO Positions in Nonionic Surfactants on Surfactant Properties and Demulsification Performance.* Colloids and Surfaces A: Physicochemical and Engineering Aspects, 2005. **252**(1): p. 79-85.

45. A.M. Al-Sabagh, N.E. Maysour, and M.R. Noor El-Din, *Investigate the Demulsification Efficiency of Some Novel Demulsifiers in Relation to Their Surface Active Properties.* Journal of Dispersion Science and Technology, 2007. **28**(4): p. 547-555.

46. F. Shehzad, et al., *Polymeric Surfactants and Emerging Alternatives used in the Demulsification of Produced Water: A Review.* Polymer Reviews, 2018. **58**(1): p. 63-101.

47. R.S. Buriks and J.G. Dolan, *Demulsifier Composition and Method of Use Thereof*, in *Google Patents*. 1986: US Patent 4 626 379, U.S.A.

48. R.S. Buriks and J.G. Dolan, *Demulsifier Composition and Method of Use Thereof*, in *Google Patents*. 1988: EP Patent 268 713, U.S.A.

49. A.M. Al-Sabagh, et al., *Demulsification Efficiency of Some New Stearate Esters of Ethoxylated and Propoxylated 1,8-Diamino-Octane for Water in Crude Oil Emulsions.* Journal of Dispersion Science and Technology, 2013. **34**(10): p. 1409-1420.

50. D.S. Treybig, D.A. Williams, and K.T. Chang, *Novel demulsifiers, Their Preparation and Use in Oil Bearing Formations*, in *Google Patents*. 2003, Ondeo Nalco Energy Services, L.P.: WO Patent 2003053536A1, U.S.A.

51. C.W. Burkhardt, *Use of Polyamines as Demulsifiers*, in *Google Patents*. 1983, Baker Hughes Inc.: US Patent 4 411 814, U.S.A.

52. A.A. Abdel-Azim, N.N. Zaki, and N.E.-S. Maysour, *Polyoxyalkylenated Amines for Breaking Water-in-Oil Emulsions: Effect of Structural Variations on the Demulsification Efficiency.* Polymers for Advanced Technologies, 1998. **9**(2): p. 159-166.

53. A. Le Follotec, et al., *Triblock Copolymers as Destabilizers of Water-in-Crude Oil Emulsions.* Colloids and Surfaces A: Physicochemical and Engineering Aspects, 2010. **365**(1): p. 162-170.

54. D. Daniel-David, et al., *Elastic Properties of Crude Oil/Water Interface in Presence of Polymeric Emulsion Breakers.* Colloids and Surfaces A: Physicochemical and Engineering Aspects, 2005. **270**: p. 257-262.

55. C.E. Carraher Jr., *Introduction to Polymer Chemistry*. 2007, U.S.A, New York: CRC Press.

56. A. Lederer and W. Burchard, *Hyperbranched Polymers: Macromolecules in between Deterministic Linear Chains and Dendrimer Structures*. RSC Polymer Chemistry Series. 2015: Royal Society of Chemistry.

57. J. Wang, et al., *Synthesis of Dendritic Polyether Surfactants for Demulsification.* Separation and Purification Technology, 2010. **73**(3): p. 349-354.

58. A. Lederer and W. Burchard. *Regularity of Branching and Branching Topologies [Figure]*. 2015 [cited 2018 21.05]; Available from: http://pubs.rsc.org/en/content/chapterhtml/2015/9781782622468-00001?isbn=978-1-78262-246-8.

59. S. Choudhary, et al., *Impact of Dendrimers on Solubility of Hydrophobic Drug Molecules.* Frontiers in Pharmacology, 2017. **8**(261).

60. Z. Zhang, et al., *Demulsification by Amphiphilic Dendrimer Copolymers.* Journal of Colloid and Interface Science, 2005. **282**(1): p. 1-4.

61. M. Yanez Arteta, R.A. Campbell, and T. Nylander, *Adsorption of Mixtures of Poly(amidoamine) Dendrimers and Sodium Dodecyl Sulfate at the Air–Water Interface.* Langmuir, 2014. **30**(20): p. 5817-5828.

62. Y. Bi, et al., *Dendrimer-Based Demulsifiers for Polymer Flooding Oil-in-Water Emulsions.* Energy & Fuels, 2017. **31**(5): p. 5395-5401.

63. H.N. Abdurahman, R.M. Yunus, and Z. Jemaat, *Chemical Demulsification of Water-in-Crude Oil Emulsions.* Journal of Applied Sciences, 2007. **7**(2): p. 196-201.

64. A.M. Al-Sabagh, et al., *Demulsification Efficiency of Some New Demulsifiers Based on 1,3,5-Triethanolhexahydro-1,3,5-triazine.* Journal of Dispersion Science and Technology, 2014. **35**(10): p. 1361-1368.

65. N.N. Zaki, M.E. Abdel-Raouf, and A.-A.A. Abdel-Azim, *Propylene Oxide-Ethylene Oxide Block Copolymers as Demulsifiers for Water-in-Oil Emulsions, I. Effect of Molecular Weight and*

Hydrophilic-Lipophylic Balance on the Demulsification Efficiency. Monatshefte für Chemie / Chemical Monthly, 1996. **127**(6): p. 621-629.

66.   C.S. Shetty, et al., *Demulsification of Water in Oil Emulsions Using Water Soluble Demulsifiers.* Journal of Dispersion Science and Technology, 1992. **13**(2): p. 121-133.

67.   D.G. Cooper, et al., *The Relevance of "HLB" to De-emulsification of a Mixture of Heavy Oil, Water and Clay.* The Canadian Journal of Chemical Engineering, 1980. **58**(5): p. 576-579.

68.   W.C. Griffin, *Classification of Surface-Active Agents by HLB.* J. Soc. Cosmet. Chem., 1949. **1**: p. 311-326.

69.   M. Rondón, et al., *Breaking of Water-in-Crude Oil Emulsions. 1. Physicochemical Phenomenology of Demulsifier Action.* Energy & fuels, 2006. **20**(4): p. 1600-1604.

70.   J. Wu, et al., *Effect of Demulsifier Properties on Destabilization of Water-in-Oil Emulsion.* Energy & fuels, 2003. **17**(6): p. 1554-1559.

71.   V.K. Rajak, et al., *Optimization of Separation of Oil from Oil-in-Water Emulsion by Demulsification Using Different Demulsifiers.* Petroleum Science and Technology, 2016. **34**(11-12): p. 1026-1032.

72.   A.-A.A. Abdel-Azim, *Excluded Volume and Hydrodynamic Properties of Polystyrene in Non-Ideal Solvents.* Polymer Bulletin, 1993. **30**(5): p. 579-586.

73.   P.D. Berger, C. Hsu, and J.P. Arendell, *Designing and Selecting Demulsifiers for Optimum Field Performance on the Basis of Production Fluid Characteristics.* 1988.

74.   C.J. Seeton, *Viscosity–Temperature Correlation for Liquids.* Tribology Letters, 2006. **22**(1): p. 67-78.

75.   R.A. Mohammed, et al., *Dewatering of Crude Oil Emulsions 3. Emulsion Resolution by Chemical Means.* Colloids and Surfaces A: Physicochemical and Engineering Aspects, 1994. **83**(3): p. 261-271.

76.   European Chemical Agency. *REACH.* 2017 [cited 2018 13.06]; Available from: https://echa.europa.eu/regulations/reach/understanding-reach.

77.   W. Landis, et al., *Introduction to Environmental Toxicology: Impacts of Chemicals upon Ecological Systems.* 3rd ed. 2005, New York, U.S.A: CRC Press.

78.   A. Kaiser, *Environmentally Friendly Emulsion Breakers: Vision or Reality?*, in *SPE International Symposium on Oilfield Chemistry.* 2013, Society of Petroleum Engineers: The Woodlands, Texas, USA.

79.   D. Leinweber, et al., *Alkoxylated Dendrimers and Use Thereof as Biodegradable Demulsifiers*, in *Google Patents.* 2009: US Patent 0100002 A1, U.S.A.

80.   M. Phukan, et al., *Biodegradable Polyorganosiloxane Demulsifier Composition and Method for Making the Same*, in *Google Patents.* 2012, Momentive Performance Materials Inc: US Patent 0329887 A1, U.S.A.

81.   H. Zhou, et al., *Development of More Environmentally Friendly Demulsifiers*, in *SPE International Symposium and Exhibition on Formation Damage Control.* 2012, Society of Petroleum Engineers: Lafayette, Louisiana, USA.

3 Experimental

3.1 General

3.1.1 Staring materials

Starting material Boltorn® H311 was supplied by Perstorp Specialty Chemicals AB, and four different surfactants (starting materials A, B, C, and D) were provided by Kao Chemicals GmbH. These are ether carboxylic derivatives with PEO units and an aliphatic alkyl R group. Boltorn H311 is described as a hydroxyl-functional dendritic polyester. The dendrimer is reported by Perstorp to have 23 terminal hydroxyl groups. Dodecylbenzenesulfonic acid (DDBSA) was used as catalyst and was supplied by Unger Fabrikker AS. All the materials used in the synthesis were viscous liquids. The starting materials are presented in Table 3.1 and their physical properties can be found in Table 3.2. The molecular weights of starting materials A, B, C, and D were determined utilizing ChemDraw Professional 17.0 (see Appendix B).

Table 3. 1 Starting materials for synthesis of demulsifier products.

STARTING MATERIALS						
Name	Chemical name	Structure	Activity	M_w [g/mole]	EO units (n)	R group
Boltorn H311	Dendritic Polyol/Polyester	-	90%	5700.0	-	-
Starting material A	Laureth-4 Carboxylic Acid	$HO_2CCH_2[OCH_2CH_2]_nOR$	> 92.5%	368.535	2.5	C_{12} / C_{14}
Starting material B	Laureth-11 Carboxylic Acid	$HO_2CCH_2[OCH_2CH_2]_nOR$	90 %	698.935	10	C_{12} / C_{14}
Starting material C	Oleth-3 Carboxylic Acid	$HO_2CCH_2[OCH_2CH_2]_nOR$	> 94%	402.615	2	C_{16} / C_{18}
Starting material D	Oleth-10 Carboxylic Acid	$HO_2CCH_2[OCH_2CH_2]_nOR$	> 89.1%	710.985	9	C_{16} / C_{18}
DDBSA	Dodecylbbenzene-sulfonic Acid	$RC_6H_4SO_3H$	97%	326.50	-	C_{12}

Table 3. 2 Physical properties for starting materials. (a) Dynamic viscosity, (b) measured at 45°C. Melting point (MP), boiling point (BP), flash point (FP), partition coefficient in octanol/water ($P_{O/W}$).

	Boltorn H311	Starting material A	Starting material B	Starting material C	Starting material D	DDBSA
PHYSICAL PROPERTIES						
MP [°C]	NA	15	0 – 5	< -10	0	0 – 10
BP [°C]	NA	NA	NA	NA	NA	>185
FP [°C]	>150	>100 (Open cup)	>100 (Open cup)	>100 (Open cup)	>100 (Closed cup)	197 – 207
pH (20°C)	NA	2.0 – 3.5 (1% w/w)	1.5 – 3.5 (10% w/w)	1.0 – 3.0 (1% w/w)	1.5 – 3.0 (10% w/w)	1.5 (10 g/L)
Density (20°C) [g/cm^3]	1.16	0.98	1.05	0.95	1.031	-
Viscosity [a] (20°C) [cP]	NA	200	500	200	120 [b]	2000
log $P_{O/W}$	>5.2	NA	NA	NA	NA	3.2 – 3.3

3.1.2   Experimental equipment

3.1.2.1   Spectroscopy and spectrometry

IR spectra were recorded on an attenuated total reflection (ATR) ALPHA FT-IR Spectrometer from Bruker. The samples were analysed neat and the absorption frequencies are given in wavenumbers, v (cm^{-1}). Intensities are given as transmittance (%).

NMR 400 MHz ^{1}H NMR and 100 MHz ^{13}C NMR spectra were recorded on a Bruker Advanced series 400 MHz spectrometer. NMR chemical shifts were recorded as δ values in parts per million (ppm) using deuterated chloroform (CDCl$_3$) with tetramethylsilane (TMS) as solvent, where TMS (δ = 0.0 ppm) functions as the internal standard for ^{1}H and ^{13}C NMR. Samples of 0.05 g were dissolved in 0.6 mL CDCl$_3$ (with TMS).

3.1.2.2   Chromatography

GPC were performed on an Agilent 1260 Infinity II GPC/SEC system. The columns used for the analyses were two series coupled organic columns, packed with PLgel – MIXED-D (5 µm, 300×75 mm, Series No. PL1110-6504) provided by Agilent Technologies. Organic solvent tetrahydrofuran, stabilized with butylated hydroxytoluene (BHT) (0.2224g/L), was used as eluent and sample solvent. The starting materials were analysed as 1% solutions. The

demulsifier products were prepared as 2% solutions. The GPC instrument was pre-calibrated according to Agilent's Narrow polydispersity EasiVial polymer standards (polyethylene glycol, PEG).

3.1.3   Methods of Analysis

pH Measurements were performed utilizing a WTW inoLab pH Level 1 pH-meter (Series No. 03420044). The pH measurements were determined in organic solvent (1% in 50:50 isopropanol:deionized water). A two-point calibration was performed before measurements and at each 10th measurement, using buffers of pH 7 and 4.

Density measurements were performed in agreement to standard ASTM D 891-09 and ASTM D 4052-11 [1, 2]. Determination of density was completed utilizing a pycnometer. The density was determined according to Eq. 3.1.

$$\rho = \frac{W_T - W_B}{V} \tag{3.1}$$

Where, ρ is the density, W_T is the total weight of the bottle and stopper filled with chemical, W_B is the weight of the empty, dry bottle and stopper, and V is the volume of the bottle (10.477 cm^3).

Solubility was measured in deionized water (1%), Solvesso 150 ND (20%), and butyl diglycol ether (BDGE, 30%).

Analytical balances used in experiments were KERN 572 (Series No. W051321) and Sartorius TE214S.

3.2   Experimental procedures

3.2.1   Synthesis

The synthesis of the demulsifier products was performed in a two-step procedure. In the first stage, water was removed from Boltorn H311 using vacuum distillation. In the second stage, Boltorn H311 was reacted with one of the four starting materials through Fisher Esterification, catalysed by DDBSA. Table 3.3 shows an overview of the products synthesised in this thesis.

Figure 3. 1 Experimental setup.

Table 3. 3 Presentation of the products, and the amounts used in the syntheses.

Starting materials	Product number	Coverage	Equivalences	Moles Boltorn H311	Moles Starting material	Moles DDBSA	$m_{Boltorn\ H311}$ [g]	$m_{Starting\ material}$ [g]	m_{DDBSA} [g]	Reaction time [hours]
Boltorn H311 + Starting material A	1	50%	11,5	0.01585	0.1823	0.01456	100.4	64.6	4.9	5.50
	2	70%	16,1	0.01587	0.2555	0.01693	100.5	90.6	5.7	4.50
	3	90%	20,7	0.01582	0.3275	0.01931	100.2	116.4	6.5	7.75
	4	100%	23	0.01584	0.3642	0.02020	100.3	129.3	6.8	5.25
Boltorn H311 + Starting material B	5	50%	11,5	0.01592	0.1830	0.02020	100.8	126.9	6.8	8.25
	6	70%	16,1	0.01584	0.2550	0.02466	100.3	177.7	8.3	8.25
	7	90%	20,7	0.01579	0.3268	0.02911	100.0	228.4	9.8	8.00
	8	100%	23	0.01581	0.3635	0.03149	100.1	253.8	10.6	8.00
Boltorn H311 + Starting material C	9	50%	11,5	0.01582	0.1819	0.01545	100.2	73.1	5.2	8.00
	10	70%	16,1	0.01585	0.2552	0.01812	100.4	104.5	6.1	6.50
	11	90%	20,7	0.01584	0.3278	0.02050	100.3	131.6	6.9	7.00
	12	100%	23	0.01581	0.3635	0.02198	100.1	146.2	7.4	7.00
Boltorn H311 + Starting material D	13	50%	11,5	0.01585	0.1823	0.02020	100.4	129.1	6.8	7.25
	14	70%	16,1	0.01737	0.2796	0.02733	110.0	199.0	9.2	7.25
	15	90%	20,7	0.01582	0.3275	0.02941	100.2	232.8	9.9	8.00
	16	100%	23	0.01584	0.3642	0.03179	100.3	258.7	10.7	7.75

3.2.1.1 Vacuum distillation (Step One)

Boltorn H311 (100.4 g, 0.01585 mol) was weighed out on an analytical balance and charged to a three-neck round bottom flask. See Figure 3.2 for setup scheme. Following, Boltorn H311 was stirred while heating to 120°C in a nitrogenous (N_2) atmosphere (approximately 9 torr). Vacuum was carefully applied as the system reached the set temperature (120°C), and the N_2-gas flow was turned off. As the boiling activity settled, the RPM of the magnetic stirrer was increased from 250 to 500. The vacuum distillation continued until there was no more water coming off the system. At this point, the collected water was weighed on an analytical balance (5.39 g).
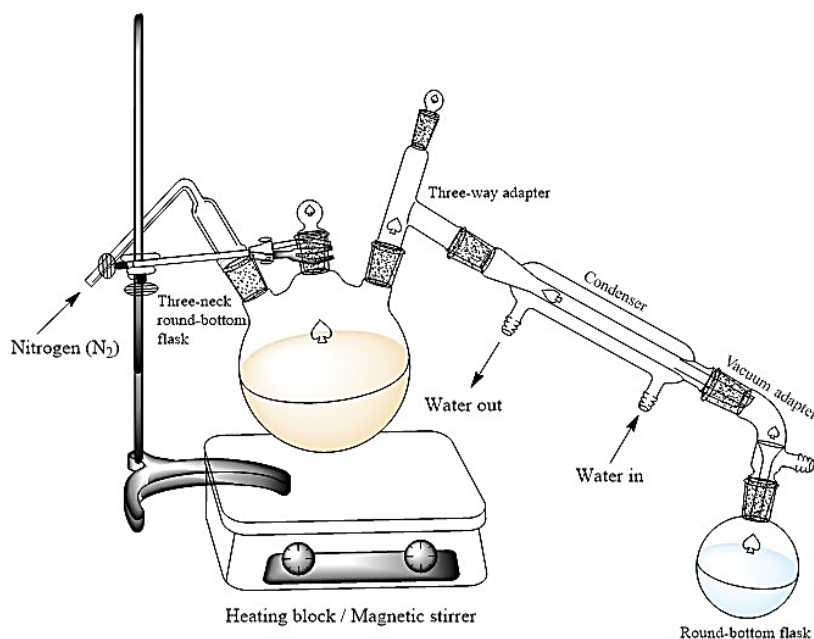
Figure 3. 2 Vacuum distillation setup for drying of Boltorn H311 (with N2 atmosphere).

3.2.1.2 Polyesterification of Boltorn H311 (Step Two)

The dried Boltorn H311 (prepared in step one) was heated to 100°C. Laureth-4 carboxylic acid (64.6 g, 0.1823 mol) was weighed out on an analytical balance and charged to the three-neck flask containing the dried Boltorn H311, at 100°C. The system was then heated to 150°C in a N_2-atmosphere. Once the temperature was reached and a homogeneous mixture observed, N_2-gas flow was turned off and vacuum was gradually applied to the system. Simultaneously, the DDBSA (4.9 g, 0.01456 mol) catalyst was added at a rate of 1 drop per 1-5 seconds, utilizing a pressure-equalizing addition funnel (see Figure 3.3). The addition rate was adjusted according to the degree of boiling activity and bumping. Overall, the catalyst had an addition time of 20 minutes. The collector flask was placed in an ice-bath with 1 tbs of sodium chloride. The acid number (AN) was analysed as a method of monitoring the progression of the reaction. The first AN (see Section 3.2.2) was analysed 2-3 hours after catalyst addition. A series of ANs were analysed until the numbers were declining by less than two units. The AN (5.1 for product **1**) was preferable < 10 when the reaction was considered finished.
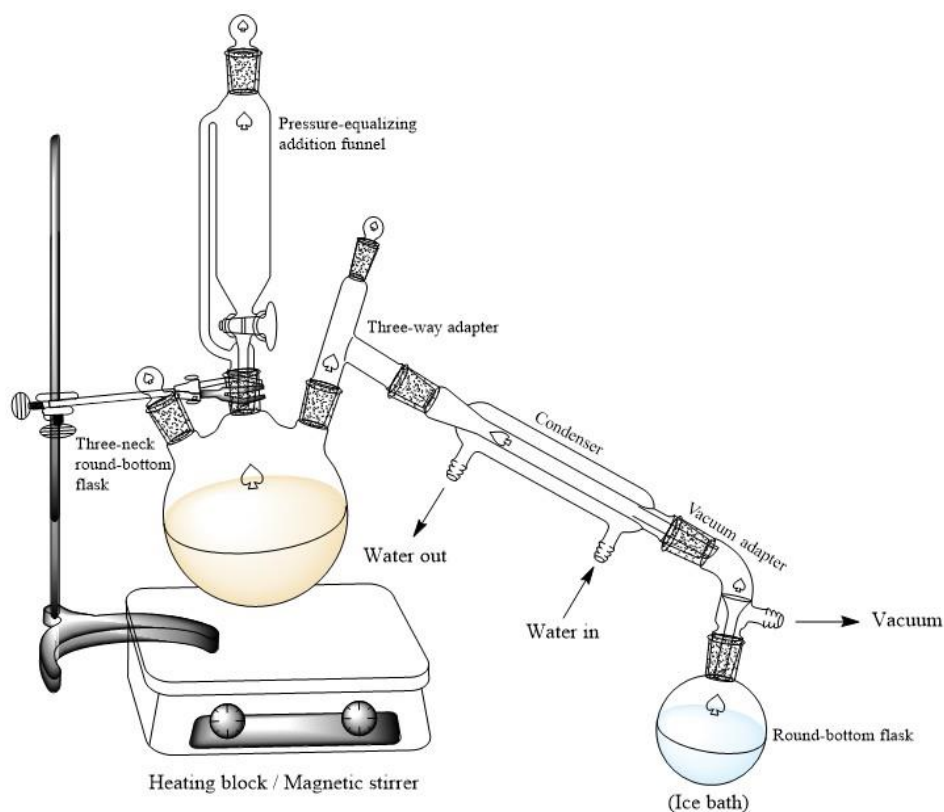
Figure 3. 3 Vacuum distillation setup for polyesterification of Boltorn H311.

3.2.2 Acid Number

The acid number (AN) procedure was performed in accordance with ASTM D974 [3]. To determine the AN, a sample were taken of the product and weighed utilizing an analytical balance. The sample was dissolved in xylene (50 mL) in a beaker (100 mL) and thoroughly mixed using a magnetic stirrer. The sample was then titrated with a 0.1 M methanolic potassium hydroxide (KOH) solution, utilizing a pipette (5 mL). A 0.9% phenolphthalein (in ethanol) solution was used as colour-indicator. For phenolphthalein, the endpoint was marked by the first colour change, clear to pink. At the end point, the volume of titrant was noted used in the calculation of the AN (see Eq. 3.2). Due to health risks, the samples were dissolved in xylene and not toluene as the ASTM D974 states. Phenolphthalein was used as indicator instead of p-naphtholbenzein, as stated in ASTM D974.

$$AN = \frac{V \cdot 56.1 \cdot 0.1}{m} \tag{3.2}$$

Where, V is the volume of titrant in mL and m is the mass of the sample in grams. ANs are given as unitless values.

3.2.3   Relative Solubility Number

This experimental method for determining relative solubility number (RSN) is based on the method developed by D.E. Williams and C.F. Meredith. However, this novel method removes the need to use benzene/dioxane. Dimethyl isosorbide (DMI, 75% w/w), butyldiglycol ether (BDGE, 20% w/w) and xylene (5% w/w) were used instead. The sample was weighed out to 1.0 g in a conical flask (100 mL), where the exact weight was recorded. Thereafter, xylene (1.5 g) and DMI (4.5 g) were added to the flask and stirred until the sample was completely dissolved. DMI (18.0 g) and BDGE (6.0 g) were added to the flask and stirred for another 5 minutes. Afterwards, the sample solution was titrated with distilled water until the solution became turbid (persistent for at least 1 minute). At this point, the volume of titrant was recorded. The results were evaluated according to:

RSN < 13 indicates water insolubility

RSN 13-17 indicates water dispersibility

RSN > 17 indicates water solubility

3.2.4   Demulsifier Performance Testing by Bottle Test

3.2.4.1   Preparation of Crude Oil 1-3

The synthesised products were tested in three different crude oils; crude oil 1, crude oil 2, and crude oil 3. The crude oil samples were sourced from three different producing fields – 2 in the North Sea and one in the South Atlantic Ocean. The exact origins of the crude oils cannot be disclosed in this thesis. The fields are known to have problems with emulsions. The crude oil samples 1-3 were heated to 70°C in a heating cabinet overnight before use.

3.2.4.2   Bottle Test

The synthetic W/O emulsion prepared for the testing, had a 30% water cut which consisted of 3% sodium chloride (NaCl) in distilled water. The preparation of the emulsions was done by utilizing a triple Hamilton Beach HMD400 3-Speed mixer (Series No. H0551L) at room temperature at 13 000 RPM. The emulsions for the crude oil samples 1, 2, and 3 were prepared by mixing the oil and water for 30-37, 45, and 10 seconds, respectively.

The water separation process was observed over a 30-minute time frame (i.e. 5, 10, 20, and 30 minutes) at a test temperature of 60°C, with a time extension to 60 minutes for additional observation. The demulsifier products were tested on dosages 40 and 80 ppm in crude oil 1. In crude oil 2 and 3, the products were only dosed at 80 ppm. Microsyringes were used for addition of demulsifier products (4 and 8 μL). The maximum of tests run at a time was eight samples. After the demulsifier products were added to the eight torpedo flasks containing the emulsion, the flasks were strapped into a rack and shaken 50 times with medium intensity (see Figure 3.4). Following, the flasks were placed in a water bath (60°C) (see Figure 3.5). The demulsifier performance was documented with water separation measurements and pictures following the time frame. The water separation measurements were converted to percent in

the results. Additionally, quality data was recorded including water quality, oil quality, and quality of the WO interface were recorded.

Figure 3. 4 Torpedo flasks in rack used for demulsifier testing.

Figure 3. 5 Bottles placed in water bath (60°C).

3.2.4.3   Basic Sediment and Water of Crude Oil Measurements by Centrifuge

Composite thief analysis and "top cut" thief analyses were performed to determine the level of dehydration of the crude oil. At times 10 and 30 minutes, thieving samples were taken just above the expected water separation line, using a 10 mL Socorex 173 syringe with a flat ended leur lock needle. The crude oil sample and xylene were charged to centrifuge tubes in a ratio of 1:1. Basic sediment and water (BS&W) measurements were recorded after 5 minutes of centrifugation at 2500 RPM (60°C), in accordance to standards ASTM D4007-81 and I.P. 359:1982 [4]. Following, another emulsion breaker was added to the centrifuge tubes to resolve any residual emulsion. The tubes were then again centrifuged under the same conditions and the total water content was determined.

3.2.5 Interfacial Tension Measurements

Interfacial tension (IFT) measurements were performed according to ASTM D1331-14, Method B [5]. For the measurements, a KVS Sigma 700 Tensiometer was used with a maximum load of 880 mN/m and maximum resolution 0.0003 mN/m. The probe used was a Du Noüy ring. Measurements were done for the 90% coverage product range (product **3**, **7**, **11**, and **15**) Additionally, a commercial product and a sample of product **3** made up with 10% additional starting material B, were also tested. The IFT for the samples was determined at dosage of 10 to 100 ppm of 0.5% w/w solutions, where the concentration was increased gradually 10 ppm at a time.

3.2.6 Ecotoxicology and Biodegradation Testing

Ecotoxicology and biodegradation testing were performed by Schlumberger Ecotox Laboratory in Bergen. Ecotoxicity and biodegradation testing were done in accordance with EC_{50} (half maximal effective concentration) of *Skeletoma costatum* and OECD 306, respectively.

The test duration for ecotoxicity testing is 96 hours where the photoperiod usually is defined by 14 hours of light and 10 hours in the dark. For seawater species, a start concentration of $2 \cdot 10^4$ cells/mL is used in the test vessel and the cell count is monitored daily.

Biodegradation is defined as the ratio of the biochemical oxygen demand to either, the theoretical oxygen demand (ThOD) or the chemical oxygen demand (COD) (see Eq. 3.3 and 3.4, respectively). ThOD is preferably used, as some chemicals are not fully oxidized in COD tests. The biodegradation was recorded as %biodegradation in 28 days. Some products were recorded on day 29 (products **5**, **7**, **8** and **16**).

$$Biodegradation\ (\%) = \frac{mg\ O_2/mg\ tested\ substance}{mg\ ThOD/mg\ tested\ substance} \cdot 100 \ = \ \frac{BOD}{ThOD} \cdot 100 \qquad (3.3)$$

$$Biodegradation\ (\%) = \frac{mg\ O_2/mg\ tested\ substance}{mg\ COD/mg\ tested\ substance} \cdot 100 \ = \ \frac{BOD}{COD} \cdot 100 \qquad (3.4)$$

COD is determined experimentally, while ThOD is calculated theoretically. An example of ThOD calculation can be seen in Eq. 3.5.

$$Glucose\ C_c H_h O_o (C_6 H_{12} O_6), M_w = 180$$

$$ThOD = \frac{16(2c + \frac{1}{2}h - o)}{M_w} \qquad (3.5)$$

3.3   References

1.   D. ASTM, *891-95. Standard test method for specific gravity, apparent, of liquid industrial chemicals*, in *ASTM International*. 2003: West Conshohocken, PA, U.S.A.

2.   D. ASTM, *4052-11, Standard Test Method for Density, Relative Density, and API Gravity of Liquids by Digital Density Meter*. ASTM International: West Conshohocken, PA, U.S.A.

3.   ASTM D974-14e2, *Standard Test Method for Acid and Base Number by Color-Indicator Titration*. 2014, ASTM International: West Conshohocken, PA, U.S.A.

4.   A. D4007-81(1995)e1, *Standard Test Method for Water and Sediment in Crude Oil by the Centrifuge Method (Laboratory Procedure)*. 1995, ASTM International: West Conshohocken, PA, U.S.A.

5.   ASTM, *D1331-14, Standard Test Methods for Surface and Interfacial Tension of Solutions of Paints, Solvents, Solutions of Surface-Active Agents, and Related Materials.* 2014, ASTM International: West Conshohocken, PA, U.S.A.

4   Results and Discussion

4.1   Synthesis

The aim of this synthesis was to produce a range of new demulsifier chemicals that were based on the reaction between Boltorn H311 and four different alkyl ether carboxylic acids. A general scheme was used as the initial guideline (see Figure 4.1). The dendrimer products were designed to be amphiphilic compounds with hydrophilic ethoxylated blocks and hydrophobic polyester dendrimer cores. The products should have a strong affinity for adsorbing at the interface water droplets in W/O emulsions. Thereby, the products will destabilize the interface and promote coalescence. An illustration of a generalized product can be seen in Figure 4.2.
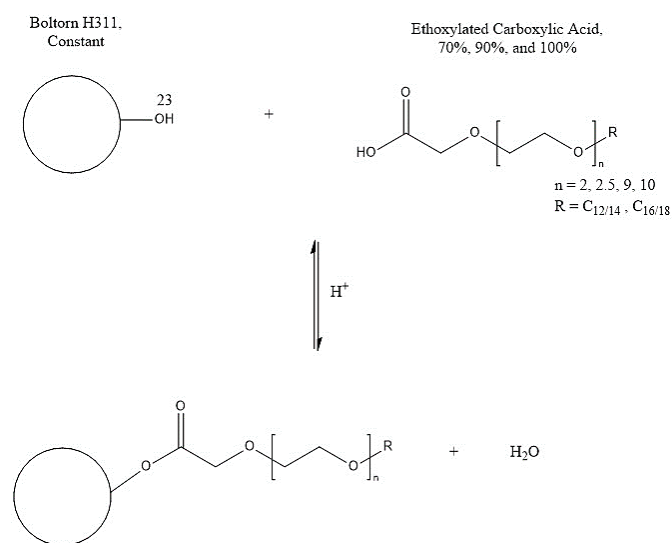
Figure 4. 1 General scheme of synthesis plan.
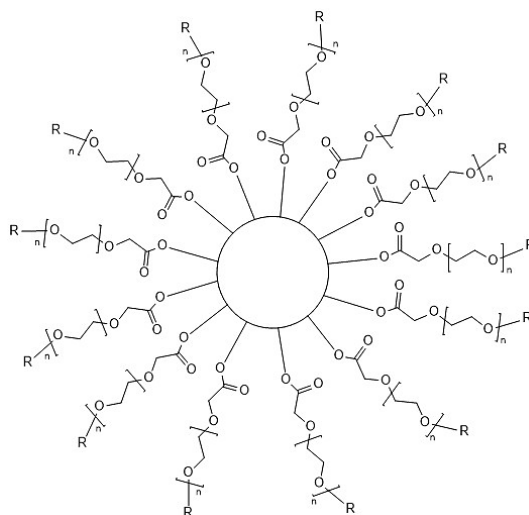
Figure 4. 2 Illustration of synthesized product.

4.1.1 Design of Experiments – Selection of starting materials

For statistical analysis and prediction of best products, the experimental design and analysis program Design-Expert® 11 form Stat-Ease Inc. was utilized. The program facilitates comparative testing, characterization, and optimization among other functions [1]. The program was primarily used for design purposes, highlighting tendencies, and for experimental optimization in this work.

The Design-Expert® program was used to optimize the experimental design and identify the four different ether carboxylic derivatives that were used for synthesis of demulsifier products. The chemicals were selected for their chemical and structural characteristics. More precisely, the carbon chain length of the R group and number of EO units were deciding factors. According to results generated by Design-Expert®, the four starting materials had combinations of longer (+) and shorter (-) carbon chains (R), and higher (+) and lower (-) number of EO units (see Table 4.1).

Table 4. 1 Summarized model of selected starting materials.

Starting material	EO units	R chain length
A	-	-
B	+	-
C	-	+
D	+	+

4.1.2 Optimization

A number of different factors were optimized to improve consistency during synthesis. These factors were considered to generate a robust procedure for the synthesis:

- Ratio of starting materials (coverage)
- Starting material activity
- Procedure
- Monitoring of reaction progress

For the scale of the reaction, it was chosen to use 100g Boltorn H311. The amount of individuals product produced ranged from approximately 170 to 360g. One important factor under consideration was the amount of the surface of the dendrimer which would be covered by functional groups. Initially the syntheses were targeted for a narrower range of coverage range 70, 90, and 100%. The coverage was an important factor in deciding the dendrimer size, in addition to the amount of residual starting material (A-D). During the initial experiments with 70-100% coverage, it was observed that the products were very similar by GPC. Thus, to

obtain a wider range of products with larger structural and physical properties, the coverage range was increased to 50, 70, 90, and 100%.

In the initial syntheses, the activity of the starting materials (A-D) were included in the calculations of the ratios. The activity ranged from 89.1 to 94% (see Table 3.1 in Section 3.1.1). However, the products of these syntheses had too large amounts of residual starting material, which was confirmed by GPC. As a result, activity of the starting materials were not included in the calculations, for products **1**-**16**. The products were found to have lower amounts of unreacted starting material because of this measure.

The reaction mechanism used in synthesis of the products was Fisher esterification. The general mechanism of the reaction is presented in Figure 4.3. Product formation in this synthesis was promoted by removal of water, with respect to the equilibrium. Hence, two methods were evaluated for the syntheses. Dehydration by Dean-stark method was first used in the synthesis. The method worked well for esterification and product formation, though the high BP solvents (xylene and toluene) were found difficult to remove from the products. The second method triald was to carrie out the procedure without solvent, i.e. under "neat" conditions. The process was thereby split into two steps. Step one was to remove the water from Boltorn H311 to give a more controlled reaction, in step two of the synthesis. The duration of the step one distillation was increased from initially 1 hour to approximately 3-4 hours, reducing the boiling activity in step two considerably. Furthermore, the addition time of the DDBSA catalyst became more consistent as the addition did not have to be interrupted or paused because of high boiling activity.
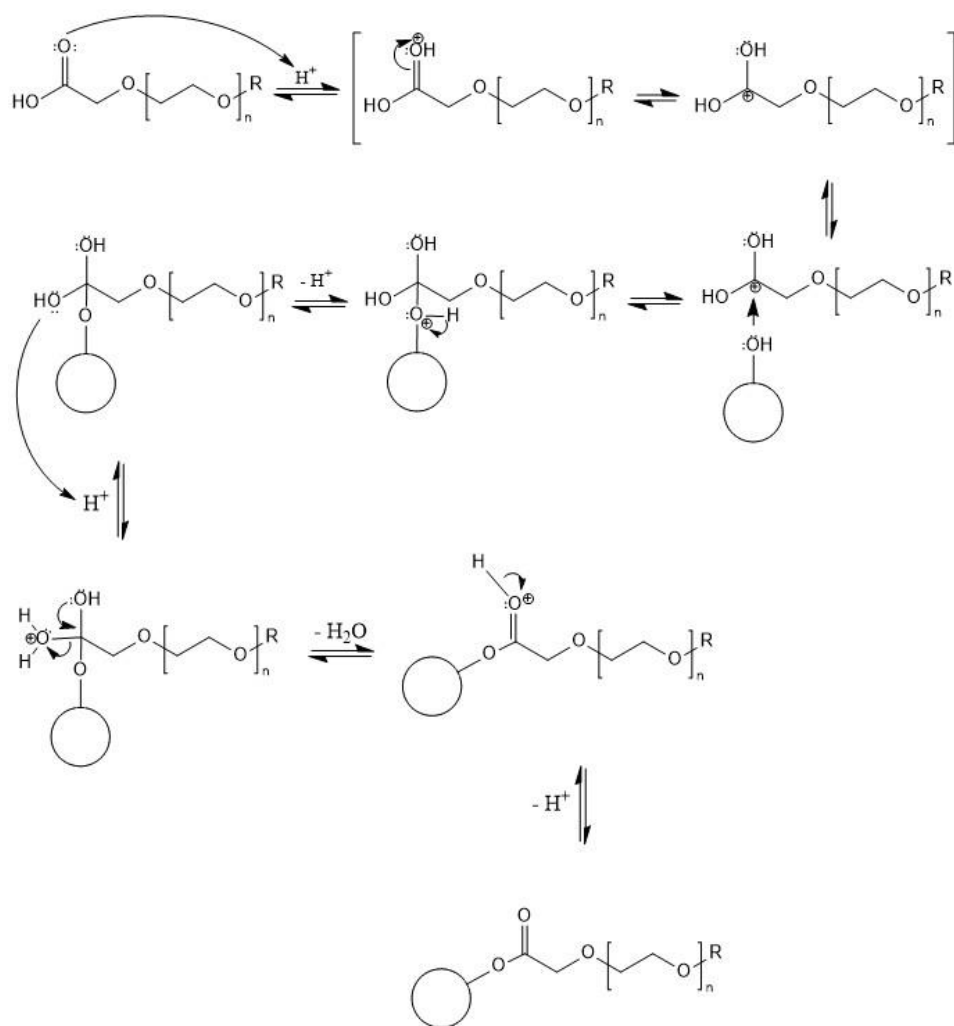
Figure 4. 3 General reaction mechanism for synthesis performed in this thesis.

The monitoring of the reaction progress was performed by acid number (AN) titrations. The AN gave an indication of the amount of unreacted acid (residual starting material) left and decreased over the course of the reaction. The AN was measured three to six times where the last AN was recorded when the decline was less than one unit. The AN was preferably below the value of 10 when the reaction was considered completed. The synthesis was initially performed with a set reaction time of approximately 4 hours. However, higher coverage products demanded longer reaction times to reach an AN < 10. Thus, the reaction time was essentially controlled by the value of the AN. The amount of distilled water was collected and recorded when there were no more water droplets left in the condenser. However, in some instances, some of the water had been extracted from the water collector flask due to strong vacuum. Thus, this method of monitoring was not considered reliable but was used as an indication of the reaction progress. The ANs and amount of collected water during syntheses are reported in Appendix A. GPC was also considered as a method of monitoring progress.

However, the method was too time consuming, requiring 40 minutes for each test run. In contrast, the AN was measured in a matter of minutes.

The molecular weights of the starting materials (A-D) were calculated using ChemDraw Professional 17. As can be seen in Appendix B, starting materials A-D are polymeric mixtures. Starting material A has four components, while starting material B, C, and D have two components. The molecular weight of the components were determined, and an average of these were used as the final molecular weight of the respective starting material.

4.2 Analytical Results

4.2.1 Gel Permeation Chromatography

Gel permeation chromatography (GPC) is a type of size exclusion chromatography [2]. This technique is particularly useful for the analysis of high molecular weight molecules and polymers. The separation and retention time depends on the effective hydrodynamic size of the analyte molecules [3].

The products, Boltorn H311, and starting materials (A-D) were analysed by GPC. Parameters such as molecular weight, polydispersity (PD), retention time, and area of the peaks were of most importance. The overview of the GPC data is reported in Table 4.2. The data was summarized from Cirrus GPC Narrow Standard Reports. The GPC results were used for the purpose of analyses where the products were compared to the starting materials.

An example of a GPC comparison of starting materials and product **3** is presented in Figure 4.4. The major peak of product **3** at approximately 19 min retention time (RT) has shifted to the left as compared to Boltorn H311. As such, the product has a larger molecular weight (11 132 g/mol, from GPC) than Boltorn H311 (5700 g/mol), which indicates that the reaction was successful.

The minor peak on product **3** at approximately 22.5 min RT overlaps with the peak for starting material A. This confirms that some residual starting material was present at the end of the reaction. No other new peaks were observed, indicating no other bi-products were formed.
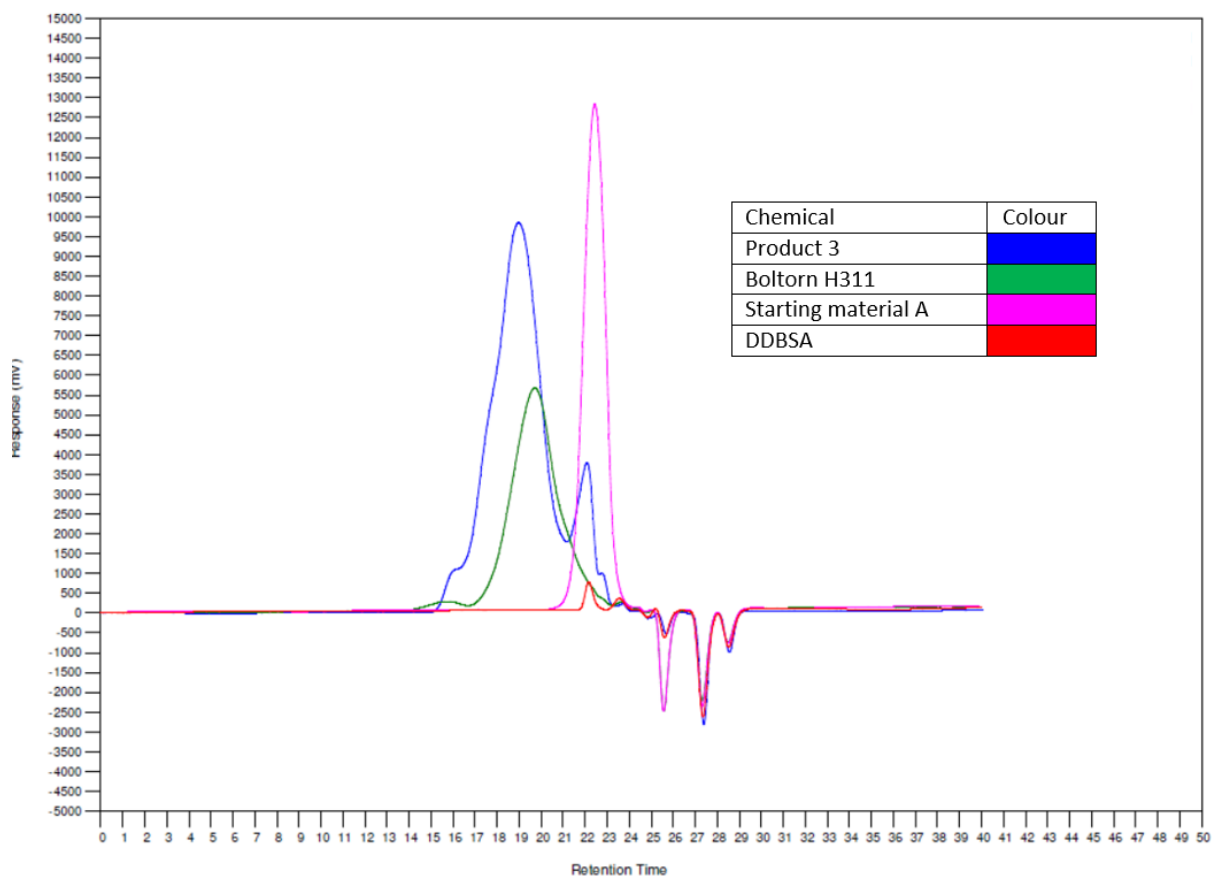
Figure 4. 4 GPC results of comparison between product range **1-4**.

In Figure 4.5, the relation between unreacted (residual) starting materials with increasing coverage for products **1**-**4** is presented. As the percent coverage increased, the area of the second peak (amount of residual) was expected to increase. This trend was clearly observed for product ranges **1**-**4**, **9**-**12,** and **13**-**16**. However, for products **5**-**8** there are much smaller differences in the residual peak area so the trend is not at clearly followed, and any descrepencies are within the margin of error.
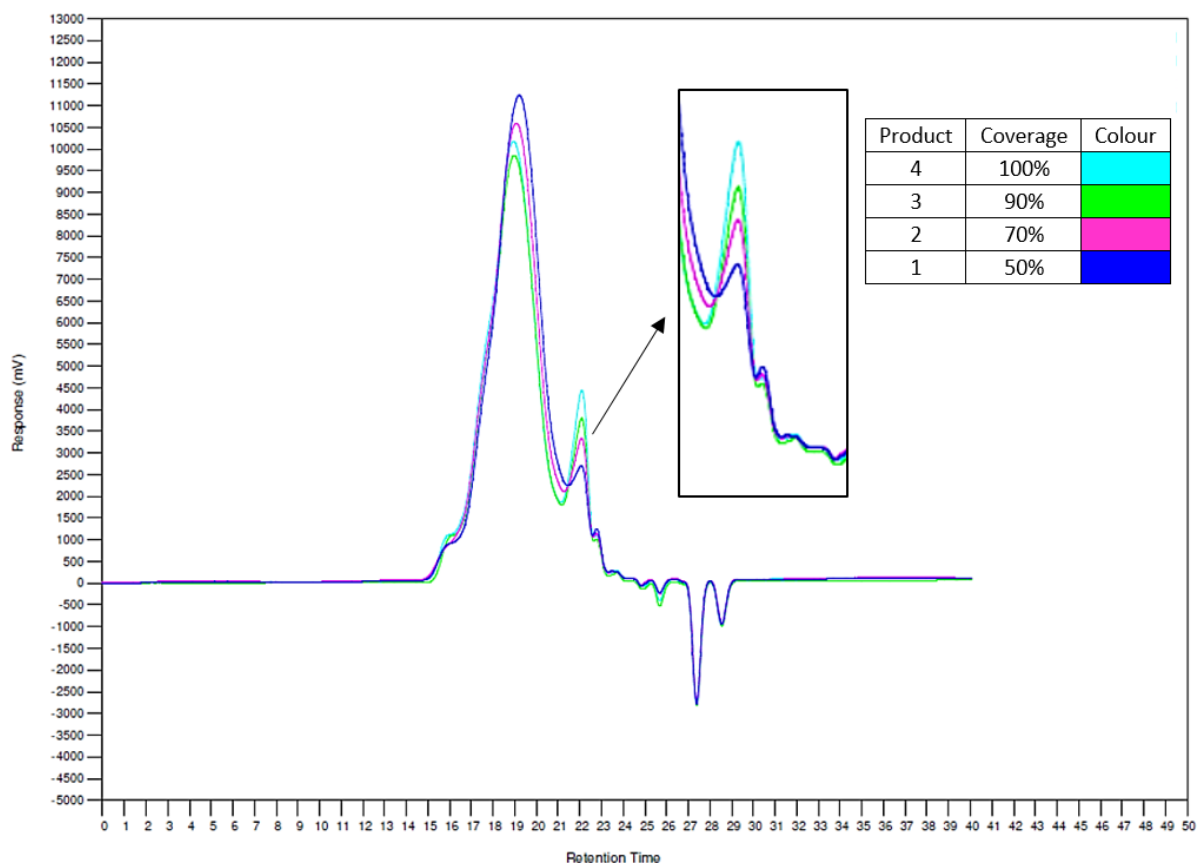
Figure 4. 5 GPC results of comparison between products **1**-**4** for residual starting material (A).

The polydispersity (PD) was reported to be > 1.2 and < 2.0 for all the products. The products were thereby determined to have a *medium* polydispersity. The products (**5**-**8** and **13**-**16**) having higher numbers of EO units, were found to have slightly lower PDs between 1.3 and 1.5. The products (**1**-**4** and **9**-**12**) having lower numbers of EO units were found to have slightly higher PD between 1.8 and 2.0.

The results of the molecular weights are relative to the PEG standards, and not absolute. The molecular weights were expected to increase with increasing percent coverage, as the added ratios of starting material were increased with increasing coverage. Results obtained by GPC generally coincided with the expected trend.

The trend was observed for products synthesised with starting materials A, B, and C (products **1**-**4**, **5**-**8**, and **13**-**16**). The molecular weight of products **5**-**8** and **13**-**16** increased from 8453 to 9363 g/mol and from 8801 to 9051 g/mol, respectively. However, these products had the

largest deviations from the theoretical molecular weights. The products were found to have the lowest molecular weight by GPC, while the opposite was expected as they had the highest degree of ethoxylation and the longest carbon chain lengths in the R group.

Product **9** was found to not be consistent with the expected trend. This product had the lowest coverage (50%) of its range, were reported to have the second highest molecular weight (in its range). On this basis, the GPC results could not be used to define the molecular weight of the products for comparison purposes.

The GPC analyses of the products proved to lack sensitivity to accurately distinguish between the small changes in dendrimer size, in addition to the amount of residual. This was hampered by overlapping peaks and the polydisperse nature of these products. The GPC spectra for the product range (**1**-**16**) can be found in Appendix C.

Table 4. 2 Overview of GPC data.

Starting materials	Product number	Coverage	M_w [g/mol]	$M_{w,Theoretical}$ [g/mol]	PD	RT_{min} [min]	RT_{max} [min]	ΔRT [min]	Area Peak 1 [%]	Area Peak 2 [%]	Area Peak 3 [%]
Boltorn H311 + Starting material A	1	50%	9882	9938.2	1.92	14.61	19.17	4.56	90.96	7.61	1.43
	2	70%	10 788	11633.4	1.90	14.57	19.04	4.47	88.38	10.28	1.34
	3	90%	11 132	13328.7	1.84	14.77	18.94	4.17	86.46	12.38	1.16
	4	100%	11 563	14176.3	1.85	14.73	18.90	4.17	85.31	13.61	1.08
Boltorn H311 + Starting material B	5	50%	8453	13737.8	1.45	16.32	18.08	1.76	86.43	13.57	-
	6	70%	8909	16952.9	1.40	15.97	18.01	2.04	86.78	13.22	-
	7	90%	9012	20168.0	1.33	16.61	18.01	1.40	83.44	16.56	-
	8	100%	9363	21775.5	1.33	16.63	17.97	1.34	83.43	16.57	-
Boltorn H311 + Starting material C	9	50%	11 371	10330.1	1.92	14.38	19.10	4.72	83.86	11.91	4.23
	10	70%	10 013	12182.1	1.78	14.61	19.12	4.51	79.61	15.73	4.66
	11	90%	12 088	14034.1	1.82	14.49	18.89	4.40	77.29	18.51	4.20
	12	100%	13 852	14960.1	1.91	14.36	18.83	4.47	76.43	19.91	3.66
Boltorn H311 + Starting material D	13	50%	8801	13876.3	1.47	15.97	18.99	3.02	85.84	14.16	-
	14	70%	8488	17146.9	1.37	16.41	19.06	2.65	83.08	16.92	-
	15	90%	8822	20417.4	1.32	16.60	18.99	2.39	79.98	20.02	-
	16	100%	9051	22052.7	1.32	16.34	18.96	2.62	78.47	21.53	-

4.2.2 IR

The IR spectroscopy provides a direct method of detecting functional groups in a molecule and gives details of the molecular structure [3]. IR spectra of the full range of products (**1**-**16**), in addition to the starting materials, are reported in Appendix D. The IR spectra were used to help confirm the formation of the products. An example is displayed in Figure 4.6, where product **3** was evaluated against Boltorn H311 and starting material A.
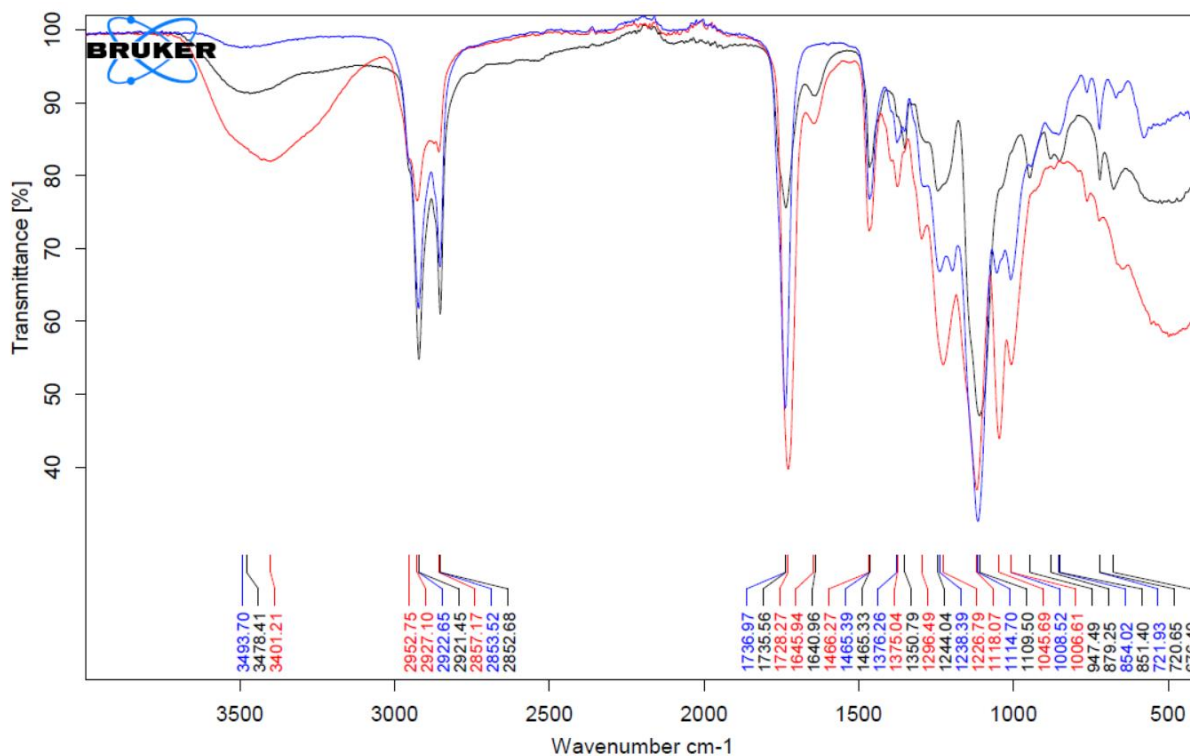
Figure 4. 6 IR spectra comparison between product **3** (blue line), starting material A (black line), and Boltorn H311 (red line).

The main peaks found in Figure 4.6 are reported in Table 4.3. The main areas of interest are found between 1600-1800 cm^{-1} and 3200-3600 cm^{-1}, which correspond to the absorbance of carbonyl and hydroxyl, respectively. Other signals found in the fingerprint region (< 1500 cm^{-1}) are detailed in Table 4.6.

Product **3** (blue line), starting material A (black line), and Boltorn H311 (red line) are active in the carbonyl region 1600-1800cm^{-1}. The carbonyl peak in starting material A and Boltorn H311 were reported at 1735 and 1728 cm^{-1} respectively, which overlap with the signal at 1737 cm^{-1} in product **3**. Little difference in the carbonyl signals was observed on changing functional groups from reaction of the acids in starting material A to esters in product **3**.

Boltorn H311 had significant activity in the OH-region (3200-3600 cm^{-1}) that could no longer be observed in product **3**. The alcohol functionality in Boltorn H311 was attributed to both water content and alcohol functionality in the dendrimer. Product **3** displayed no alcohol functional groups in the IR spectrum. This supported both removal of water and the conclusion that the alcohols had reacted with the carboxylic acids to form esters.

40

A smaller OH-signal was reported for starting material A in the 3200-3600 cm^{-1} region. This also could not be detected in product **3**. The OH-signal was linked to the acids present and provides additional evidence for reaction to form polymeric esters in product **3**.

Table 4. 3 Overview of main peaks in Figure 4.6.

Chemical	Peak	Intensity	Functional group
Boltorn H311	3391	Medium	OH Alcohol
	2857-2927	Medium	Aliphatic C-H
	1728	Strong	Ester C=O
	1466	Medium	Alkanes C-H
	1119	Strong	C-O
Starting Material A	3466	Weak	OH
	2853-2922	Medium	Aliphatic C-H
	1736	Medium-weak	Carbonyl C=O
	1465	Weak	CH Alkanes
	1109	Strong	Aliphatic ether
Product 3	2854-2923	Medium	Aliphatic C-H
	1737	Strong	Ester C=O
	1466	Weak	Alkanes C-H
	1050-1300	Strong	C-O, Aliphatic Ether

4.2.3 NMR

In nuclear magnetic resonance (NMR) spectroscopy, elucidation of chemical structures is based on the measure of absorption by nuclei of electromagnetic radiation in the radio-frequency region (approximately 4-900 MHz) [3]. In this thesis, both ^{1}H-NMR and ^{13}C-NMR analyses were performed for the products (**1**-**16**) in addition to the starting materials. The spectra can be found in Appendix E.

An example of ^{1}H-NMR spectra of product **3** and respective starting materials are presented in Figures 4.7, 4.8, and 4.9. There are many common NMR signals between Boltorn H311 and product **3**, showing the core of the dendritic polyester remained intact during the reaction.

An increase can be observed in the integration of the signals at 1.20-1.30 ppm in product **3** ^{1}H-NMR relative to Boltorn H311, showing an increase in the alkyl groups present in product **3**. As no signals for carboxylic acids (> 10 ppm in ^{1}H-NMR) can be observed, this gives additional evidence that starting material A is attached to the dendrimer core.

The signals linked to carbonyl functionality in the ^{13}C-NMR would be expected between 170-175 ppm. This were not observed in the spectra, see Appendix XX. This was believed to be due to signal broadening as it was polymers being analysed, and insufficient concentrations to enhance the signal-to-noise ratio, even though high concentrations were used for this analysis.
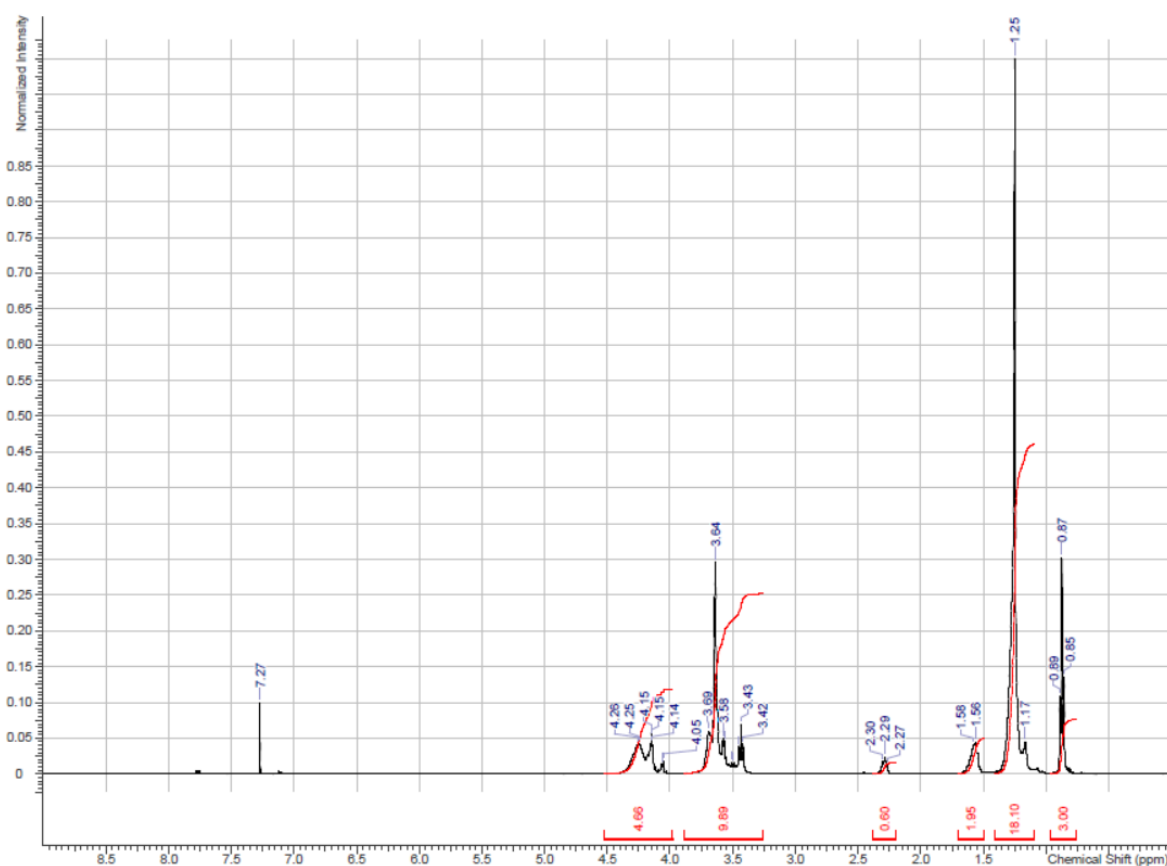
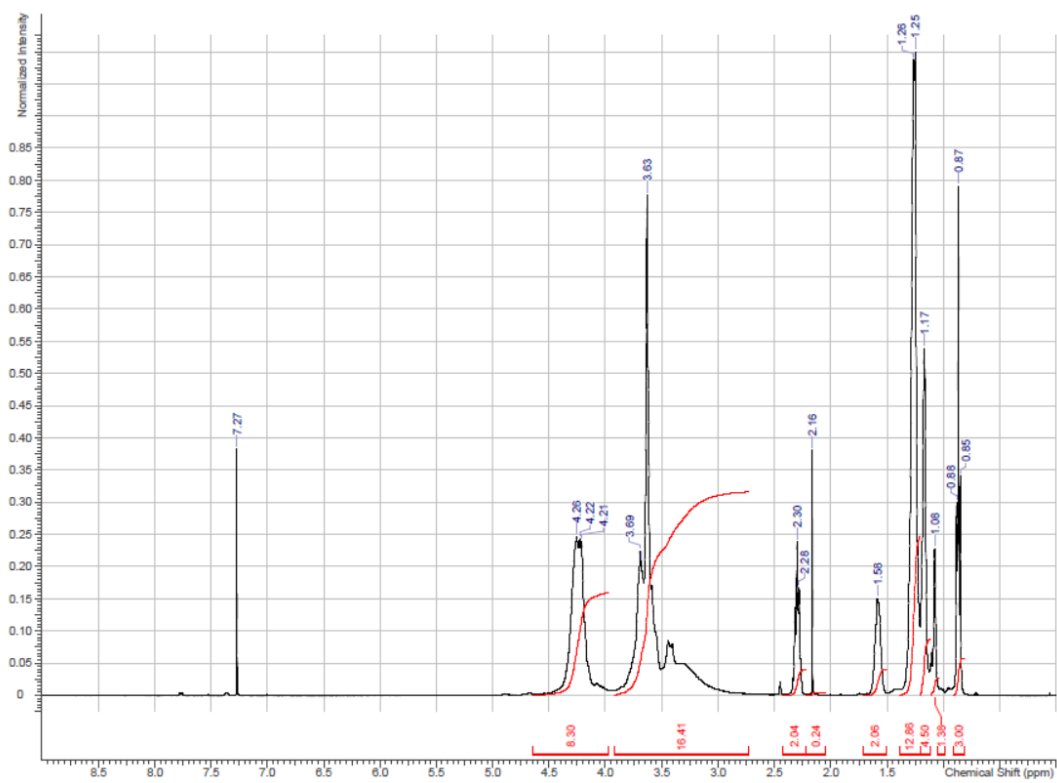

Figure 4. 7 ^{1}H-NMR spectrum of product **3**.
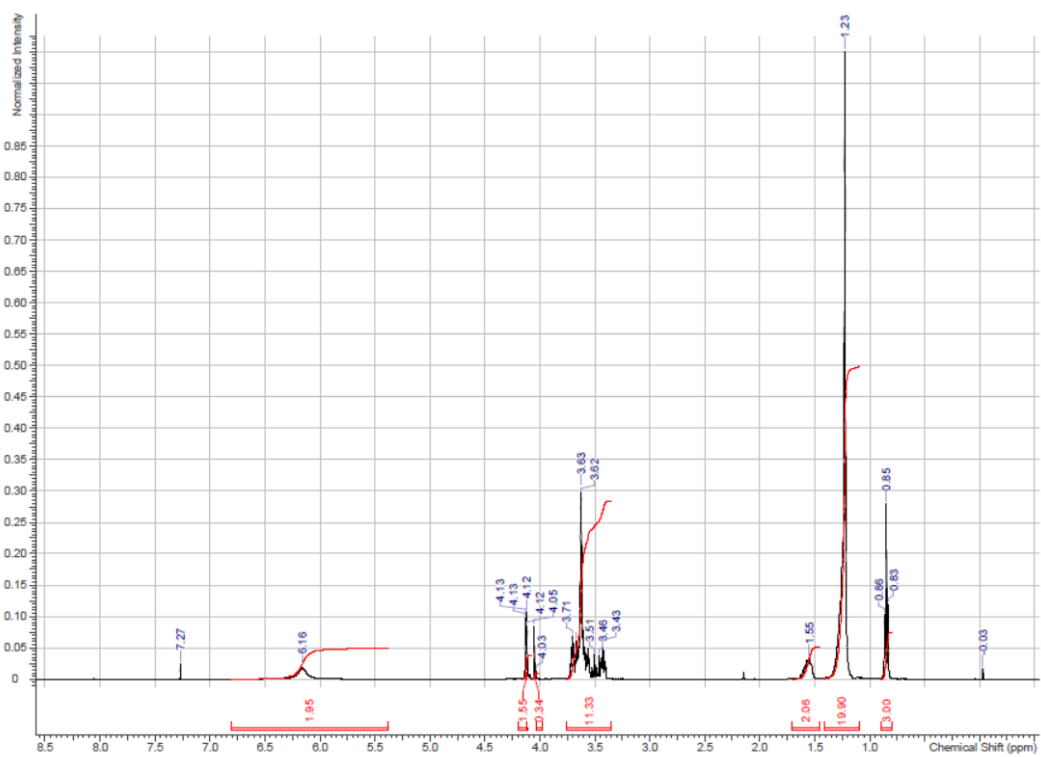
Figure 4. 8 ^{1}H-NMR spectrum of Boltorn H311.

Figure 4. 9 ^{1}H-NMR spectrum of starting material A.

4.2.4 RSN and HLB

The relative solubility number (RSN) was determined experimentally for all products (**1**-**16**). The hydrophilic-lipophilic balance (HLB) was determined theoretically for all products (**1**-**16**). The results are presented in Table 4.4.

Table 4. 4 Overview of RSN and HLB results for products **1**-**16**.

Starting materials	Product number	Coverage	RSN	HLB
Boltorn H311 + Starting material A	1	50%	4.1	2.61
	2	70%	3.5	3.12
	3	90%	3.2	3.50
	4	100%	3.0	3.66
Boltorn H311 + Starting material B	5	50%	6.1	7.54
	6	70%	5.5	8.56
	7	90%	5.4	9.25
	8	100%	5.1	9.52
Boltorn H311 + Starting material C	9	50%	3.4	2.01
	10	70%	3.2	2.38
	11	90%	2.5	2.66
	12	100%	2.4	2.77
Boltorn H311 + Starting material D	13	50%	5.0	6.72
	14	70%	4.9	7.62
	15	90%	4.2	8.22
	16	100%	3.8	8.46

The HLB is a numerical expression of the hydrophilic-lipophilic balance within a molecule, where the degree of ethoxylation is a determining factor. For non-ionic surfactants, HLB carries a dimensionless value ranging from 0-20. Oil soluble surfactants will have a HLB value < 9, while water solubles will have a HLB value > 11 [4]. The majority of the products were found to have a HLB < 9. Product **7** and **8** were exceptions and were reported to have HLB values slightly above 9 (9.25 and 9.52, respectively). Each product range displayed the trend of increasing HLB values with increasing coverage (see Figure 4.10). The products (**5**-**8** and **13**-**16**) synthesized with starting materials B and D that had higher degrees of ethoxylation, and it follows that they had higher HLB values.

The RSN is a measure of the solubility properties for a chemical. RSN measured < 13 indicates water insolubility, while RSN > 17 indicates water solubility. A measurement between 13 and 17 suggest water dispersibility. The measured RSN values for the demulsifier products were generally low, ranging from 2.4 to 6.1. This indicates that the products interact better with the oil phase, meaning that they are oil soluble and water insoluble or dispersible. As shown in Figure 4.11, the RSNs decrease with increasing coverage, indicating lower water solubility as the coverage of the dendrimer increases. The products synthesized with starting material B and D, containing more ethoxylation, had higher RSN values ranging from 3.8 to 6.1.

The relative solubility number (RSN) can be correlated to the hydrophilic-lipophilic balance (HLB) as they are both measures of the water-oil solubility of a substance. The HLB values obtained here show the inverse trend to the RSN; increasing HLB value and decreasing RSN with higher coverage (see Figure 4.10 and 4.11).
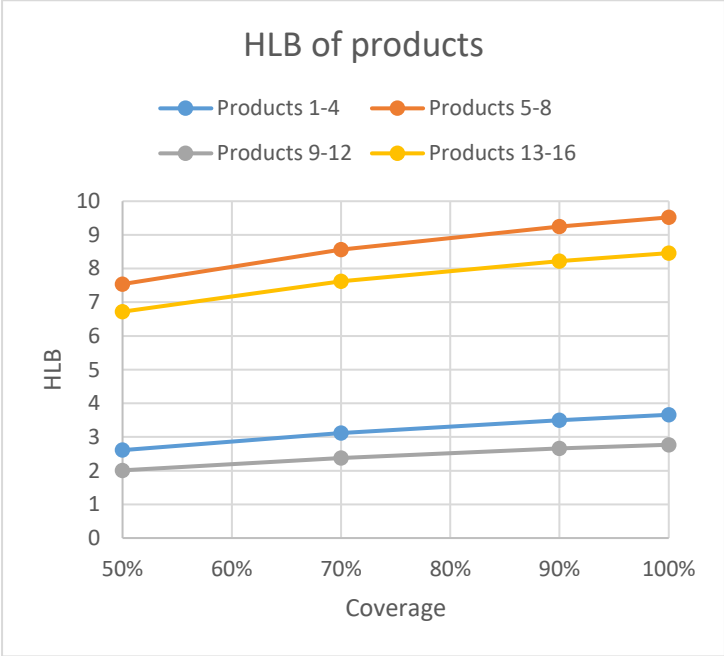

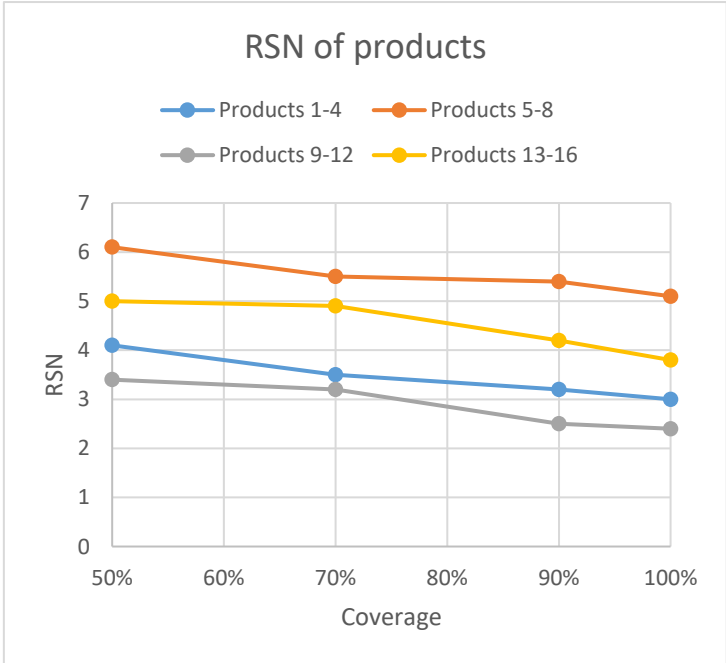Figure 4. 10 Results of theoretically calculated HLB for products **1**-**16**.

Figure 4. 11 Results of RSN measurements for products **1**-**16**.

4.2.5 Physical property data

Physical property data of the products (**1**-**16**) was measured and found consistent over the range of products. The average pH measurements were found to be between 3.7 to 4.3. The pH measurements show the tendency to decline as the coverage and ratio of acid increase. The density measurements were between 1.018 to 1.085 g/cm^3. The products were found to be dispersible in deionized water (1%), while soluble in BDGE (30%) and Solvesso 150 ND (20%). The full overview of the physical data (pH, density, and solubility) can be found in Table 4.5.

Table 4. 5 Overview of recorded physical property data.

Starting materials	Product number	Coverage	pH	Density [g/cm³]	Solubility in deionized water (1%)	Solubility in Solvesso 150 ND (20%)	Solubility in BDGE (30%)
Boltorn H311 + Starting material A	1	50%	4.17	1.074	Dispersible	Soluble	Soluble
	2	70%	4.05	1.060			
	3	90%	3.93	1.047			
	4	100%	3.72	1.041			
Boltorn H311 + Starting material B	5	50%	4.04	1.085	Dispersible	Soluble	Soluble
	6	70%	4.04	1.081			
	7	90%	3.99	1.074			
	8	100%	3.90	1.071			
Boltorn H311 + Starting material C	9	50%	4.32	1.058	Dispersible	Soluble	Soluble
	10	70%	3.88	1.036			
	11	90%	3.88	1.023			
	12	100%	3.95	1.018			
Boltorn H311 + Starting material D	13	50%	4.37	1.074	Dispersible	Soluble	Soluble
	14	70%	4.25	1.064			
	15	90%	4.05	1.055			
	16	100%	4.08	1.053			

4.4 Demulsification Performance

4.4.1 Design of Experiments – Modelling results of performance

For the analysis of the performance data, a model in Design-Expert® was made. A model is a mathematical model used to find relations between factors and responses. Four factors were used in the program to generate the model: (factor A) carbon chain length, (factor B) EO units, (factor C) dosage concentration, and (factor D) coverage. After analysis, an equation was made relating the mathematical model to the factors. The equation in terms of so-called coded factors can be used to make predictions about the response for given levels of each factor. The coded equation is useful for identifying the relative impact of the factors by comparing the factor coefficients. An example of a coded equation of the resulting mathematical model for water separation is presented in Table 4.6. The responses used in the model were water separation, BS (residual emulsion), RSN and HLB. Quality data was not included in the model.

Table 4. 6 Example of generated mathematical model for water separation.

Water separation [mL]	=	
+10.72		(Constant)
+2.77	* A	carbon chain length
+6.40	* B	EO units
+2.84	* C	Dosage Concentration
-0.3140	* D	Coverage
+0.3158	* AB	
+1.18	* AC	
-0.5444	* AD	
+1.08	* BC	
+2.75	* BD	
-1.20	* CD	

The model suggested in this case is a 2FI (two factor interaction) model (see Table XX). According to the model, longer carbon chain length, higher number of EO units, and higher concentration will increase the amount of water separated. This is shown by the positive values of +2.77, +6.40, and +2.84 respectively in Table 4.6. Conversely, increasing the coverage will have a negative effect on the water separation. However, the negative constant is not very significant (-0.314), and will not hold as much weight as for example the constant for EO units. In this model, the number of EO units is predicted to have the highest relative impact on water separation.

In the model, the EO units and carbon chain length factors are modelled in such a way that the factors are interpreted at two levels, as either "high" (10 and 16, respectively) or "low" (2 and 12, respectively). Thus, starting material C having 2.5 EO units is modelled under lower level (2) of the EO units factor. Similarly, starting material D with 9 EO units is modelled under

the higher level (10) of the EO units factor. The same principle is applied to the carbon chain length.

It is important to note that the model only presents the trends of the results. An example of how the actual measurements (responses) may vary from the model as can be seen in Figure 4.12.
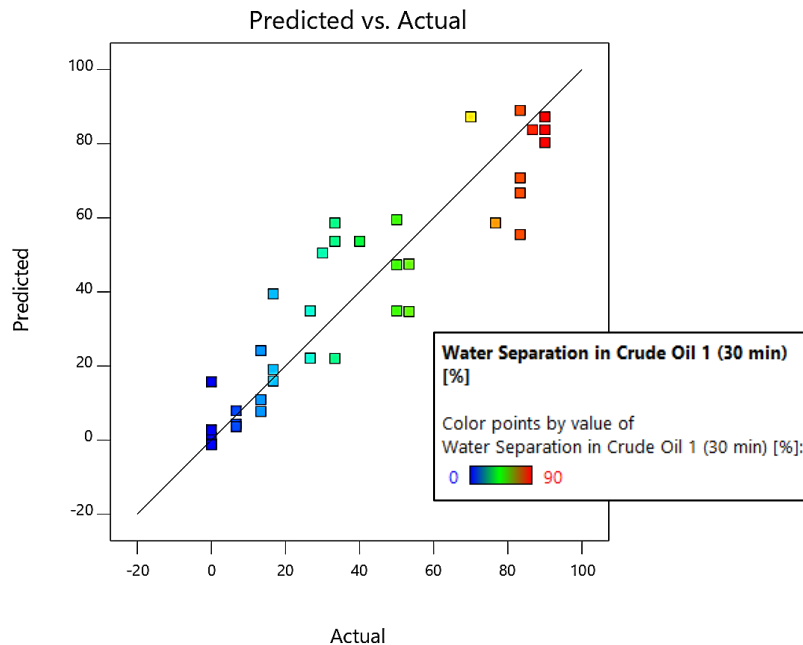

Figure 4. 12 Actual measurements plotted versus predicted model.

The Design-Expert® program was also used to predict the best performing products. The prediction was generated by evaluating all the factors in the range of their experimental values, while the settings for water separation was set to "maximize" and the highest importance was chosen. The residual emulsion (BS) was set to be evaluated in the range of its values. In the optimizing, the limiting values were set to be from zero to maximum amount of residual emulsion recorded. For an example of the numerical optimization criteria that were fed to the model, see Table 4.7.

Table 4. 7 Example of numerical optimization model for products.

Factors and responses	Goal	Lower limit	Upper limit	Importance
A: R chain length	In range	12	16	3
B: EO units	In range	2	10	3
C: Dosage Concentration [ppm]	In range	40	80	3
D: Coverage [%]	In range	50	100	3
Water separation in Crude Oil 1 (30 min) [mL]	Maximize	0	27	5
Water separation in Crude Oil 1 (30 min) [%]	Maximize	0	90	5
BS in Crude Oil 1 (10 min) [mL]	In range	0	21	3

The model may not always generate values that are reproducible experimentally. For example, nearing coordinate (0,0,0) in Figure 4.17 a "kink" can be observed in the plot where the model suggests negative values for water separation. This, for obvious reasons, is obviously not realistic, and the y_{min} (water separation) value was thereby set to zero, resulting in the "kink". By the same reasoning, the goal of "BS in Crude Oil 1 (10 min) [mL]" was selected to be "in range", instead of "minimize".

4.4.2 Bottle Test

Demulsifier bottle tests were carried out according to procedure in Section 3.2.4. The results were analysed and the best performing demulsifier products were identified. These will be presented here. The complete set of demulsifier test data can be found in Appendix F-H.

The bottle tests were evaluated and scored with regards to different factors, including water separation efficiency, quality data, and thieving sample parameters such as amount of residual emulsion (BS) and free water. The most important factor was water separation efficiency. Although, the amount of residual emulsion in the crude oil was also considered very important, especially as products **1**-**16** were readily oil soluble.

Products 1-16 underwent performance testing on three different crude oils (1, 2, and 3). The crude oils were sourced from producing fields known to have problems with emulsions (see Table 4.8).

Table 4. 8 Characteristics for crude oils 1, 2, and 3.

Crude oil sample	Source	API Gravity
Crude oil 1	North Sea	33.6
Crude oil 2	North Sea	31.8
Crude oil 3	South Atlantic Ocean	29.7

The bottle test was designed to simulate a "typical" oil field system. The system had two separators maintained at 60°C with a resident time of 30 minutes per separator. Thus, the products were observed over a 30-minute period, with an extension to 65 minutes. The results recorded at 30 minutes were of most significance and were used in subsequent analysis.

The bottle test technique is a comparative method, meaning that there are no analytical methods available for evaluation of instant percent water separation. The most challenging aspect was to produce an emulsion that responded exactly the same for each test run. Pictures of the produced emulsions were taken to observe the consistency. Representative pictures of the emulsions produced can be seen in Figure 4.13. The pictures of the emulsions were taken immediately after they were prepared using a regular microscope, on a heated (70°C) glass slide. For testing with crude oil 1, preparing a consistent emulsion for each run was especially challenging. As can be seen in Figure 4.13a, the size of the dispersed water droplets is significantly larger than the droplets in emulsions prepared by crude oils 2 and 3. Thus, the emulsions prepared with crude oil 1 were considered the least stable. For some test runs, this resulted in the testing having to be repeated because of too large inconsistencies between test runs. The blank untreated test and the commercial product sample were used as controls to check and measure of consistency. The commercial reference naturally had small variances from each test run, but as the product performed out of its regular performance pattern, the test was repeated.

Others have reported emulsion stability lasting for more than 1 day [5]. The stability of the emulsion prepared with crude oil 1 was evaluated to be stable for 3-4 hours. The emulsions for prepared with crude oil 2 was stable for around 5-6 hours. The emulsion prepared with crude oil 3 was stronger and were evaluated to be stable for 1 day.
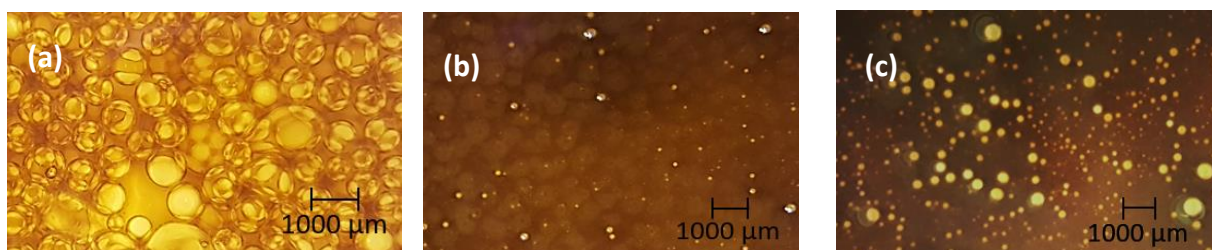

Figure 4. 13 Pictures of emulsions of crude oils 1-3. (a) Crude oil 1 emulsion, (b) Crude oil 2 emulsion, (c) Crude oil 3 emulsion.

The scope of this testing was not to break an extremely stable and tight emulsion, but to simulate a realistic emulsion found in the oil field system and observe how products **1**-**16** behave as demulsifiers. The emulsions found in oil filed systems have a range of different droplet sizes. This is challenging to recreate using equipment such as blenders to prepare the emulsion. The blenders often end up "cutting" the water droplets into smaller and smaller droplets, resulting in a "perfect" emulsion. Therefore, the lowest speed setting (13 000 RPM) was chosen for the preparation of the emulsions. Additionally, the shortest possible mixing times to create a stable emulsion were used for the different crude oils.

To determine the dosage rates for testing with crude oil 1, a commercial demulsifier product was screened at 5, 10, 20, 40, 80, and 120 ppm (results not reported here). De demulsifier products were still tested on 40 and 80 ppm in crude oil 1, while testing in crude oil 2 and 3 were only performed at 80 ppm.

The quality data was evaluated by observation only. As only one person performed the evaluations, the recordings were executed as consistently as possible. The oil quality data was the most challenging to evaluate, as the changes were often subtle and harder to make out as crude oils 1 and 2 were quite dark in colour. The quality data were divided up by water, oil, and interfacial quality. Water quality was scored from 1 to 5. If the sample was scored with 1, there was no water separated to evaluate. Samples scored with 5 had completely clear water. The oil quality was evaluated by the degree of dirtiness (D), i.e. the shininess of the oil and the amount of particles. The interfacial quality was evaluated by degree of mobility (M) and the presence of "balls" or rags on the IF. If none of these traits were present, the IF was marked as sharp (S). Higher degrees of the different factors were marked with (+) or (++), while lower degrees were marked with (-) or (--).

Thieving samples were taken at 10 and 30 minutes. These were to assess the amount of residual emulsion (BS) left in the oil, effectively measuring the dryness of the oil. The samples were taken approximately 10 mL above the expected interface (IF) (at 30 mL) to simulate a weir-type separator. The products displayed a decrease in the residual emulsion and water content in measurements from 10 to 30 minutes. However, because of how the emulsions were dispersed in the sample flasks, an increased amount of residual emulsion could be observed.

To simulate the remixing between the two separators, the test tubes were re-shaken after measurements at 30 minutes. After the re-shake and second 30 minutes standing (65 min), the samples were expected to reach the same or higher separation ratio achieved at 30 minutes. However, due to slower demulsification mechanism or re-emulsification slowing down the process, some samples may experience a decrease in water separation.

The Expert-Design® program was used to model and present the trends of the results obtained in bottle testing. Additionally, the program was used to generate predictions of the best performing products in the respective crude oil. The predictions from the Expert-Design® program offered valuable information, but it should be noted that the predicted data should always be evaluated against the experimental data.

In the next sections 4.4.2.1 to 4.4.2.4 a deitailed description and analysis of the demusifier testing in each crude oil is given.

4.4.2.1   Results of Testing in Crude Oil 1

Demulsification testing was performed for the full range of products (**1**-**16**) at 40 and 80 ppm in crude oil 1. The complete results are presented in Appendix F.

Two dosages were selected to study the effect on both water separation and amount of residual emulsion and check for any effects on over or underdosing. After the results from the screening with the commercial product were analysed, it was determined to test the products at both 40 and 80 ppm. The resulting data collected from the demulsification testing with the synthesised products was then processed. It was determined that the 80 ppm dosage concentration was related to higher performance, with respects to both water separation and amount of residual emulsion (see Figure 4.14 and 4.15, respectively). In Figure 4.14, the performance of products dosed at 80 ppm was varied (0-90% water separation), but the products with the highest performance were all dosed at 80 ppm. For the products dosed at 40 ppm, the performance range is much narrower (0-50% water separation).
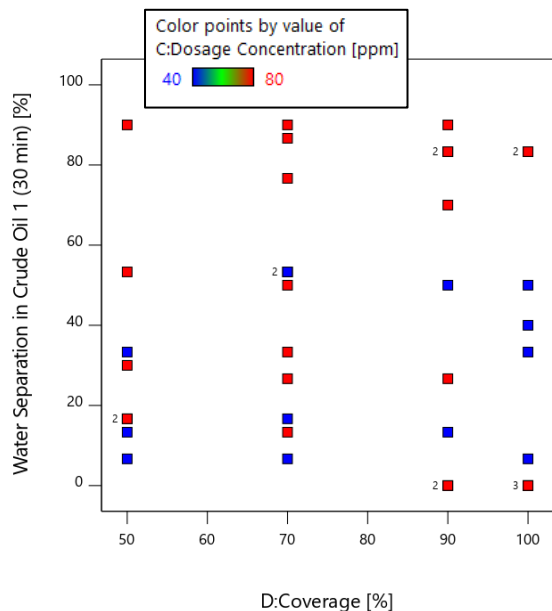
Figure 4. 14 Water separation (%) in crude oil 1 with varying coverage, related to dosages 40-80 ppm. The small numbers in the plot represent number of replicas.
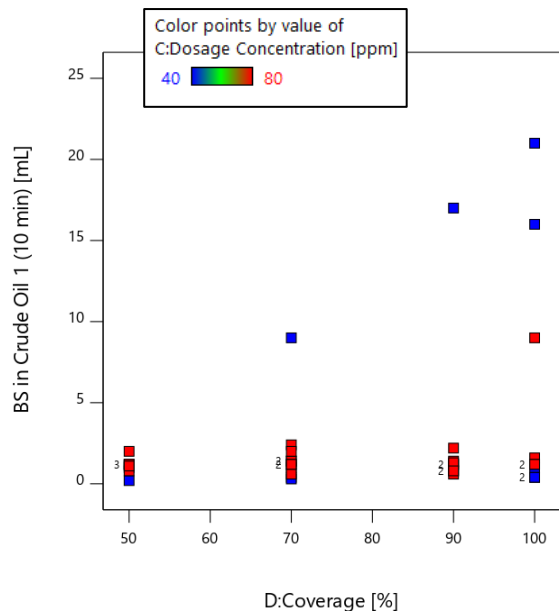
Figure 4. 15 Amount of residual emulsion (BS) in crude oil 1 with varying coverage, related to dosages 40-80 ppm. The small numbers in the plot represent number of replicas.

The products dosed at 40 ppm generally displayed higher amounts of residual emulsion, than the products dosed at 80 ppm. The 80 ppm dosage increased the measure of residual emulsion for products **1**, **2**, **5**, **6**, **8**, **11**, **16** and **13**-**15** (see Tables F.2 and F.4 in Appendix F). However, the measures for products **11** and **16** increased only by 0.2 mL, while products **13** and **15** experienced an increase of 0.1 mL. This could be within the margin of error. A decline in the amount of residual emulsion was observed for the other six products. Overall better levels of residual emulsion were seen at 80 ppm dosage rate.

Thereby, the optimum dosage concentration was found to be 80 ppm. Rajak et al. also found that the optimum dosage varied from 60 to 80 ppm for different demulsifiers [6]. Thus, the results of testing with 80 ppm dosage will be discussed here. The results for testing at 80 ppm can be found in Appendix F (Tables F.3 and F.4).

As the experimental data was analysed, the 90 and 100% coverage ranges were evaluated to have the best performance, although the same trends described below hold true for the 50 and 70% coverage ranges. Expert-Design® was utilized to plot water separation against both the number of EO units and the carbon chain length. Figures 4.16 and 4.17 present the results at 90 and 100% coverage, respectively. The strongest trend for enhanced water separation was an increase in the number of EO units. The effect of the carbon chain length was less pronounced. Longer R groups seemed to give slightly better water separation.
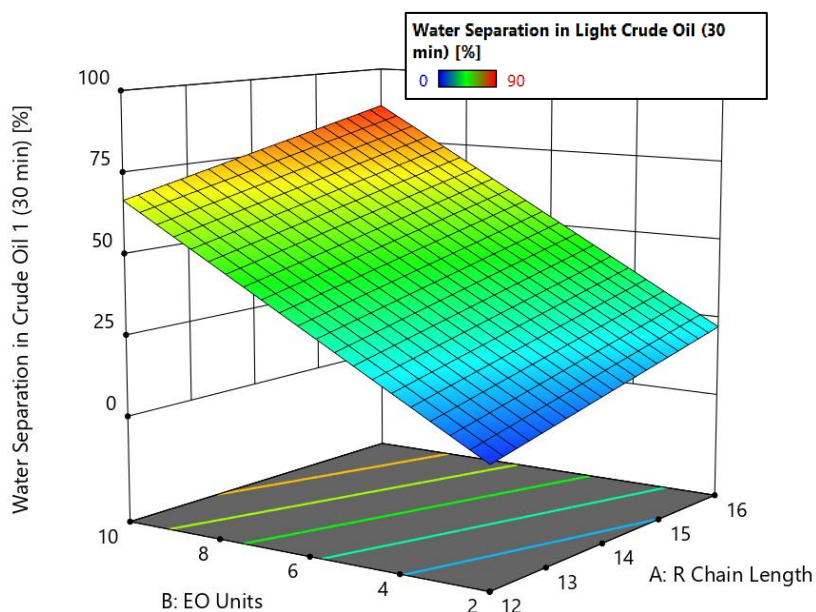

Figure 4. 16 Water separation results from 90% coverage products at 80 ppm tested in crude oil 1, modelled with Expert-Design®.

Of the four products with 90% coverage, products **7** and **15** had both high numbers of EO units and water separation efficiency. However, the highest separation ratio was recorded for product **15** (90%), which had a longer R group. The measure of water separation for product **11** was 26.67%. Product **3** did not display any water separation over time.
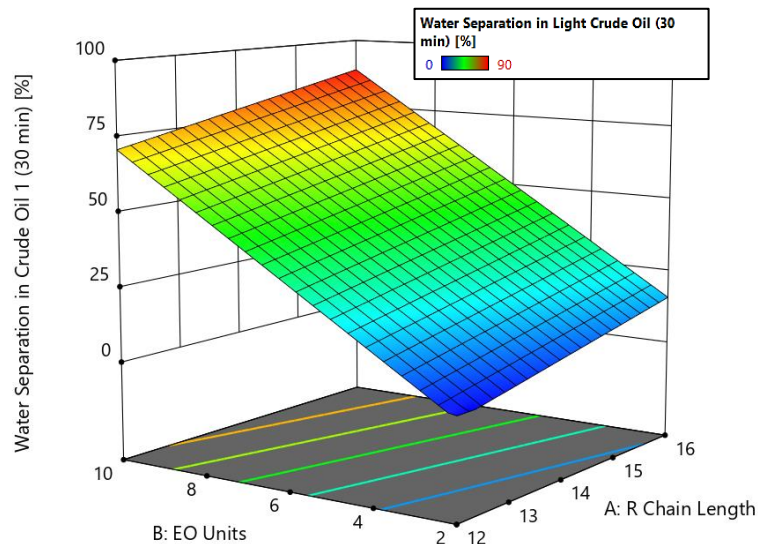

Figure 4. 17 Water separation results from 100% coverage products at 80 ppm tested in crude oil 1, modelled with Expert-Design®.

For the products with 100% coverage, having the highest number of EO units and the longest carbon chains, products **8** and **16** had the best water separation efficiency. Both products had a water separation ratio of 83.33%. Neither of products **4** and **12** had any water separation.

In the thieving samples, product **8** and **16** had similar results regarding amount of residual emulsion. The products had comparable water and IF quality, while product **8** demonstrated better reduction of the oil dirtiness.

In Appendix F (Table F.3), the results show that every product in the 100% coverage range have 0% separation in the first 5 minutes. This is illustrated in Figure 4.18. Although the 100% coverage products had no separation in the 5 first minutes, the water separation increases rapidly afterwards. However, this increase was only observed for the 100% coverage products with higher EO content (product **8** and **16**). The lower EO content products had 0% separation efficiency across the testing (product **4** an **12**). The initially slower demulsification process for the 100% coverage range, seem to have had negative effects on the amount of residual emulsion as it is quite high for these products.
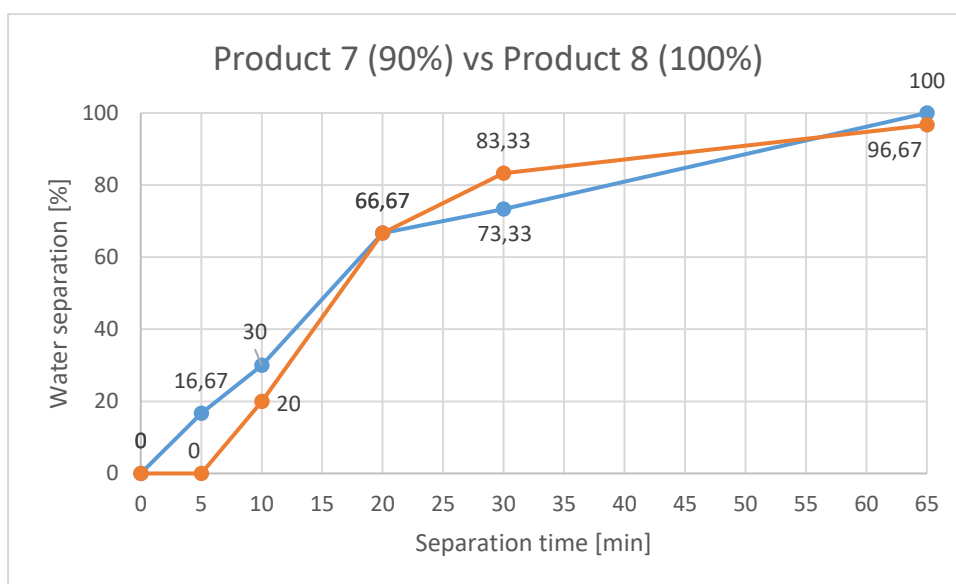
Figure 4. 18 Water separation efficiency for products **7** and **8**.

After modelling the emperical data, the Design-Expert® program generated a numerical optimization result, presenting the theoretically best performing products. The results are presented in Table 4.9.

Table 4. 9 Numerical optimization results for product performance in crude oil 1 emulsion.

Nr.	R chain length	EO units	Dosage [ppm]	Coverage [%]	BS [mL]	Water separation [mL]	Water separation [%]
1	C_{16}	10	79.999	91.066	0	26.092	86.975
2	C_{16}	10	80	89.744	0.132	26.032	86.775
3	$C_{15.962}$	10	80	91.094	0	26.031	86.770
4	$C_{15.999}$	10	79.969	89.530	0.154	26.014	86.714
5	$C_{15.999}$	10	79.631	91.121	0.003	26.010	86.699

The program suggests that the best performing product would have ten EO units, C_{16} carbon chain length, and a 90-91% coverage. This correlates to product **15**. Product **15** did indeed have the highest water separation efficiency. The model suggests an optimized water separation efficiency of 87%, and product **15** was measured to have a separation ratio of 90% (at 30 minutes) in the actual bottle test. Thus, there was good correlation between predicted and experimental results.

From the experimental data, product **7** was evaluated to have the best overall performance. Product **7** had a separation efficiency of 73.33%. Additionally, the amount of residual emulsion for product **7** (0.4 mL, 10 min) was less than a third of the BS for product **15**. The amount of residual emulsion for product **7** was the lowest recorded in the bottle testing with crude oil 1. Product **7** was also the only product to reach 100% separation (at 60 minutes). By 30 minutes, this product had removed all of the free water in the residual emulsion meaning that

only smaller droplets of water were left (0.4 mL). Product **15** had trace amount of free water left at 30 minutes, which amounted to 0.6 mL of water at the end. Both products **7** and **15** performed better than the commercial product used as a reference in the testing procedure (see Figure 4.19 and 4.20, respectively).
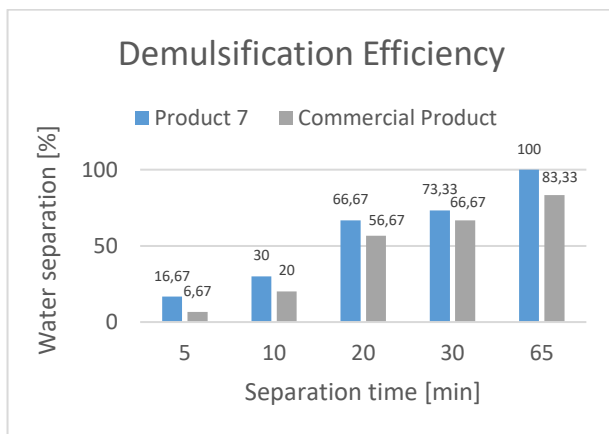

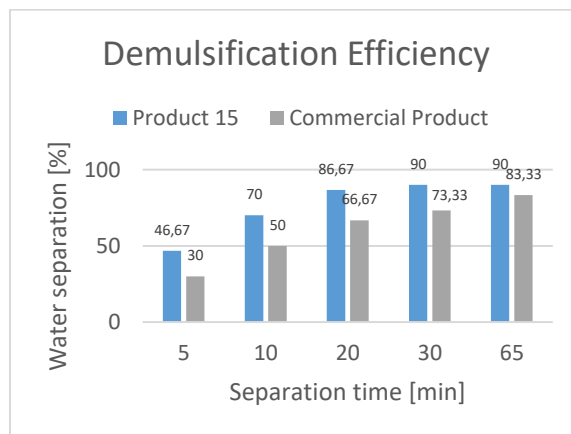Figure 4. 19 Performance of product **7** vs. commercial product.

Figure 4. 20 Performance of product **15** vs. commercial product.

4.4.2.2   Results of Testing in Crude Oil 2

The demulsification efficiency testing was performed for the full range of products (**1**-**16**) at 80 ppm in crude oil 2. A full overview of the results is reported in Appendix G (Tables G.1 and G.2).

The 90 and 100% coverage ranges were evaluated to have the best performance from analysis of the experimental data. Expert-Design® was used to plot water separation against both the number of EO units and the carbon chain length. Figure 4.21 and 4.22 present the results at 90 and 100% coverage, respectively. The strongest trend for enhanced water separation in crude oil 2 was observed for longer carbon chains. The influence of varied degrees of ethoxylation was found to be less significant. Nevertheless, the model show a slight increase in water separation for higher numbers of EO units.
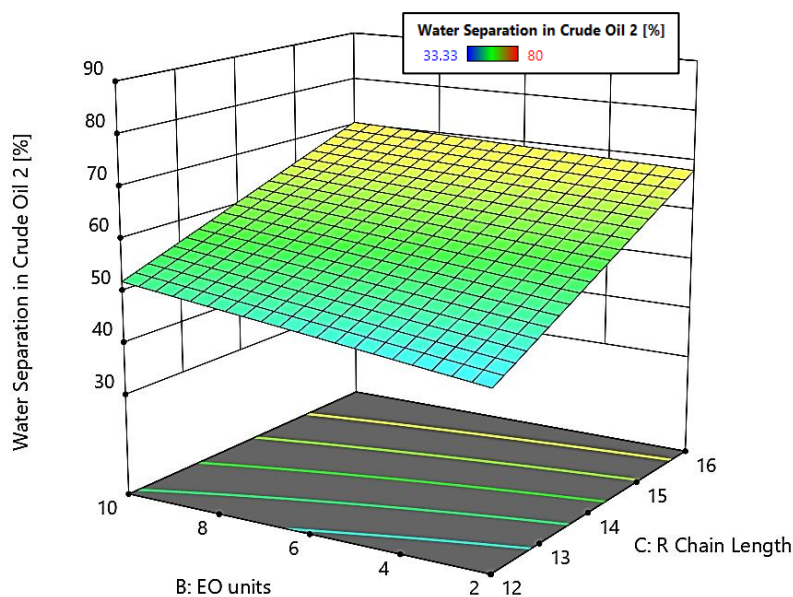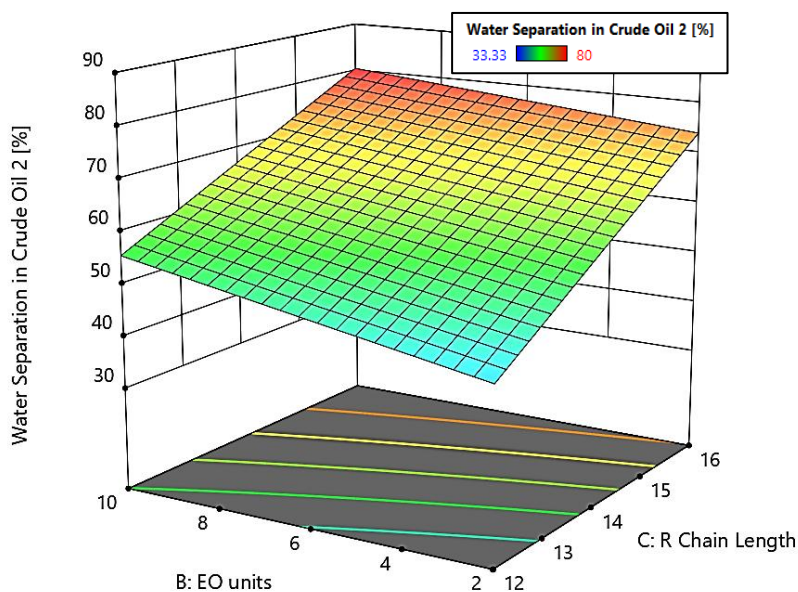
Figure 4. 21 Water separation results from 90% coverage products at 80 ppm tested in crude oil 2, modelled with Expert-Design®.

Product **11** and **15** had the highest separation efficiency within the 90% coverage range. Both products had longer R groups (C_{16}/C_{18}). Product **15** and **11** had nine and two EO units, respectively. The water separation efficiency of product **3** and **7** were both lower than efficiencies for product **11** and **15**. Higher numbers of EO units did not seem to have much influence on water separation for the 90% coverage range.

Product **15** had only a trace amount of residual emulsion left at the 10-minute thief sample but had a small increase to 0.5 mL at 30 minutes. The residual emulsion for product **11** remained unchanged over time (1.0 mL). The two products had similar quality data for water and oil dirtiness. Some small rags were observed at the IF for product **11**, while the IF for product **15** was sharp.

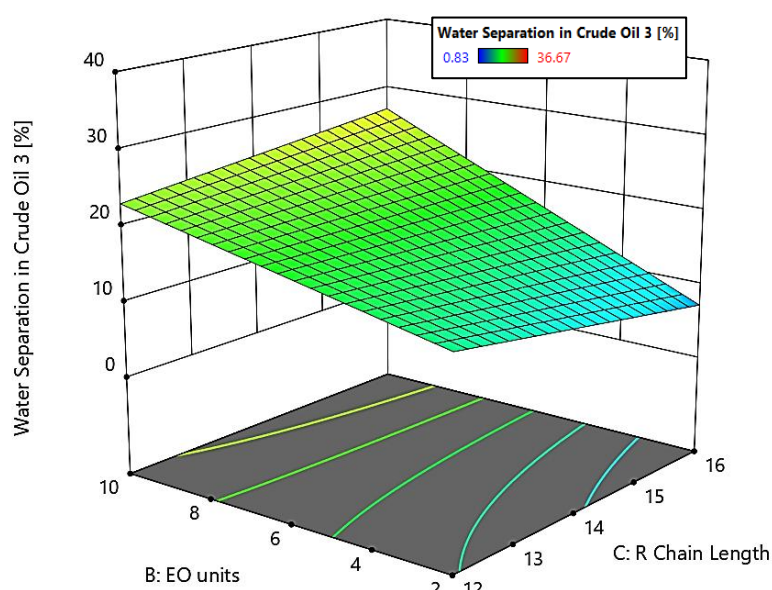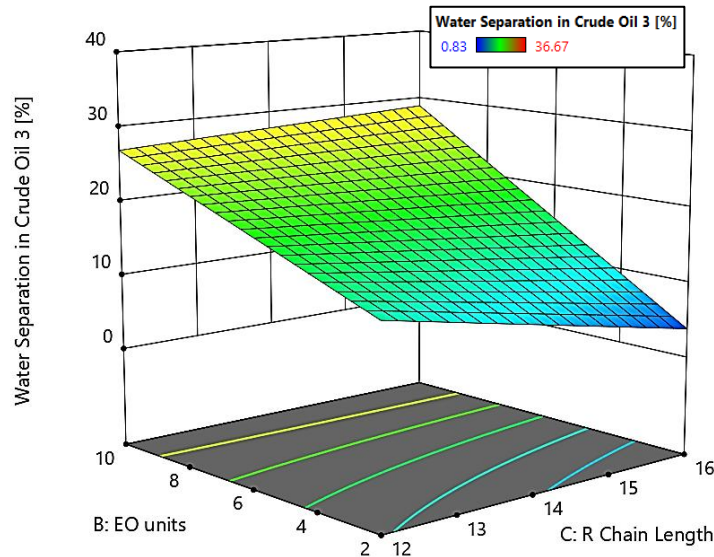Figure 4. 22 Water separation results from 100% coverage products at 80 ppm tested in crude oil 2, modelled with Expert-Design®.

The 100% coverage range was found to have generally higher water separation efficiencies, compared to the 90% range. Products **12** and **16** had the highest separation efficiencies. Both products had carbon chain length of C_{16}/C_{18}. Product **12** had two EO units, while product **16** had nine. In this case, product **16** with more EO units had the highest water separation. Product **8**, having C_{12}/C_{14} carbon chain length, had lower separation efficiency than products **12** and **16**. With few EO units and a short R group, product **4** had the lowest water separation ratio of the 100% coverage range.

Products **12** and **16** perform similarly in the first thieving samples (0.5 mL, 10 min) but product **12** experienced an increase in residual emulsion at 30 minutes. No change was observed in the amount of residual emulsion over time for product **16**. The two products were evaluated with the same scores for water and oil dirtiness. Some small rags were observed at the IF for product **12**, while the IF for product **16** was sharp.

The optimized products suggested by the model are reported in Table 4.10.

Table 4. 10 Numerical optimization results for product performance in crude oil 2 emulsion.

Nr.	R group	EO units	Dosage [ppm]	Coverage [%]	BS [mL]	Water separation [mL]	Water separation [%]
1	$C_{13.681}$	5.178	80	89.888	0.719	16.188	53.958
2	C_{12}	10	80	90	0.719	16.188	53.958
3	C_{12}	2	80	100	0.719	16.188	53.958
4	C_{16}	2	80	70	0.719	16.188	53.958
5	C_{12}	10	80	70	0.719	16.188	53.958

Based on the experimental data, the model suggests a variance of different structured products that may obtain the same water separation efficiency. The optimized product was predicted to have a structure with a C_{14} carbon chain, five EO units and a coverage of 90%. This does not represent any of the products synthesised in this thesis. However, the prediction 2 to 5 correlate to products **7**, **4**, **10**, and **6**, respectively. In relation to separation efficiency, the four products perform similarly with product **7** having the highest ratio of water separation (50%). Although the products discussed above (**11**, **12**, **15**, **and 16**) had higher separation ratios, product **7** was the only product to have no residual emulsion left at 10 minutes. As water separation is regarded as the most important factor, product **16** may be evaluated to have the overall best performance in crude oil 2 although the thieving sample showed 0.5 mL of residual emulsion.

4.4.2.3 Results of Testing in Crude Oil 3

The demulsification efficiency testing was performed on the full range of products (**1**-**16**) at 80 ppm with crude oil 3. The complete results can be found in Appendix H (Tables H.1 and H.2).

In these bottle tests, both emulsions and micro-emulsions were observed. Furthermore, overall numbers observed for water separation in crude oil 3 were found to be low. The W/O emulsion was correspondently much harder to resolve.

From analysis of the experimental data, the 90 and 100% coverage ranges were recognized to have the best performance. Expert-Design® was utilized to plot water separation against both the number of EO units and the carbon chain length. Figures 4.23 and 4.24 present the results at 90 and 100% coverage, respectively. The model for the 90% coverage range showed that the products with higher numbers of EO units will have enchanced performance with increasing carbon chain length. Conversely, the opposite trend was observed for products with lower numbers of EO units. The model for the 100% coverage range showed that products with low numers of EO units will experience a decrease in water separation efficiency with increasing length of R group. The trend for the higher EO content products were almost insignificant regarding the carbon chain length.

Figure 4. 23 Water separation results from 90% coverage products at 80 ppm tested in crude oil 3, modelled with Expert-Design®.

Product **7** and **15** had the highest water separation efficiencies (36.67 and 26.67%, respectively). Both products had high degrees of ethoxylation. Product **7** had a shorter carbon chain length, while product **15** had a longer R group. Product **3** with few EO units an a short R group had lower water separation than products **7** and **15**. The lowest separation ratio were recorded for product **11**.

59

In the thieving samples, products **7** and **15** had smiliar results. The products had little effect on the micro-emulsion. Both samples displayed low water quality and had no effect on the dirtiness of the crude oil. For product **16**, small rags characterized the IF. Product **7** had a moderate amount of "balls" on the IF.

Figure 4. 24 Water separation results from 100% coverage products at 80 ppm tested in crude oil 3, modelled with Expert-Design®.

Product **16** had the highest separation in the 100% coverage range, having both a high number of EO units and a long R group. Product **4** and **8** performed similarly, only distinguished by 3% in water separation efficiency despite product **8** having a high number of EO units. Product **12** had the lowest separation ratio.

For product **16**, the amount of residual emulsion (BS) was observed to decrease from the 10 to 30-minute thieving samples. The water quality was evaluated to be low and the product did not seem to have any effect on the oil dirtiness. Some small rags were observed at the IF.

The optimized products suggested by the model are reported in Table 4.11.

Table 4. 11 Numerical optimization results for product performance in crude oil 3 emulsions.

Nr.	R group	EO units	Dosage [ppm]	Coverage [%]	BS [mL]	Water separation [mL]	Water separation [%]	Micro-emulsion [mL]
1	$C_{12.707}$	4.153	80	62.772	2.094	5.259	17.531	46.75
2	C_{16}	10	80	100	2.094	5.259	17.531	46.75
3	C_{16}	10	80	70	2.094	5.259	17.531	46.75
4	C_{16}	2	80	50	2.094	5.259	17.531	46.75
5	C_{12}	10	80	100	2.094	5.259	17.531	46.75

The optimized product was predicted to have a carbon chain length of C_{13} ($C_{12.707}$), four EO units and a coverage of 62.772%. Such a product is not represented in the products synthesised in this thesis. Optimized products 2 to 5 can be correlated to products **16**, **14**, **9**, and **8**. Out of these products, only product **16** was evaluated to be high performing. However, all of the products with the exception of product **8** (13.33%), had a higher separation ratio than predicted (17.531%). Products **16** and **14** had lower measurements of residual emulsion (1 mL) than predicted (2.094), while product **9** and **8** had similar measurements (2 mL).

4.4.2.4   *General Comparison of Demulsifier Results*

The result range obtained from testing with crude oil 1 were substantially more wide spread with larger variance, compared to that of crude oil 2 and 3. For crude oil 1, the results ranged from 0 to 90% separation efficiency. The result range from testing with crude oil 2 were much narrower, ranging from 33.33 to 80% water separation ratio. Likewise, the results collected when testing with crude oil 3 were more concentrated. The results ranged from 0.83 to 36.67% water separation efficiency. The highest to lowest separation ratios were recorded in crude oil 1, crude oil 2, to crude oil 3, respectively. As such, the lower separation ratios gave an indication of how hard the emulsions were to treat. Although it is noteworthy that the products (**1**-**16**) tested in crude oil 2 reached the highest water separation at 65 minutes, compared to results from testing in crude oils 1 and 3.

In the thieving samples for crude oil 1 emulsions the amount of residual emulsion was recorded between a trace amount to 9 mL at 10 minutes. Good reduction of the residual emulsion was generally observed from the products at the 30-mintue thieving samples. The amounts of free water recorded in this testing were the lowest, compared to crude oils 2 and 3. The results seen in the 10-minute thieves in crude oil 2, were more narrow ranging from 0 to 3 mL. However, no improvement on amount of residual emulsion was observed over time (10-30 minutes) in the crude oil 2 emulsion. Still, several samples had only trace amounts of residual emulsion left at 30 minutes. The measurements of free water in testing with crude oil 2 were high, but some reduction of these were recorded. The amounts of residual emulsion recorded in testing with crude oil 3 ranged from 0.5 to 6 mL. Some reduction of the residual emulsion was observed over time, but the majority of the measurements remained high. In this testing, the highest amounts of free water were observed, and the reduction of these were minimal. Micro-emulsions were also recorded in the testing with crude oil 3, but the products had little or no effect on these.

The quality data recorded from testing in crude oil 1 was again the most varied. The water quality varied from scores of 1 to 5. Some products displayed good reduction in oil dirtiness, while others had no effect on the oil quality. The IF was generally characterized by balls present. The highest water quality data was observed in the testing with crude oil 2, scoring from 4 to 5. However, the products did not seem to have much effect on the oil dirtiness. The IF was generally sharp if no rags were present. The lowest water quality scores were recorded in testing with crude oil 3, where the scores ranged from 3 to 4. No significant changes in oil dirtiness were observed during this testing. The IF quality for product **13**-**16** were moderately

sharp (S-/R--), while the balls were generally present on the IF for the majority of the other products. The product range with high content of EO and longer R group (**13**-**16**), had higher IF quality across the testing with crude oils 1, 2, and 3.

4.4.3 Synergistic Relationships

Synergistic relationships of a group of selected products were studied. The products were tested in ratios of 75:25, 50:50, and 25:75. Products **14** and **6** were combined to observe potential synergistic effects between a longer and shorter R chain. Products **10** and **14** were tested to observe the potential synergistic effect between a lower and higher number of EO units. Lastly, product **15** was tested with product **7** to study the synergistic effects between two high performing products having the same percent coverage. However, none of the blends demonstrated any synergistic effects for water separation or residual emulsion. The results can be found in Appendix I (Figures I.1-I.3).

It was theorized that small amounts of residual starting material could have beneficial effects on water separation efficiency and residual emulsion. Smaller surfactants could enhance the water separation efficiency by displacing natural surfactant at the IF of smaller water droplets. If few natural surfactants are present, the smaller demulsifiers could readily reduce the interfacial tension (IFT) of the smaller droplets and promote demulsification with the dendrimer product.

After analysing the results from testing with crude oil 1, product **7** was identified as one of the best performing products. A test run was conducted testing the effect of different ratios of residual starting material (B) (i.e. 2, 5, 10, 15 and 20%) on the demulsification efficiency (complete results not reported here). The samples with 10 and 20% residual staring material B was found to have the highest water separation efficiency. Thereby, products **7a** and **7b** were also tested with crude oils 2 and 3. Table 4.12 shows the constituents of products **7a** and **7b**. These products could not be included in the mathematical model.

Table 4. 12 Components in product **7a** and **7b**.

Product Number	Ratio of starting material B	$M_{Starting\ material\ B}$ [g]	$m_{Product\ 7}$ [g]	m_{BDGE} [g]	Solution [% w/w]
7a	10%	0.15	1.35	3.5	30
7b	20%	0.30	1.20	3.5	30

As seen in Table 4.12, the effective amount of dendrimer product decreases with increasing amount of added starting material. The weight percent of active demulsifier was kept constant.

The results from testing in crude oil 1 showed that products **7a** and **7b** performed better than product **7** (see Figure 4.25). Although the performance related to water separation was similar, the difference in amount of residual emulsion is significant. Product **7** had 0.6 mL of residual emulsion (10 min), while products **7a** and **7b** only have a trace amount. The samples with residual starting materials may thereby assist in the flocculation of the smaller droplets. No differences were observed between the three products with respects to water quality (4 out of 5). Regarding the oil and interfacial quality, product **7b** was superior to products **7** and **7a**.
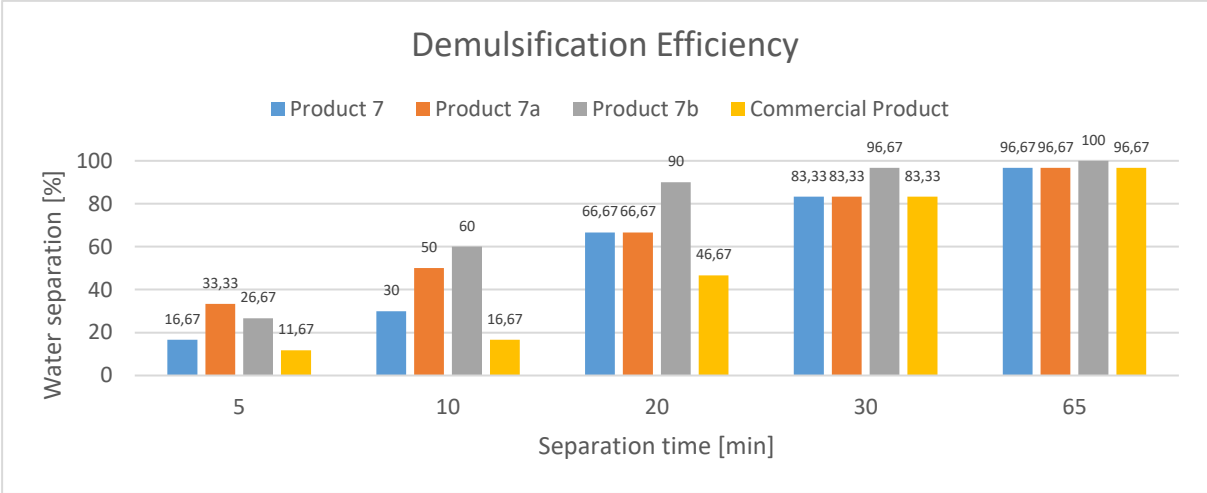
Figure 4. 25 Performance of product **7**, **7a**, **7b**, and commercial product in crude oil 1 emulsion (80 ppm).

The results of further testing with crude oil 2 showed that products **7a** and **7b** performed higher than product **7**. The water separation increased from 50% (**7**) to 60% (**7a**, **7b**) at 30 minutes (see Figure 4.26). Both products **7a** and **7b** had only trance amounts of residual emulsion at 10 and 30 minutes. The amount of free water in the thieving samples of these products was lower than for product **7**, indicating enhanced coalescence and water separation. Of the three products, **7b** had the best water quality (score 5 out of 5).
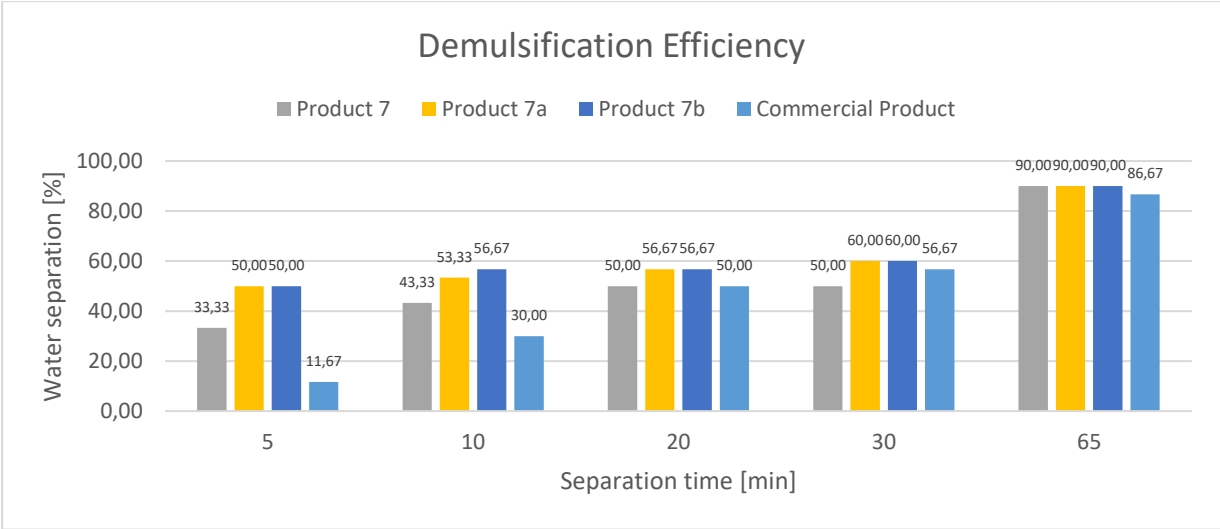
Figure 4. 26 Performance of product **7**, **7a**, **7b**, and commercial product in the crude oil 2 emulsion (80 ppm).

In crude oil 3, product **7a** outperformed product **7** in the testing with crude oil 3. Product **7a** also had higher separation efficiency than the commercial product (see Figure 4.27). However, in this test, product **7** had a higher water separation ratio than product **7b**. Still, products **7a** and **7b** reduced the amount of residual emulsion down to only a trace amount (30 min). Compared to product **7** and **7b**, product **7a** was the only product that seemed to affect the micro-emulsion, reducing it from 40 mL (10 min) to 34 mL (30 min). However, the quality data of products **7a** and **7b** did not differ from the quality data of product **7**.

Demulsification Efficiency
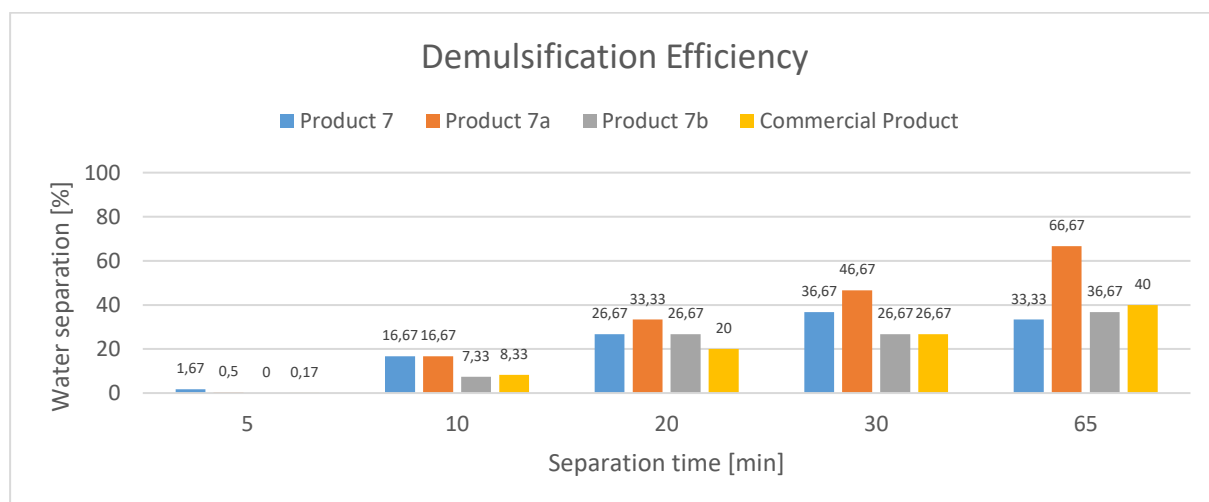
Figure 4. 27 Performance of product **7**, **7a**, **7b**, and commercial product in the crude oil 3 emulsion (80 ppm).

4.4.4   EO Content, HLB and RSN

As stated in Section 2.3.2, demulsifier products with higher HLB have been reported to have better performance. Shetty et.al found that water soluble, low molecular weight polymer demulsifiers with a high content of EO performed very well [7]. Here, we found that the demulsifier product **7** having the second highest EO content (46%) and HLB (9.25), had the overall best performance. This product had one of the highest (theoretical) molecular weights (20 000 g/mol), although this may not be regarded as "high" in the context of polymer weights.

The best water separation is observed from the products with highest content of EO (products **7**, **8**, **15**, and **16**), thus also having the highest HLB and lower RSN (within their respective ranges; **5**-**8** and **13**-**16**). Increased performance correlated to these factors could suggest that the products that have a higher affinity for water are initially and generally more stable at the interface of the dispersed water droplets. Thus, there will effectively be a higher demulsifier concentration at the interface compared to the other products with lower degrees of HLB.

The high performing products synthesised in this work seem to function better as "coalescers" or "water droppers" than as "flocculators" of smaller water droplets. As the products are quite large they may move slower through the oil phase and diffuse slower across the IF. Hence, the interaction with the smaller water droplets may not be optimal. Increasing the amount of

residual starting material (as done for product **7a** and **7b**), thus increasing the EO content and giving a higher HLB value, has been observed to enhance the water separation and reduction of residual emulsion. A general working mechanism for the products is proposed in Figure 4.28.
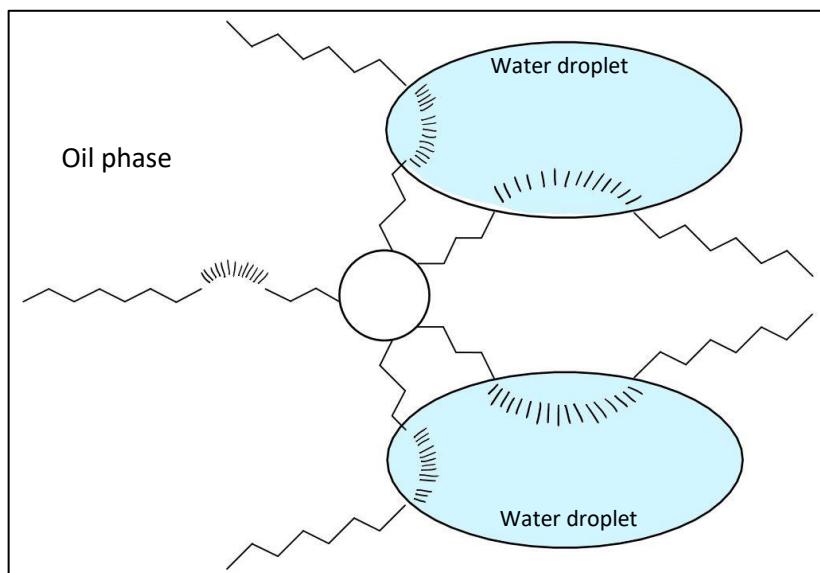
Figure 4. 28 Proposed demulsification mechanism for synthesized products.

In Appendix J, the water separation is reported in correlation with HLB for the three different crude oils. In crude oil 1, the products having the highest separation ratios also have higher HLB (coloured red, orange, yellow) (see Appendix J, Figure J.1). The products with higher HLB but lower demulsification (~40%) efficiency are products tested at 40 ppm. Moreover, all the product having a separation ratio < 30% have lower HLB (coloured blue). These are also some of the products with the highest amount of residual emulsion (see Figure J.3).

For the results reported for testing in crude oil 2 (see Appendix J, Figure J.2), two products with lower HLB are among the top five products with respect to water separation ratio. However, these also have higher amounts of residual emulsion. The remaining three other top products have higher HLB.

In the testing with crude oil 3, the three products with the highest water separation efficiency are reported to have higher HLB. Figure J.6 in Appendix J show that the products with higher HLB have lower amounts of residual emulsion, although a few of the lower HLB products are equal to these.

Although it can conclusively be stated that the higher performing products have higher HLB values, a general or statistical trend relating HLB and performance for all the products cannot be determined. The RSN values were observed to decrease with increasing. However, it was difficult to relate the trend for RSN to the results seen in the bottle tests.

4.4.5 Alkyl Chain Length

The effect of alkyl chain length on demulsification efficiency was discussed in Section 2.3.1. In this work, the general trend indicates that increasing length of R group may promote water separation. However, the trend seems to be of less importance compared to the trends observed for EO content.

The general trends for the effect of different R groups on water separation ratio were presented by the result plots modelled with Expert-Design® in Sections 4.4.2.1 – 4.4.2.3. In the models used for analysis of demulsifier results for testing in crude oil 1, increasing length of R groups were shown to have slightly higher water separation (see Figures 4.16 and 4.17). In the testing with crude oil 2, the trend was much stronger (see Figures 4.21 and 4.22). In the model for crude oil 3 results (see Figures 4.23 and 4.24), an increased carbon chain length had beneficial effects for the 90% coverage products with high EO content. The same trend was observed for the 70% coverage range. For the 100% coverage products with high EO content, the effects of the carbon chain length were less obvious. This was also true for the 50% coverage range.

The amount of residual emulsion correlated to carbon chain length is reported in Appendix K. However, the trends for the effects of carbon chain length on amount of residual emulsion were less clear.

4.4.6   Molecular weight

The effect of molecular weight on demulsification efficiency was discussed in Section 2.3.4. As many factors effected the GPC results with respect to molecular weight, it was concluded to use the theoretical molecular weights for comparisons with chemistry and demulsification efficiency. This was due to large deviations between theoretical molecular weight and molecular weight analysed by GPC. The theoretical molecular weights are presented in Table 4.13.

Table 4. 13 Theoretical molecular weights (M_w) of products **1**-**16**.

Product number	Coverage	M_w [g/mol]
1	50%	9938.2
2	70%	11633.4
3	90%	13328.7
4	100%	14176.3
5	50%	13737.8
6	70%	16952.9
7	90%	20168.0
8	100%	21775.5
9	50%	10330.1
10	70%	12182.1
11	90%	14034.1
12	100%	14960.1
13	50%	13876.3
14	70%	17146.9
15	90%	20417.4
16	100%	22052.7

From Figure 4.29, the general trend showed that water separation ratio increased for products with higher molecular weight. Products **7** and **16** were identified as some of the highest performing products for water separation in crude oil 1. These products can be seen to have some of the highest molecular weights, where product **16** had the highest. Conversely, the products with lower molecular weights had lower water separation. Similar trends could be observed for water separation results obtained in crude oil 2 and 3.
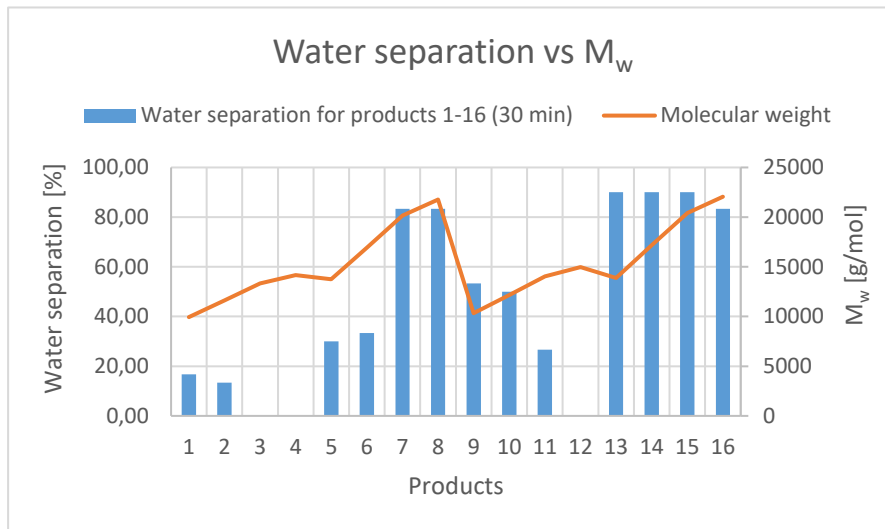
Figure 4. 29 Trend between water separation and molecular weight (M_w).

4.5   Interfacial tension

The interfacial tension (IFT) was investigated for the 90% coverage products, i.e. products **3**, **7**, **11**, and **15**, in a water-toluene system. Additionally, a commercial product from Schlumberger was measured and used as a reference. The IFT of water-toluene was measured to 34.1 mN/m. The results are reported in Figure 4.30.
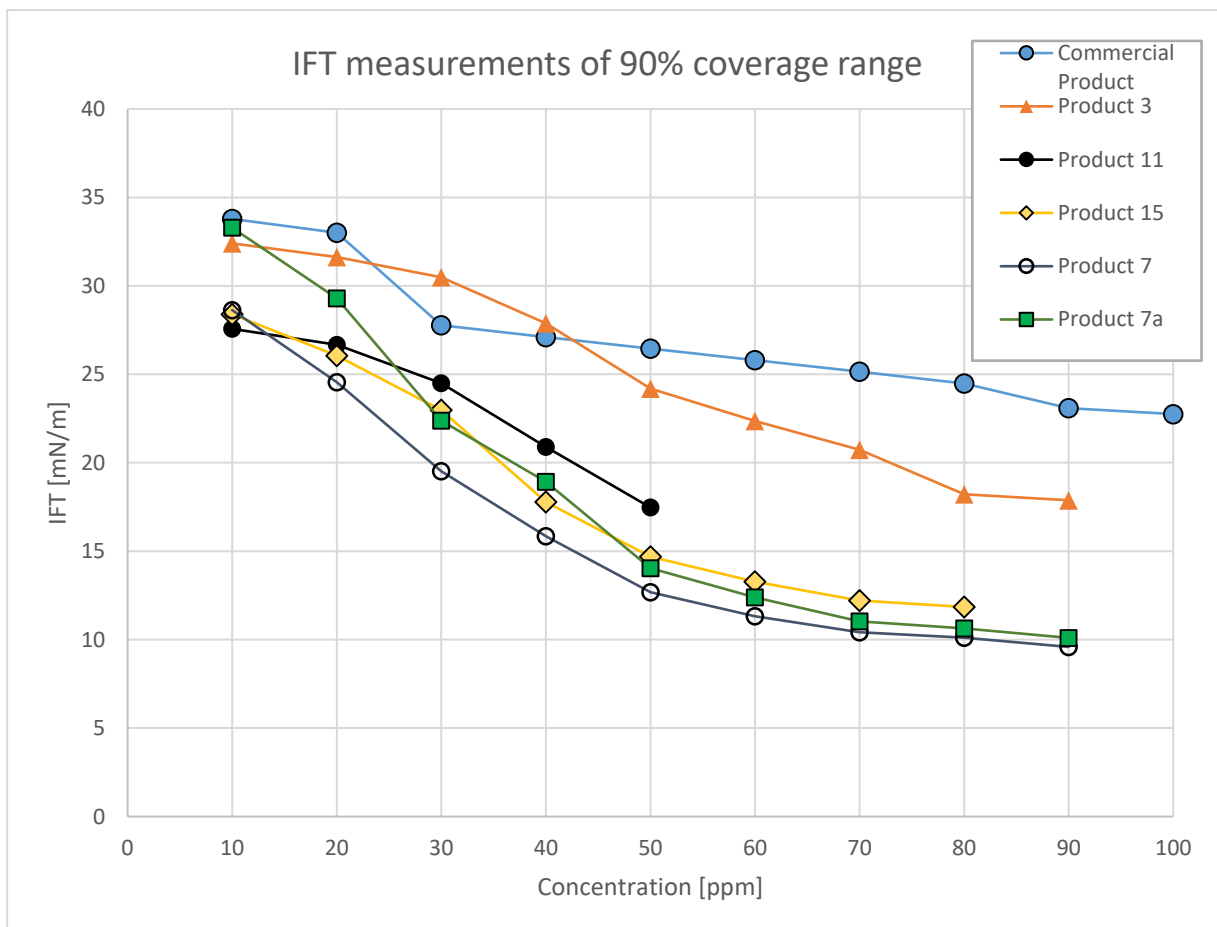
Figure 4. 30 IFT measurements in a water-toluene system for commercial product and products **3**, **7**, **7a**, **11**, and **15**.

Only a selection of products was tested. As the 90% coverage product range contains some of the best performing products, these were examined closer. The products were selected to have a constant coverage to examine the effect of different starting materials (A-D).

Very low concentrations were used in the measurements of IFT (10-100 ppm of 0.5% solutions). The measurements had to be performed below the critical micelle concentration (CMC). At higher concentrations, the IF was saturated instantly and no measurable testing could be done. This could be an indication of a very strong adsorption of the product to the IF.

However, others have reported occurrence of CMC around 200-800 ppm with polymeric demulsifiers [8]. The effect of dendritic demulsifiers has been studied, though with some varied results [9-11]. Dendrimer-based demulsifiers may have a more unique mechanism compared to conventional demulsifiers.

As the concentration of demulsifier was increased stepwise, the IFT was observed to decrease for all the products tested. This indicates a good interaction with the I, and hence the potential to work as demulsifiers.

Lowering of IFT has been correlated to performance measurements as discussed in Section 2.2.2. As the data indicate, products **7**, **7a**, and **15** lower the IFT further than the other products. This is also reflected in the bottle testing results, where these products are considered some of the most efficient. Product **7** and **7a** had very similar measurements, and could not be distinguished with regard to IFT.

Product **3** and **11** had both few EO groups. However, product **11** having a longer carbon chain had larger effect on the reduction of the IFT than product **3**.

The commercial product had the least effect on the IFT. This was not reflected in the bottle testing where the commercial product performed better than both products **3** and **11**. However, as the commercial product was a finished blend, the blend of chemicals might have interacted differently with the IF. Nevertheless, it is difficult to conclude why this phenomenon occurred.

4.6 Ecotoxicity

The ecotoxicity and biodegradation testing were performed by Schlumberger Ecotox Laboratory, Bergen. The results are reported in Table 4.14.

Table 4. 14 Results of toxicity and biodegradation testing. The product ranges are arranged after increasing coverage. *Samples were tested on day 29, not 28, as stated in the procedure (Section 3.2.6).

Product number	EO	R	OECD 306 Biodegradation	EC$_{50}$ *Skeletonema*	Classification
1			29%	> 96 mg/L	Y2
2	2.5	C$_{12/14}$	24%	80 mg/L	Y2
3			26%	82 mg/L	Y2
4			29%	> 45 mg/L	Y2
5			15%*	> 49 mg/L	Red
6	10	C$_{12/14}$	21%	> 28 mg/L	Y2
7			22%*	> 28 mg/L	Y2
8			23%*	> 25 mg/L	Y2
9			25%	> 151 mg/L	Y2
10	2	C$_{16/18}$	29%	> 99 mg/L	Y2
11			29%	155 mg/L	Y2
12			26%	45 mg/L	Y2
13			22%	12 mg/L	Y2
14	9	C$_{16/18}$	23%	32 mg/L	Y2
15			24%	31 mg/L	Y2
16			29%*	28 mg/L	Y2

Since it is the individual chemical's environmental properties that is important for classification, the active molecules have been screened for toxicity as well as biodegradation. The bioaccumulation is less important as the molecular weight of the dendrimers is much higher than 700 Da, which is considered as the size of molecules to pass lipophilic cell membranes.

The products (**1**-**16**) had a biodegradation between 20-30%, with the exception of product **5** (15%). A small increase in biodegradation with increasing percent coverage was observed in some cases, but the trend was not significant. No significant trends could be correlated to chemical structure changes between Boltorn H311 reacted with starting materials A-D.

All the products (**1**-**16**) obtained an EC$_{50}$ > 10 mg/L. The product ranges with higher numbers of EO units were found to be the most toxic. Product ranges **5**-**8** had an average EC$_{50}$ of 32.5 mg/L. An average EC$_{50}$ of 26 mg/L was recoded for product range **13**-**16**. The product ranges with lower degrees of ethoxylation (**1**-**4** and **9**-**12**) had average EC$_{50}$ of 76 and 112.5 mg/L, respectively. The effect of the carbon chain length was less significant.

The products were classified as Y2 chemicals (Yellow, level 2), with the exception of product **5** as the biodegradation was < 20%. Although yellow chemicals are often used without restriction in the North Sea, the products could not be classified as "green" or PLONOR chemicals (Pose Little or NO Risk to the marine environment).

4.7   Summary and Future Thoughts

In this thesis, 16 products were synthesized through esterification with Boltorn H311 and four different ethoxylated carboxylic acids. The four different starting materials were chosen utilizing a mathematical model in the Design-Expert® program.

Analytical techniques, such as GPC, IR, and NMR were used to confirm formation of the dendrimer products. The HLB has been used extensively in research of demulsifiers. The HLB values were theoretically calculated for the synthesised products, ranging from 2.01 to 9.52. The RSNs were determined experimentally, ranging from 2.4 to 6.1. The RSN was used as an experimental verification of the HLB. Physical properties of the products were determined by pH (3.7-4.3), density (1.018-1.085 g/cm^3), and solubility. The products were found the be soluble in both Solvesso 150 ND (20%) and BDGE (30%), while dispersible in deionized water (1%).

The demulsification performance of the products was measured utilizing bottle testing and the results were analysed by Expert-Design®. The Expert-Design® program was especially useful for elucidation of trends within the demulsifier testing results.

The product range (**1**-**16**) was tested in three different crude oils (1, 2, and 3). In the crude oil 1, the products were tested at 40 and 80 ppm. After analysis of the results, 80 ppm was recognized as the optimum dosage concentration. As such, the products were only tested at 80 ppm in crude oils 2 and 3 for comparison purposes.

Several products were observed to have good demulsification efficiency. Products **7** and **16** were identified as the best performing products. These two products had the same water separation efficiency in crude oil emulsion 1 (83.33%, 80 ppm, 30 min). However, product **7** had a significantly lower amount of residual emulsion (0.6 mL) compared to product **16** (1.2 mL), at 10 minutes. In crude oil 2, product **16** had a water separation ratio of 80%, while product **7** achieved 50% water separation. In crude oil 3, product **7** had a slightly higher water separation efficiency (36.67%) than product **16** (33.33%). The HLB and RSN of product **7** was determined to be 9.25 and 5.4, respectively. Product **16** had an HLB of 8.46 and RSN of 3.8. Thus, higher HLB (correlated to higher EO ratios) seemed to promote water separation.

Variations of product **7**, were tested where the residual starting material (B) was adjusted. Products **7a** and **7b** generally increased the performance of product **7** and reduced the amount of residual emulsion down to a trace amount in crude oil emulsions 1 and 2. The two additional products performed similarly with respects to water separation in crude oil 1 and 2 emulsions. However, product **7a** achieved a significantly higher separation ratio in crude oil 3 emulsion (65 min) and was therefore evaluated to be the overall best performing product. However, the physical and environmental properties of products **7a** and **7b** received relatively little attention in this work and should be further investigated.

Demulsification optimization was only studied for product **7** and should be extended to other products, such as product **16**, in the future. Additionally, the optimized products suggested in the numerical optimization model should be studied further. The performance of the starting materials was not measured in this thesis, but the results could offer valuable information of the demulsifier mechanism of the constituents of the products. The IFT was only investigated

for a selected group of products as the method was very time consuming. The IFT should naturally be measured for the full range of products and the individual starting materials.

Few results were found in the synergistic studies apart from the results of products **7a** and **7b**. The synergistic studies could be extended to testing with other polymeric demulsifiers.

Bottle testing is strictly a comparative method of testing. Therefore, other methods are often used in conjunction with bottle test to confirm the performance of the demulsifiers. Other methods often used are measurement of zeta potential, rheology, micropipette experiments, atomic force microscopy, turbidimetric measurements, and X-ray photoelectron spectroscopy [5, 12-14]. Results alone from these methods and others alike, will not necessarily translate to demulsifier performance. However, when related to results of bottle testing, information for these methods can be valuable. Such methods could be considered for future work.

The variable factors in the bottle testing were kept as constant as possible to obtain more consistent results. In future work, these may be changed or varied to more clearly observe the effect of different parameters. Such may include temperature, brine concentration and composition, mixing procedures of emulsions, addition of other natural or oil field production surfactants, asphaltenic content, and lower API gravity crude oils. Turbiscan could be used in future work to directly observe emulsion consistency and changes with added demulsifiers. Other physical parameters such as viscosity and surface tension may also be investigated.

The products had biodegradation ranging from 20 to 30%, with the exception of product **5** (15%). No significant trends were observed in the biodegradation results. All the products (**1**-**16**) obtained an $EC_{50} > 10$ mg/L. Ecotoxicity was found to increase with higher degrees of ethoxylation. Having the lowest number of EO units, products **9**-**12** had the highest average EC_{50} (112.5 mg/L) and hence the lowest toxicity. The majority of the products were classified as Y2. In future work, extended biodegradation testing should be performed in order to improve the environmental profile even further.

4.8 References

1. D.C. Montgomery, *Design and Analysis of Experiments*. 9th ed. 2017, New Jersey, U.S.A: John Wiley & Sons.
2. C. Wu, ed. *Handbook of Size Exclusion Chromatography and Related Techniques*. 2nd ed. 2004, Marcel Dekker: New York, U.S.A.
3. D.A. Skoog, F.J. Holler, and S.R. Crouch, *Principles of Instrumental Analysis*. 6th ed. 2017, Canada: Cole Cengage Learning.
4. L.L. Schramm, *Emulsions, Foams, and Suspensions: Fundamentals and Applications*. 2005, Germany: John Wiley & Sons.
5. E. Pensini, et al., *Demulsification Mechanism of Asphaltene-Stabilized Water-in-Oil Emulsions by a Polymeric Ethylene Oxide–Propylene Oxide Demulsifier.* Energy & Fuels, 2014. **28**(11): p. 6760-6771.
6. V.K. Rajak, et al., *Optimization of Separation of Oil from Oil-in-Water Emulsion by Demulsification Using Different Demulsifiers.* Petroleum Science and Technology, 2016. **34**(11-12): p. 1026-1032.
7. C.S. Shetty, et al., *Demulsification of Water in Oil Emulsions Using Water Soluble Demulsifiers.* Journal of Dispersion Science and Technology, 1992. **13**(2): p. 121-133.
8. A.M. Al-Sabagh, E. Elsharaky, and A.E. El-Tabey, *Demulsification Performance and the Relative Solubility Number (RSN) of Modified Poly (Maleic Anhydride-alt-1-dodecene) on Naturally Asphaltenic Crude Oil Emulsion.* Journal of Dispersion Science and Technology, 2017. **38**(2): p. 288-295.
9. Y. Bi, et al., *Dendrimer-Based Demulsifiers for Polymer Flooding Oil-in-Water Emulsions.* Energy & Fuels, 2017. **31**(5): p. 5395-5401.
10. J. Wang, et al., *Demulsification of Crude Oil Emulsion Using Polyamidoamine Dendrimers.* Separation Science and Technology, 2007. **42**(9): p. 2111-2120.
11. X. Yao, et al., *Synthesis of a Novel Dendrimer-Based Demulsifier and its Application in the Treatment of Typical Diesel-in-Water Emulsions with Ultrafine Oil Droplets.* Energy & Fuels, 2014. **28**(9): p. 5998-6005.
12. D. Pradilla, S.b. Simon, and J. Sjöblom, *Mixed Interfaces of Asphaltenes and Model Demulsifiers, Part II: Study of Desorption Mechanisms at Liquid/Liquid Interfaces.* Energy & Fuels, 2015. **29**(9): p. 5507-5518.
13. F. Shehzad, et al., *Polymeric Surfactants and Emerging Alternatives used in the Demulsification of Produced Water: A Review.* Polymer Reviews, 2018. **58**(1): p. 63-101.
14. D. Daniel-David, et al., *Elastic Properties of Crude Oil/Water Interface in Presence of Polymeric Emulsion Breakers.* Colloids and Surfaces A: Physicochemical and Engineering Aspects, 2005. **270**: p. 257-262.

5 Conclusion

In this thesis, 16 products were synthesised and evaluated using different techniques. Boltorn H311 was reacted with four different alkyl ether carboxylic acids, where the coverages of the dendrimer were 50, 70, 90 and 100%. A robust 2-step procedure using AN titration for reaction progress monitoring was established. The chemical structures were evaluated by IR, NMR, and GPC. Esterification of Boltorn H311 were confirmed by IR and GPC. The NMR spectra confirmed that Boltorn H311 and reactant (starting materials A-D) were intact in the product. The GPC results were also used in the detection of residual starting material in the products. The physical properties were studied by pH, density, RSN, HLB, and ANs.

The products (**1**-**16**) were subjected to extensive performance testing utilizing bottle testing method. The demulsification efficiency was measured for the products in three different crude oils. Included in this testing were two additional products (**7a**, **7b**) that were optimized versions of product **7**. A dosage concentration of 80 ppm was found to enhance the water separation efficiency. The results were also evaluated using the Design-Expert® program, providing predictions of optimized products. Higher degrees of ethoxylation were found to have the strongest effect on water separation efficiency. Generally, longer R groups seemed to slightly increase the water separation. The best performing products had 90 or 100% coverage.

Products **7** and **16** were identified to have the highest demulsification efficiencies. In crude oil 1, these products had a separation efficiency of 83.33%. In crude oil 2, the water separation of product **7** and **16** were recorded to be 50 and 80%, respectively. Lastly, the separation efficiency measured in crude oil 3 for these products, was 36.67 and 33.33% respectively. The two products had low amounts of residual emulsion across the bottle tests, although the lowest amount was recorded for product **7**.

The optimized products **7a** and **7b** had generally higher performance than product **7**. In the crude oil 1 emulsion these products had water separation efficiencies of 83.33 and 96.67%, respectively. The products were measured to have a 60% separation ratio in crude oil 2. In the crude oil 3 emulsion, product **7a** and **7b** had water separation efficiency of 46.67 and 26.67%, respectively. However, product **7a** were evaluated to have the overall best performance, having both high water separation efficiency and low amounts of residual emulsion.

The HLB of products **7** and **16** were found to be 9.25 and 8.46, respectively. These values were some of the highest across the product range (**1**-**16**). Being a measure of EO content, water separation was generally observed to increase with increasing HLB. The two products had RSNs of 5.4 and 3.8, respectively. The RSN was observed to decrease with increasing HLB and percentage coverage.

IFT measurement were conducted for the 90% coverage range (products **3**, **7**, **7a**, **11**, and **15**). Product **7a** reduced the IFT the most, which related well to the product having the highest demulsification performance. The IFT was reduced approximately 24 mN/m by product **7a**.

Product **3**, having the lowest demulsification performance out of these products, reduced the IFT the least.

The products had biodegradation ranging from 20 to 30%, with the exception of product **5** (15%). All the products (**1**-**16**) obtained an $EC_{50} > 10$ mg/L. Ecotoxicity was found to increase with higher degrees of ethoxylation. The product ranges (**13**-**16**, **5**-**8**, **1**-**4**, and **9-12**) had average EC_{50} of 25, 32.5, 76, and 112.5 mg/L, respectively. Fifteen of the products were classified as Y2.

Appendix A

Table A. 1 Results of acid numbers and amounts of water collected, related to experimental data.

Starting materials	Product number	Coverage	Equivalences	Moles			$m_{Boltorn\ H311}$ [g]	$m_{Starting\ material}$ [g]	m_{DDBSA} [g]	Reaction time [hours]	Acid Number	Water collected [g]
				Boltorn H311	Starting material	DDBSA						
Boltorn H311 + Starting material A	1	50%	11,5	0.01585	0.1823	0.01456	100.4	64.6	4.9	5.50	5.1	8.38
	2	70%	16,1	0.01587	0.2555	0.01693	100.5	90.6	5.7	4.50	5.23	11.80
	3	90%	20,7	0.01582	0.3275	0.01931	100.2	116.4	6.5	7.75	4.99	13.37
	4	100%	23	0.01584	0.3642	0.02020	100.3	129.3	6.8	5.25	7.23	19.20
Boltorn H311 + Starting material B	5	50%	11,5	0.01592	0.1830	0.02020	100.8	126.9	6.8	8.25	5.23	22.77
	6	70%	16,1	0.01584	0.2550	0.02466	100.3	177.7	8.3	8.25	6.16	24.75
	7	90%	20,7	0.01579	0.3268	0.02911	100.0	228.4	9.8	8.00	8.08	33.13
	8	100%	23	0.01581	0.3635	0.03149	100.1	253.8	10.6	8.00	8.44	33.97
Boltorn H311 + Starting material C	9	50%	11,5	0.01582	0.1819	0.01545	100.2	73.1	5.2	8.00	4.04	8.53
	10	70%	16,1	0.01585	0.2552	0.01812	100.4	104.5	6.1	6.50	8.17	7.82
	11	90%	20,7	0.01584	0.3278	0.02050	100.3	131.6	6.9	7.00	5.25	12.98
	12	100%	23	0.01581	0.3635	0.02198	100.1	146.2	7.4	7.00	4.98	15.83
Boltorn H311 + Starting material D	13	50%	11,5	0.01585	0.1823	0.02020	100.4	129.1	6.8	7.25	4.75	19.65
	14	70%	16,1	0.01737	0.2796	0.02733	110.0	199.0	9.2	7.25	4.62	29.87
	15	90%	20,7	0.01582	0.3275	0.02941	100.2	232.8	9.9	8.00	5.18	29.98
	16	100%	23	0.01584	0.3642	0.03179	100.3	258.7	10.7	7.75	6.17	33.91

Appendix B
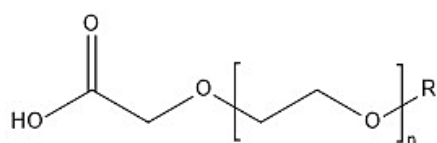
Starting Material A, n = 2.5, R = C_{12} / C_{14}

1a. Staring material A, n = 2, R = C_{12}
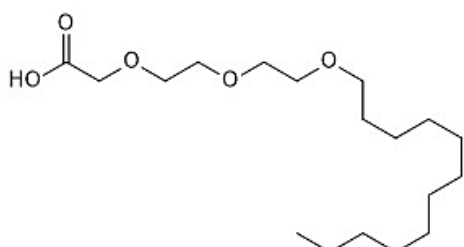
2-(2-(2-(dodecyloxy)ethoxy)ethoxy)acetic acid
Chemical Formula: $C_{18}H_{36}O_5$
Molecular Weight: 332,48 g/mol

1b. Staring material A, n = 2, R = C_{14}
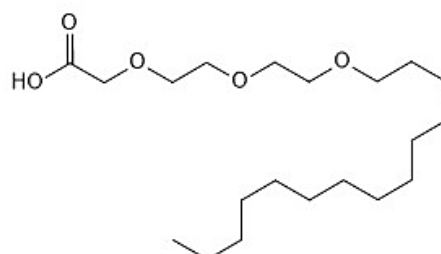
2-(2-(2-(tetradecyloxy)ethoxy)ethoxy)acetic acid
Chemical Formula: $C_{20}H_{40}O_5$
Molecular Weight: 360,54 g/mol

2a. Starting material A, n = 3, R = C_{12}
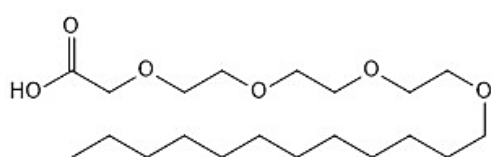
3,6,9,12-tetraoxatetracosanoic acid
Chemical Formula: $C_{20}H_{40}O_6$
Molecular Weight: 376,53 g/mol

2b. Starting material A, n = 3, R = C_{14}
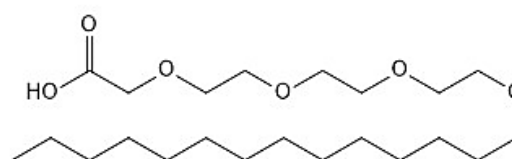
3,6,9,12-tetraoxahexacosanoic acid
Chemical Formula: $C_{22}H_{44}O_6$
Molecular Weight: 404,59 g/mol

Average Molecular Weight: 368.535 g/mol

Figure B. 1 Calculated average molecular weight of starting material A.
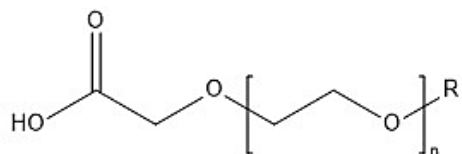
Starting Material B, n = 10, R = C_{12} / C_{14}

1. Starting material B, n = 10, R = C_{12}
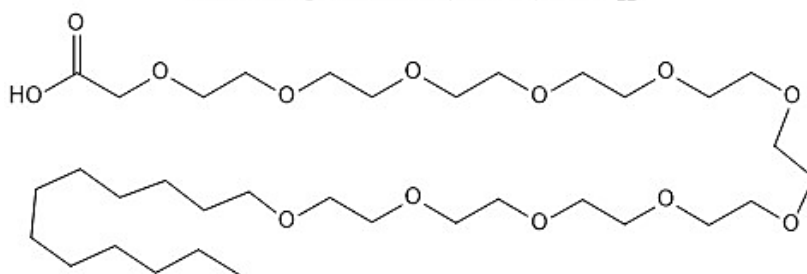
3,6,9,12,15,18,21,24,27,30,33-undecaoxapentatetracontanoic acid
Chemical Formula: $C_{34}H_{68}O_{13}$
Molecular Weight: 684,91 g/mol

2. Starting material, n = 10, R = C_{14}
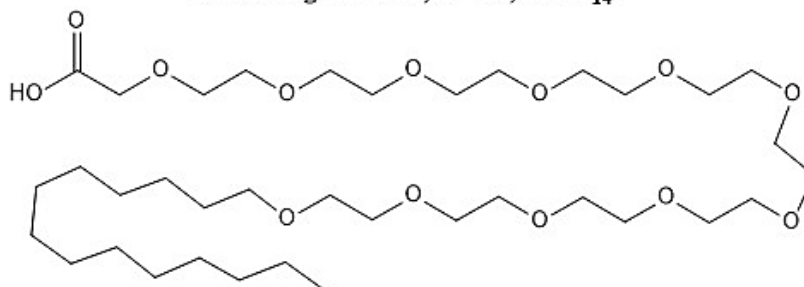
3,6,9,12,15,18,21,24,27,30,33-undecaoxaheptatetracontanoic acid
Chemical Formula: $C_{36}H_{72}O_{13}$
Molecular Weight: 712,96 g/mol

Average Molecular Weight: 698,935 g/mol

Figure B. 2 Calculated average molecular weight of starting material B.
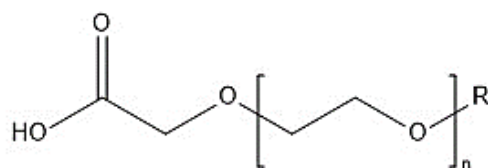
Starting Material C, n = 2, R = C$_{16}$ / C$_{18}$

1. Starting material C, n = 2, R = C$_{16}$
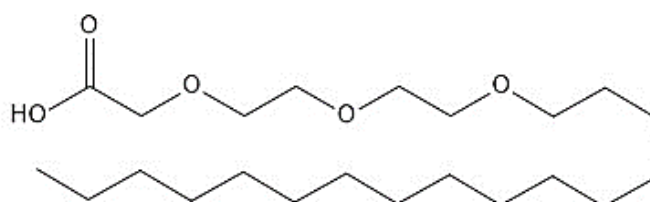
2-(2-(2-(hexadecyloxy)ethoxy)ethoxy)acetic acid
Chemical Formula: C$_{22}$H$_{44}$O$_5$
Molecular Weight: 388,59 g/mol

2. Starting material C, n = 2, R = C$_{18}$
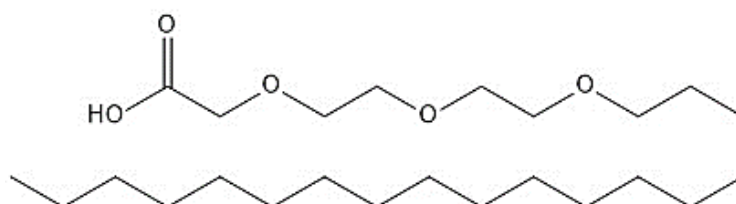
2-(2-(2-(octadecyloxy)ethoxy)ethoxy)acetic acid
Chemical Formula: C$_{24}$H$_{48}$O$_5$
Molecular Weight: 416,64 g/mol

Average Molecular Weight: 402.615 g/mol

Figure B. 3 Calculated average molecular weight of starting material C.
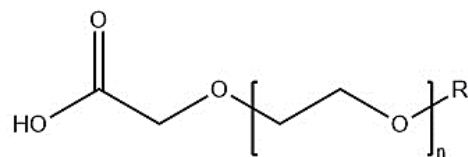
Starting Material D, n = 9, R = C$_{16}$ / C$_{18}$

1.Starting material D, n = 9, R = C$_{16}$
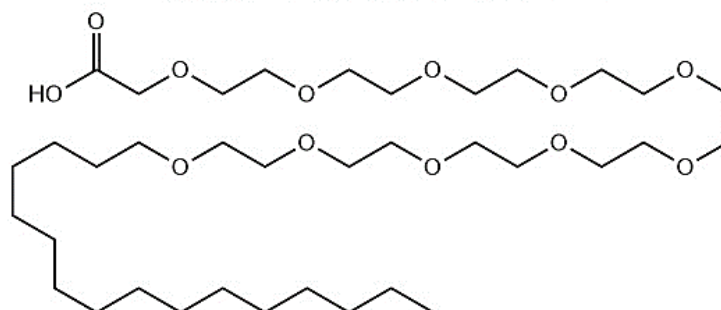
3,6,9,12,15,18,21,24,27,30-decaoxahexatetracontanoic acid
Chemical Formula: C$_{36}$H$_{72}$O$_{12}$
Molecular Weight: 696,96 g/mol

2. Starting material D, n = 9, R = C$_{18}$
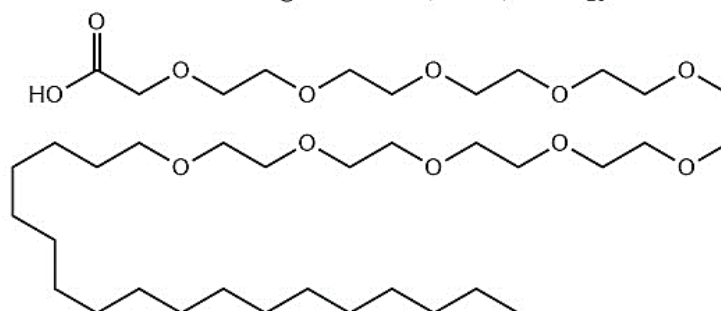
3,6,9,12,15,18,21,24,27,30-decaoxaoctatetracontanoic acid
Chemical Formula: C$_{38}$H$_{76}$O$_{12}$
Molecular Weight: 725,01 g/mol

Average Molecular Weight: 710.985 g/mol

Figure B. 4 Calculated average molecular weight of starting material C.

Appendix C
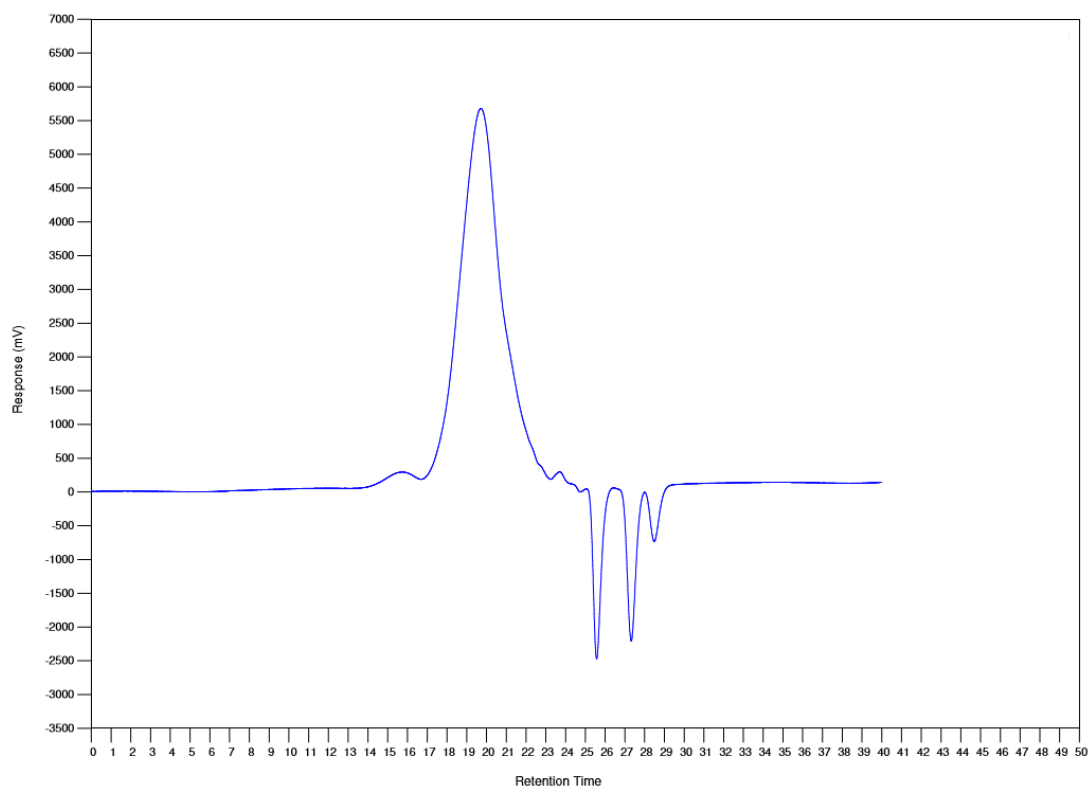
Figure C. 1 GPC spectrum of Boltorn H311.
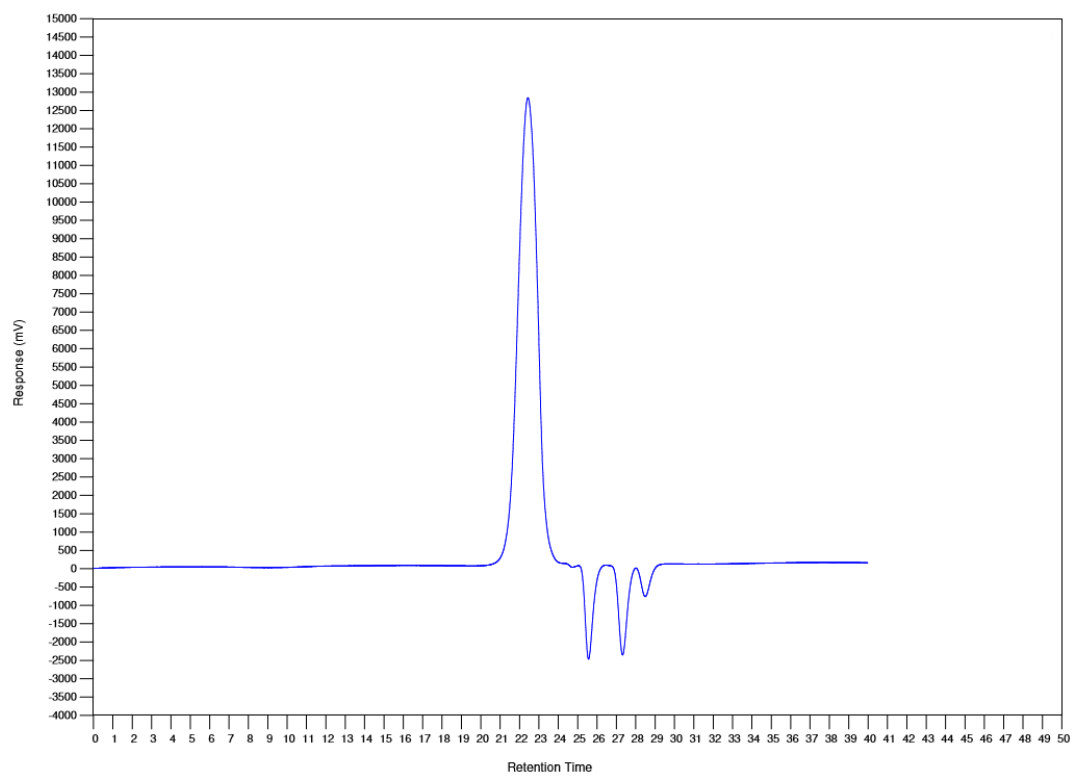
Figure C. 2 GPC spectrum of starting material A.
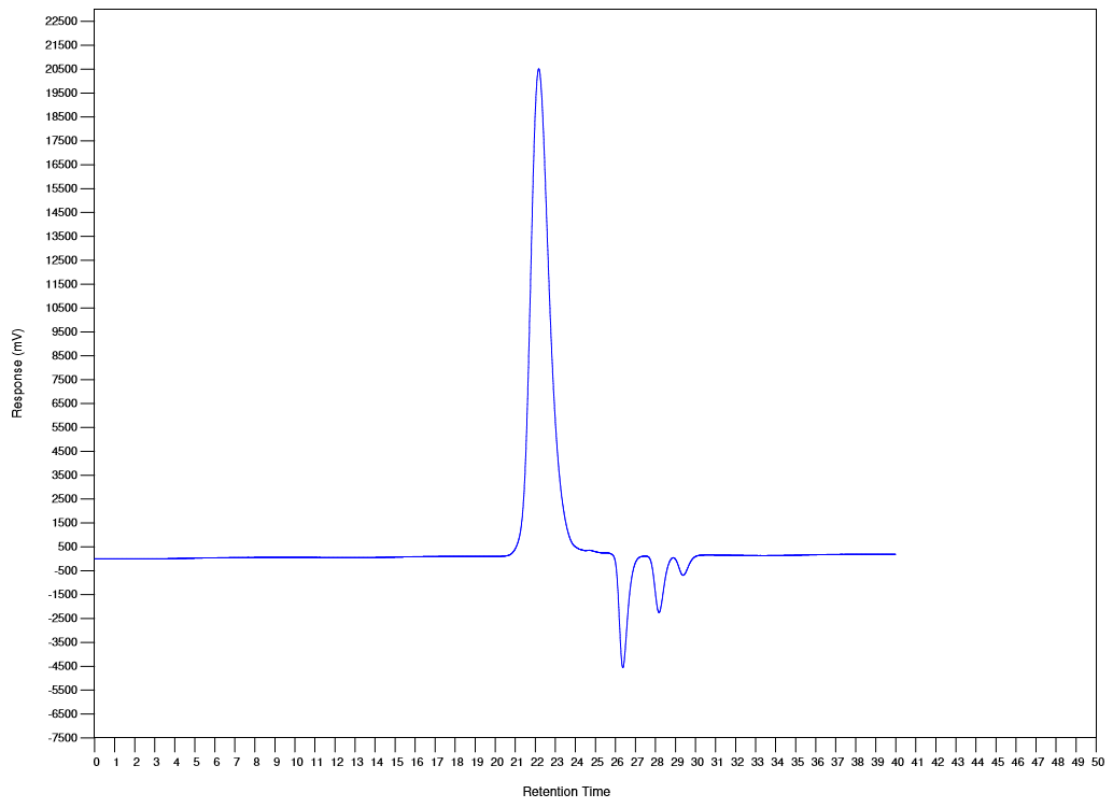
Figure C. 3 GPC spectrum of starting material B.
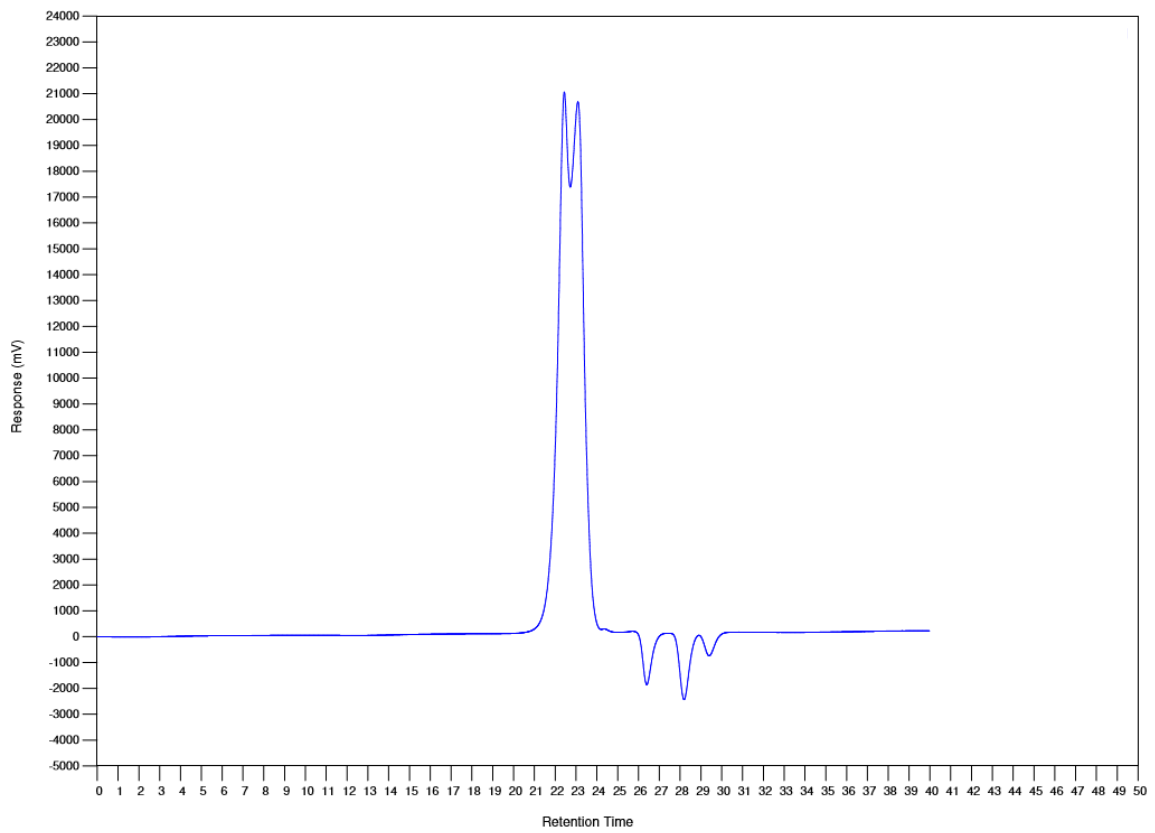
Figure C. 4 GPC spectrum of starting material C.
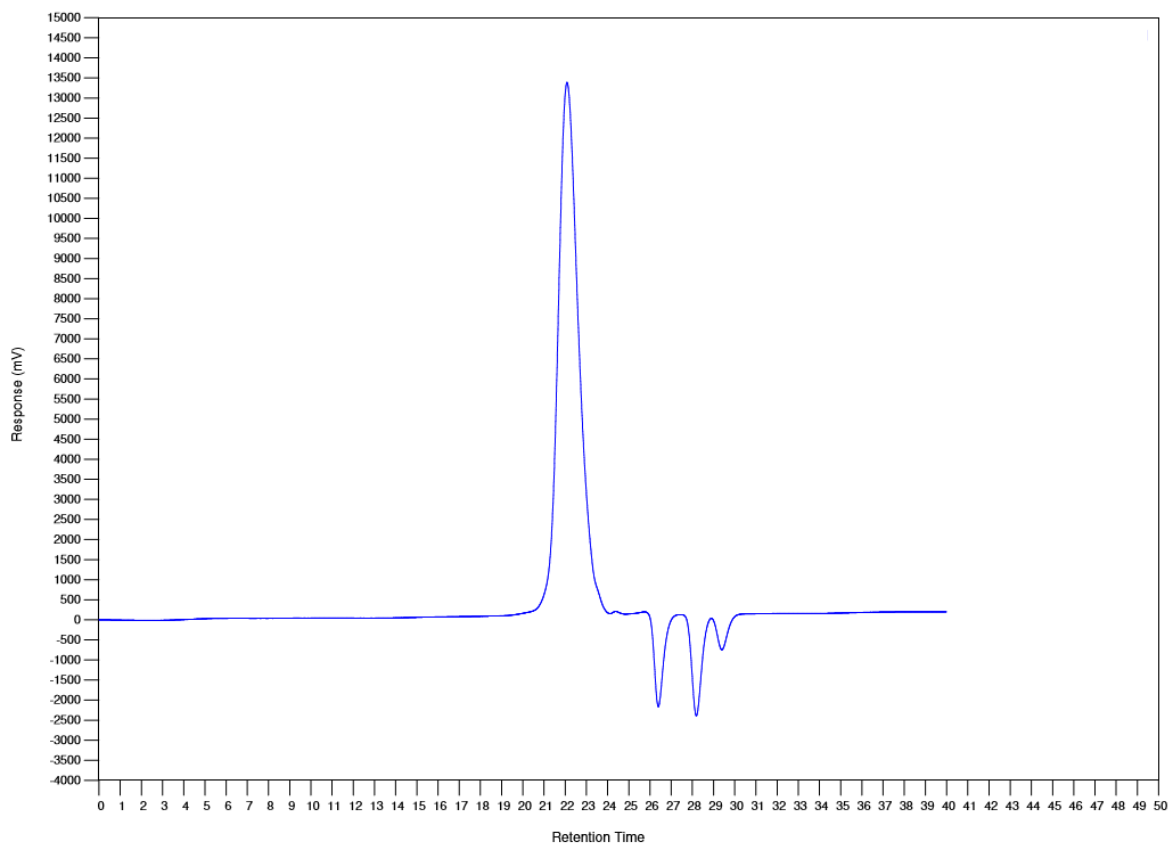
Figure C. 5 GPC spectrum of starting material D.
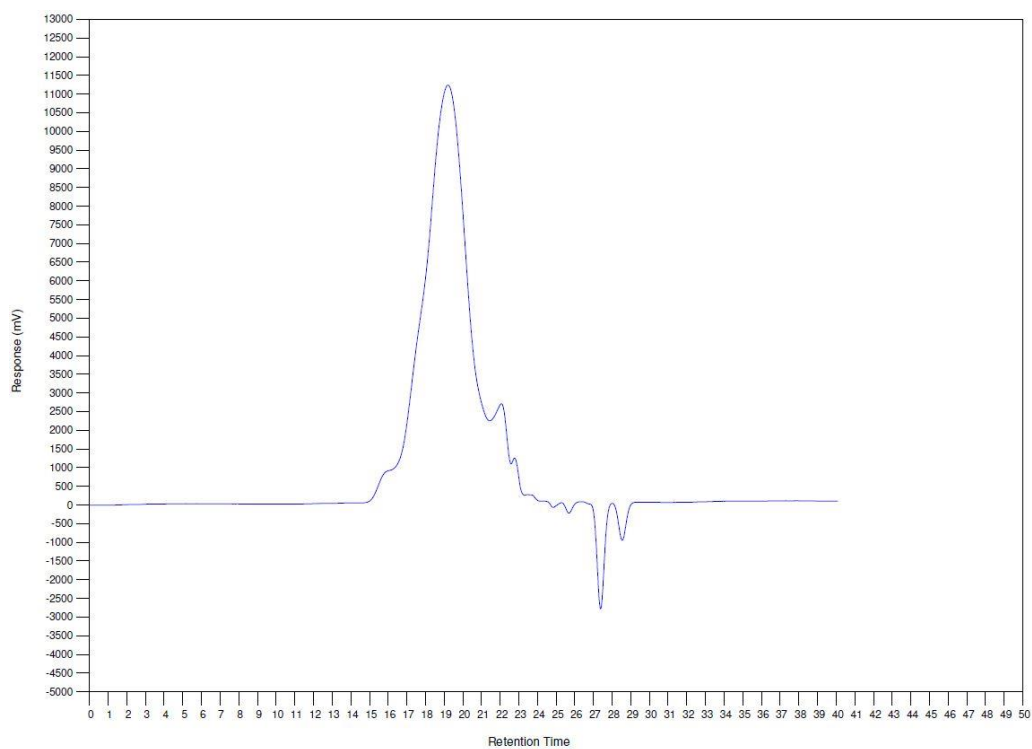
Figure C. 6 GPC spectrum of product **1**.
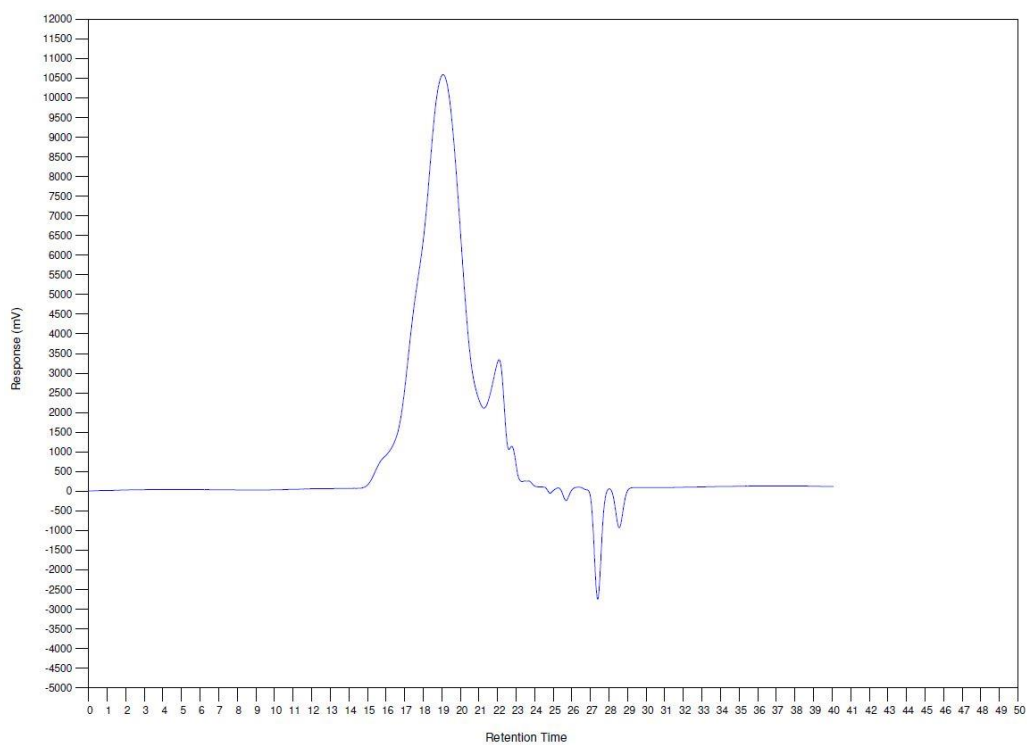
Figure C. 7 GPC spectrum of product **2**.
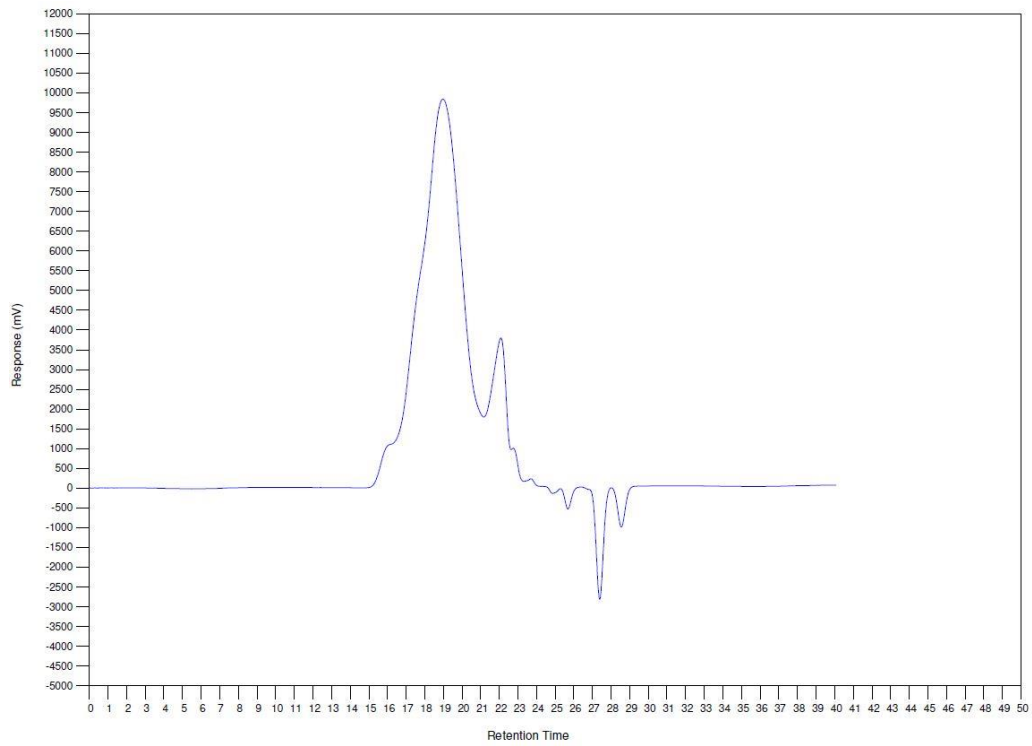
Figure C. 8 GPC spectrum of product **3**.
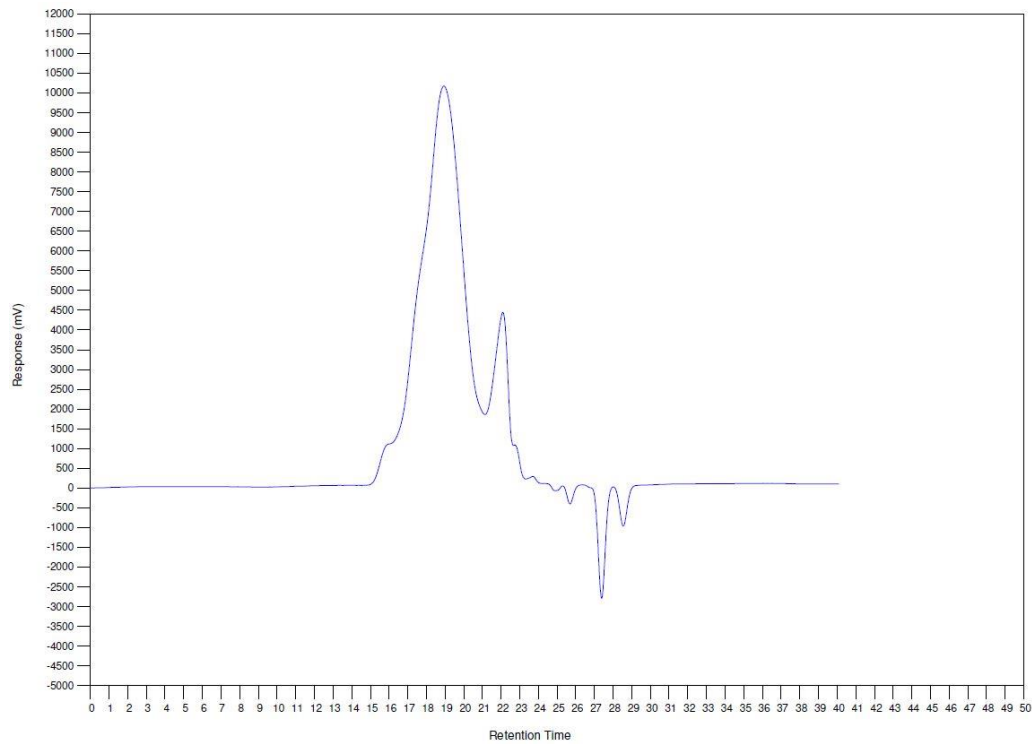
Figure C. 9 GPC spectrum of product **4**.
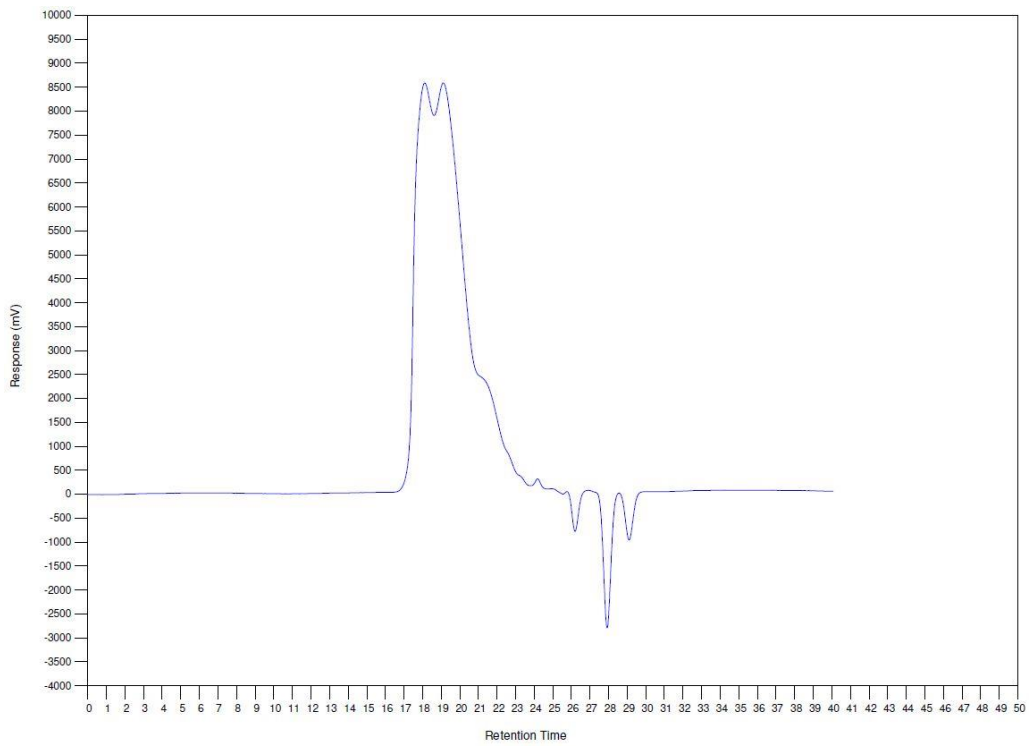
Figure C. 10 GPC spectrum of product **5**.
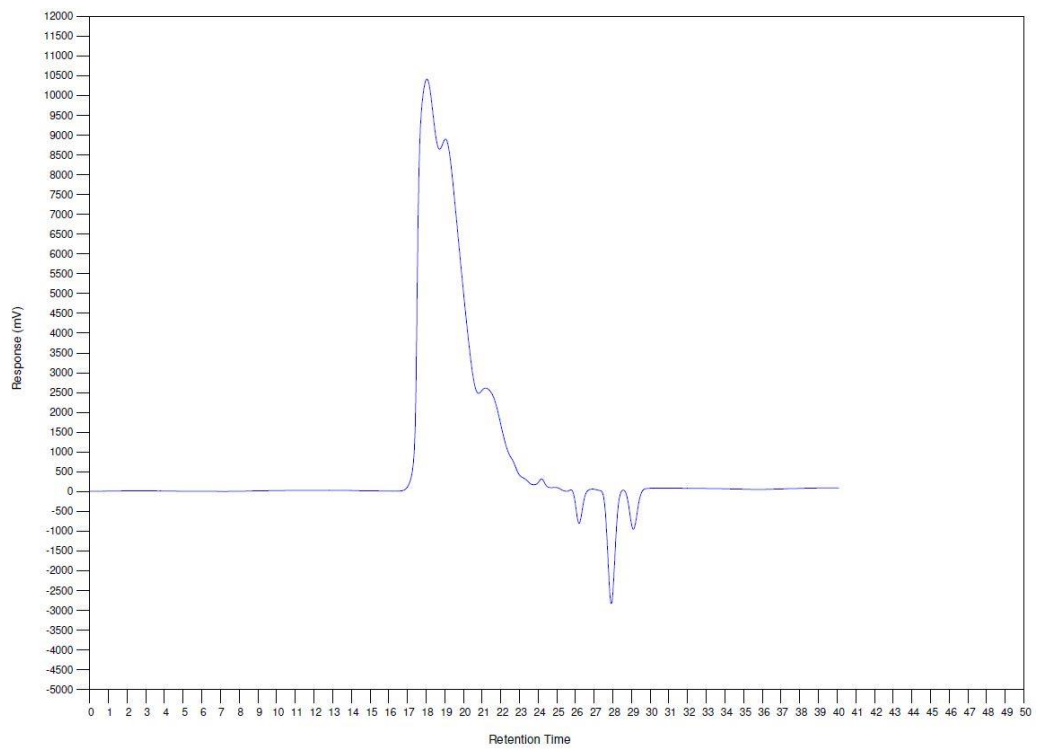
Figure C. 11 GPC spectrum of product **6**.

XI
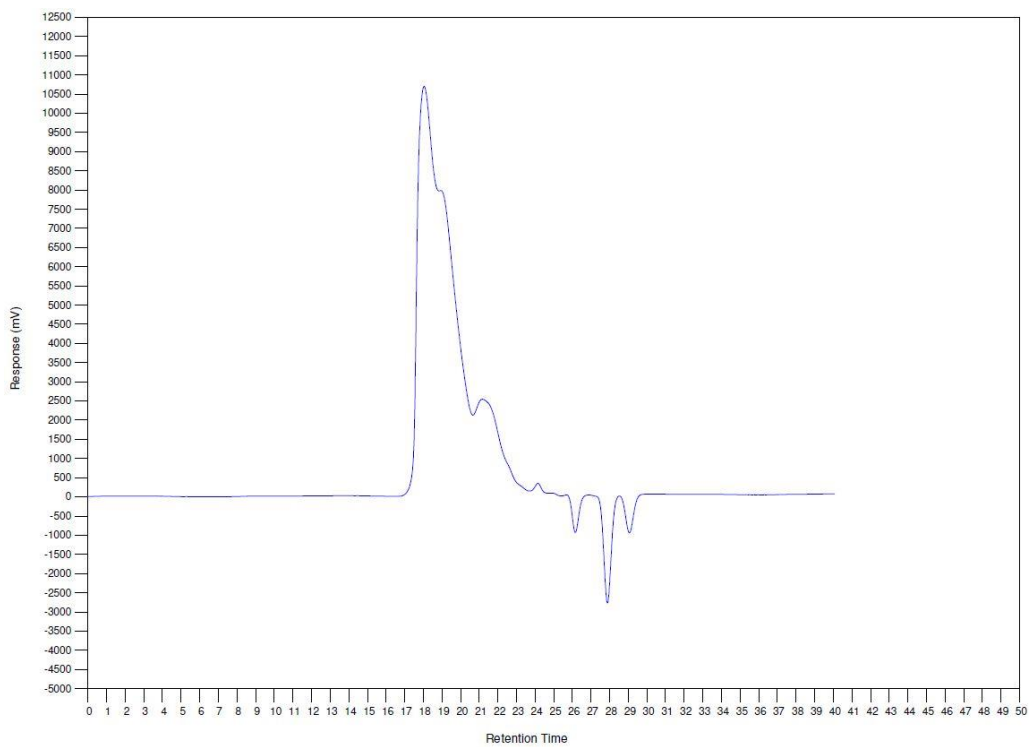
Figure C. 12 GPC spectrum of product **7**.
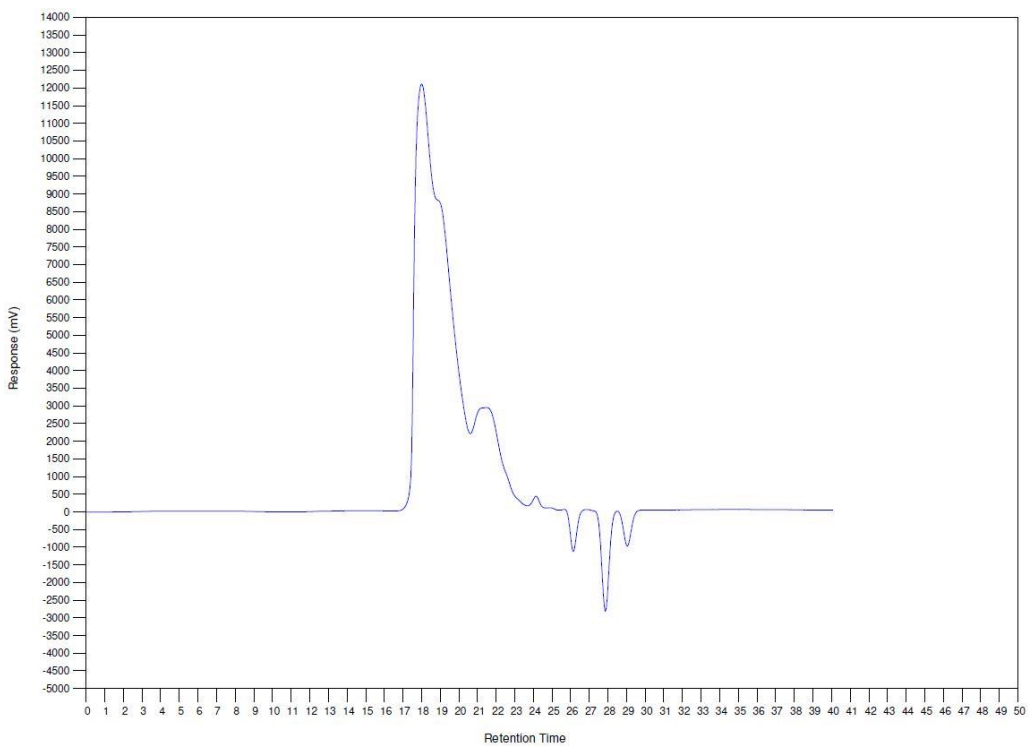
Figure C. 13 GPC spectrum of product **8**.
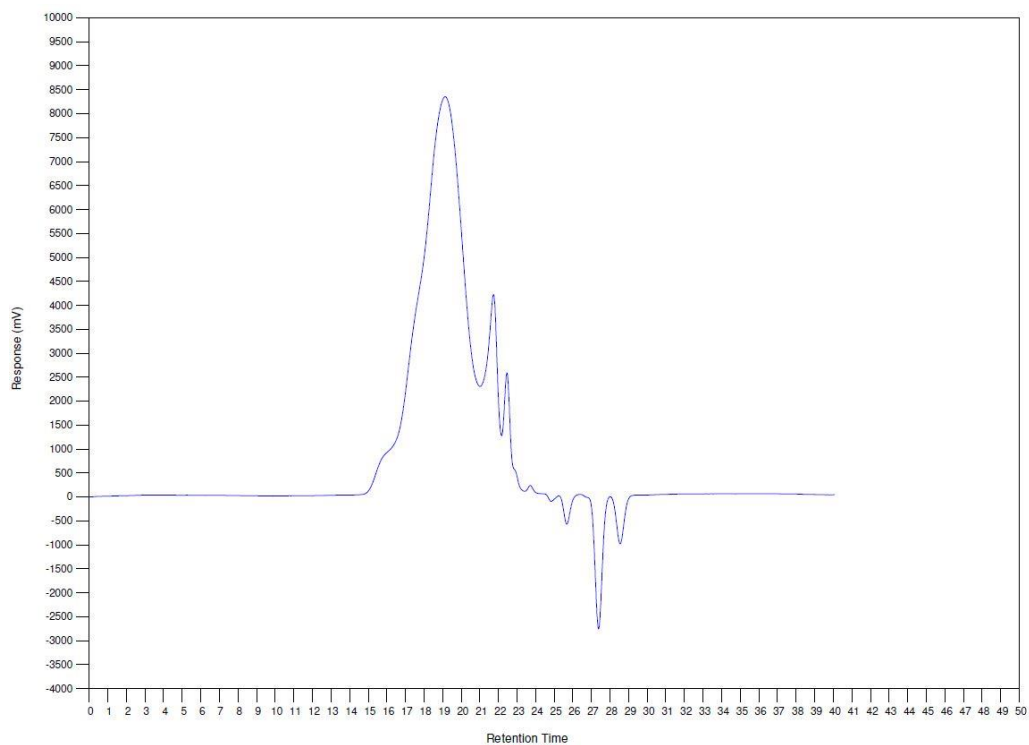
Figure C. 14 GPC spectrum of product **9**.
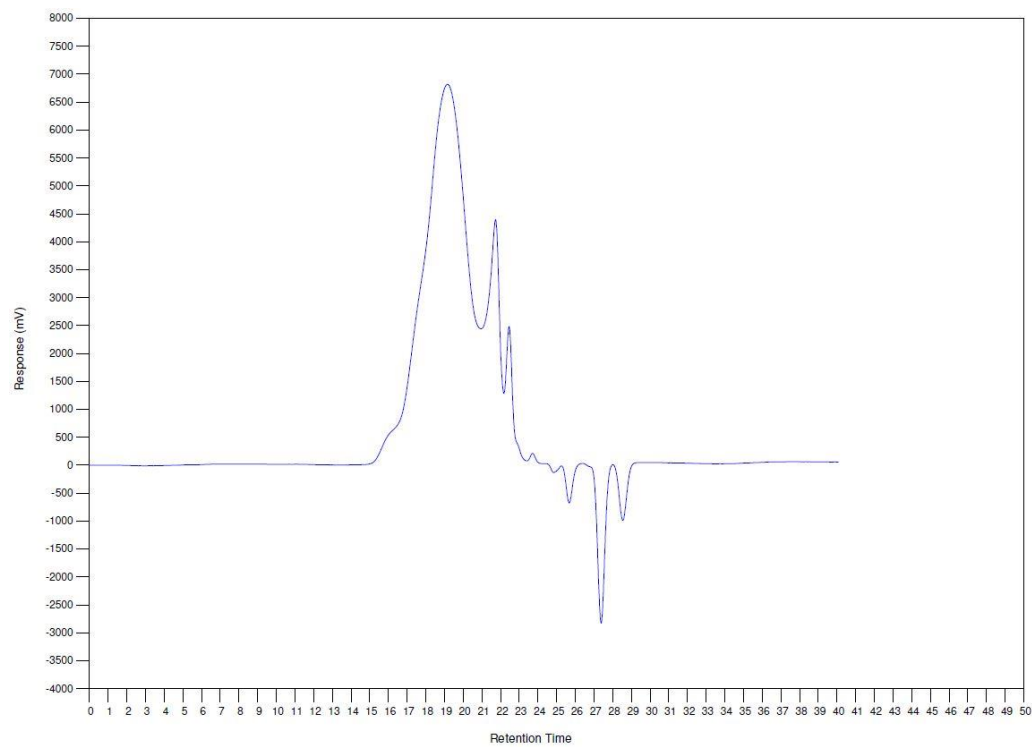
Figure C. 15 GPC spectrum of product **10**.
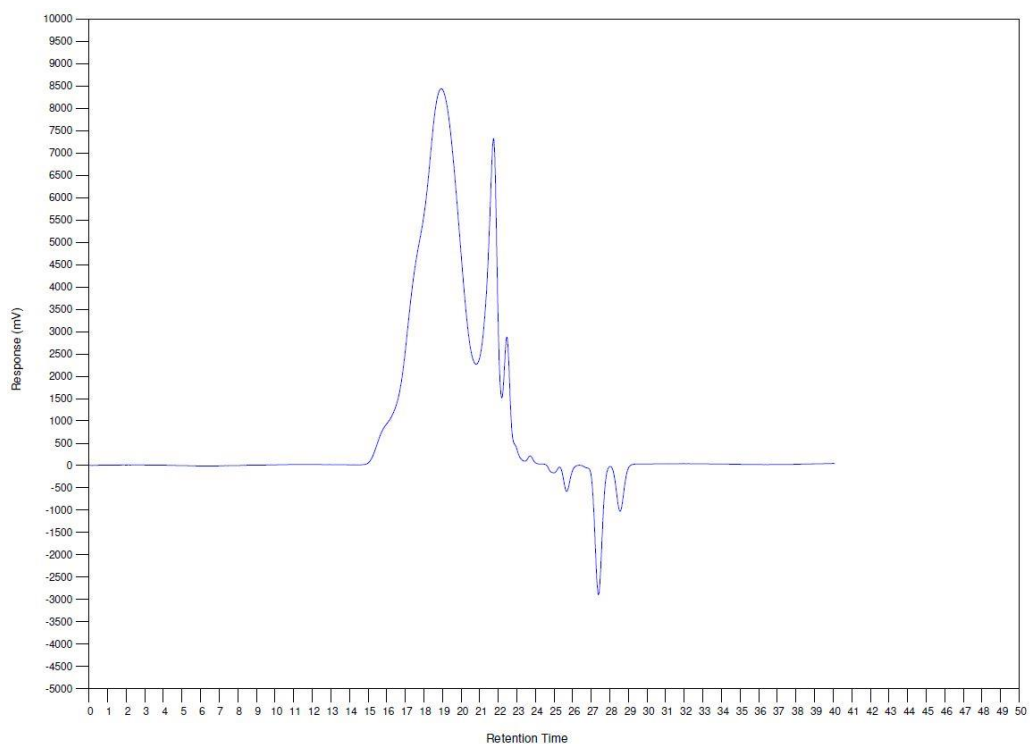
Figure C. 16 GPC spectrum of product **11**.
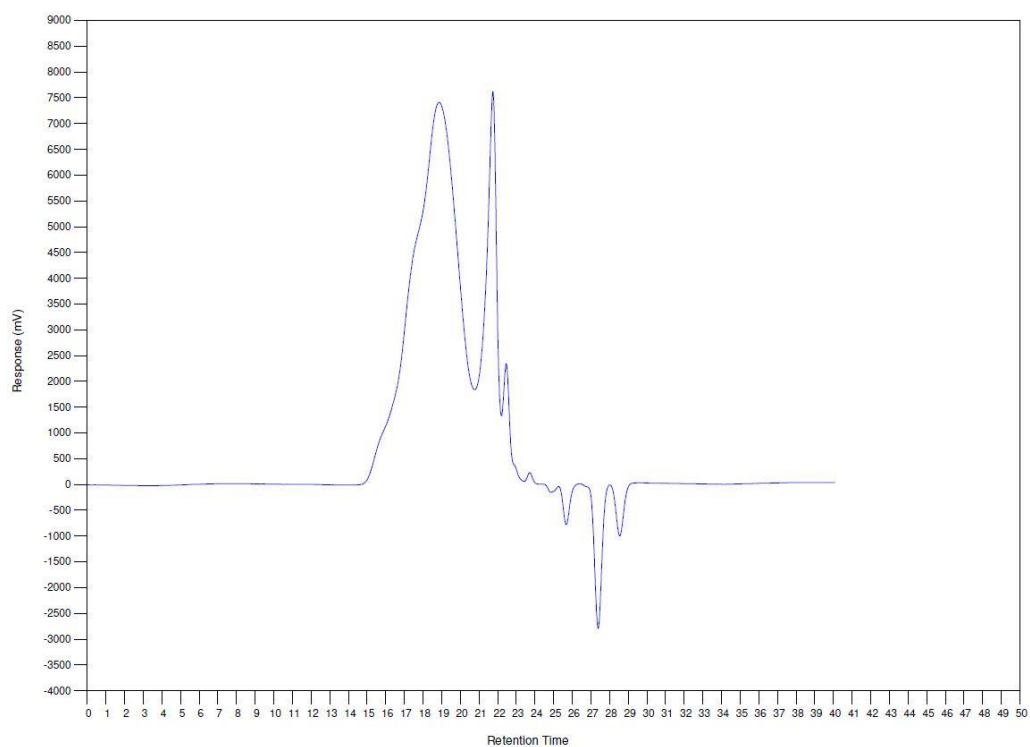
Figure C. 17 GPC spectrum of product **12**.

XIV
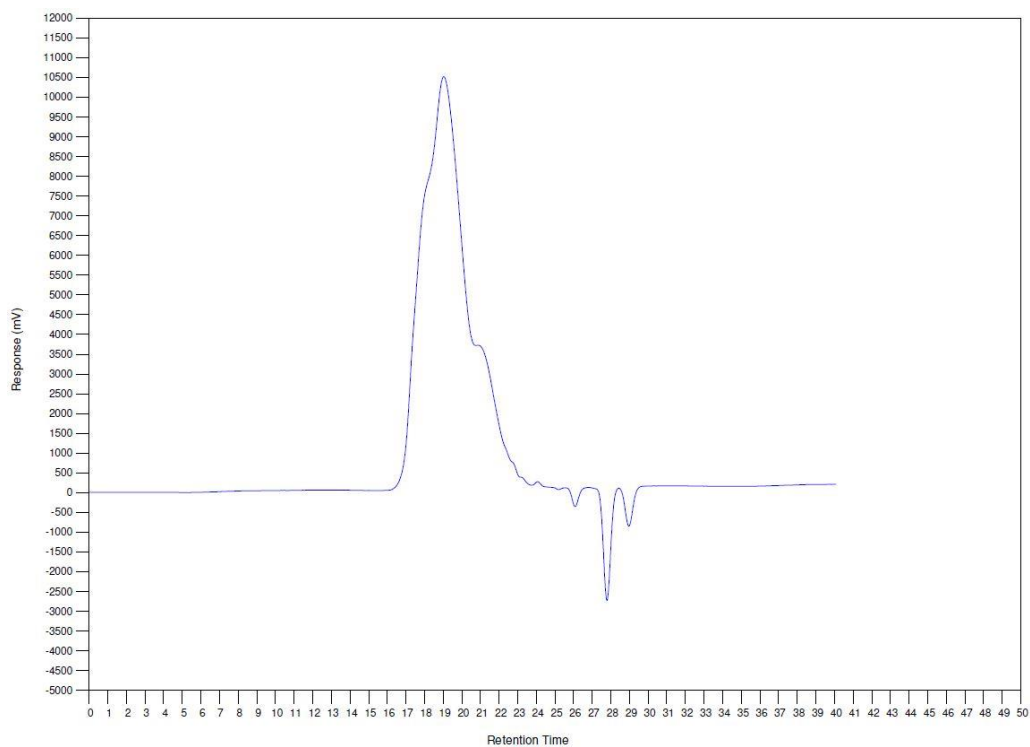
Figure C. 18 GPC spectrum of product **13**.
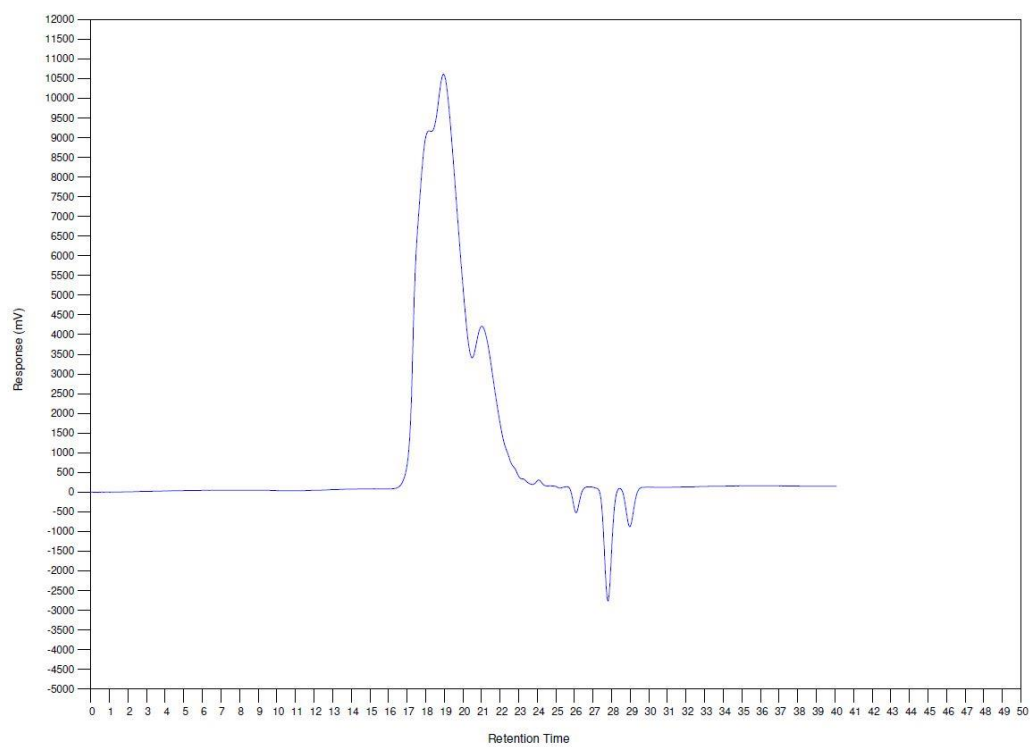
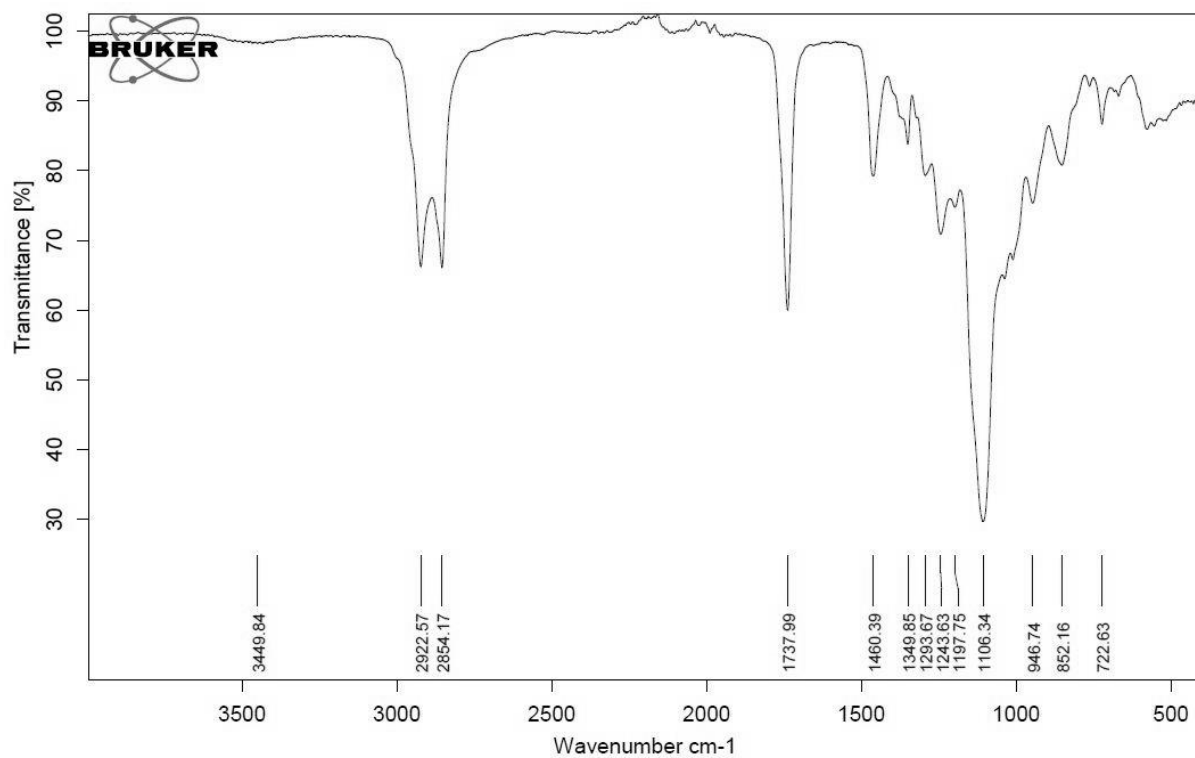Figure C. 19 GPC spectrum of product **14**.
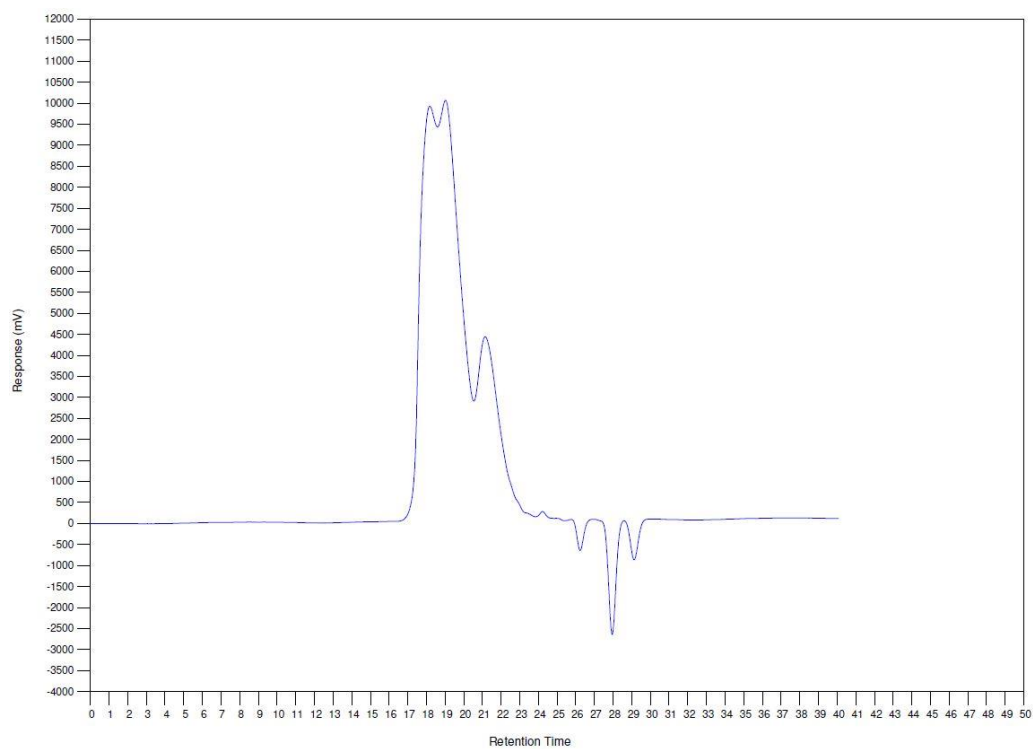
Figure C. 20 GPC spectrum of product **15**.
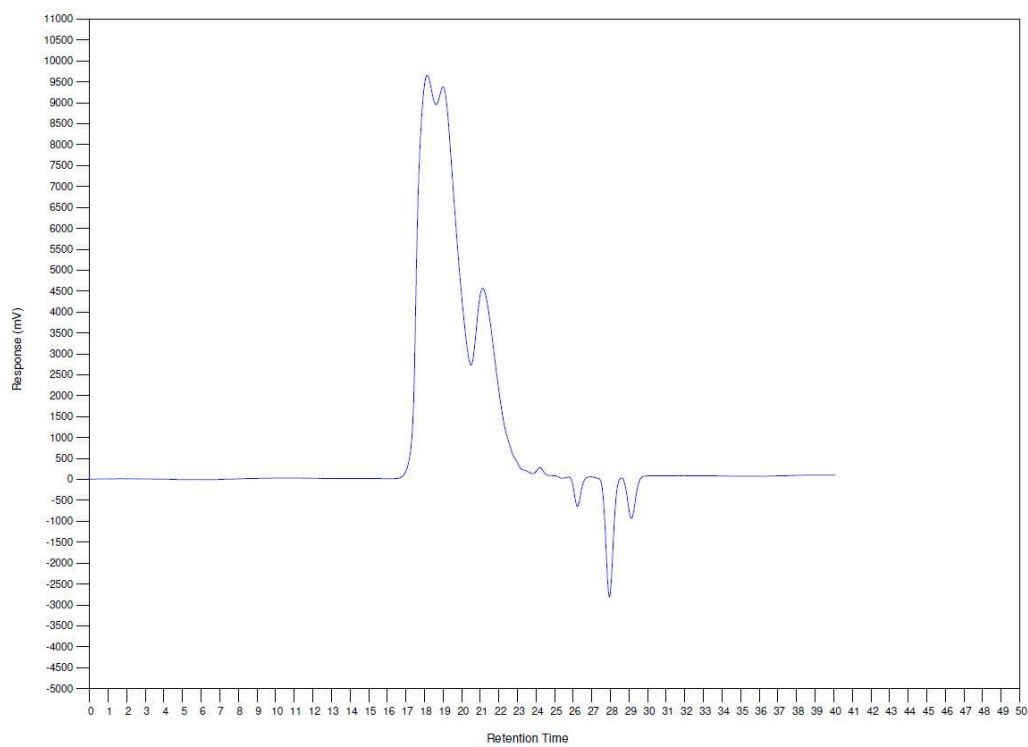
Figure C. 21 GPC spectrum of product **16**.

Appendix D
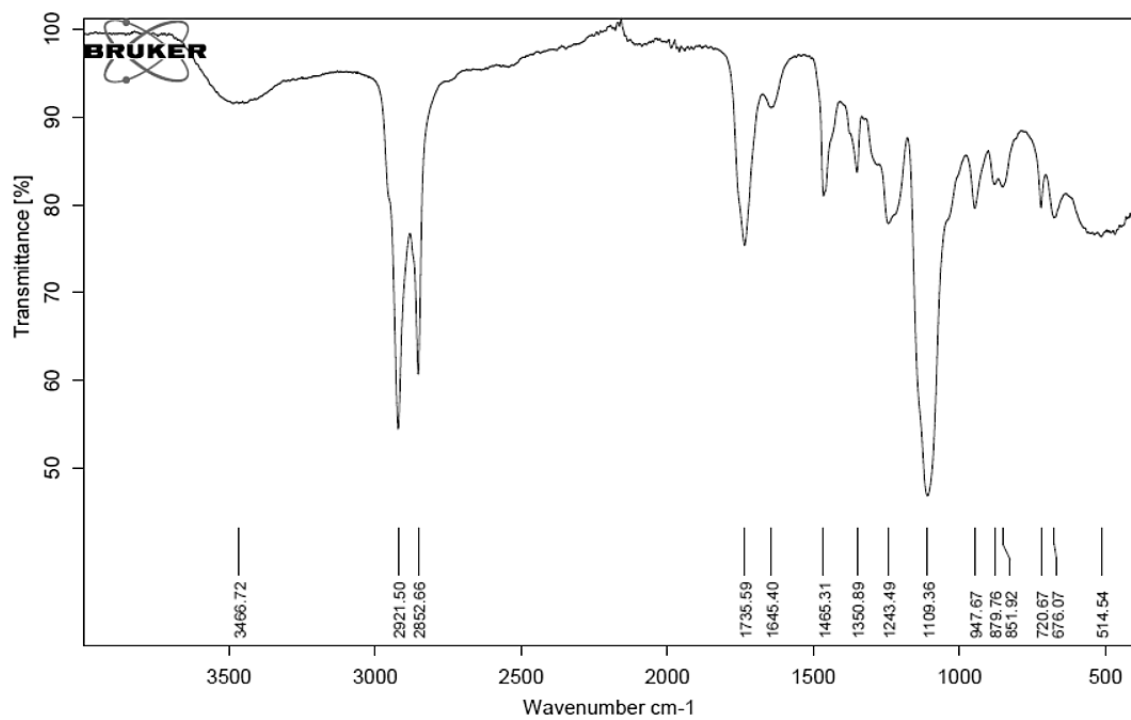
Figure D. 1 IR spectrum of Boltorn H311.
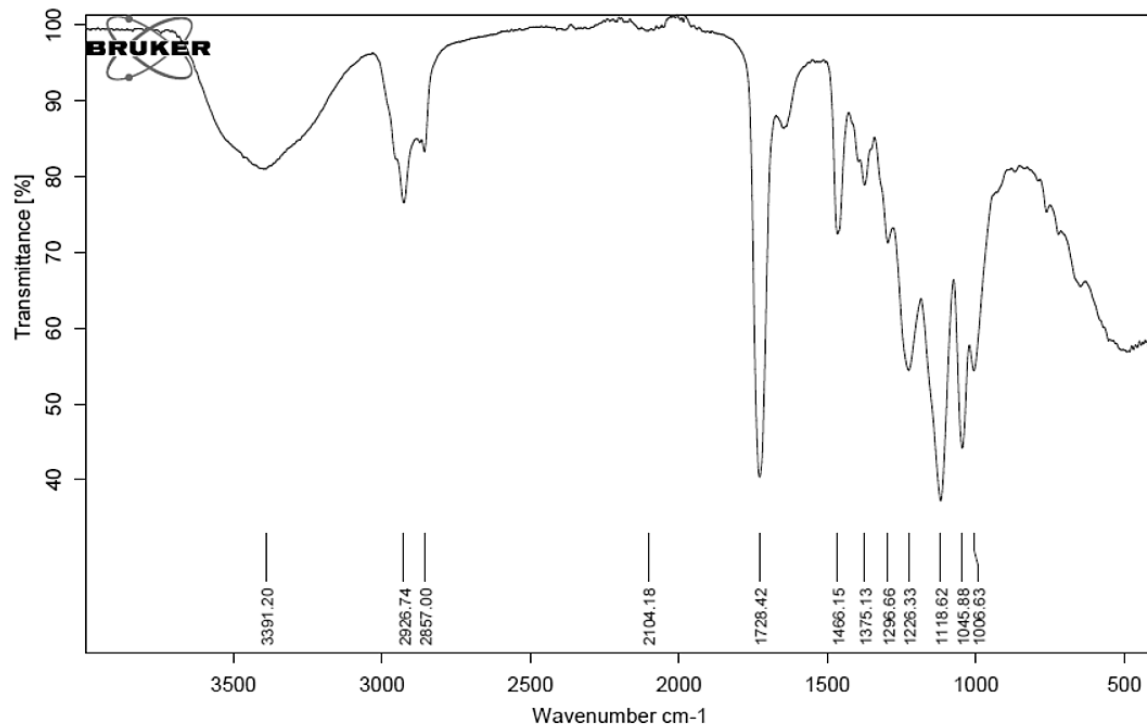
Figure D. 2 IR spectrum of starting material A.

XVII
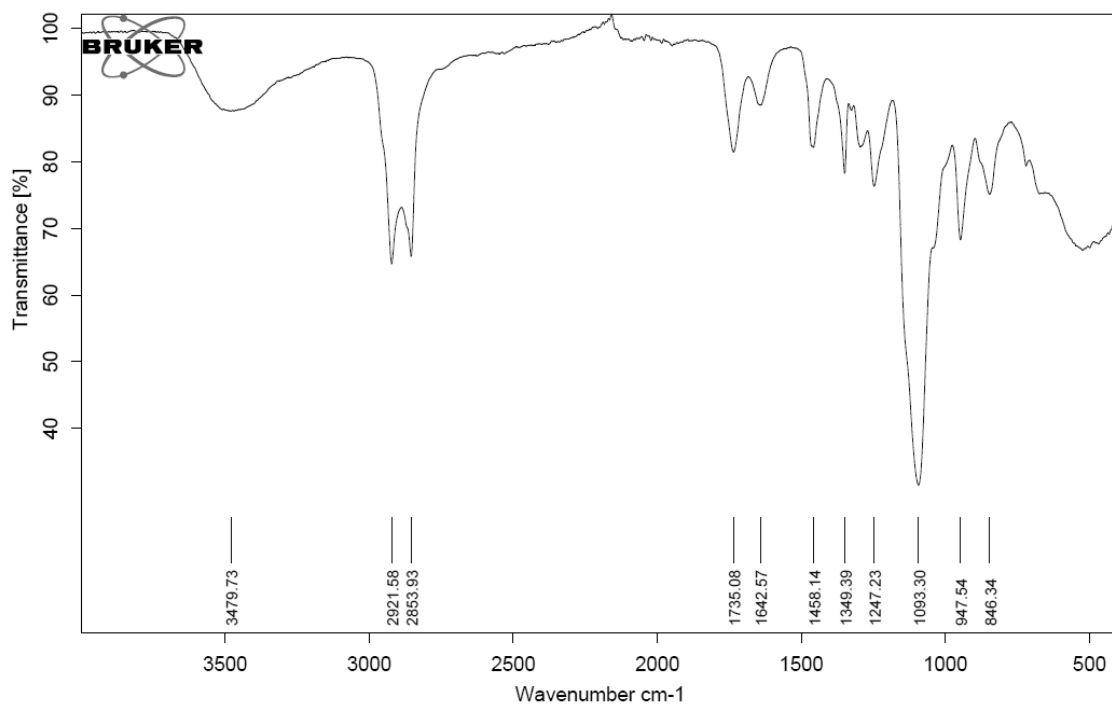
Figure D. 3 IR spectrum of starting material B.
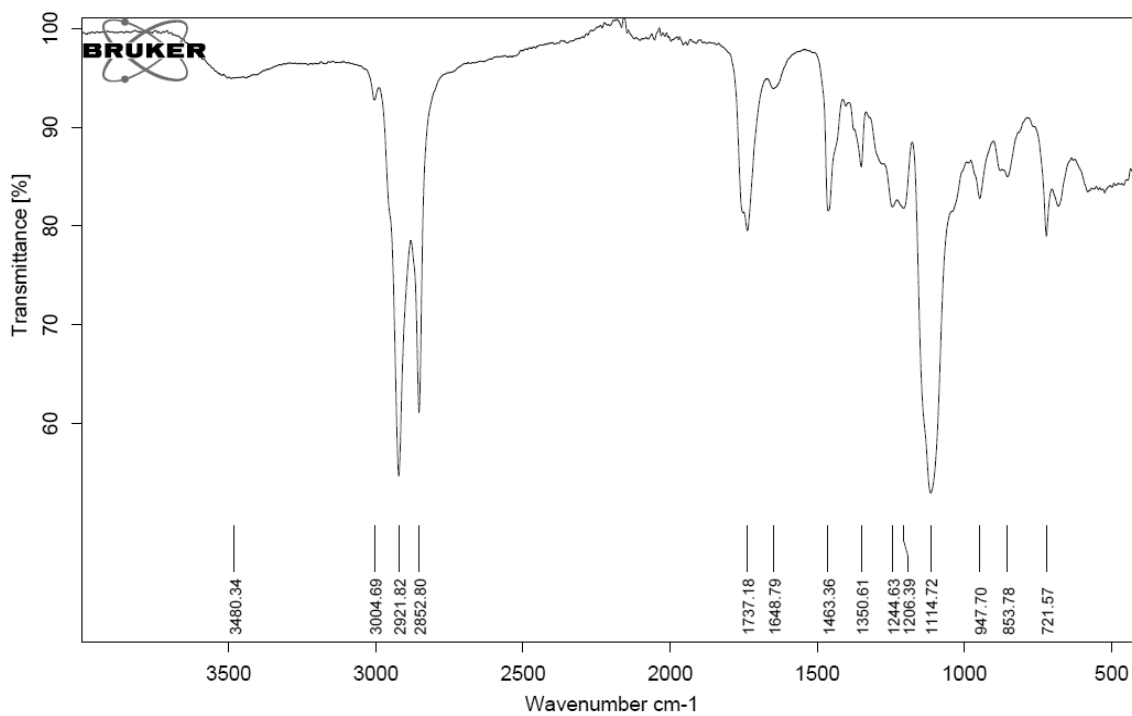
Figure D. 4 IR spectrum of starting material C.
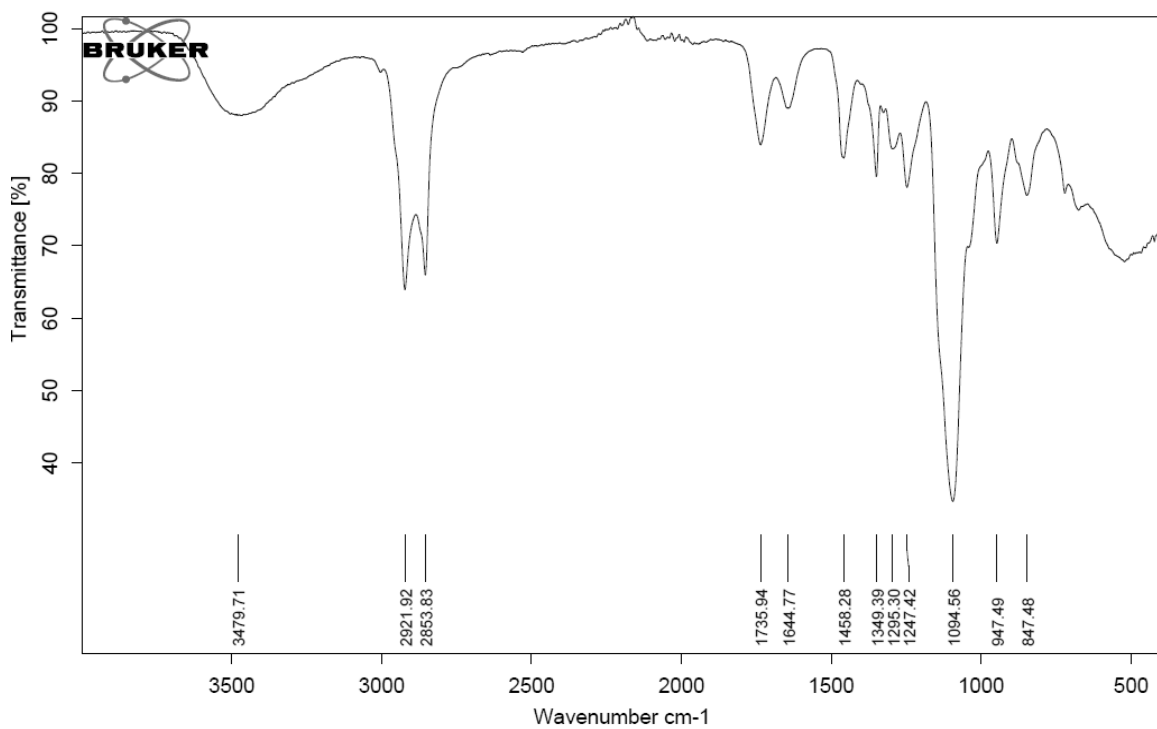
Figure D. 5 IR spectrum of starting material D.
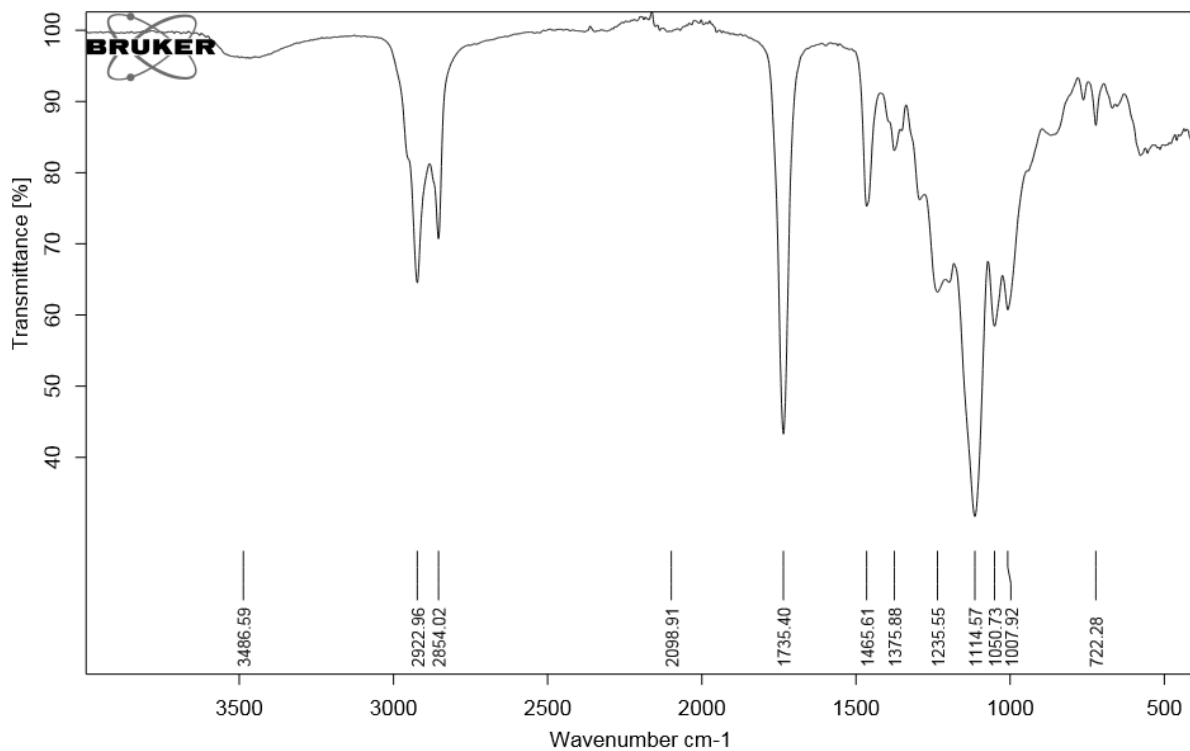
Figure D. 6 IR spectrum of product **1**.
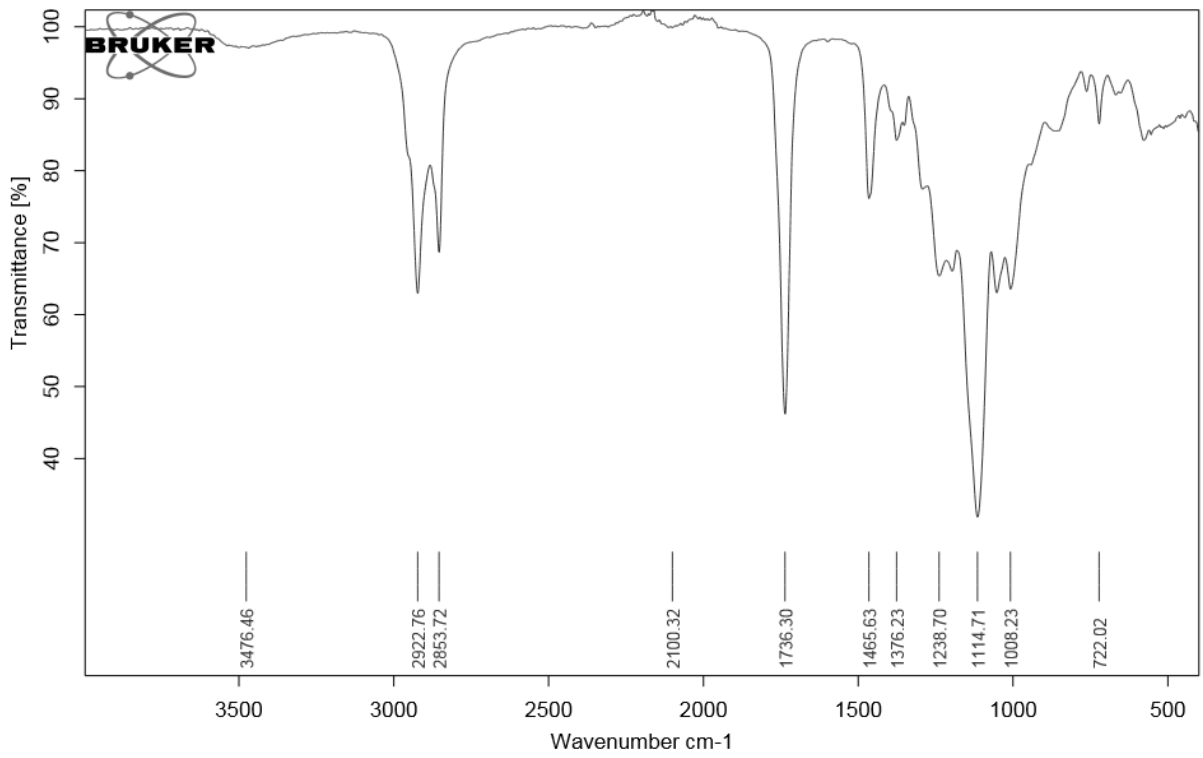
Figure D. 7 IR spectrum of product **2**.
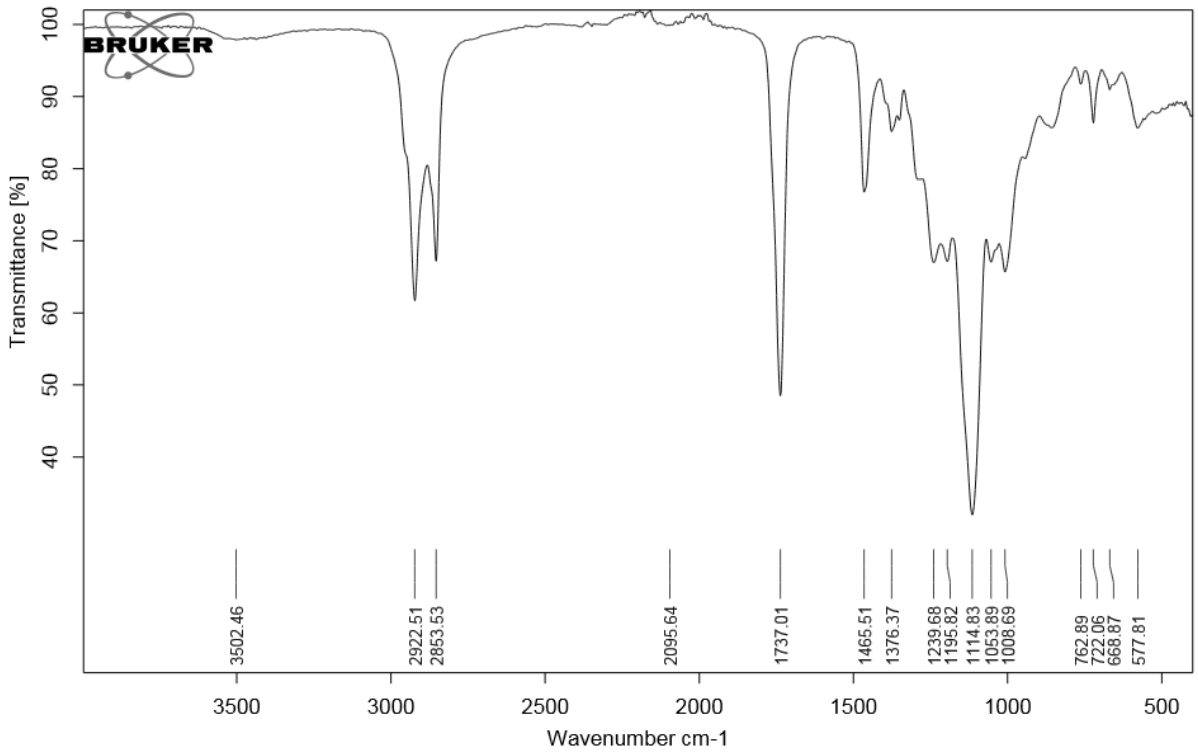
Figure D. 8 IR spectrum of product **3**.
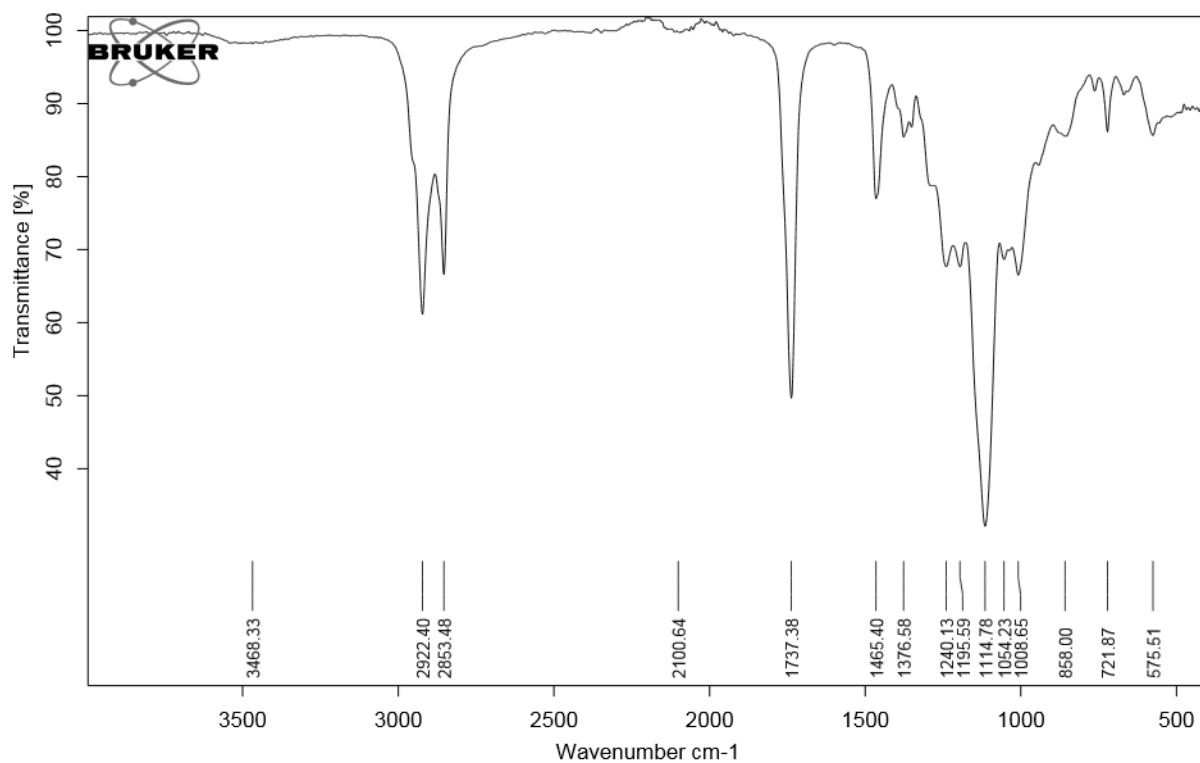
Figure D. 9 IR spectrum of product **4**.
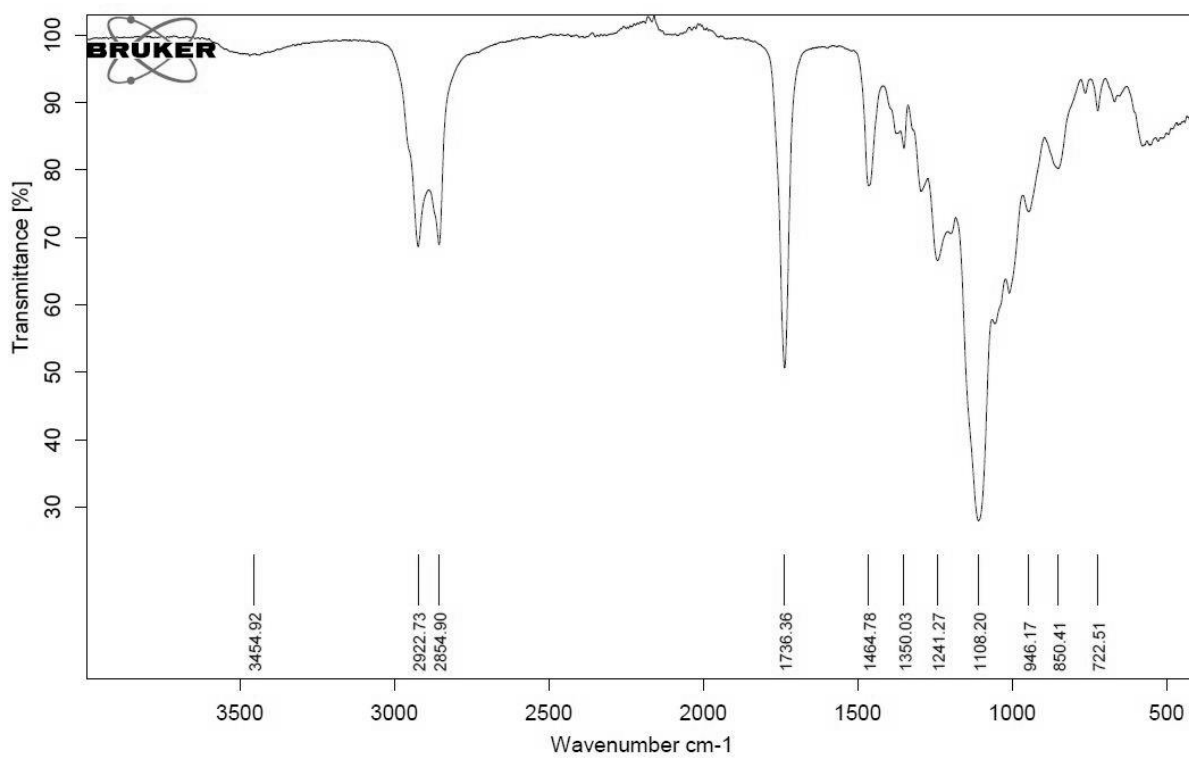
Figure D. 10 IR spectrum of product **5**.
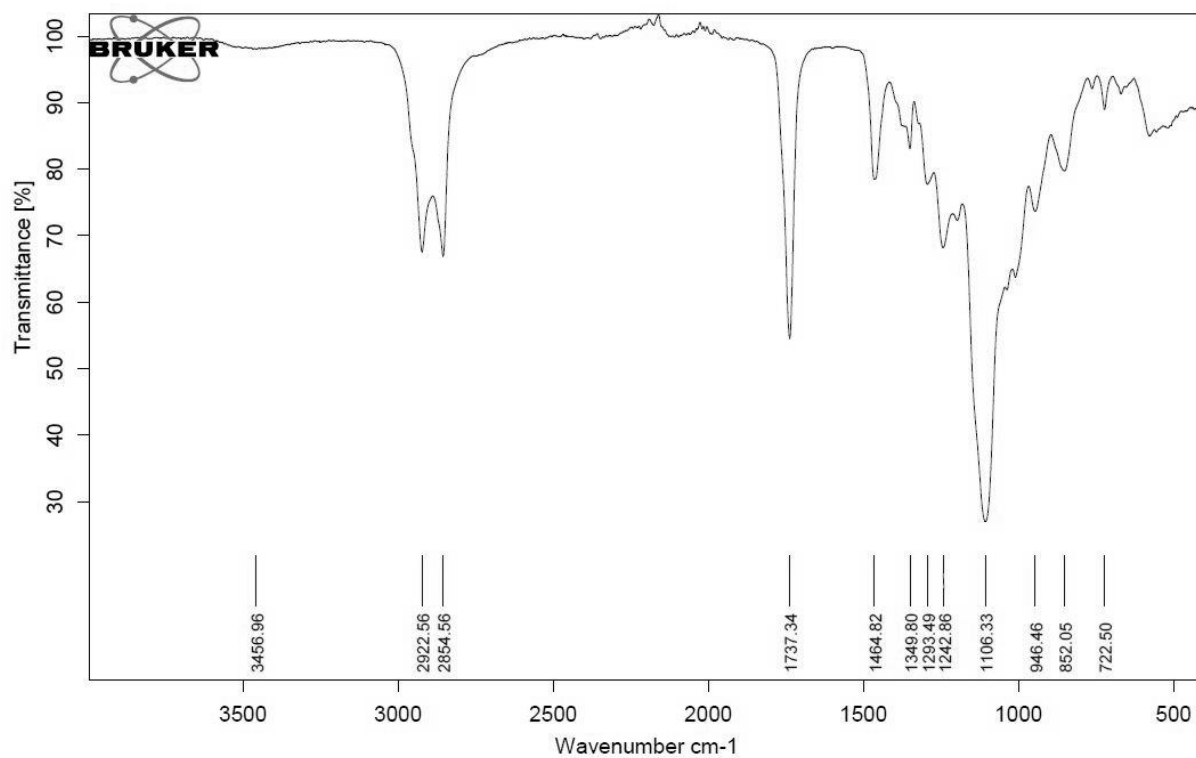
Figure D. 11 IR spectrum of product **6**.
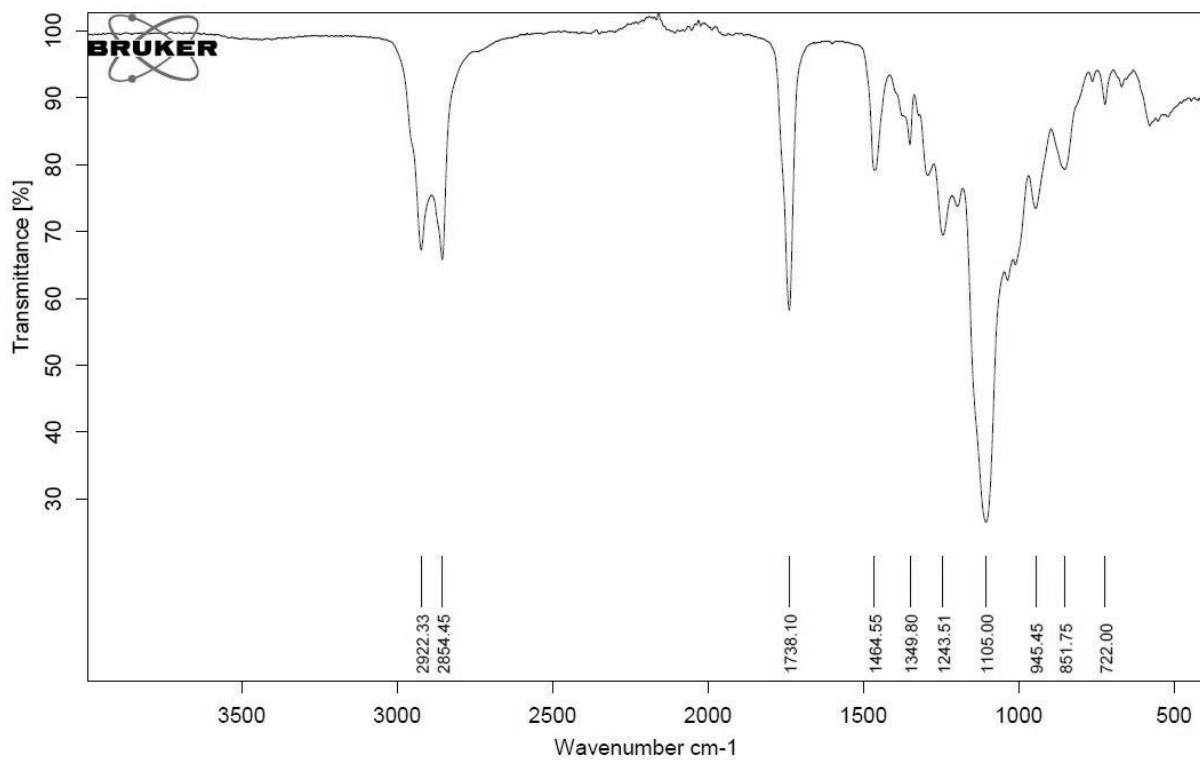
Figure D. 12 IR spectrum of product **7**.
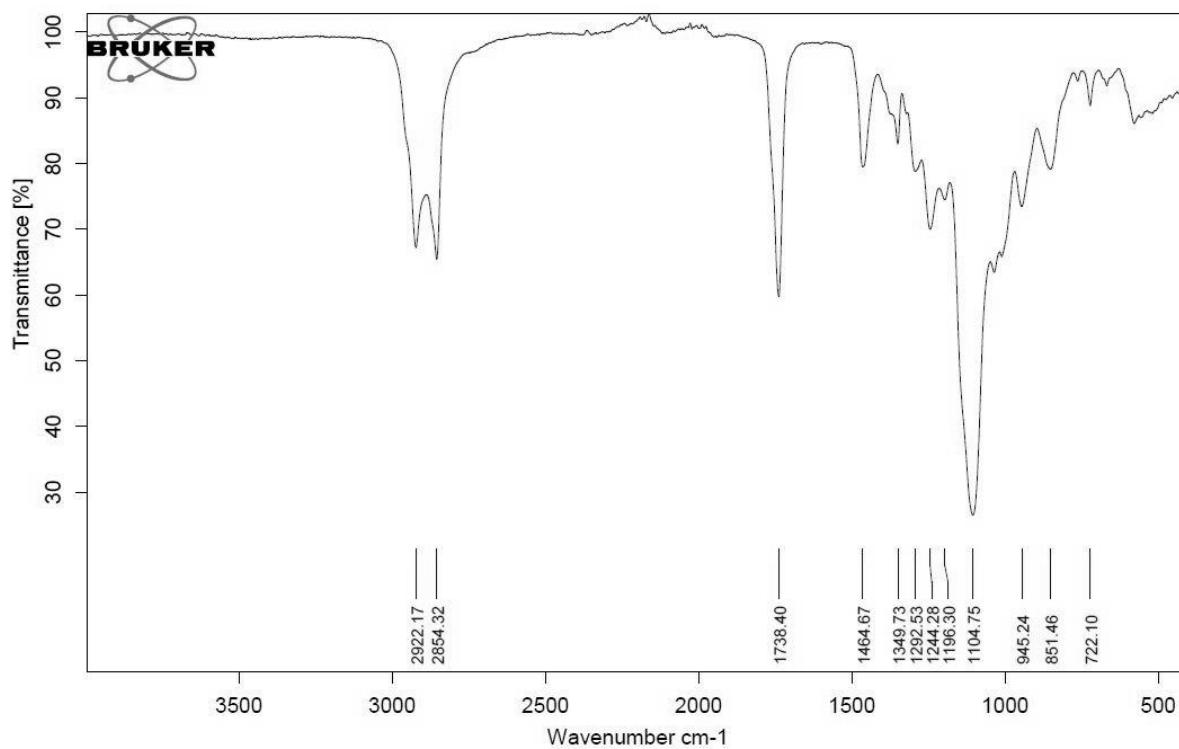
Figure D. 13 IR spectrum of product **8**.
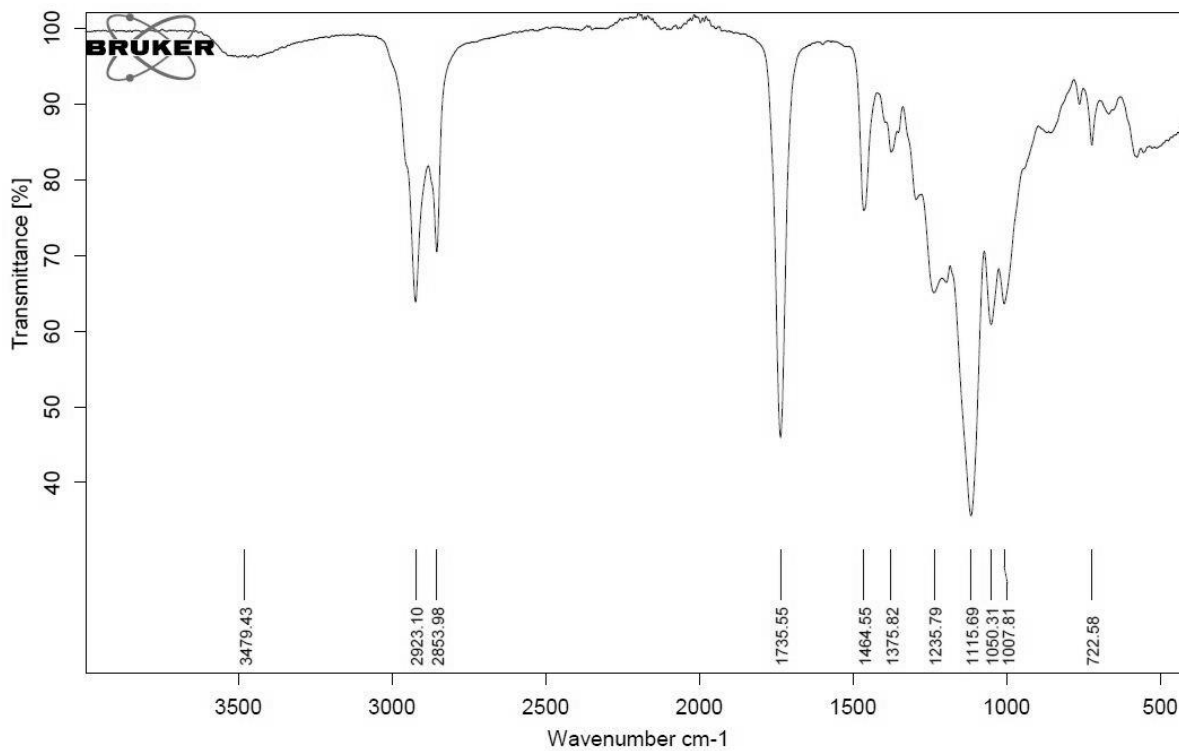
Figure D. 14 IR spectrum of product **9**.

XXIII
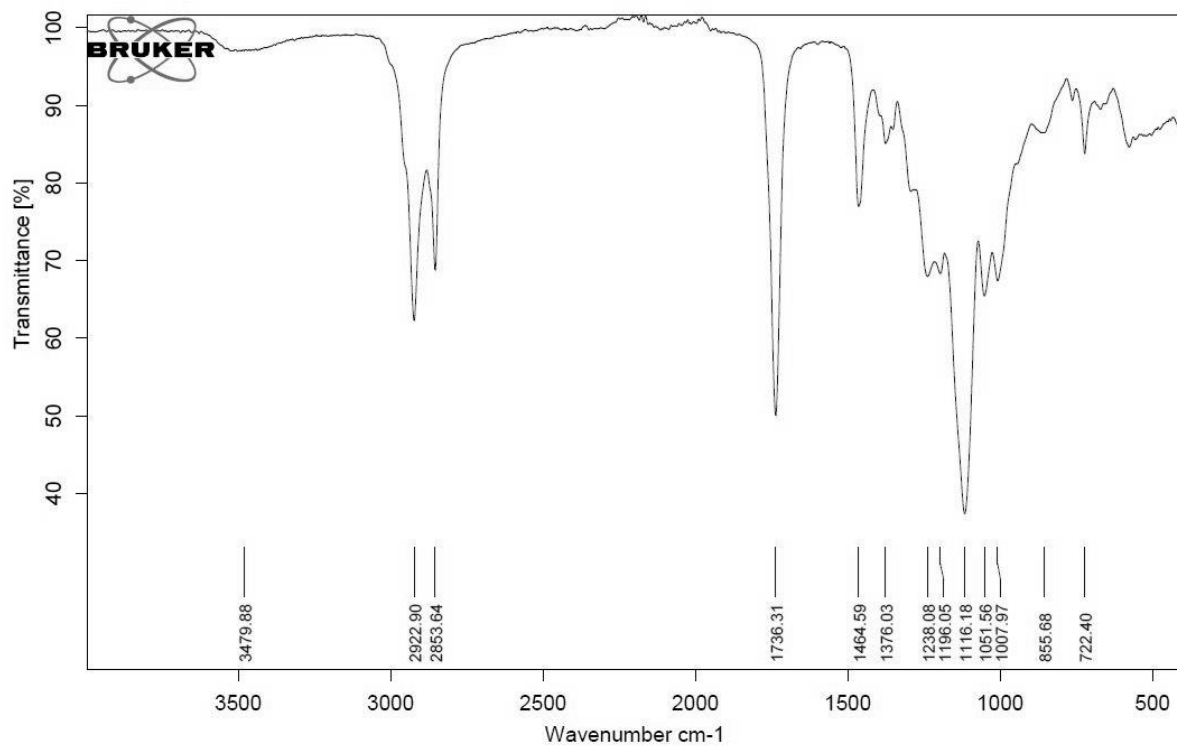
Figure D. 15 IR spectrum of product **10**.
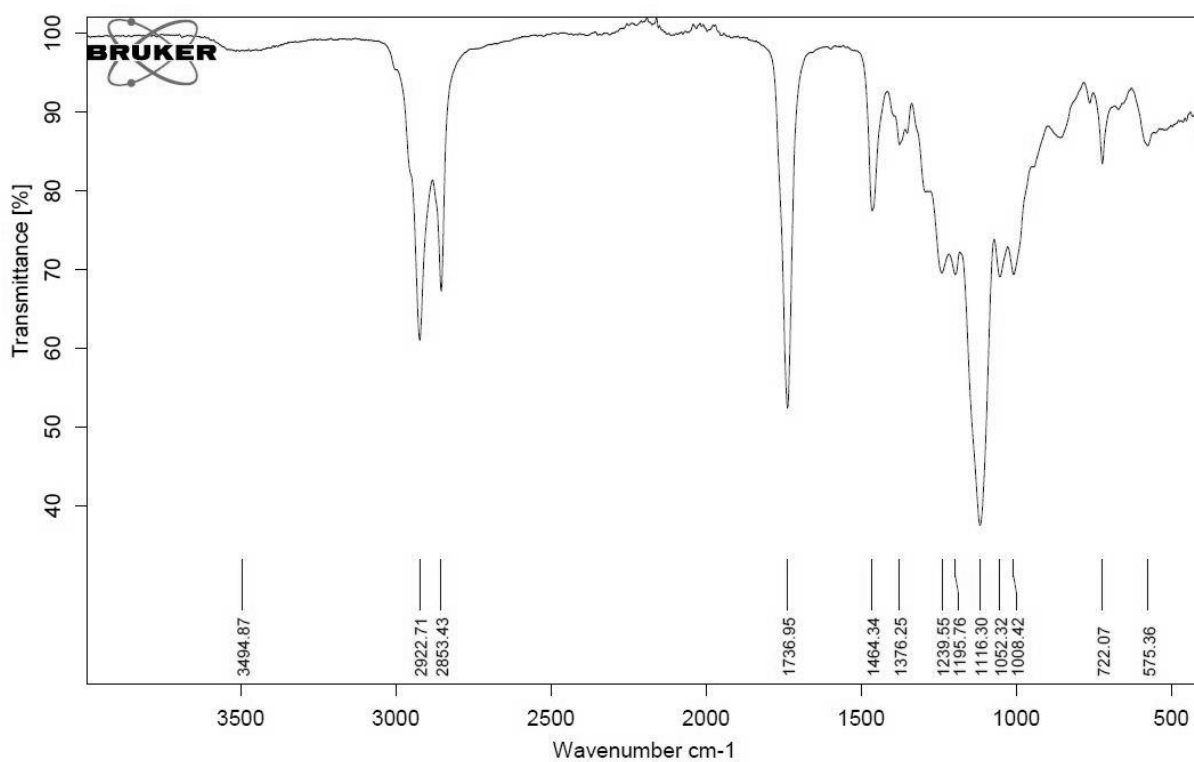
Figure D. 16 IR spectrum of product **11**.

XXIV
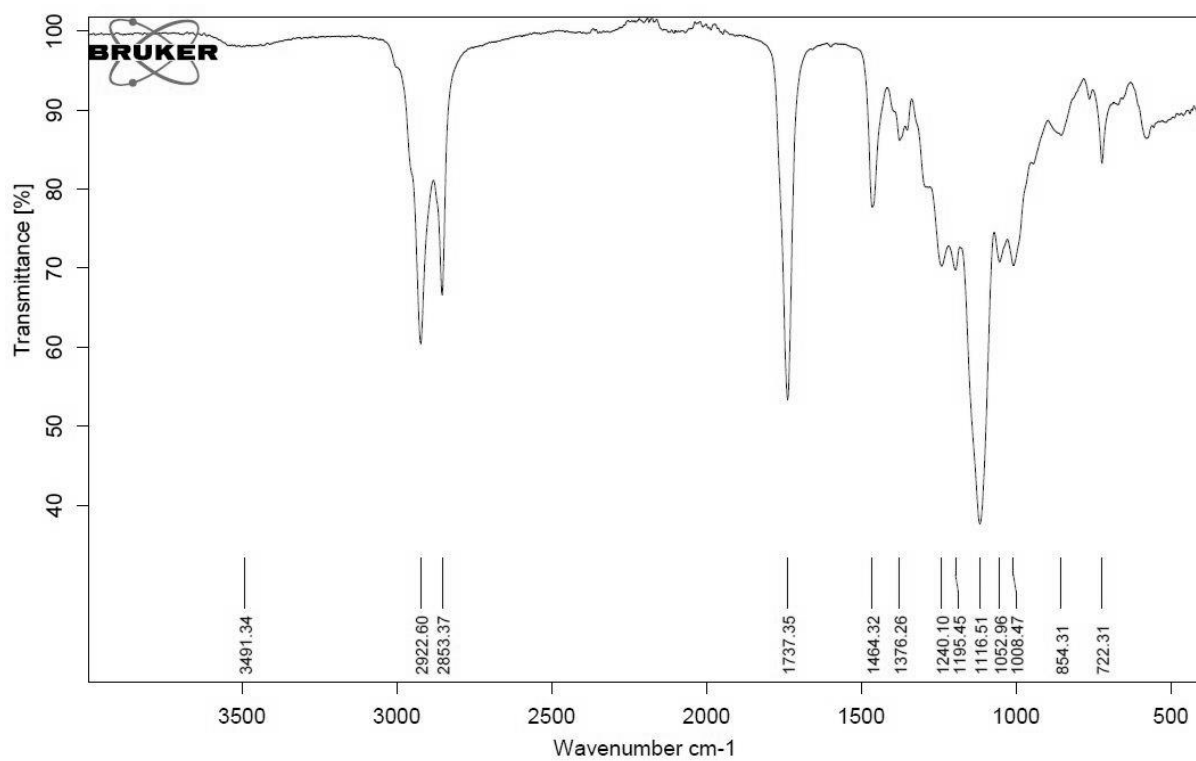
Figure D. 17 IR spectrum of product **12**.
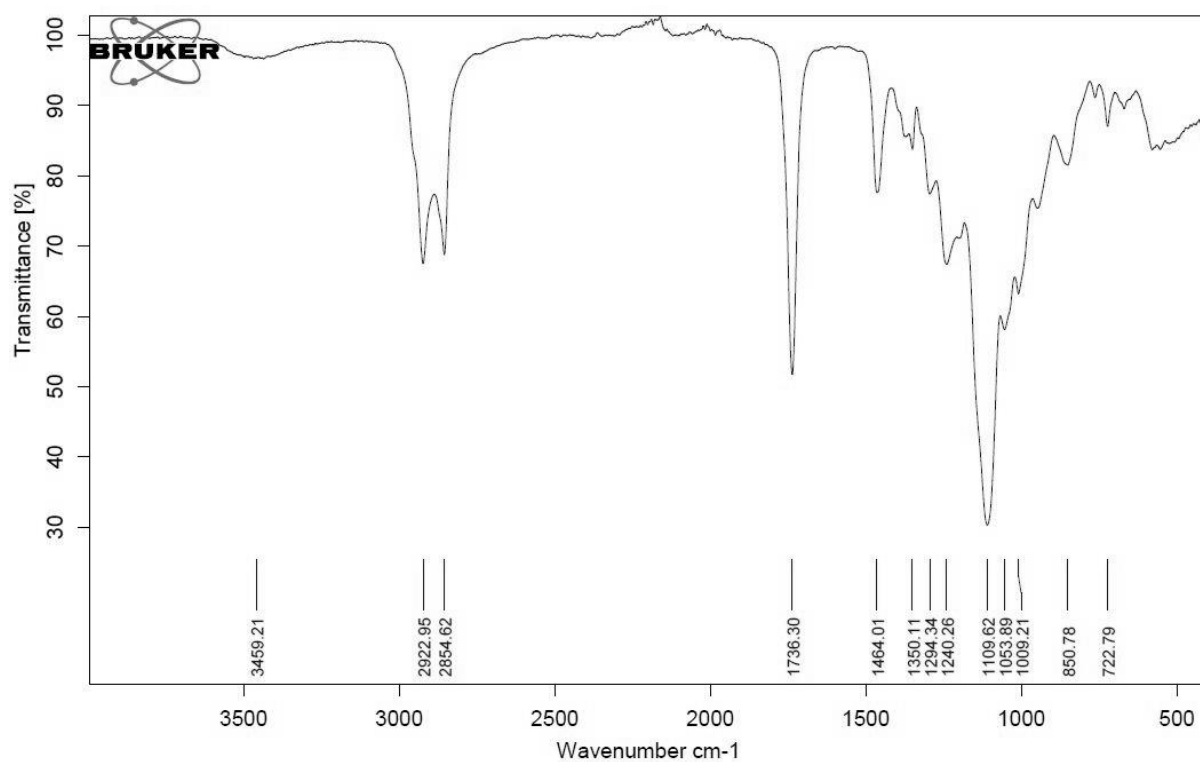
Figure D. 18 IR spectrum of product **13**.
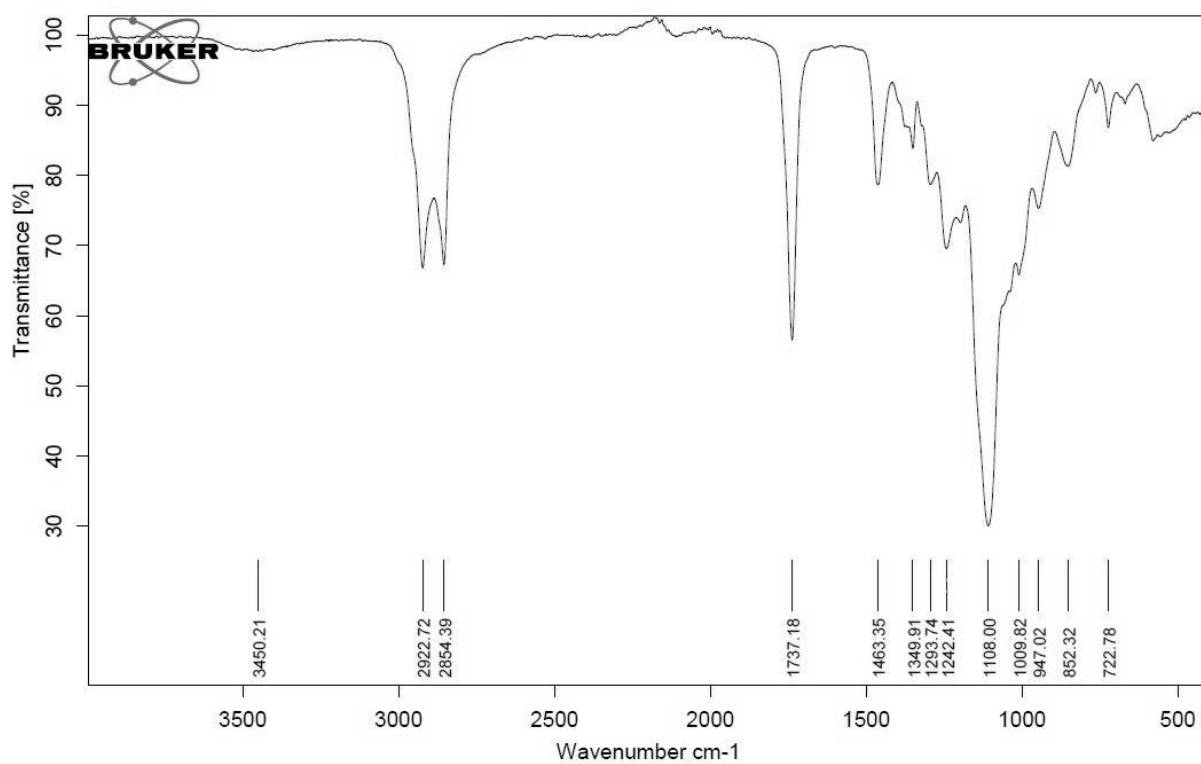
Figure D. 19 IR spectrum of product **14**.

Figure D. 20 IR spectrum of product **15**.
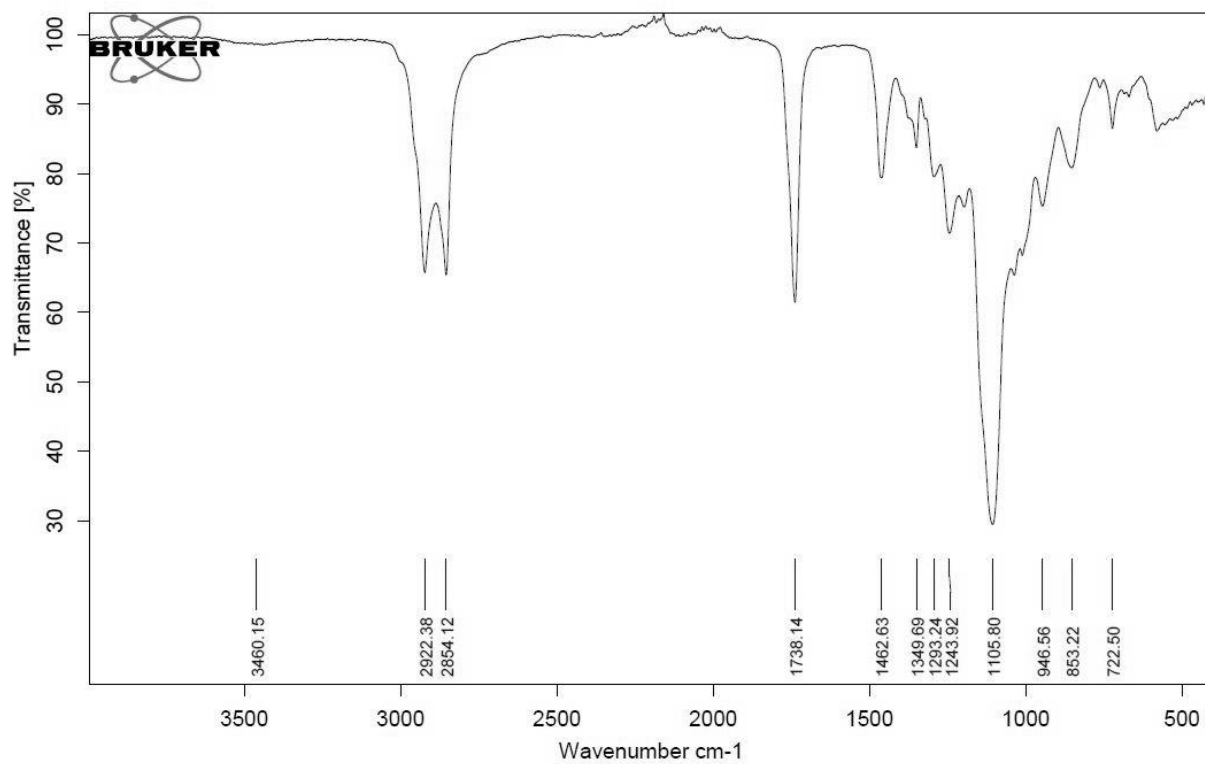
Figure D. 21 IR spectrum of product **16**.

Appendix E
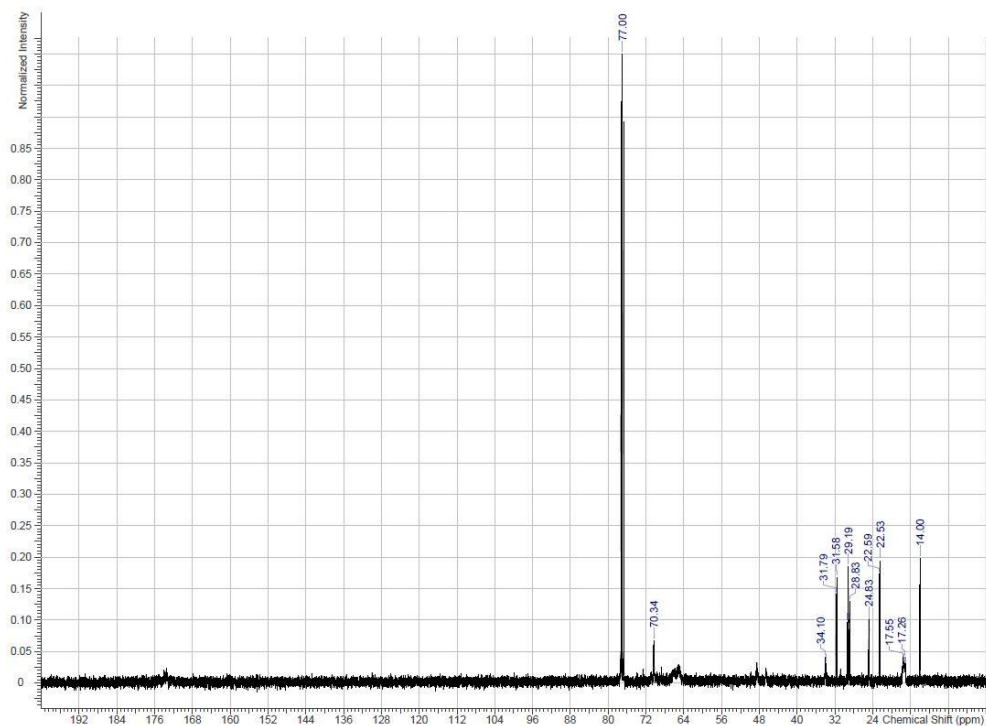
Figure E. 1 ^{13}C-NMR spectrum of Boltorn H311.
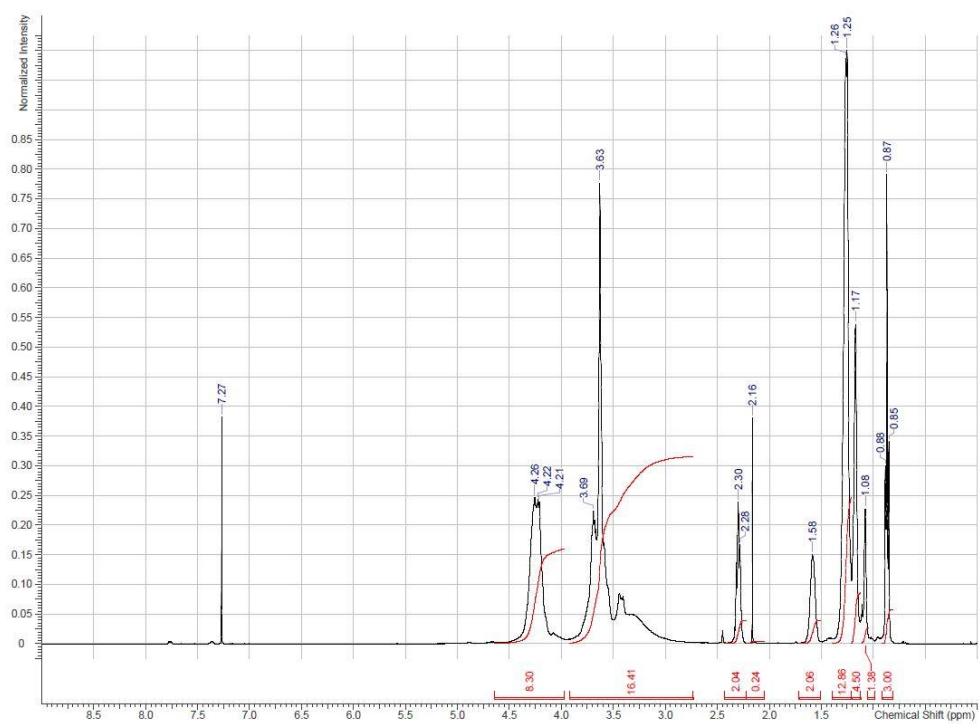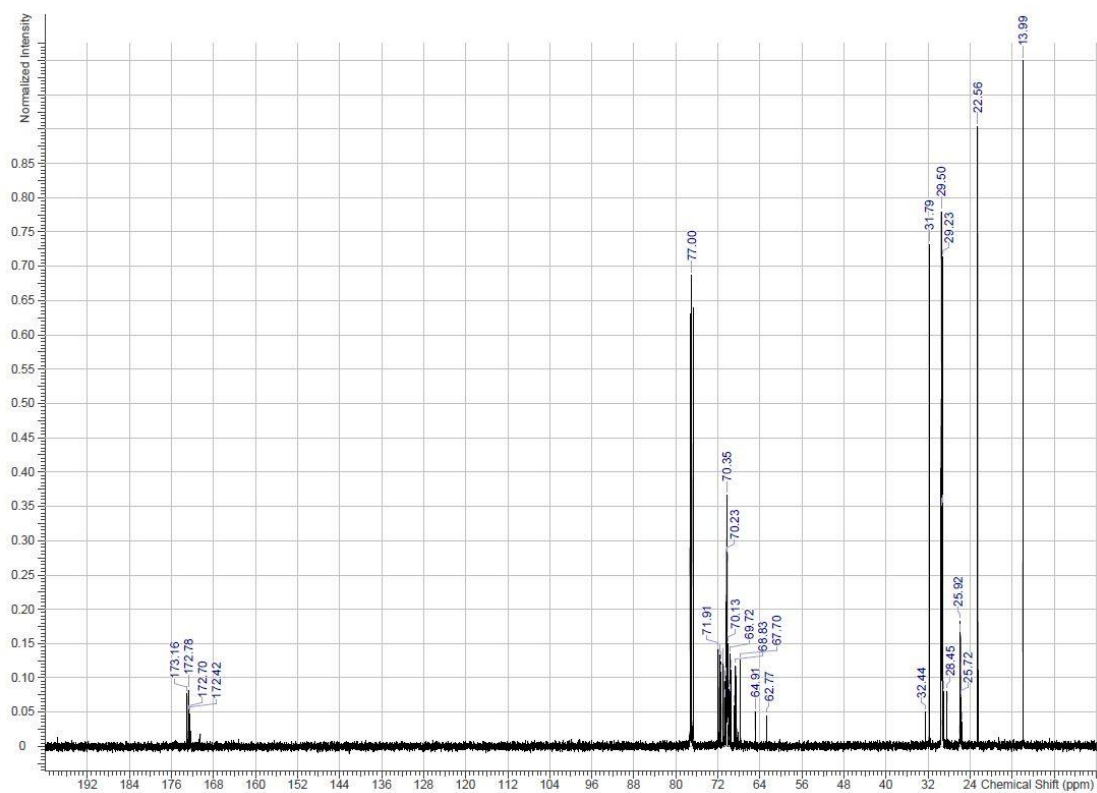

Figure E. 2 ^{1}H-NMR spectrum of Boltorn H311.

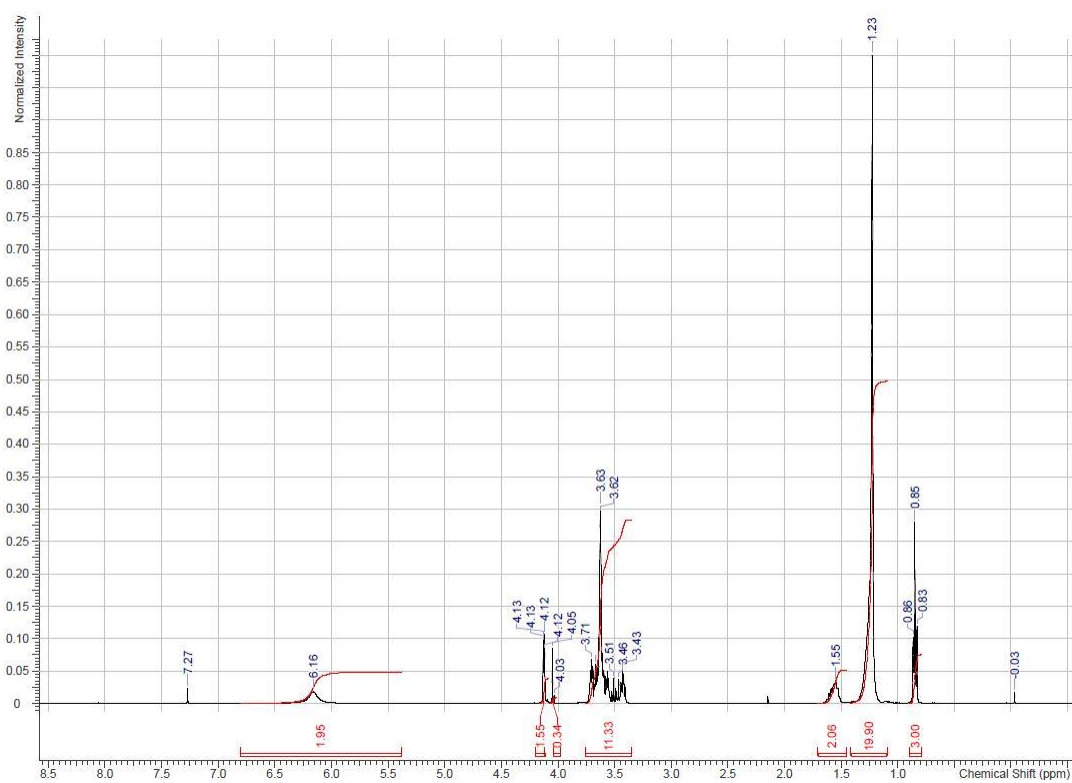Figure E. 3 ^{13}C-NMR spectrum of starting material A.
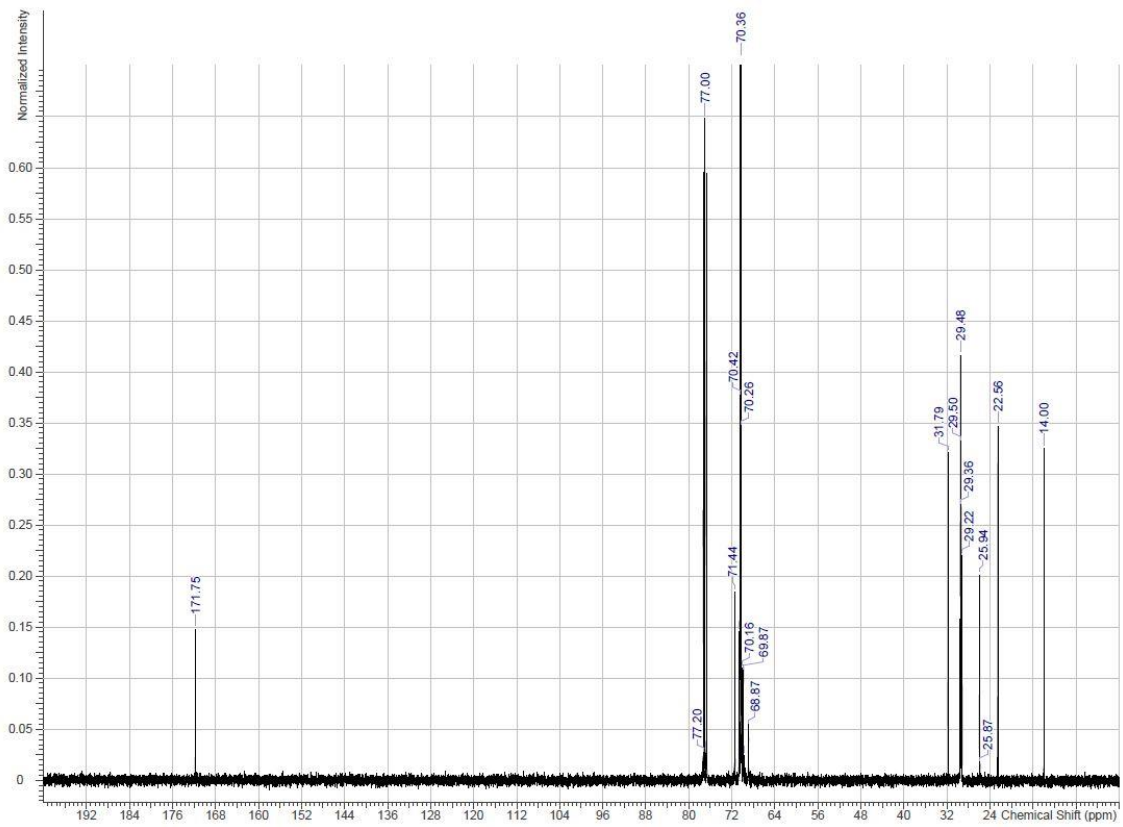

Figure E. 4 ^{1}H-NMR spectrum of starting material A.

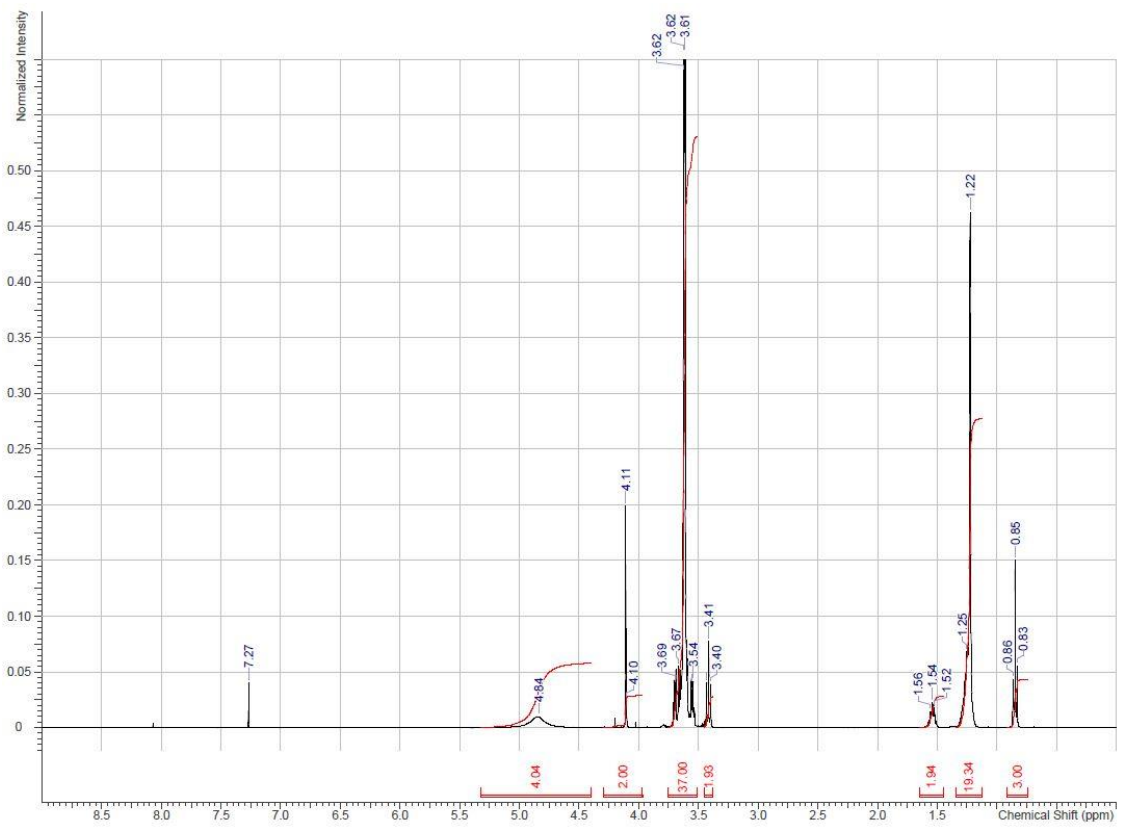Figure E. 5 ^{13}C-NMR spectrum of starting material B.

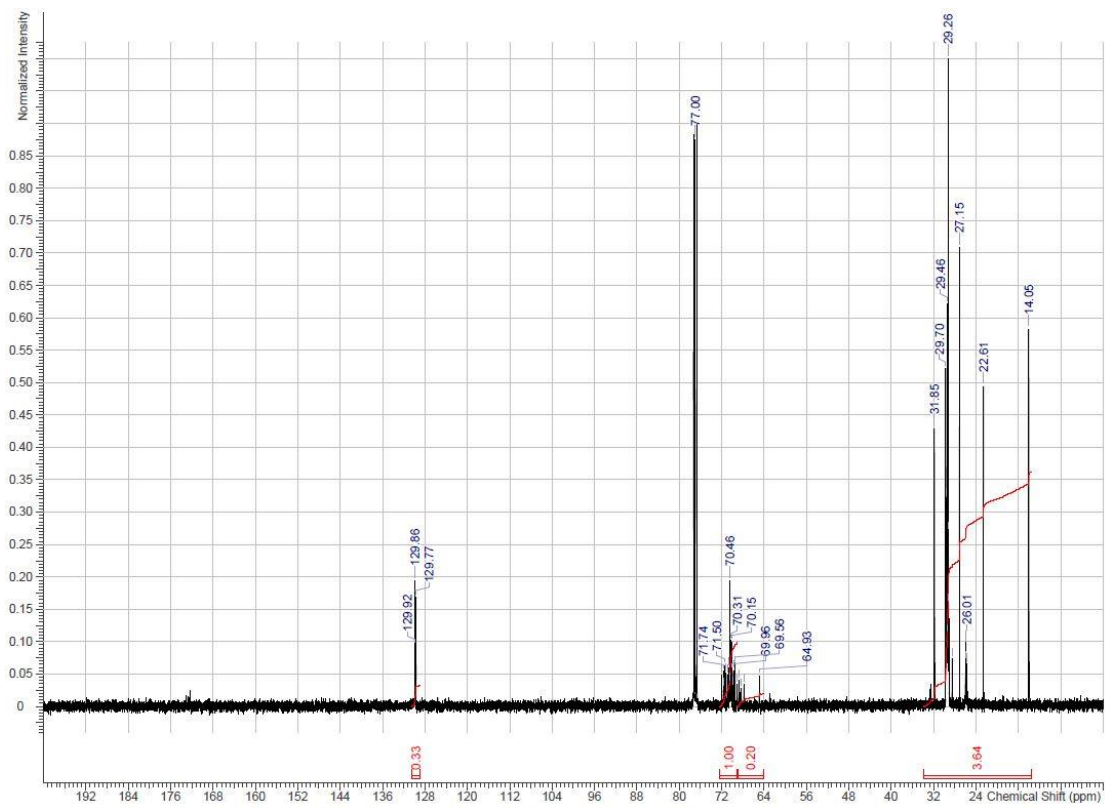Figure E. 6 ^{1}H-NMR spectrum of starting material B.

XXX

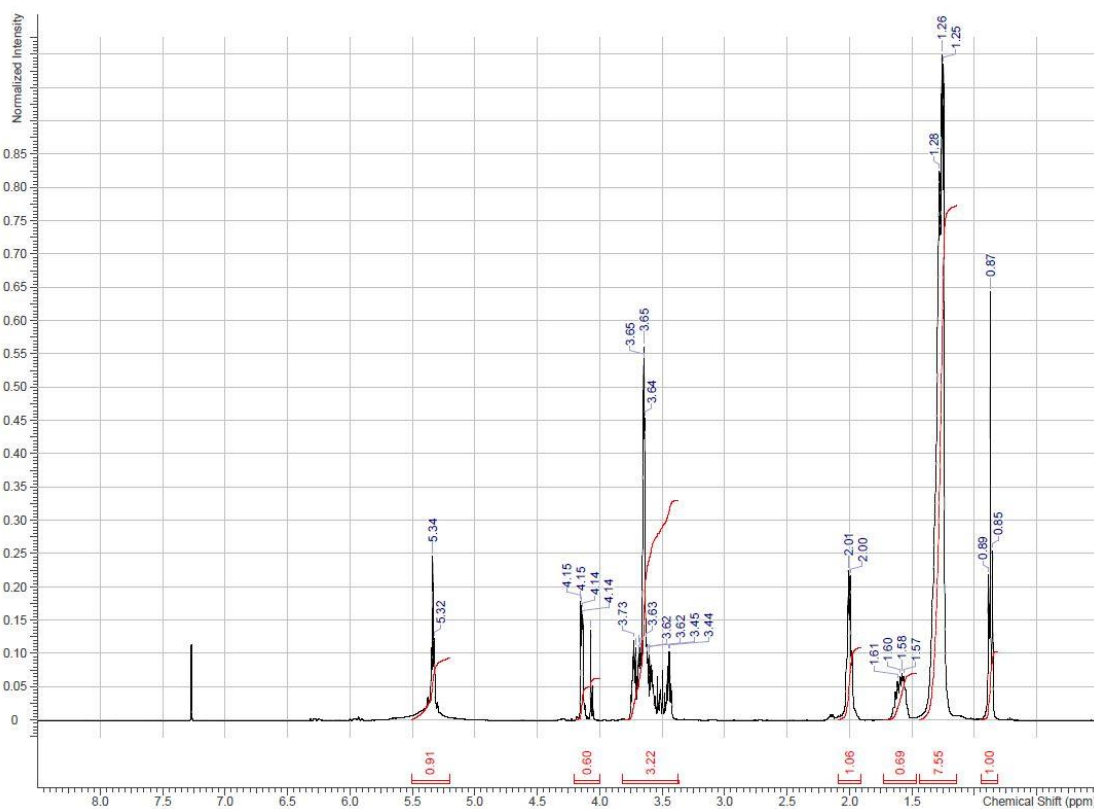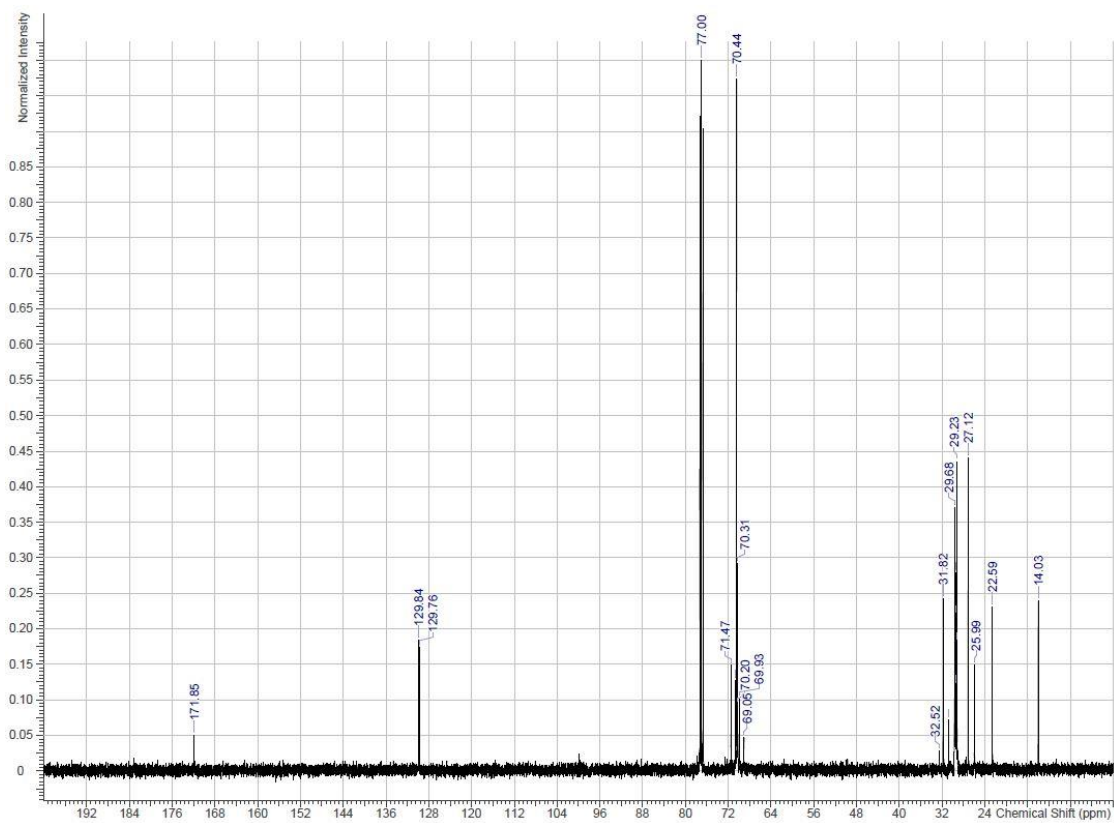Figure E. 7 ^{13}C-NMR spectrum of starting material C.

Figure E. 8 ^{1}H-NMR spectrum of starting material C.

Figure E. 9 ^{13}C-NMR spectrum of starting material D.

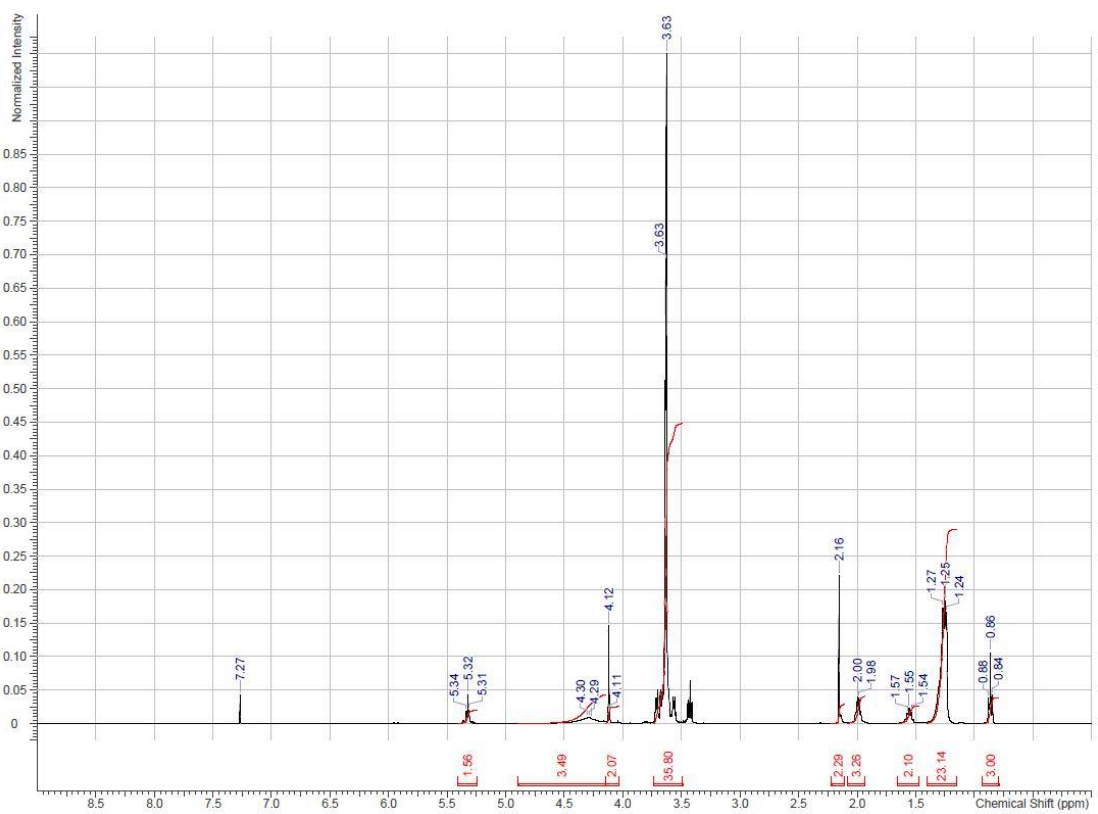Figure E. 10 ^{1}H-NMR spectrum of starting material D.

XXXII

Figure E. 11 ^{13}C-NMR spectrum of product **1**.
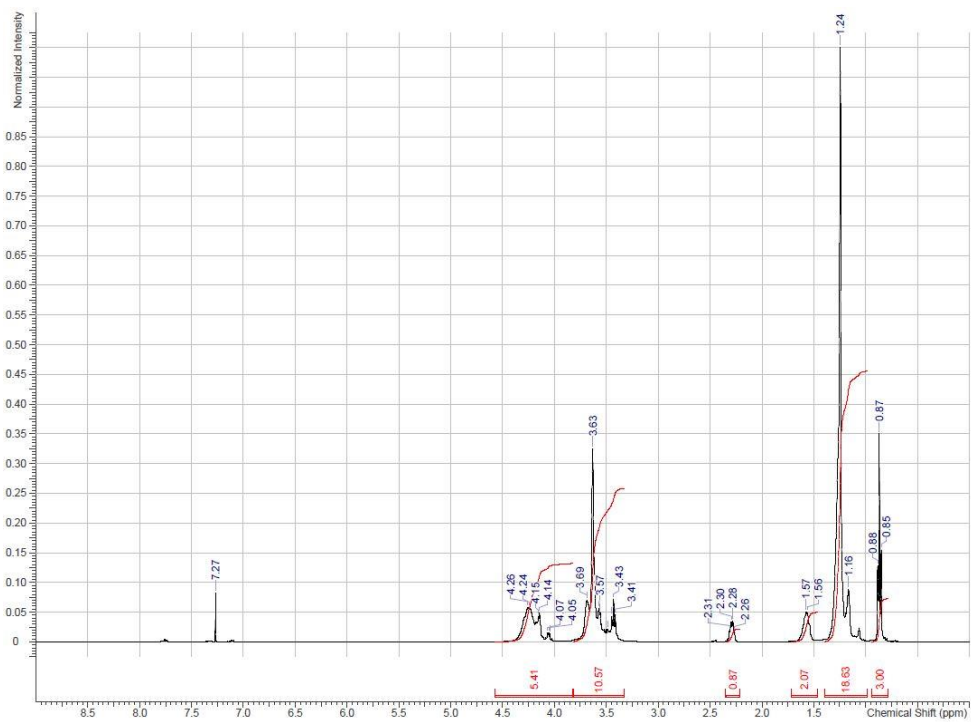
Figure E. 12 ^{1}H-NMR spectrum of product **1**.
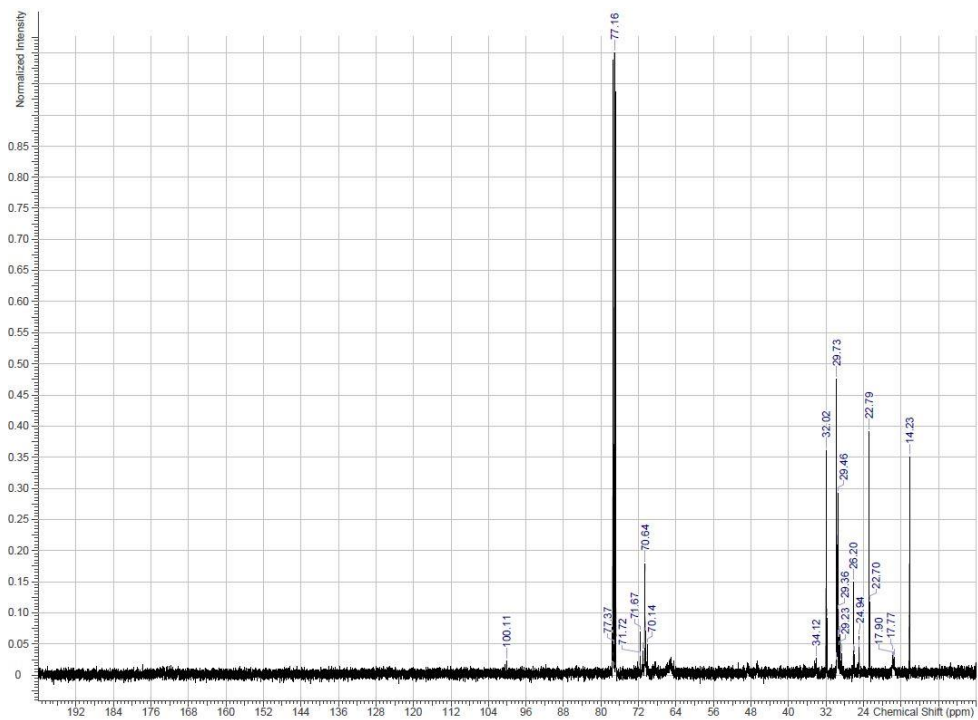
Figure E. 13 ^{13}C-NMR spectrum of product **2**.
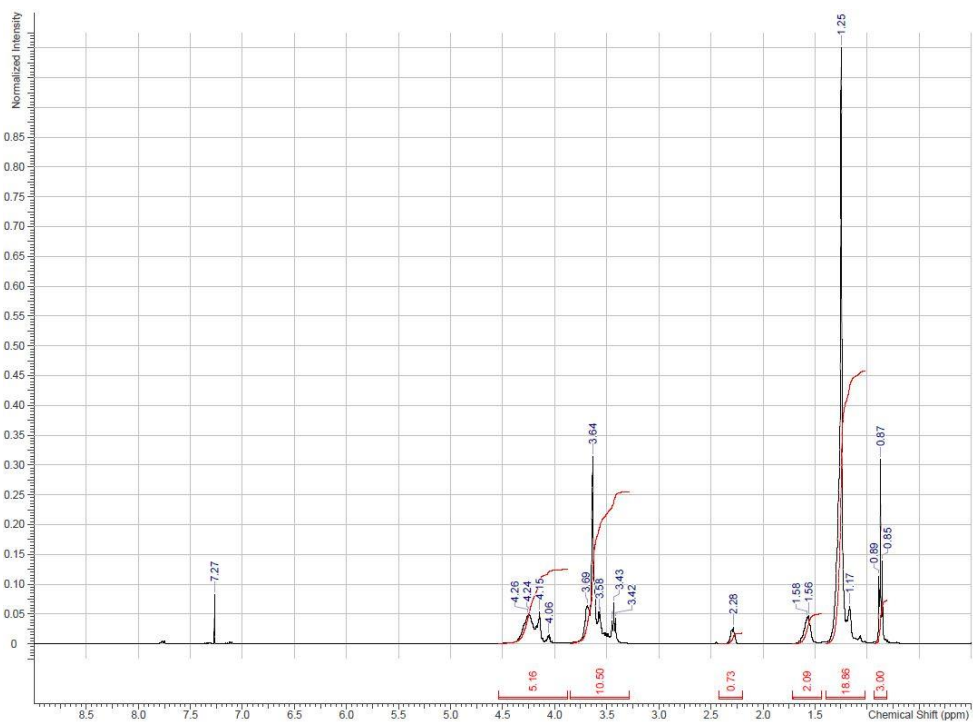
Figure E. 14 ^{1}H-NMR spectrum of product **2**.

Figure E. 15 ^{13}C-NMR spectrum of product **3**.

Figure E. 16 ^{1}H-NMR spectrum of product **3**.

Figure E. 17 ^{13}C-NMR spectrum of product **4**.

Figure E. 18 ^{1}H-NMR spectrum of product **4**.

Figure E. 19 ^{13}C-NMR spectrum of product **5**.

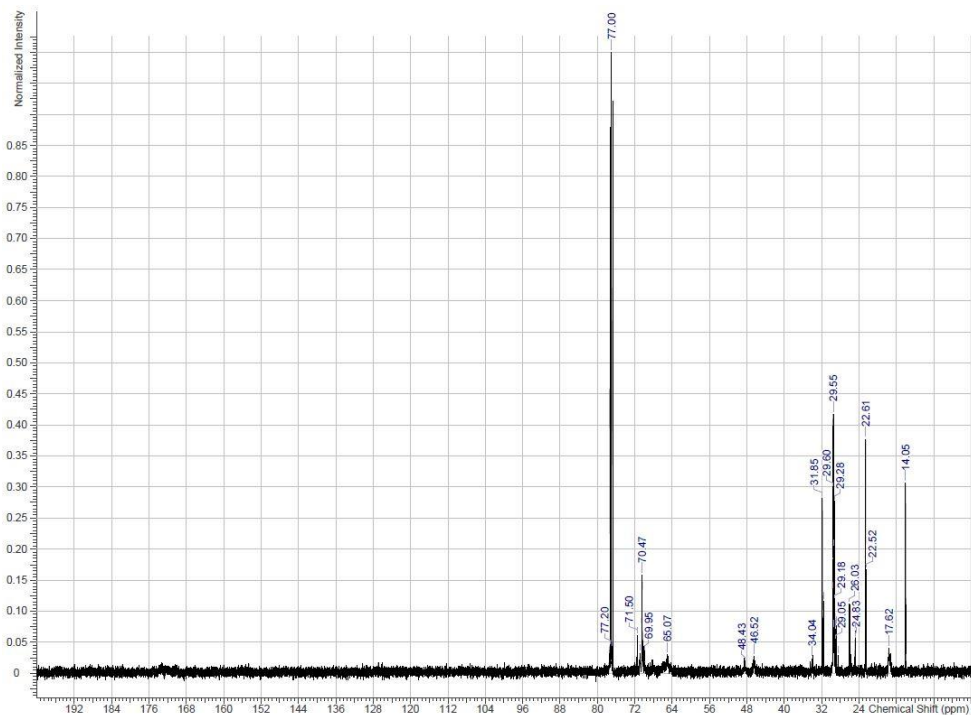Figure E. 20 ^{1}H-NMR spectrum of product **5**.
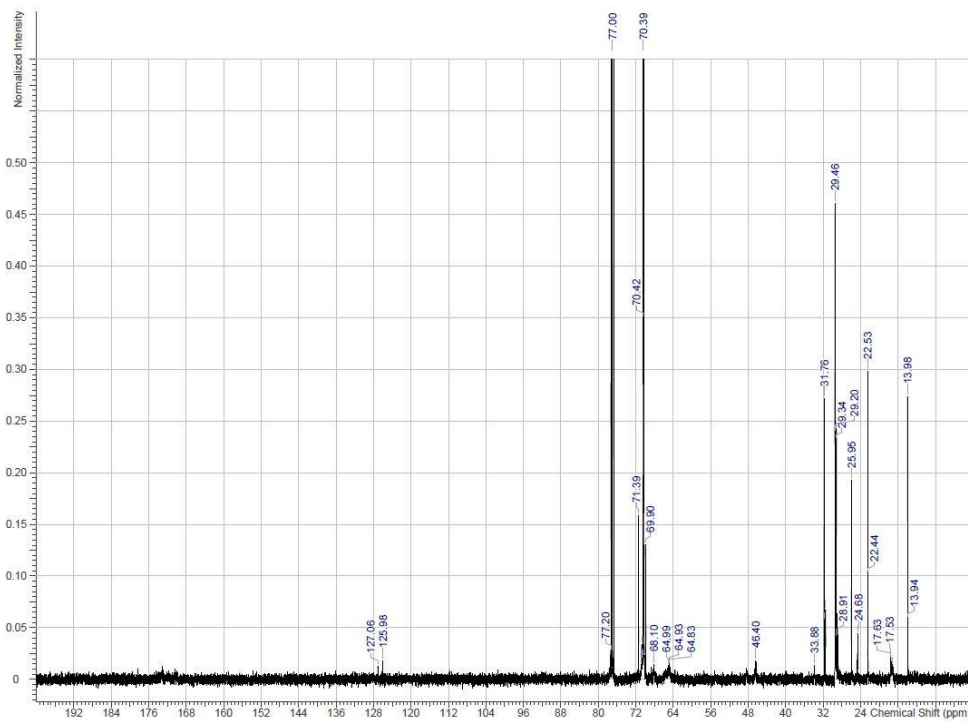
Figure E. 21 ^{13}C-NMR spectrum of product **6**.

Figure E. 22 ^{1}H-NMR spectrum of product **6**.

Figure E. 23 ^{13}C-NMR spectrum of product **7**.

Figure E. 24 ^{1}H-NMR spectrum of product **7**.

Figure E. 25 ^{13}C-NMR spectrum of product **8**.

Figure E. 26 ^{1}H-NMR spectrum of product **8**.

Figure E. 27 ^{13}C-NMR spectrum of product **9**.
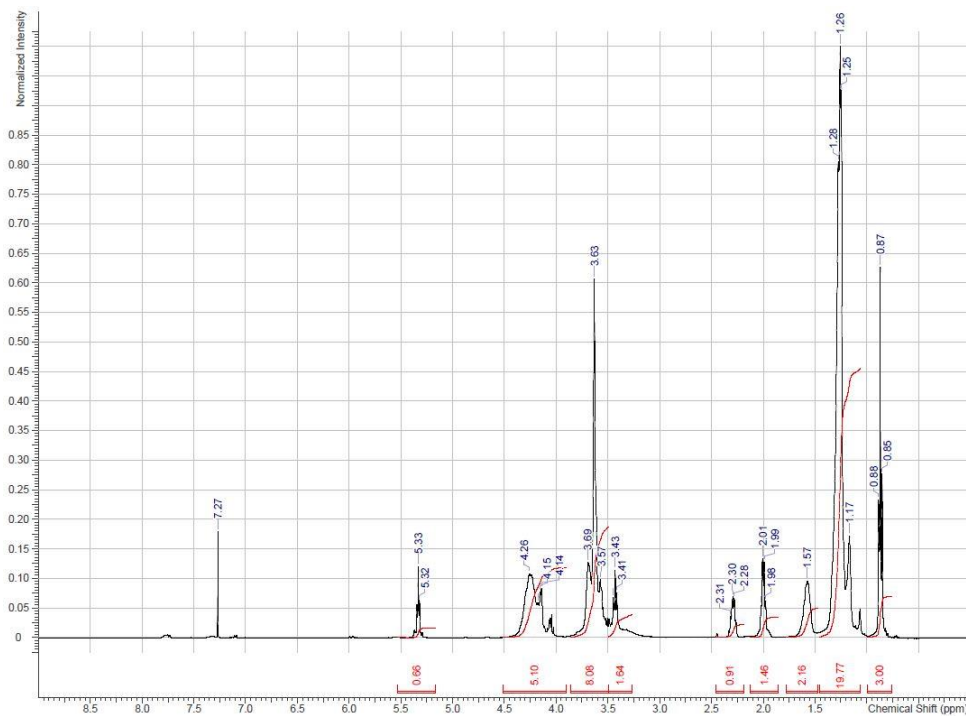
Figure E. 28 ^{1}H-NMR spectrum of product **9**.
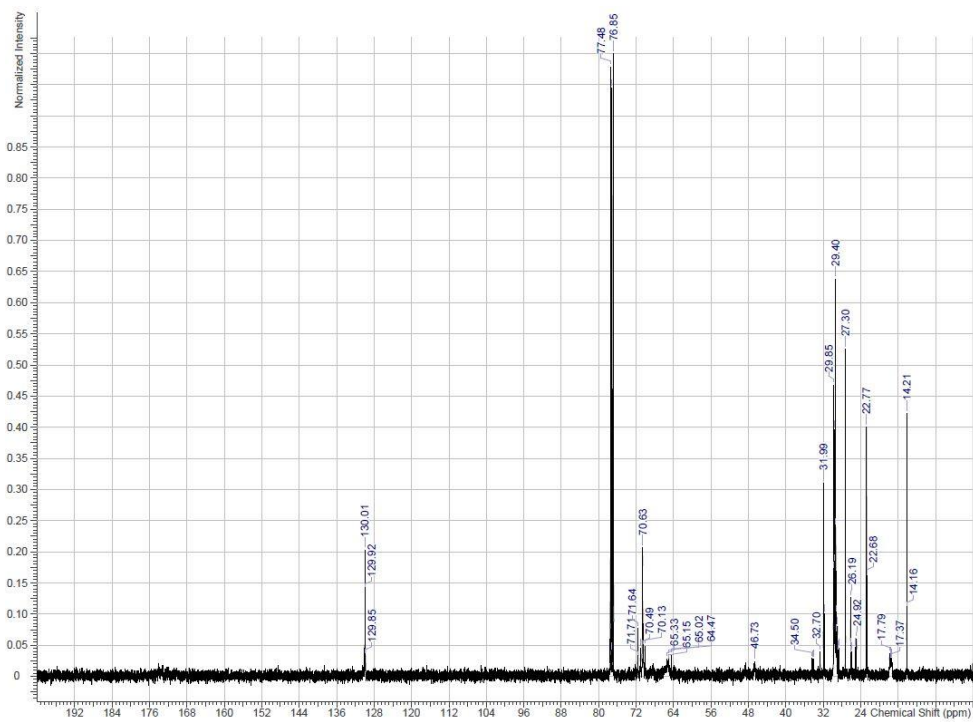
Figure E. 29 ^{13}C-NMR spectrum of product **10**.
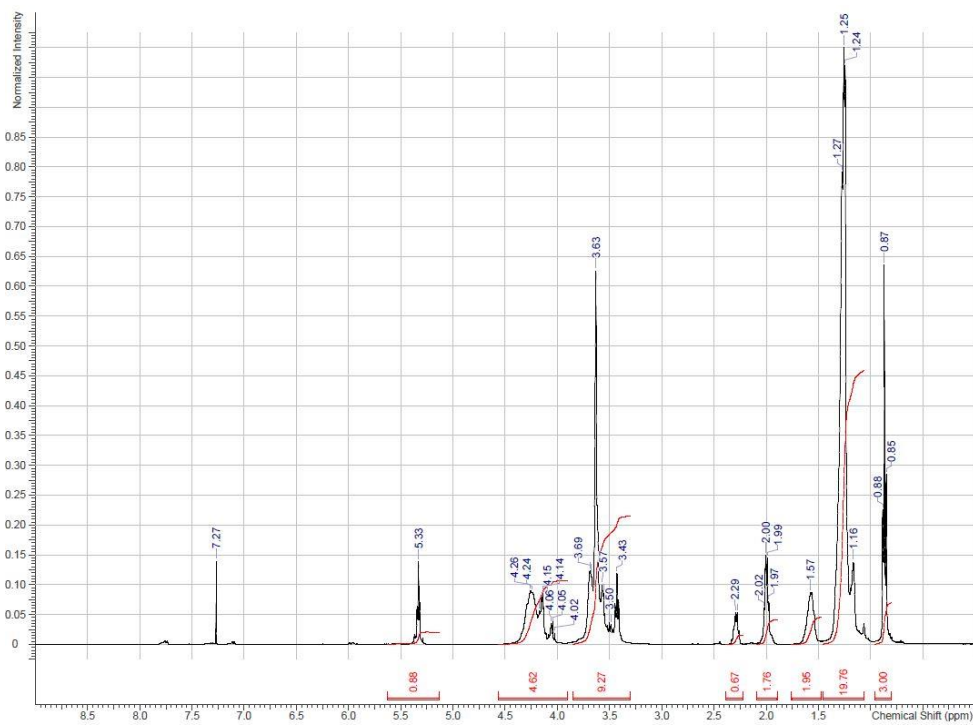
Figure E. 30 ^{1}H-NMR spectrum of product **10**.
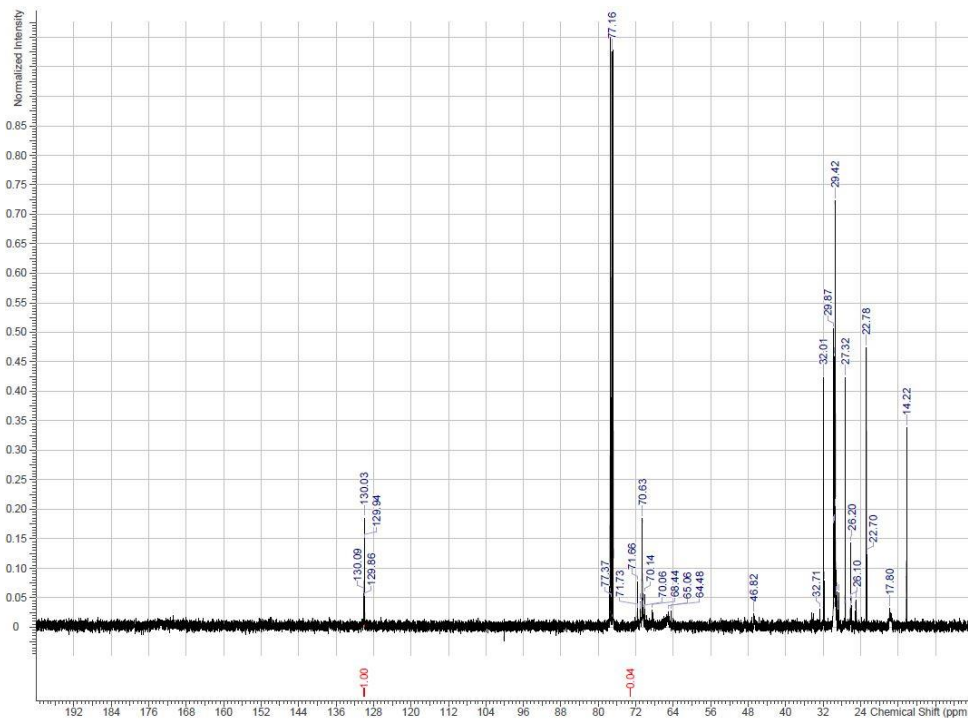
Figure E. 31 ^{13}C-NMR spectrum of product **11**.
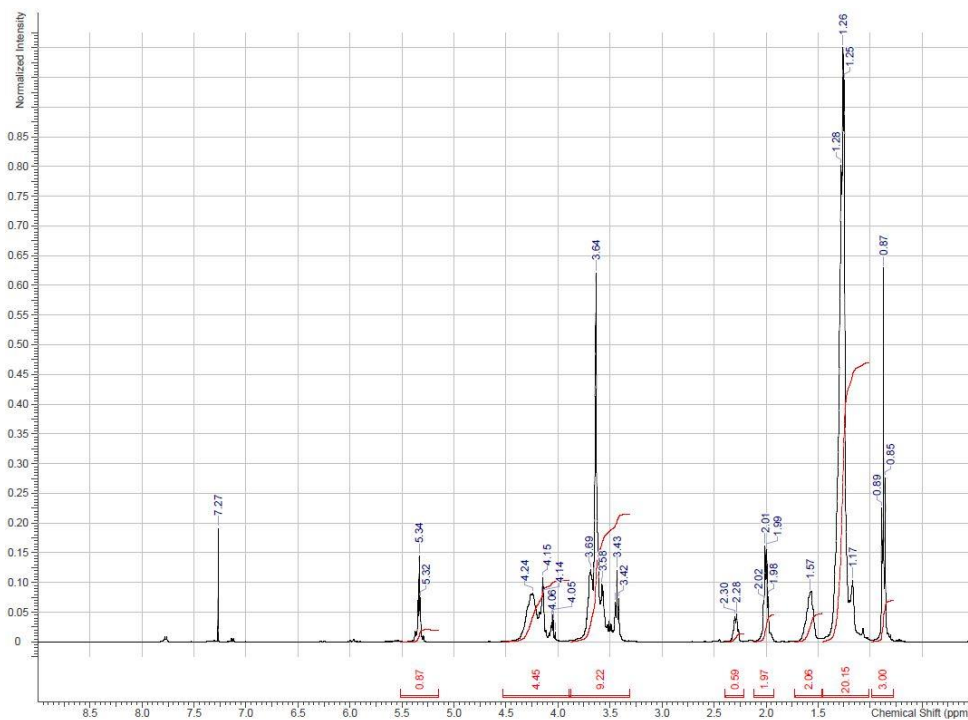
Figure E. 32 ^{1}H-NMR spectrum of product **11**.
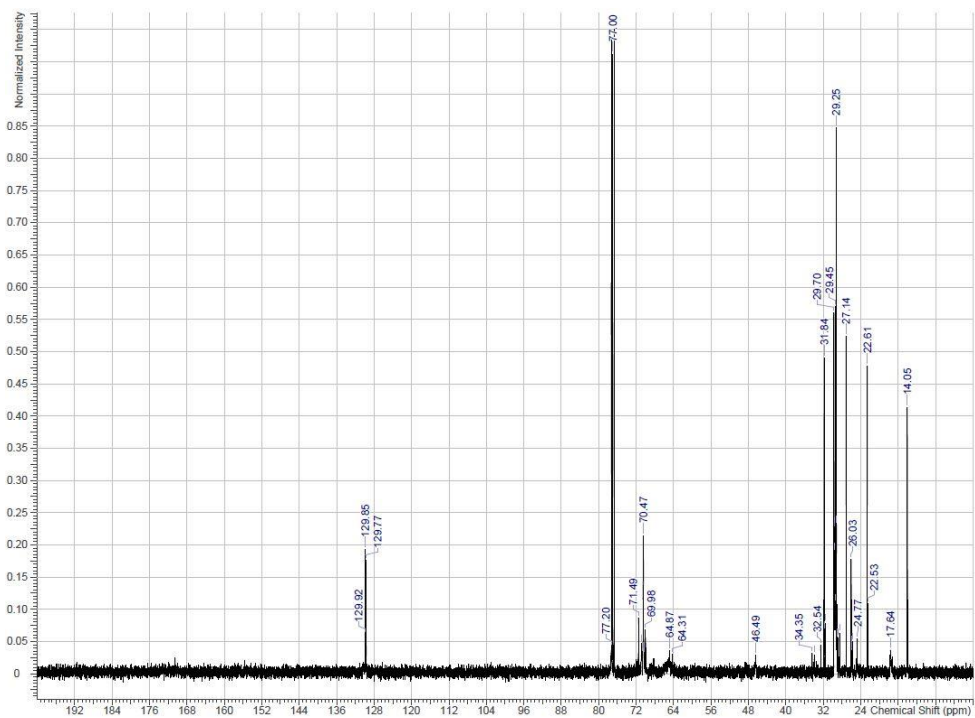
Figure E. 33 ^{13}C-NMR spectrum of product **12**.
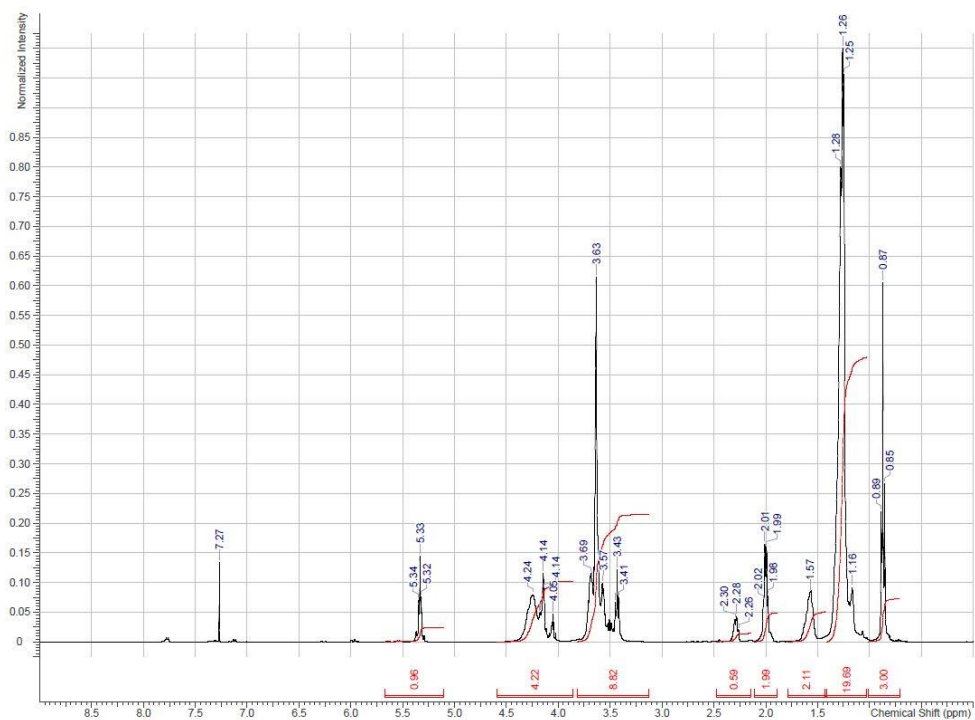
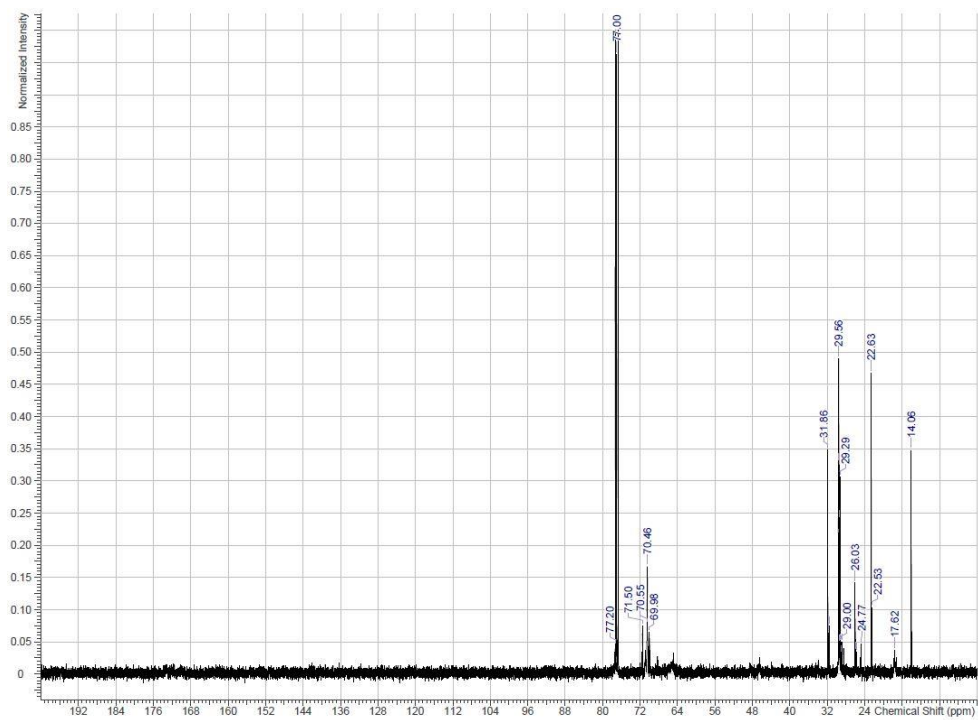Figure E. 34 ^{1}H-NMR spectrum of product **12**.
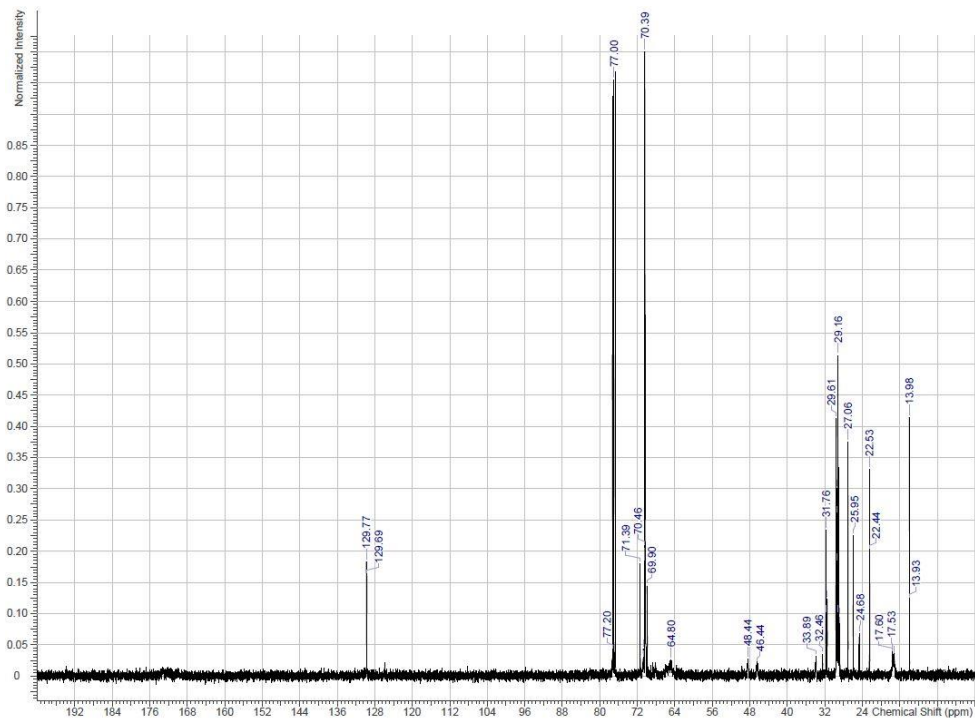
Figure E. 35 ^{13}C-NMR spectrum of product **13**.
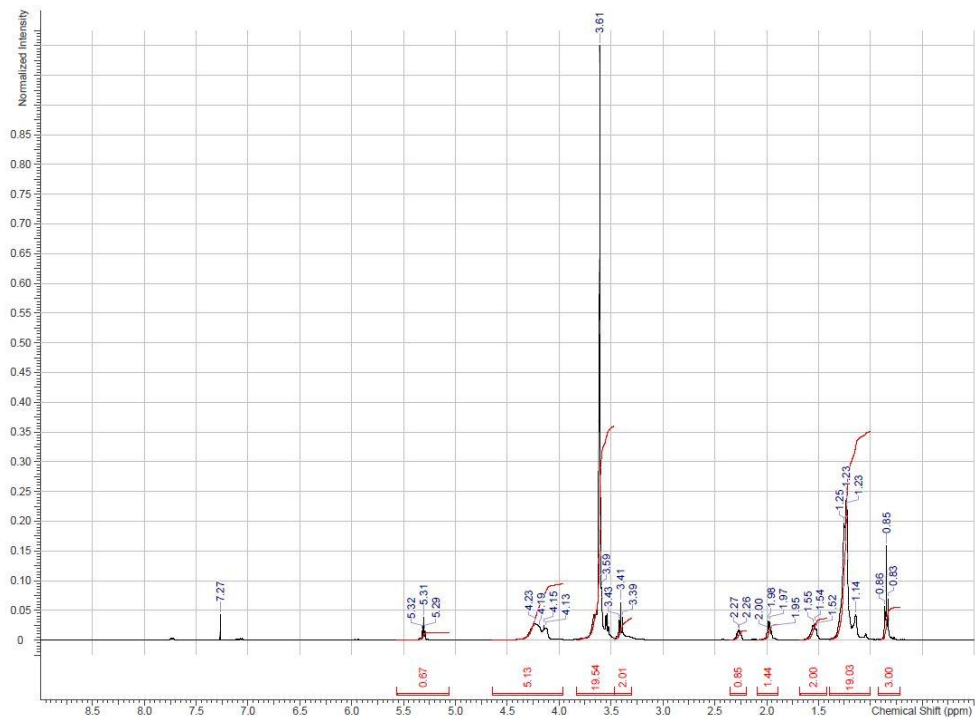
Figure E. 36 ^{1}H-NMR spectrum of product **13**.
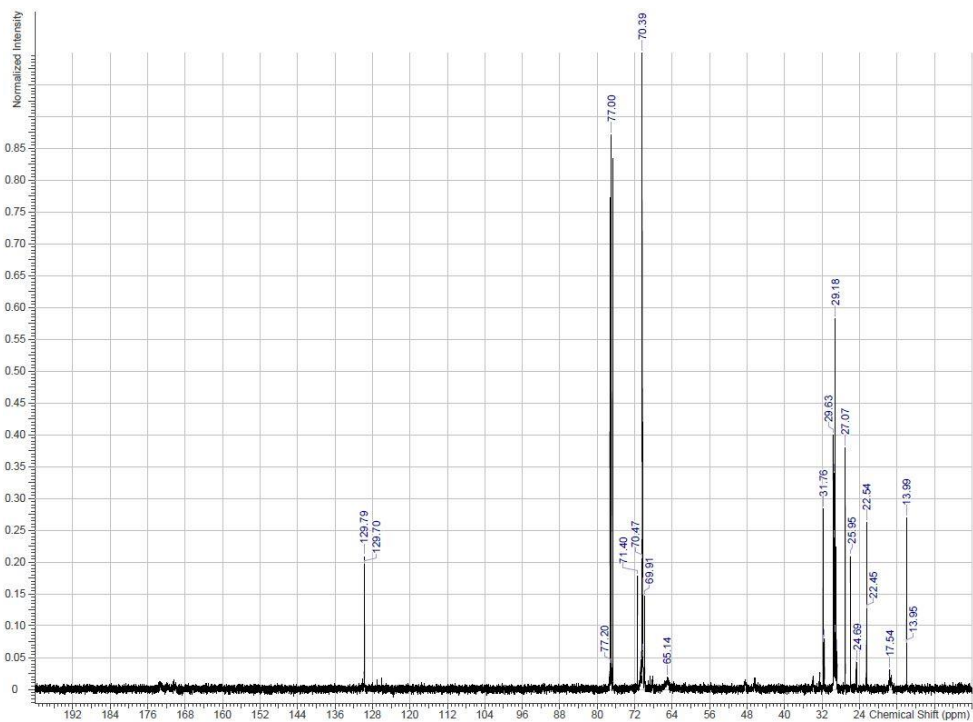
Figure E. 37 ^{13}C-NMR spectrum of product **14**.
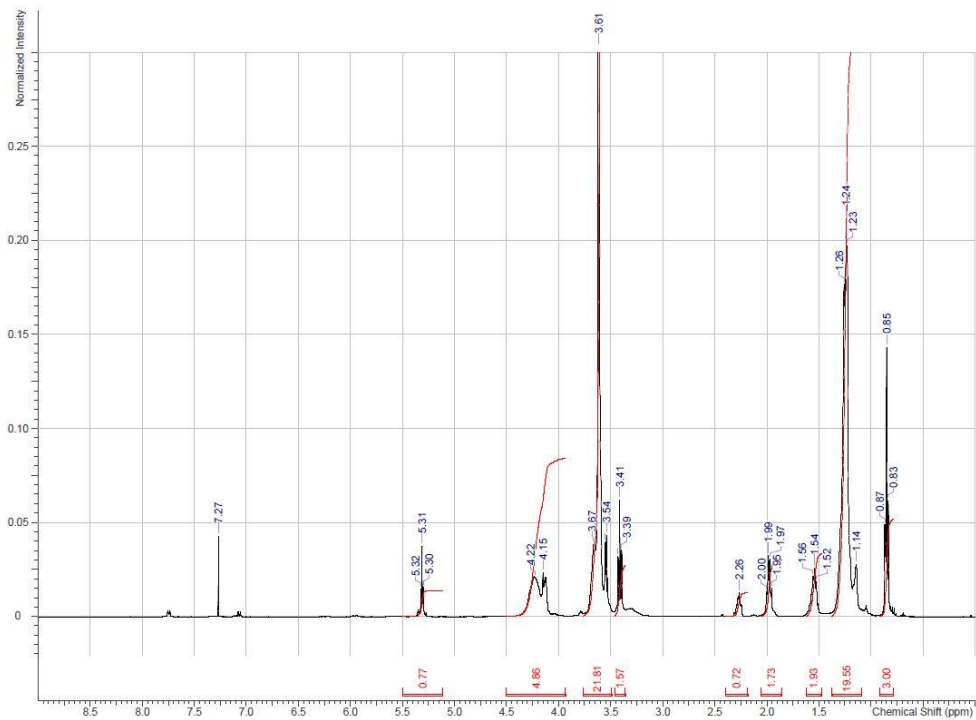
Figure E. 38 ^{1}H-NMR spectrum of product **14**.

XLVI
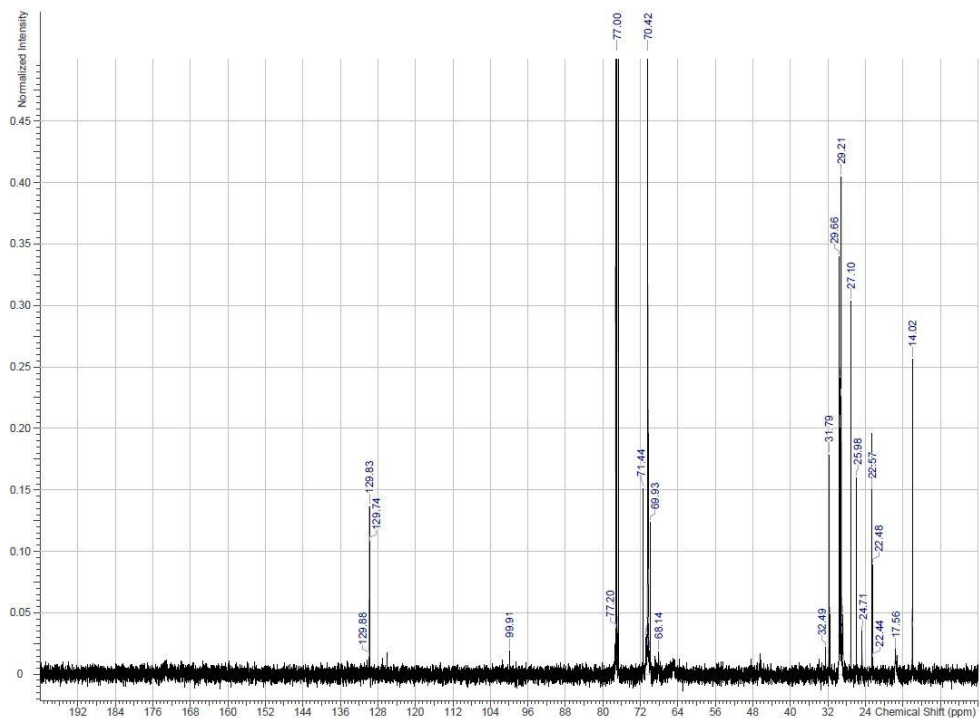
Figure E. 39 ¹³C-NMR spectrum of product **15**.
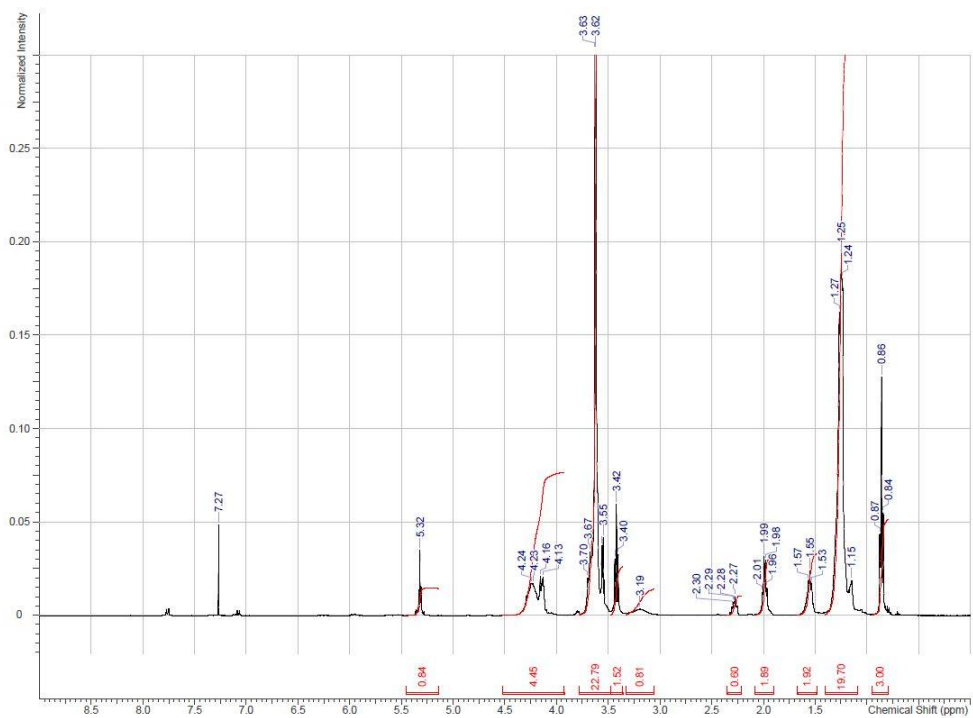
Figure E. 40 ¹H-NMR spectrum of product **15**.
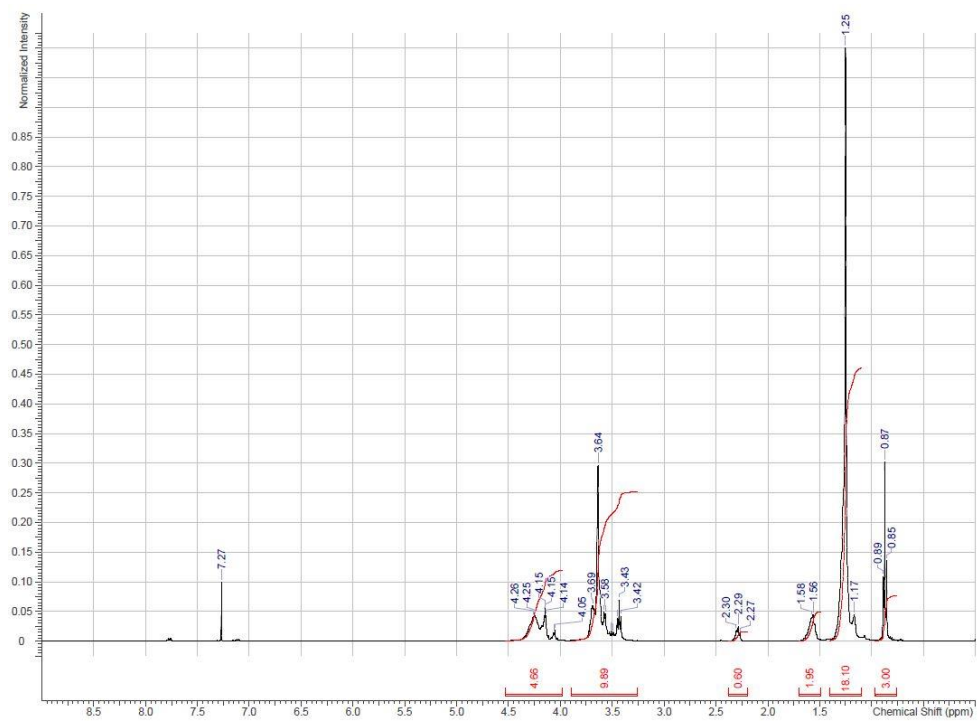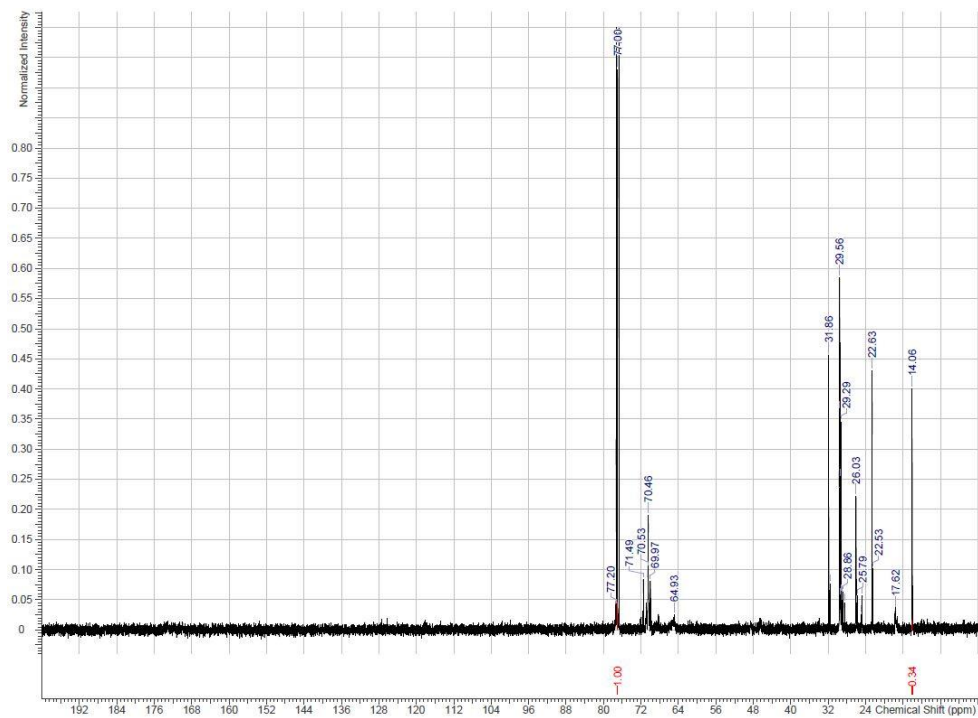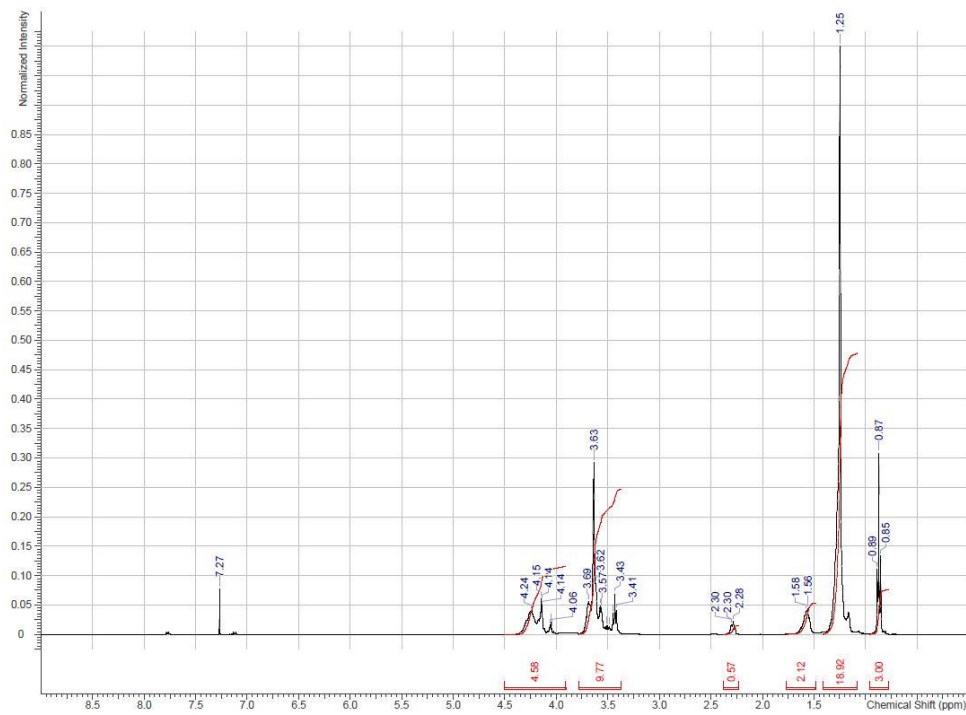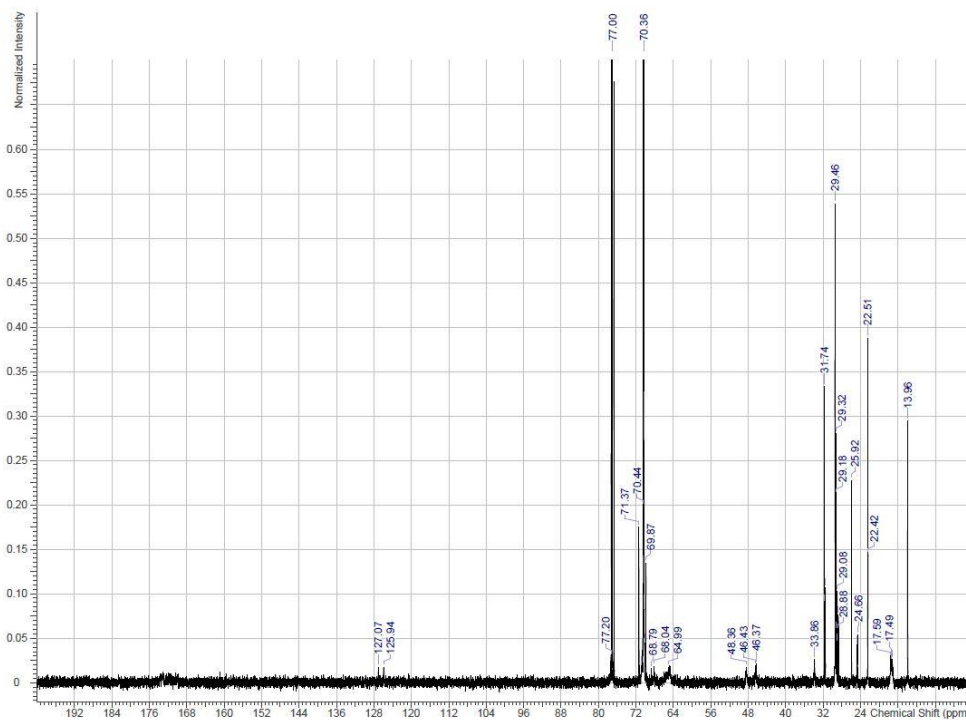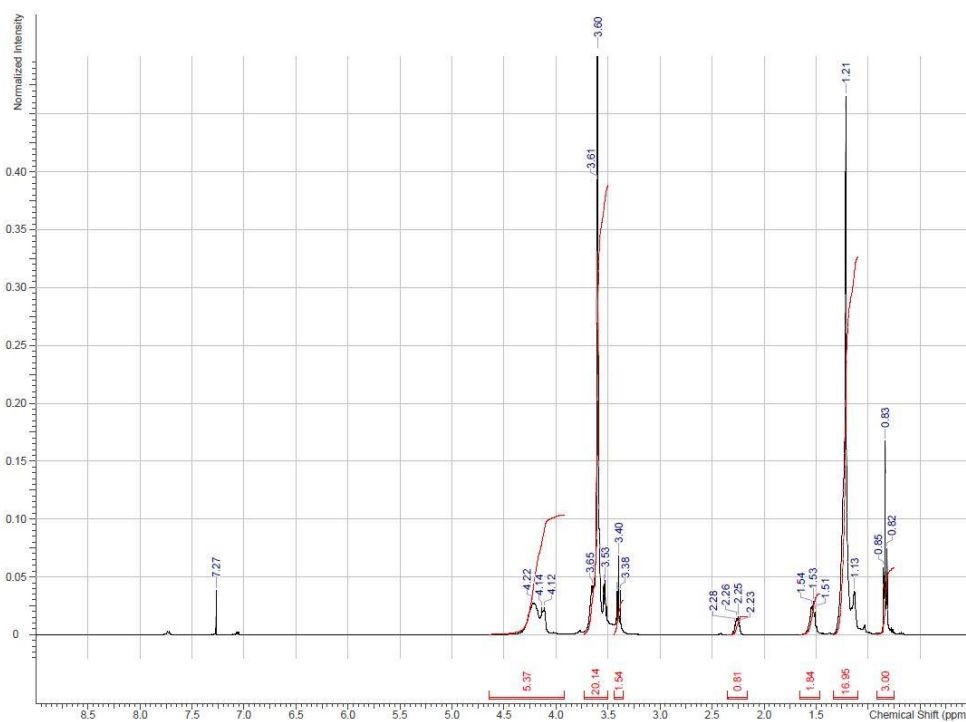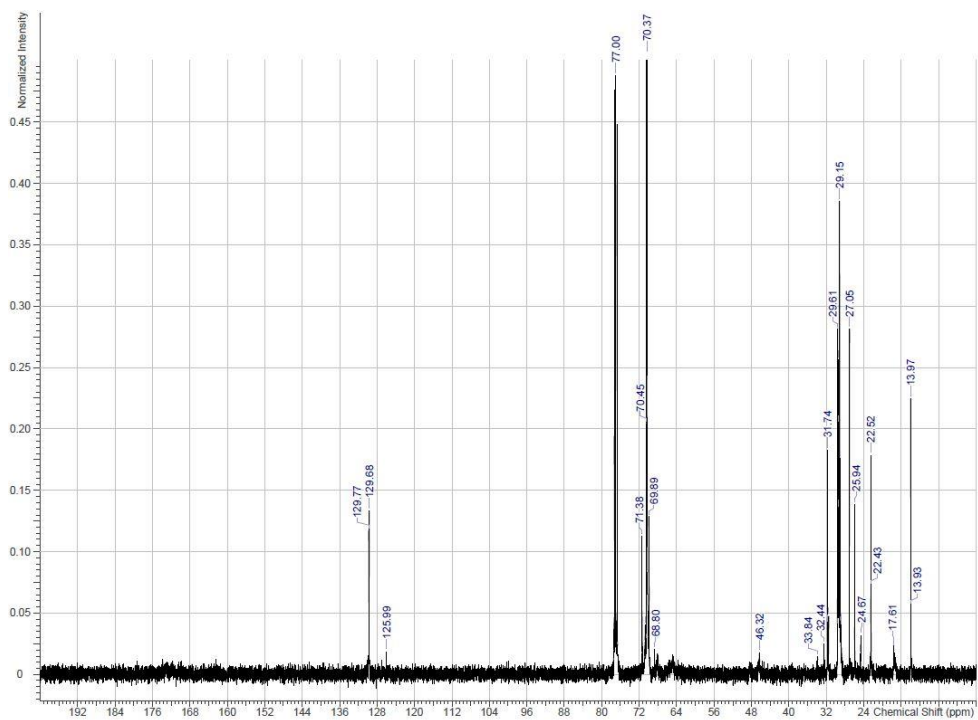
Figure E. 41 ^{13}C-NMR spectrum of product **16**.
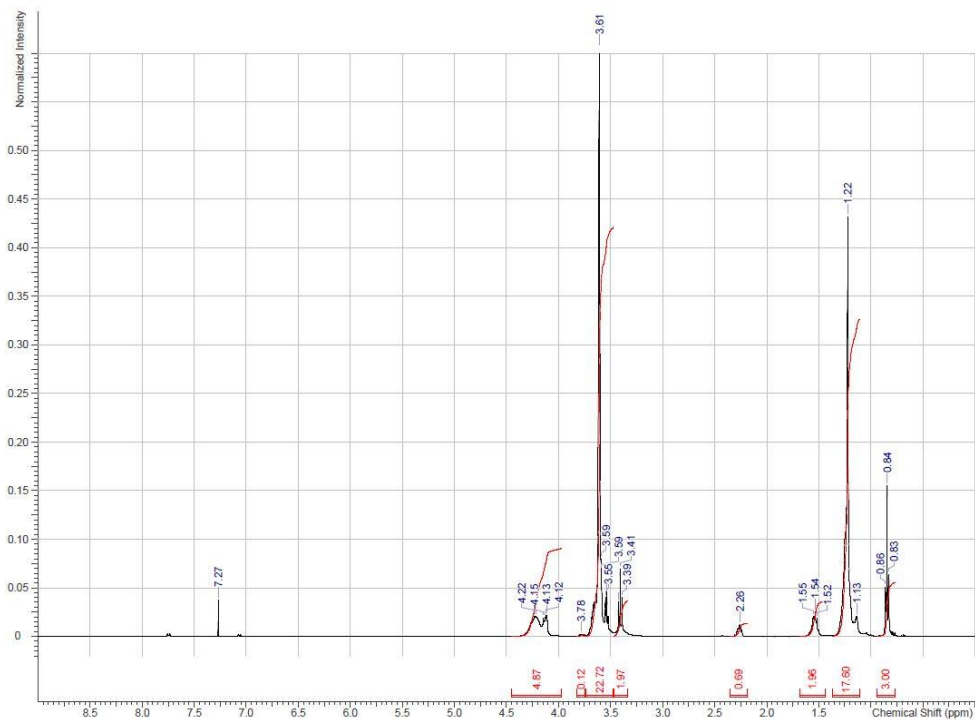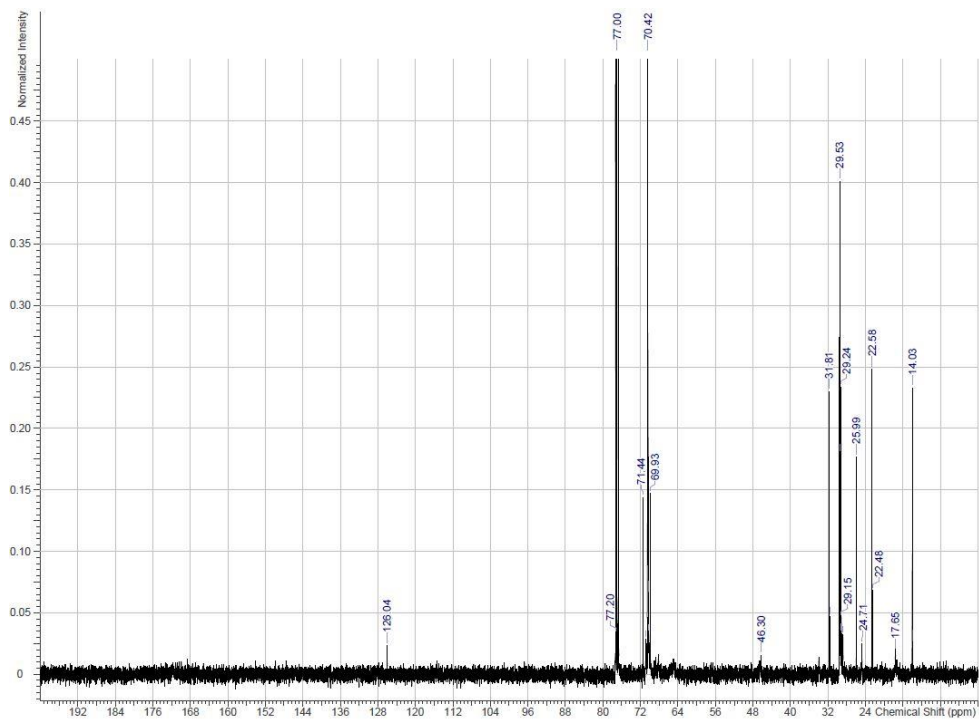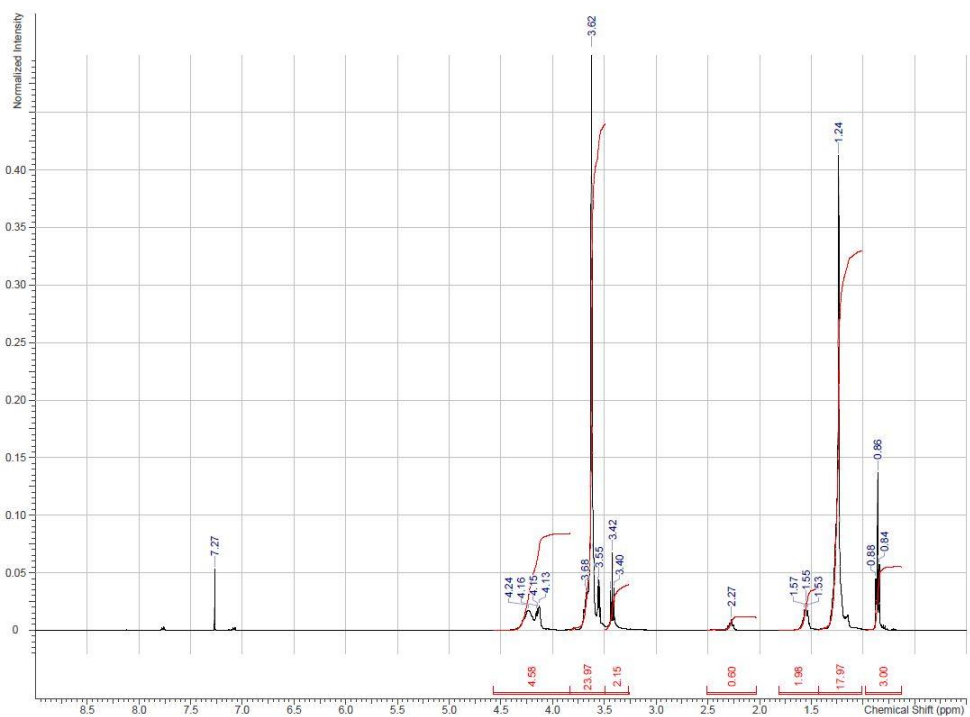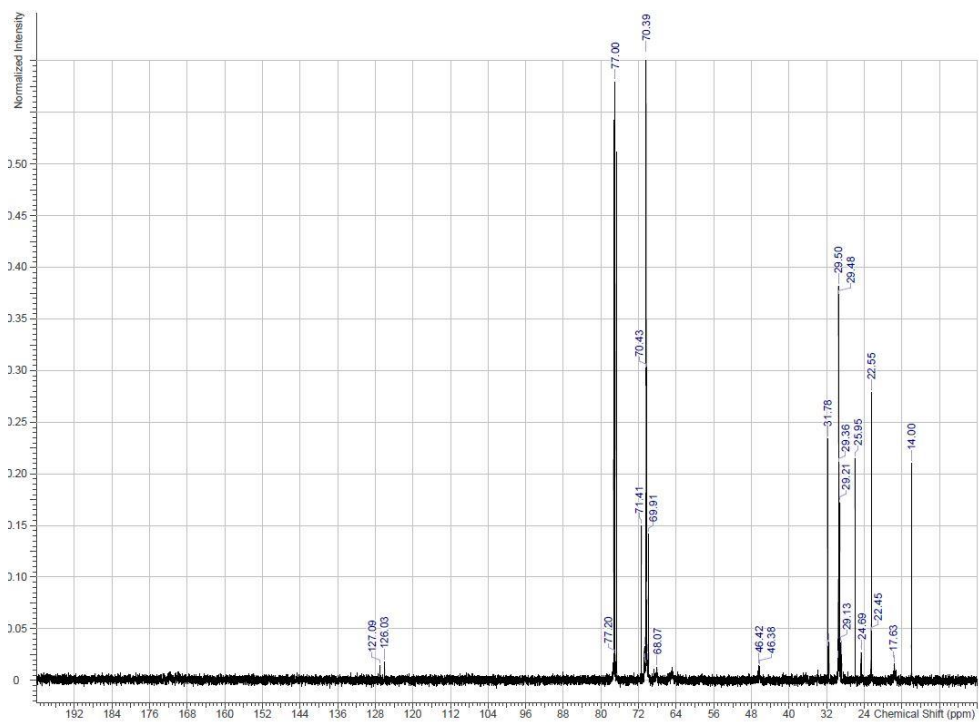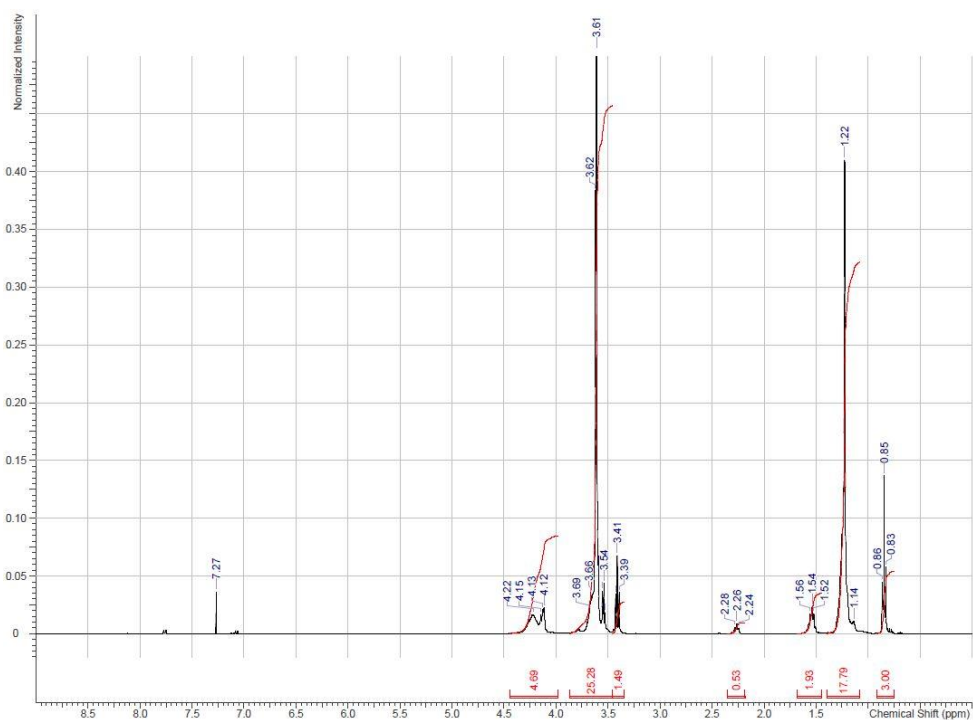

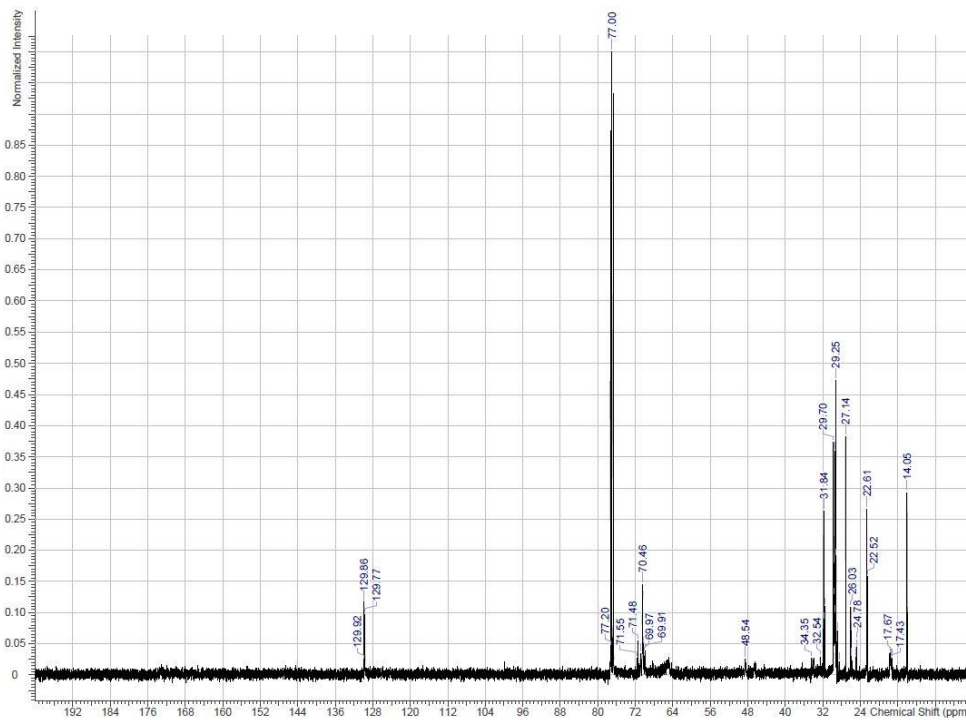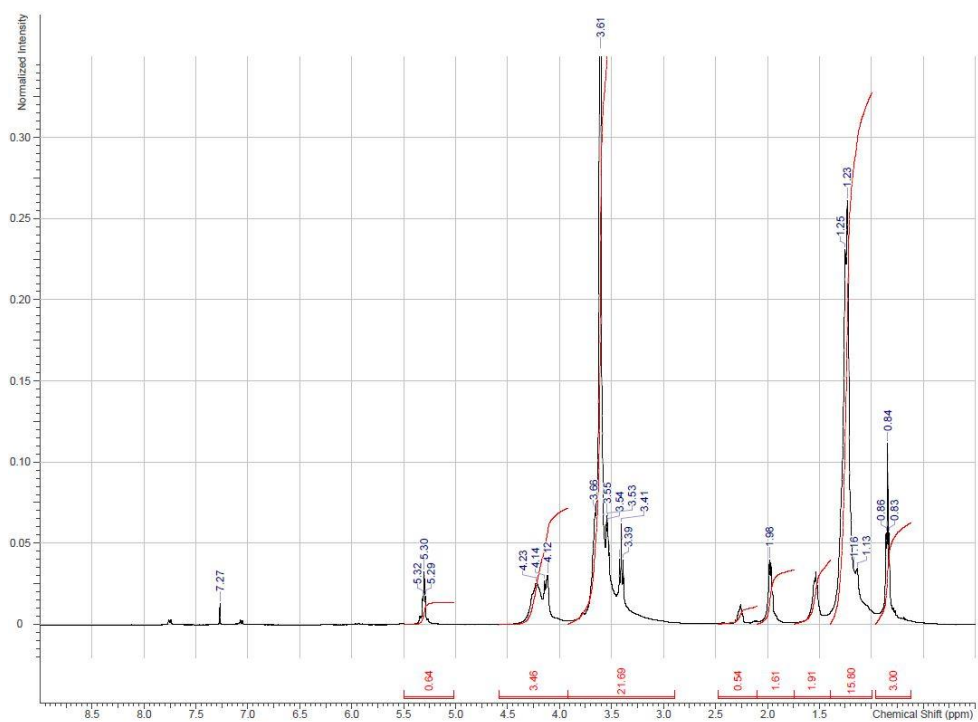Figure E. 42 ^{1}H-NMR spectrum of product **16**.

Appendix F

Table F. 1 Demulsifier testing results from testing in crude oil 1 at 40 ppm. Water separation at times 5, 10, 20, 30, and 65 min is given in percent (%).

Starting materials	Product number	Coverage	EO	R	Time [min]					RSN	HLB	Water quality data		
					5	10	20	30	65			Water	Oil	IF
Boltorn H311 + Starting material A	1	50%	2.5	C_{12}-C_{14}	1.67	3.33	3.33	6.67	16.67	4.1	2.61	4 +	D	M, B +
	2	70%			1.67	3.33	3.33	6.67	6.67	3.5	3.12	4 +	D	M, B +
	3	90%			0	0	0	0	1.67	3.2	3.50	2	D	M-, B ++
	4	100%			0	0	0	0	0	3.0	3.66	1	D	-
Boltorn H311 + Starting material B	5	50%	10	C_{12}-C_{14}	1.67	10	20	33.33	83.33	6.1	7.54	4	D	M+, B +
	6	70%			0	10	23.33	53.33	86.67	5.5	8.56	4	D	M+, B
	7	90%			0	20	46.67	50	50	5.4	9.25	4	D -	M+, B +
	8	100%			0	0	26.67	33.33	23.33	5.1	9.52	3	D	M+, B++
Boltorn H311 + Starting material C	9	50%	2	C_{16}-C_{18}	1.67	3.33	8.33	13.33	13.33	3.4	2.01	4 +	D	M, B +
	10	70%			1.67	5	13.33	16.67	16.67	3.2	2.38	4	D	M, B +
	11	90%			0	0	6.67	13.33	26.67	2.5	2.66	4	D	M+, B ++
	12	100%			0	0	0	6.67	13.33	2.4	2.77	3-4	D	M+, B ++
Boltorn H311 + Starting material D	13	50%	9	C_{16}-C_{18}	5	6.67	13.33	16.67	66.67	5.0	6.72	4	D	M, B +
	14	70%			23.22	33.33	50	53.33	90	4.9	7.62	4	D	M+, B +
	15	90%			23.33	40	66.67	83.33	96.67	4.2	8.22	4 +	D -	M+, B
	16	100%			10	20	33.33	50	83.33	3.8	8.46	4 +	D	M+, B ++

Table F. 2 Results of thieving samples in crude oil 1 emulsion measured in mL (40 ppm). Emulsion breaker (EB).

Starting materials	Product number	Coverage	EO	R	Thief Time: 10 min		Thief (10% EB) Time: 10 min		Thief Time: 30 min		Thief (10% EB) Time: 30 min	
					BS	H_2O	BS	H_2O	BS	H_2O	BS	H_2O
Boltorn H311 + Starting material A	1	50%	2.5	C_{12}-C_{14}	1.2	0.4	-	1.2	0.4	0.2	-	0.8
	2	70%			1.4	T	-	1.4	0.6	0.2	-	1
	3	90%			17	T	-	17	1	T	-	1
	4	100%			21	T	-	22	0.6	T	-	0.8
Boltorn H311 + Starting material B	5	50%	10	C_{12}-C_{14}	0.2	0.9	-	1.4	0.4	0.36	-	0.8
	6	70%			0.4	1	-	15	0.2	0.2	-	0.7
	7	90%			0.8	0.8	-	1.2	0.4	0.2	-	0.8
	8	100%			0.4	0.7	-	1.6	0.4	0.2	-	0.8
Boltorn H311 + Starting material C	9	50%	2	C_{16}-C_{18}	1.2	T	-	1.6	0.6	0.2	-	1
	10	70%			9	T	-	9	0.8	T	-	0.9
	11	90%			1.2	0.4	-	1.2	0.5	0.2	-	1.2
	12	100%			16	T	-	15	0.4	0.2	-	1
Boltorn H311 + Starting material D	13	50%	9	C_{16}-C_{18}	1	T	-	1.2	0.4	0.2	-	0.8
	14	70%			0.3	0.4	-	0.8	0.4	0.2	-	0.6
	15	90%			1.2	0.44	-	1.2	0.7	T	-	0.6
	16	100%			1	0.8	-	1.2	0.4	T	-	0.6

L

Table F. 3 Demulsifier testing results from testing in crude oil 1 at 80 ppm. Water separation at times 5, 10, 20, 30, and 65 min is given in percent (%).

Starting materials	Product number	Coverage	EO	R	Time [min]					RSN	HLB	Water quality data		
					5	10	20	30	65			Water	Oil	IF
Boltorn H311 + Starting material A	1	50%	2.5	C_{12}-C_{14}	0	0	16.67	16.67	16.67	4.1	2.61	3-4	D +	M, B +
	2	70%			3.33	6.67	10	13.33	13.33	3.5	3.12	3-4	D +	M-, B +
	3	90%			0	0	0	0	0	3.2	3.50	1	D +	-
	4	100%			0	0	0	0	0	3.0	3.66	1	D +	-
Boltorn H311 + Starting material B	5	50%	10	C_{12}-C_{14}	3.33	20	26.67	30	66.67	6.1	7.54	4 -	D -	M+, B
	6	70%			11.67	16.67	33.33	33.33	80	5.5	8.56	5	D	M+, B
	7	90%			26.67	40	76.67	83.33	96.67	5.4	9.25	4	D-	M+, B
	7a	90%			33.33	50	66.67	83.33	96.67	-	-	4	D -	M+, B
	7b	90%			26.67	60	90	96.67	100	-	-	4	D - -	M+, S
	8	100%			0	20	66.67	83.33	96.67	5.1	9.52	4 -	D - -	M+, B -
Boltorn H311 + Starting material C	9	50%	2	C_{16}-C_{18}	6.67	13.33	40	53.33	96.67	3.4	2.01	4 +	D	M+, B
	10	70%			0	10	33.33	50	90	3.2	2.38	5	D -	M+, B +
	11	90%			0	0	16.67	26.67	66.67	2.5	2.66	4 +	D	M+, B ++
	12	100%			0	0	0	0	0	2.4	2.77	2	D	-
Boltorn H311 + Starting material D	13	50%	9	C_{16}-C_{18}	50	73.33	90	90	90	5.0	6.72	4	D -	M+, B -
	14	70%			50	73.33	86.67	90	90	4.9	7.62	4 +	D	M+, B -
	15	90%			46.67	70	86.67	90	90	4.2	8.22	4 +	D -	M+, B -
	16	100%			0	30	63.33	83.33	93.33	3.8	8.46	4 -	D	M+, B

Table F. 4 Results of thieving samples in crude oil 1 emulsion measured in mL (80 ppm). Emulsion breaker (EB).

Starting materials	Product number	Coverage	EO	R	Thief Time:	10 min	Thief (10% EB) Time:	10 min	Thief Time:	30 min	Thief (10% EB) Time:	30 min
					BS	H_2O	BS	H_2O	BS	H_2O	BS	H_2O
Boltorn H311 + Starting material A	1	50%	2.5	C_{12}-C_{14}	2	0.2	-	2	1.2	T	-	1
	2	70%			2.4	T	-	2	1.2	T	-	1.2
	3	90%			2.2	T	-	2	1.2	T	-	0.76
	4	100%			9	T	-	9.2	0.8	T	-	1.1
Boltorn H311 + Starting material B	5	50%	10	C_{12}-C_{14}	0.8	1.2	-	1.7	0.4	0.4	-	0.8
	6	70%			1	1	-	1.7	0.6	0.2	-	0.8
	7	90%			0.6	0.6	-	1.1	0.7	T	-	0.6
	7a	90%			T	1.1		1.2	0	0.6	-	0.6
	7b	90%			T	1		1	T	0.4	-	0.5
	8	100%			1.2	0.4	-	1	0.4	0.2	-	0.6
Boltorn H311 + Starting material C	9	50%	2	C_{16}-C_{18}	1.2	0.4	-	1.2	1.2	T	-	1.2
	10	70%			1.4	0.5	-	1.6	1.3	T	-	1.3
	11	90%			1.4	0.5	-	1.5	1	0.2	-	1.2
	12	100%			1.6	0.4	-	1.6	0.5	0.2	-	1
Boltorn H311 + Starting material D	13	50%	9	C_{16}-C_{18}	1.1	0.4	-	0.9	0.8	T	-	0.8
	14	70%			1.2	0.4	-	1.2	0.8	T	-	0.8
	15	90%			1.3	0.4	-	1.2	0.6	T	-	0.6
	16	100%			1.2	0.4	-	1.2	0.6	T	-	0.6

Appendix G

Table G. 1 Demulsifier testing results from testing in crude oil 2 at 80 ppm. Water separation at times 5, 10, 20, 30, and 65 min is given in percent (%).

Starting materials	Product number	Coverage	EO	R	Time [min]					RSN	HLB	Water quality data		
					5	10	20	30	65			Water	Oil	IF
Boltorn H311 + Starting material A	1	50%	2.5	C$_{12}$-C$_{14}$	11.67	25	43.33	50	66.67	4.1	2.61	5	D	R -
	2	70%			13.33	23.33	33.33	36.67	73.33	3.5	3.12	4 +	D	R -
	3	90%			30	43.33	50	50	83.33	3.2	3.50	5 +	D	S
	4	100%			13.33	26.67	36.67	40	76.67	3.0	3.66	4	D	R -
Boltorn H311 + Starting material B	5	50%	10	C$_{12}$-C$_{14}$	11.67	20	26.67	33.33	86.67	6.1	7.54	5	D	S
	6	70%			30	40	46.67	50	90	5.5	8.56	5	D	S
	7	90%			33.33	43.33	50	50	90	5.4	9.25	5	D	S
	7a	90%			50	53.33	56.67	60	90	-	-	5 -	D	S
	7b	90%			50	56.67	56.67	60	90	-	-	5 -	D	S
	8	100%			30	43.33	53.33	56.67	90	5.1	9.52	5	D	S
Boltorn H311 + Starting material C	9	50%	2	C$_{16}$-C$_{18}$	26.67	36.67	43.33	50	80	3.4	2.01	5	D	R -
	10	70%			15	26.67	40	43.33	73.33	3.2	2.38	4 +	D	S -
	11	90%			30	60	70	73.33	90	2.5	2.66	5	D	R -
	12	100%			16.67	50	70	76.67	90	2.4	2.77	5	D	R -
Boltorn H311 + Starting material D	13	50%	9	C$_{16}$-C$_{18}$	3.33	15	26.67	33.33	83.33	5.0	6.72	4	D	S
	14	70%			9.33	30	43.33	50	86.67	4.9	7.62	5	D	S
	15	90%			16.67	53.33	66.67	70	90	4.2	8.22	5 -	D	S
	16	100%			18.33	66.67	76.67	80	93.33	3.8	8.46	5	D	S

Table G. 2 Results of thieving samples in crude oil 2 emulsion measured in mL (80 ppm). Emulsion breaker (EB).

Starting materials	Product number	Coverage	EO	R	Thief Time: BS	10 min H_2O	Thief (10% EB) Time: BS	10 min H_2O	Thief Time: BS	30 min H_2O	Thief (10% EB) Time: BS	30 min H_2O
Boltorn H311 + Starting material A	1	50%	2.5	C_{12}-C_{14}	3	17	-	19	3	11	-	13.5
	2	70%			1	17	-	19	7	12	-	18
	3	90%			1	13.5	-	15	4	10	-	15
	4	100%			0.5	17	-	18	2	14	-	15
Boltorn H311 + Starting material B	5	50%	10	C_{12}-C_{14}	0	20	-	20	0	18	-	18
	6	70%			0.5	18	-	19	T	13.5	-	14
	7	90%			0	17	-	18	T	13	-	13
	7a	90%			T	13	-	14	T	12	-	12.5
	7b	90%			T	13	-	14	T	12	-	12
	8	100%			T	13	-	14	T	12	-	12
Boltorn H311 + Starting material C	9	50%	2	C_{16}-C_{18}	2	17	-	18	1	11	-	13
	10	70%			2	15	-	17	2	13	-	15
	11	90%			1	10	-	10	1	8	-	9
	12	100%			0.5	7	-	8	2	6	-	7.5
Boltorn H311 + Starting material D	13	50%	9	C_{16}-C_{18}	T	20	-	20	T	16	-	17
	14	70%			T	17	-	17	T	14	-	14
	15	90%			T	11	-	11	0.5	10	-	10.5
	16	100%			0.5	7	-	7	0.5	8	-	8

Appendix H

Table H. 1 Demulsifier testing results from testing in crude oil 3 at 80 ppm. Water separation at times 5, 10, 20, 30, and 65 min is given as percent (%).

Starting materials	Product number	Coverage	EO	R	Time [min]					RSN	HLB	Water quality data		
					5	10	20	30	65			Water	Oil	IF
Boltorn H311 + Starting material A	1	50%	2.5	C_{12}-C_{14}	0.33	5	11.67	15	16.67	4.1	2.61	3	D+	M+, B-
	2	70%			0.83	6	13.33	18.33	30	3.5	3.12	3	D+	M, B-
	3	90%			3.33	9.33	15	20	20	3.2	3.50	4 -	D+	M, B-
	4	100%			0.17	1	3.33	10	16.67	3.0	3.66	3	D+	M+, B
Boltorn H311 + Starting material B	5	50%	10	C_{12}-C_{14}	0	0.83	6.67	8	16.67	6.1	7.54	3	D+	M, S-
	6	70%			0.17	5	11.67	15	26.67	5.5	8.56	3	D+	M, S-
	7	90%			1.67	16.67	26.67	36.67	33.33	5.4	9.25	3	D+	M+, B
	7a	90%			0.5	16.67	33.33	46.67	66.67	-	-	3	D+	M+, B
	7b	90%			0	7.33	26.67	26.67	36.67	-	-	3	D+	M+, B
	8	100%			0.33	5	10	13.33	26.67	5.1	9.52	3	D+	M+, S
Boltorn H311 + Starting material C	9	50%	2	C_{16}-C_{18}	1.67	5	13.33	23.33	23.33	3.4	2.01	4 -	D+	M+, B
	10	70%			1	5.33	13.33	16.67	20	3.2	2.38	4 -	D+	M+, B
	11	90%			0	0.03	0.17	0.83	5	2.5	2.66	3	D+	M-, R+
	12	100%			0	0.17	2.67	5	6.67	2.4	2.77	3	D+	M, R+
Boltorn H311 + Starting material D	13	50%	9	C_{16}-C_{18}	0.33	4.33	13.33	18.33	23.33	5.0	6.72	3	D+	M+, S-
	14	70%			0.17	3.33	16.67	20	23.33	4.9	7.62	3	D+	M+, S-
	15	90%			0	3	23.33	26.67	31.67	4.2	8.22	3	D+	M+, S-
	16	100%			2.33	10	26.67	33.33	43.33	3.8	8.46	3	D+	M+, R--

Table H. 2 Results of thieving samples in crude oil 3 emulsion measured in mL (80 ppm). Emulsion breaker (EB).

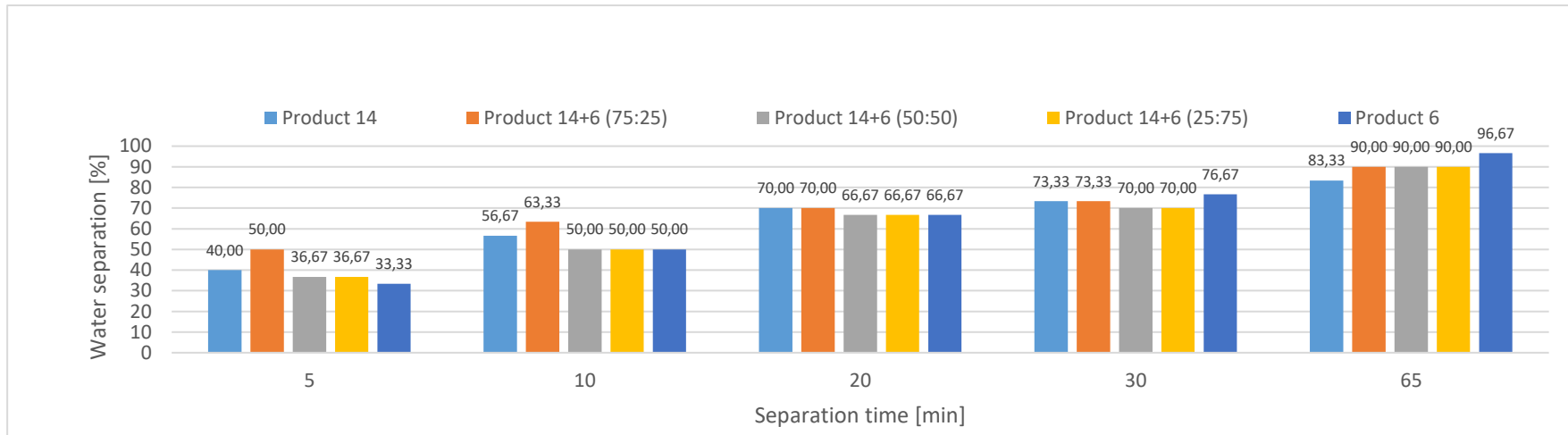| Starting materials	Product number	Coverage	EO	R	Micro-emulsion Time: 10 min	Thief Time: 10 min		Thief (10% EB) Time: 10 min		Micro-emulsion Time: 30 min	Thief Time: 30 min		Thief (10% EB) Time: 30 min	
						BS	H$_2$O	BS	H$_2$O		BS	H$_2$O	BS	H$_2$O
Boltorn H311 + Starting material A	1	50%	2.5	C$_{12}$-C$_{14}$	56	4	20	-	24	40	3	17	-	20
	2	70%			50	2	18	-	20	34	1	19	-	20
	3	90%			36	2	18	-	19	46	4	13	-	17
	4	100%			34	4	20	-	24	42	2	20	-	22
Boltorn H311 + Starting material B	5	50%	10	C$_{12}$-C$_{14}$	60	1	19	-	25	50	1	20	-	20
	6	70%			40	2	19	-	20	50	1	18	-	18
	7	90%			40	1	18	-	19	40	0.5	17	-	16
	7a	90%			44	1	14	-	15	36	T	14	-	14
	7b	90%			40	1	20	-	23	40	T	18	-	18
	8	100%			40	2	20	-	22	54	2	22	-	26
Boltorn H311 + Starting material C	9	50%	2	C$_{16}$-C$_{18}$	48	2	10	-	12	40	1	10	-	11
	10	70%			60	2	20	-	22	36	1	16	-	17
	11	90%			42	2	22	-	23	44	2	18	-	21
	12	100%			42	6	20	-	26	36	6	16	-	22
Boltorn H311 + Starting material D	13	50%	9	C$_{16}$-C$_{18}$	52	1	20	-	21	50	2	17	-	19
	14	70%			56	1	21	-	22	48	1	16	-	17
	15	90%			44	0.5	18	-	19	34	0.5	15	-	17
	16	100%			48	1	20	-	19	52	0.5	16	-	18

Appendix I

Figure I. 1 Water separation (%) for synergistic testing of products **6** and **14**.
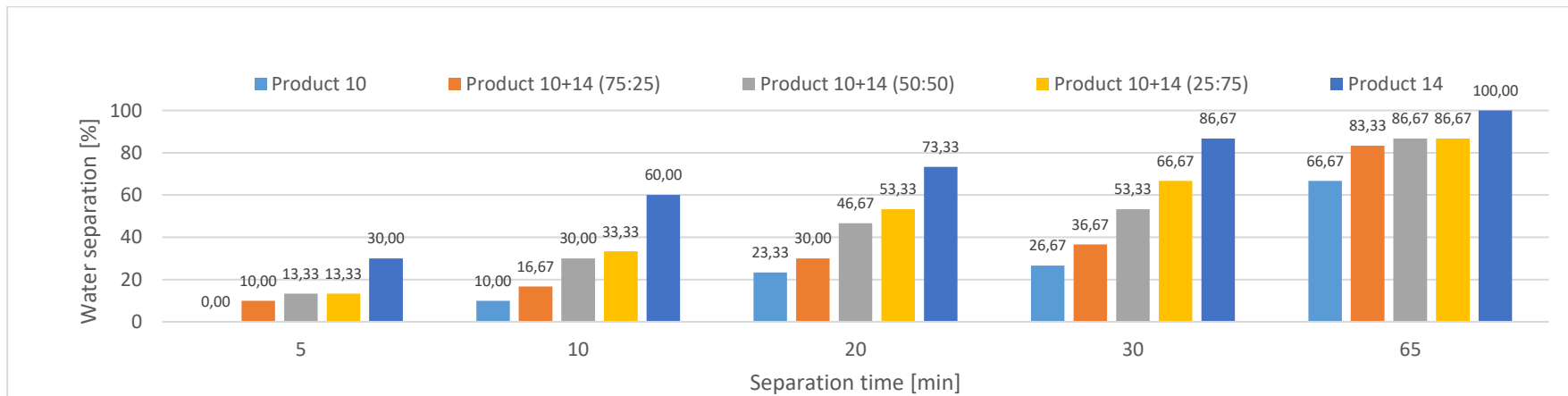

Figure I. 2 Water separation (%) for synergistic testing of products **10** and **14**.
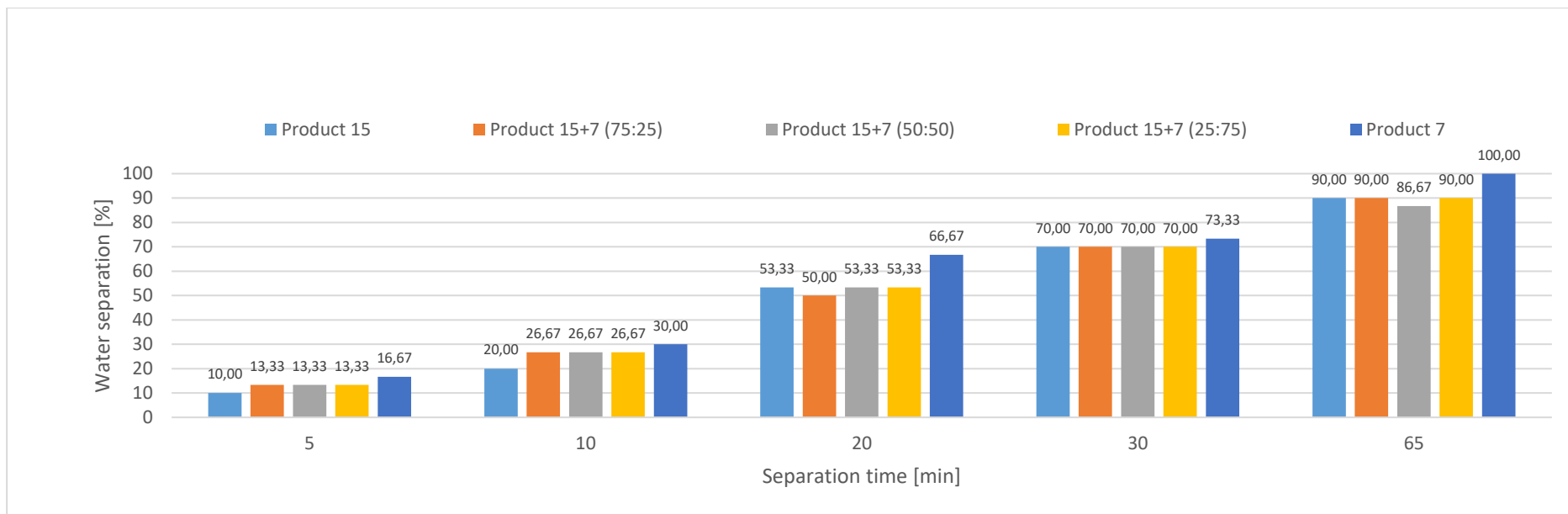
Figure I. 3 Water separation (%) for synergistic testing of products **7** and **15**.
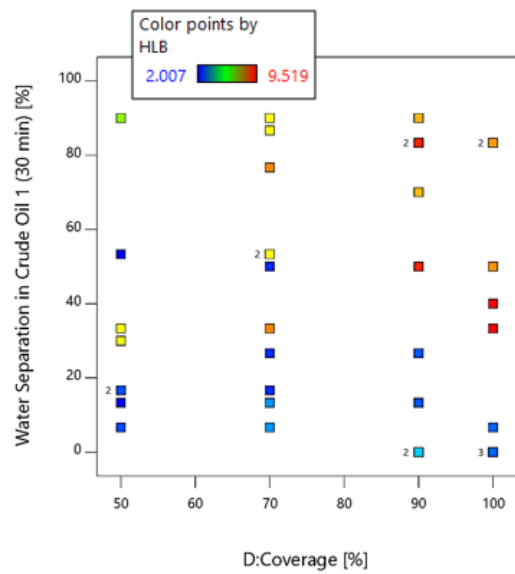
Appendix J

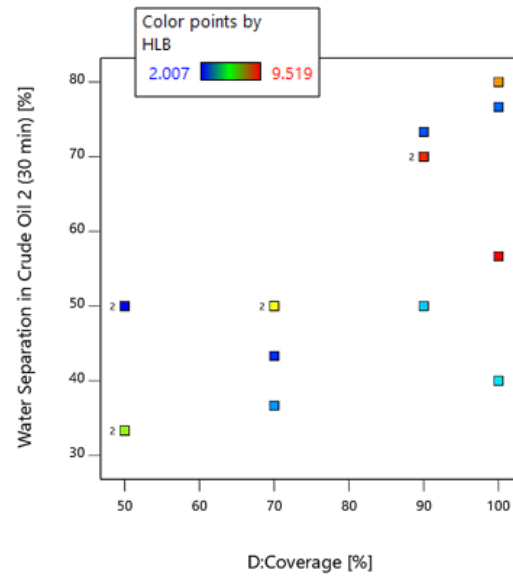Figure J. 1 Water separation (%) in crude oil 1 related to percentage coverage and HLB values.

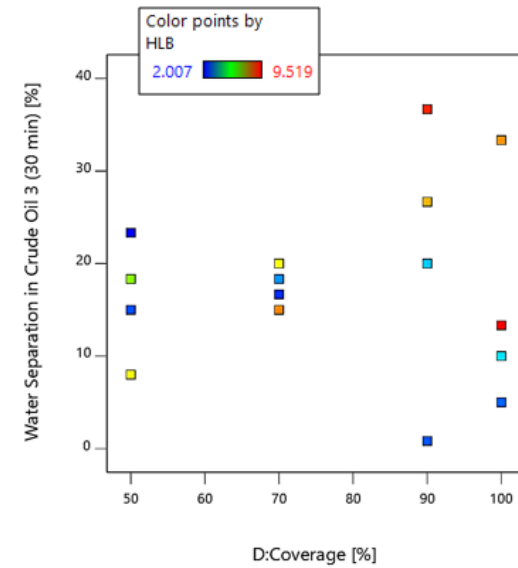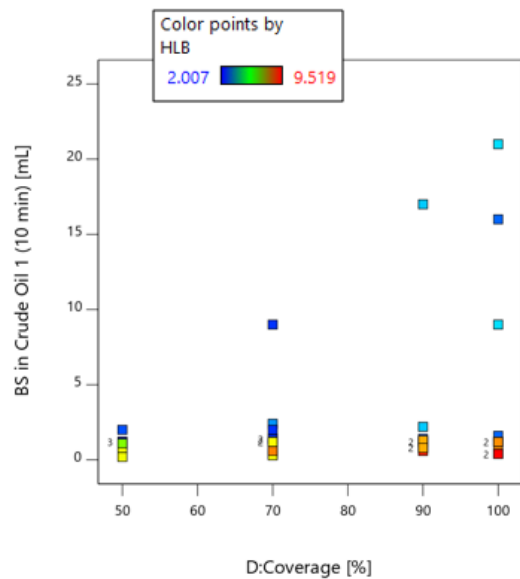Figure J. 2 Water separation (%) in crude oil 2 related to percentage coverage and HLB values.

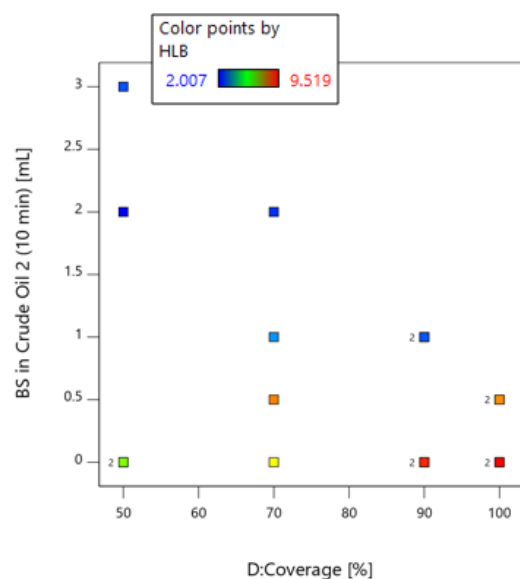Figure J. 3 Water separation (%) in crude oil 3 related to percentage coverage and HLB values.

Figure J. 4 Amount of residual emulsion (BS, mL) in crude oil 1 related to percentage coverage and HLB values.

Figure J. 5 Amount of residual emulsion (BS, mL) in crude oil 2 related to percentage coverage and HLB values.
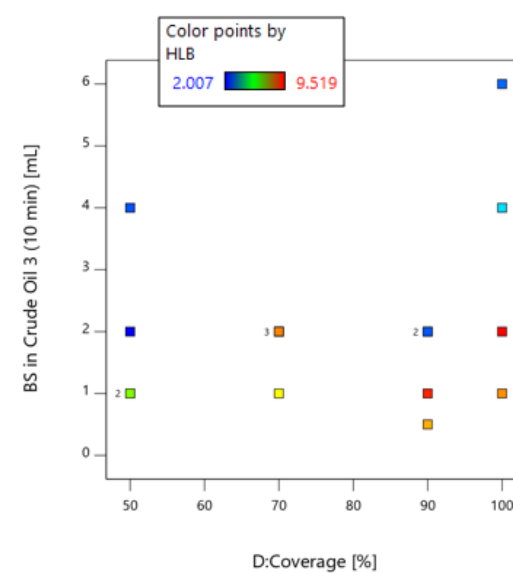

Figure J. 6 Amount of residual emulsion (BS, mL) in crude oil 3 related to percentage coverage and HLB values.
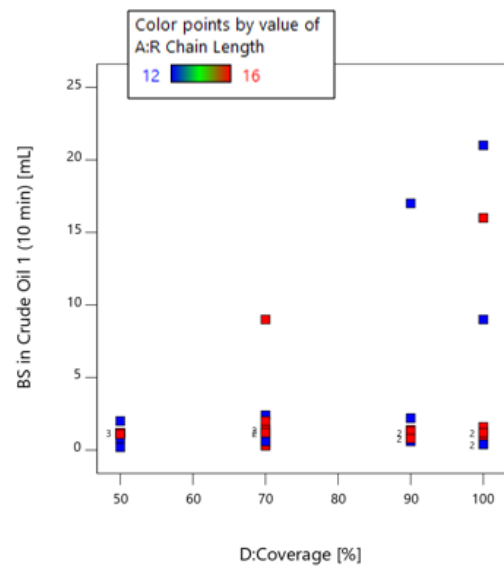
Appendix K

Figure K. 1 Amount of residual emulsion (BS, mL) in crude oil 1 related to percentage coverage and alkyl chain length.
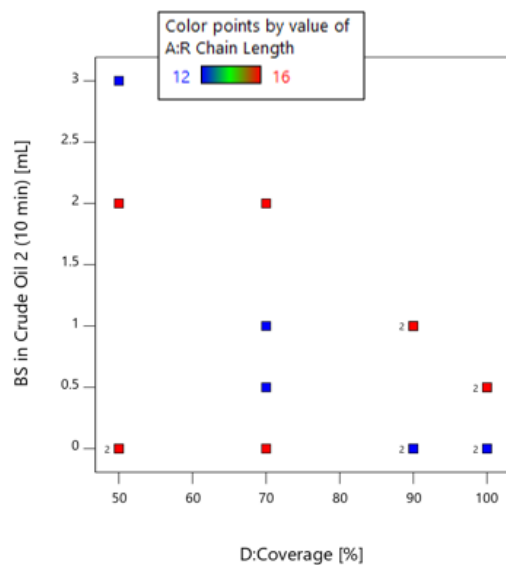

Figure K. 2 Amount of residual emulsion (BS, mL) in crude oil 2 related to percentage coverage and alkyl chain length.
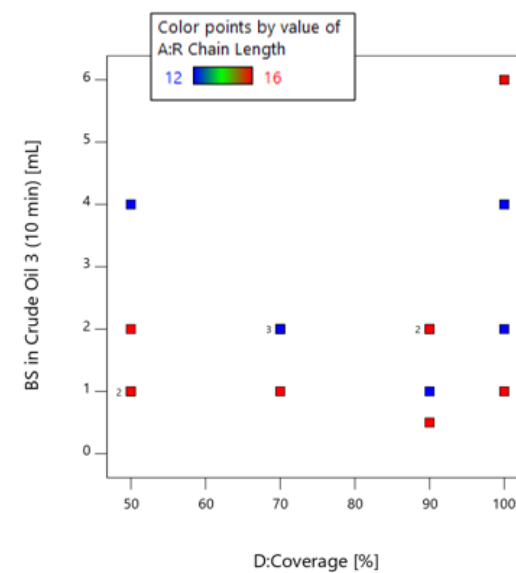

Figure K. 3 Amount of residual emulsion (BS, mL) in crude oil 3 related to percentage coverage and alkyl chain length.